UNIVERSITY OF CALIFORNIA

Los Angeles

Evolution of drought tolerance within and across species

A dissertation submitted in partial satisfaction of the

requirements for the degree Doctor of Philosophy

in Biology

by

Leila Rose Fletcher

2021

ABSTRACT OF THE DISSERTATION

Evolution of drought tolerance within and across species

by

Leila Rose Fletcher

Doctor of Philosophy in Biology

University of California, Los Angeles, 2021

Professor Lawren Sack, Chair

Plants experience a wide range of environmental stresses, and are expected to face more frequent and severe droughts under climate change. Understanding the impacts of stress on plant performance will allow us to predict changes in the distribution and abundance of plants across habitats. Despite this, few studies have analyzed plant drought tolerance within a lineage or species, rather than at a broad scale. I demonstrated the utility of the leaf osmotic potential at turgor loss point (π_{TLP}; wilting point) for predicting drought tolerance across closely-related species of *Ceanothus*. I extended this work to examine how the osmotic potential at full turgor (π_o), the main determinant of the π_{TLP}, could be used to assess drought tolerance across individuals of a given species using model organism, *Arabidopsis thaliana* (Arabidopsis). I showed that the lack of a trade-off between growth and both drought tolerance traits and climatic drought in Arabidopsis could allow for the occupation of a large geographic and climatic range. I then combined an in-depth study of trait-trait and trait-climate relationships in Arabidopsis with

an expansive study of genotypes spanning the species' natural range to show that Arabidopsis can adapt to stress through both stress tolerance and avoidance, leading to unexpected trait relationships, and creating the potential to evolve under climate change. Adaptation to drought is influenced by many traits, including leaf venation architecture, which supplies water to the leaves allowing for photosynthesis to occur. I showed that major vein length per area (VLA) scaled with leaf size across ontogenetic stages, and provided evidence that while this scaling potentially leads to larger leaves having reduced hydraulic benefit relative to the increased construction and photosynthetic costs of leaf veins, they can offset this cost through vein tapering. Finally, I found that Arabidopsis vein mutants generally have reduced growth rates, opening the door to further research on the connection between vein traits and plant growth with applications to agricultural systems. Overall, this work demonstrates that in order to gain a deeper understanding of the complexities of plant drought tolerance we must examine it at multiple scales.

The dissertation of Leila Rose Fletcher is approved.

Nathan J. B. Kraft

Matteo Pellegrini

Felipe Zapata

Lawren Sack, Committee Chair

University of California, Los Angeles

2021

"Just remember in the winter
far beneath the bitter snows
lies the seed that with the sun's love
in the spring becomes the Rose"
~Amanda McBroom

Dedicated with love to my parents and sibling
for inspiring me creatively,
supporting me unconditionally
and challenging me to keep achieving.
Fletchers do more!

TABLE OF CONTENTS

LIST OF TABLES

LIST OF SUPPLEMENTARY TABLES

CHAPTER 5

CHAPTER 6

LIST OF FIGURES

LIST OF SUPPLEMENTARY FIGURES

ACKNOWLEDGEMENTS

We are all connected in the web of life, nurturing and sustaining each other. My path has been influenced by many, and the completion of this dissertation would not have been possible without their support. Foremost I would like to thank my advisor and mentor, Dr. Lawren Sack, for sharing your knowledge and enthusiasm for plant science and the world. I am deeply appreciative of the many hours you dedicated to meeting with me, discussing ideas, and propelling my career forward. I am so lucky to have had an advisor with such broad and deep knowledge of science who I know will also always support me in my future endeavors. I am also grateful to you for enriching my time as a student with plant pop-culture moments and various lab outings in Los Angeles, including a visit to the Hammer Museum.

To my labmates—I could not have made it through without you! You have all brought so much light to my grad school experience and have all been there for me in different ways. To Camila and Christian—thank you for going through it all with me. I can't express enough how lucky I have been to have had you two by my side from day one. To Christian—thank you for letting me feel comfortable to be my goofy self and for being my deskmate! Thank you also for all the adventures with boxes and bubble wrap, *Arctostaphylos*, and for introducing me to Aunty Bev. To Camila—thank you for giving me hugs when I needed them, cooking amazing dinners and desserts and listening to me when I needed a friend. You'll always be the Mimu in my heart. To Grace, Christine, Megan and Marissa C.—you are stars and I aspire to be like you! To Grace—thank you for teaching me all the lab techniques and for bringing life and fun to the lab; it hasn't been the same without you. To Christine—thank you for sharing your beautiful way of interacting with the world and for introducing me to Aix. To Megan—thank you for having infinite wisdom in all things, and for being a great bunny-mom. To Marissa C.—thank you for

being a ray of sunshine. To Alec—thank you for our days taking the dogs to the park and for the talks about life. To Marvin—thank you for the interesting video suggestions during our late-night lab days, for starting the Crossworders, and for coding all the things. To Marissa O.—thank you for being a confidant, always listening to and supporting me, and for showing me how to do lovely interior decorating. To Nishia—thank you for sharing your enthusiasm for vegan cooking and for the style inspirations. To Jess—thank you for helping me get things done in a crunch and for giving me excellent life advice. To Ruihua—thank you for pushing me to go to the gym and for being a wonderful friend. I miss you! To Joseph—thank you for carrying on the *Ceanothus* tradition and I can't wait to work together again soon!

My friends and the other members of my cohort also provided support in so many ways and I am grateful to them all. I especially want to thank Gaurav "The Big G" for getting me through first-year and having endless patience in explaining things, Zack for Thursday trivia and making me fall in love with California, and Scott for living with me and helping me with many random tasks.

I had wonderful mentors before arriving at UCLA. I would not have entered the world of botany if not for Professor Hilary Callahan—thank you for taking me under your wing and introducing me to research. I am so appreciative of your guidance and for you setting the course of my career through the unPAK project. I also would like to thank Professor Jon Snow for supporting me and offering advice even after all these years, and Drs. Courntey Murren and Matt Rutter, and Clare Kohler for welcoming me to your labs and projects.

I am grateful to my many collaborators and to my committee members, Nathan Kraft, Matteo Pellegrini and Felipe Zapata for your guidance, feedback and support, and for setting the standard of scientific excellence. Much of my scientific work has been done collaboratively with

people at the Centre National de la Recherche Scientifique in Montpellier, France, including Cyrille Violle, Francois Vasseur, Kevin Sartori and Lauren Gillespie. I had a wonderful experience visiting and working in your lab. Kevin—I am grateful for our friendship and adventures at home and abroad! I am also thankful to the CIRTL Community at UCLA for helping me grow as a person and teacher, and to Jocelyn Yamadera and Tessa Villaseñor for finding answers to my questions about all the practical aspects of grad school.

To my incredible family, Jim, Rebecca, Florence and Sam Fletcher—you have all inspired me in so many ways throughout my life. I am very appreciative to have been able to spend so much time together, even more so during the pandemic year. Dad, you have always been my idol for creativity and you make me believe I can follow my dreams. You bring joy and light to our home. Mom, you are the rock of our family and you instilled in me such a great appreciation for the natural world. Thank you for your unconditional love. Florence, I have always admired your courage and fearlessness in being exactly who you are no matter the adversity. Your strength inspires me every day. Grandpa Sam—thank you for your inspirational stories and for your support of my career. I love you all so much.

Finally, to my fur-fin-and-photosynthetic-family of the past six years including Trixie, Lily, Biff, Simba, William Catner, Tommy, Kahotep, other fishy friends and house plants—I know you will never read this but I hope I can and have expressed my gratitude without words. You have been my emotional supports and I wouldn't want to imagine a life without you. I am fortunate to be connected to everyone acknowledged here, and so many more.

Coauthored work: **Chapter 2** is from Fletcher, L. R., H. Cui, H. Callahan, C. Scoffoni, G. P. John, M. K. Bartlett, D. O. Burge, and L. Sack. (*2018*). Evolution of leaf structure and drought

tolerance in species of Californian *Ceanothus*. *American Journal of Botany* 105, 1–16. doi:10.1002/ajb2.1164. H. Cui, C. Scoffoni, G.P. John and M. K. Bartlett contributed to data collection, C. Callahan mentored the project and suggested analyses, D. O. Burge contributed to analyses, L. Sack mentored all stages of the project. All co-authors provided feedback on the manuscript. **Chapter 3** is from Fletcher, L. R., C. Scoffoni, C. Farrell, T. N. Buckley, M. Pellegrini, and L. Sack. (*in prep*). Variation in relative growth and adaptation to aridity across *Arabidopsis* ecotypes: does lack of a trade-off contribute to a wide species range? C. Scoffoni contributed to data collection, C. Farrell and T. N. Buckley contributed to analyses, M. Pellegrini and L. Sack mentored the project. **Chapter 4** is from Fletcher, L. R., C. Scoffoni, C. D. Medeiros, K. Sartori, F. Vasseur, C. Violle, and L. Sack. (*in prep*). Breaking the law: mixed climate adaptation strategies results in contrary trait-climate relationships across *Arabidopsis* ecotypes. C. Scoffoni, C. D. Medeiros, K. Sartori and F. Vasseur contributed to data collection, K. Sartori also planned and set up one of the experiments, C. Violle and L. Sack mentored all stages of the project. **Chapter 5** is from Fletcher, L. R., K. Sartori, F. Vasseur, C. D. Medeiros, C. Farrell, M. Pellegrini, C. Violle, and L. Sack. (*in prep*). Scaling of venation architecture within leaves of diverse ecotypes of *Arabidopsis thaliana*. K. Sartori, F. Vasseur and C. Violle planned the experiment and collected samples, C. D. Medeiros contributed to data collection, C. Farrell contributed to analyses, C. Violle, M. Pellegrini and L. Sack mentored the project. **Chapter 6** is from Fletcher, L. R., J. Song, C. Scoffoni, S. Fitz-Gibbon, C. Farrell, C. D. Medeiros, M. Pellegrini, and L. Sack (*in prep*). Variation in growth and venation architecture across *Arabidopsis* leaf vein mutants. J. Song and C. D. Medeiros contributed to data collection, S. Fitz-Gibbon, C. Farrell and M. Pellegrini contributed to analyses, M. Pellegrini and L. Sack mentored the project.

Funding: This work was generously supported by the Vavra Fellowship and research grants, the UCLA Edwin W. Pauley Fellowship, the UCLA Dissertation Year Fellowship, grants from the Barnard College Biology Department and the UCLA Department of Ecology and Evolutionary Biology, the National Science Foundation (microMORPH Research Coordination Network Undergraduate Training Grant to L. Fletcher, and grants IOS-#1457279, 1557906 and1951244 to L. Sack and M. Pellegrini) and the European Research Council (ERC; 'CONSTRAINTS': grant ERC-StG-2014-639706- CONSTRAINTS to C. Violle).

VITA

PROFESSIONAL PREPARATION

2015 B. A. in Art History (Visual Arts) and Biology (Barnard College, Columbia University)

PUBLICATIONS

Published work

Henry C, John GP, Pan R, Bartlett MK, **Fletcher LR,** Scoffoni C, Sack L. 2019. A stomatal safety-efficiency trade-off constrains responses to leaf dehydration. *Nature Communications* 10, 3398.

Fletcher LR, Cui H, Callahan H, Scoffoni C, John G, Bartlett M, Burge D, Sack L. 2018. Evolution of leaf structure and drought tolerance in species of Californian *Ceanothus*. *American Journal of Botany* 105, 1672–1687. (Selected as a highlighted article: https://bsapubs.onlinelibrary.wiley.com/doi/pdf/10.1002/ajb2.1177)

Scoffoni C, Albuquerque C, Cochard H, Buckley TN, **Fletcher LR**, Caringella MA, Bartlett M, Brodersen CR, Jansen S, McElrone AJ, Sack L. 2018. The causes of leaf hydraulic vulnerability and its influence on gas exchange in *Arabidopsis thaliana*. *Plant Physiology* 178, 1584-1601.

Paper in review

Kevin Sartori, Violle C, Vile D, Vasseur F, de Villemereuil P, Bresson J, Gillsepie L, **Fletcher LR**, Sack L, Kazakou E. (*in review*). Does leaf nitrogen resorption dynamics reflect adaptation to the slow-fast continuum? A test across ecotypes of *Arabidopsis thaliana. Functional Ecology*.

SYNERGISTIC ACIVITIES

- Scholar at the Center for the Integration of Research, Teaching and Learning (CIRTL; 2019-present)
- Teaching Assistant Consultant for UCLA's Department of Ecology and Evolutionary Biology (EEB) and for the Life Sciences Division (2019-2020)
- Conference presentations at the Ecological Society of America (2018, 2020), the CIRTL@UCLA Teaching and Research Event (2020), UCLA's EEB/MCDB Plant Seminar Series (2019), UCLA's EEB Department Symposium (2019), the American Geophysical Union (2019) and the Evolution Conference (2016).
- Volunteer docent at the Mildred E. Mathias Botanical Garden at UCLA (2015-2020), volunteer for various outreach programs at UCLA including the Diversity Project REU (2016), UCLA's AWiSE (Advancing Women in Science and Engineering, 2016), EEB Department recruitment (2018) and orientation events (2017, 2018),
- Coordinator of the EEB department first year trip (2016) and Cohort Ambassdaor (2020-present)
- Mentor of 22 undergraduates from diverse backgrounds (2016-2021)
- Reviewer for *Physiologia Plantarum* (2019)
- Participant in the Jepson Herbarium Workshop Program on *Arctostaphylos* (2016)
- Member of the Ecological Society of America (2016-present) and the Botanical Society of America (2015-present)

CHAPTER 1

PREMISE OF THE DISSERTATION

For evolution by natural selection to occur, there must be variation across ecotypes or species in the genome upon which selection can act, and there must be functional or phenotypic differences that scale up to cause fitness differences, resulting in differential survival in given environmental conditions. Drought is one of the major environmental stresses that plants face, and is expected to become more severe for plants globally (Sheffield & Wood 2008). By studying the mechanisms and genetic bases for drought tolerance, we can understand what leads to species' success in different habitats. The goal of my dissertation research is to better understand the basis of the great diversity in plants, and how that is generated and maintained by investigating species' drought tolerance mechanisms, genetic backgrounds, and how plants are adapted for diverse climates through their traits.

Functional traits have important influences on plant growth, survival and reproduction, which can scale up to influence species distributions under climate change (Medeiros *et al.* 2019). Studies across diverse species have shown that certain traits are key in mediating plant response to drought and plant survival in harsh environmental conditions (Hacke & Sperry 2001; Dunbar-Co *et al.* 2009; Sack & Scoffoni 2013; Pivovaroff *et al.* 2014). However, trait relationships to each other, climate and ancestry are not always clear and can vary across scales (Sack *et al.* 2013). In fact, studying trait-trait and trait-climate relationshsips across closely-related species or across individuals within a single species has the benefit of fewer confouding factors and greater signal to resolve genetic linkages. Some work has been dedicated to studying trait-climate relationships at a more narrow sampling scheme, but many of these studies do not

focus on drought-related traits, and only sometimes incorporate phylogenetic methods. Several studies have focused on the evolution of physiological traits (Edwards 2006; Dunbar-Co *et al.* 2009; Brodribb *et al.* 2013; Jordan *et al.* 2013; Brodribb *et al.* 2014; Larter *et al.* 2017), but none analyze the most direct measures of drought tolerance, such as the osmotic potential at turgor loss point (π_{TLP}; leaf wilting point) and its main biophysical determinant, the osmotic potential at full turgor (π_o; Bartlett *et al.* 2012). In particular, little work has tested how these leaf drought tolerance traits within a given lineage or species have diversified across climatic gradients, and such tests are necessary to indicate whether micro-scale evolution of drought tolerance within a lineage or species mirrors comparative trends found across diverse species.

My dissertation research takes several key steps toward determining the genetic and geographical basis of drought tolerance both within and across species. In Chapter 2 I explore the evolution of drought tolerance within a lineage through a detailed study of anatomy, structure, and drought tolerance of 10 *Ceanothus* (Rhamnaceae) species. This work establishes that leaf traits related to drought tolerance, such as the π_{TLP}, can evolve across an aridity gradient even when looking across closely-related species. This study highlights the utility of the π_{TLP} for drought tolerance, and emphasizes that to find a fundamental understanding of the bases for plant drought tolerance, we must examine it at many scales. In Chapter 3 I extend the findings of work across biomes, diverse and closely related species to show that the π_o can adapt to climate across naturally occurring genotypes (ecotypes) of model organism, *Arabidopsis thaliana* (Arabidopsis; Brassicaceae). This work also shows how decoupling of growth from drought and cold tolerance allows for many successful trait combinations which could confer species' ability to occupy a large climatic range. My work in Chapter 4 uses a combination of two datasets, one on a group of 12 diverse Arabidopsis ecotypes grown in greenhouse at UCLA for which I examined detailed

physiological traits, and another on a group of 152 ecotypes grown in greenhouse in France and measured for π_o and other leaf traits, to demonstrate the complexity of plant drought adaptation at multiple scales. This work clarifies how suites of traits can allow plants to adapt to climatic stress through avoidance and tolerance, and shows that the π_o and other key mechanistic traits can have unexpected relationships with climate if they are confounded with rapid growth.

Leaf veins include both xylem and phloem that are essential for water and sugar transport, and thus sustaining the growth of the whole plant. This leaf vein system also accounts for much of the hydraulic resistance in plants (Sack & Holbrook 2006), thus leaves must develop a cost-effective strategy for building veins. In Chapter 5 I use a vein scaling approach to show how large leaves can still have cost effective vein systems through vein tapering, and I demonstrate the importance of considering vein scaling trends at different ontogenetic stages. Finally, in Chapter 6 I use Arabidopsis mutants to open the door for future research to examine the relationship of leaf vein traits and plant growth, and to uncover genes related to leaf venation, with applications in many fields including crop science (Liu 2010; Chew & Halliday 2011; Cobb *et al.* 2013). Overall, my thesis work helps determine the roles of environment, genes, development and ancestry in shaping drought tolerance and thus species distributions and ecosystem organization.

REFERENCES

Bartlett, M.K., Scoffoni, C. & Sack, L. (2012). The determinants of leaf turgor loss point and prediction of drought tolerance of species and biomes: a global meta-analysis. *Ecol. Lett.*, 15, 393-405.

Brodribb, T.J., Jordan, G.J. & Carpenter, R.J. (2013). Unified changes in cell size permit coordinated leaf evolution. *New Phytologist*, 199, 559-570.

Brodribb, T.J., McAdam, S.A.M., Jordan, G.J. & Martins, S.C.V. (2014). Conifer species adapt to low-rainfall climates by following one of two divergent pathways. *Proc. Natl. Acad. Sci. U. S. A.*, 111, 14489-14493.

Chew, Y.H. & Halliday, K.J. (2011). A stress-free walk from *Arabidopsis* to crops. *Current Opinion in Biotechnology*, 22, 281-286.

Cobb, J.N., DeClerck, G., Greenberg, A., Clark, R. & McCouch, S. (2013). Next-generation phenotyping: requirements and strategies for enhancing our understanding of genotype-phenotype relationships and its relevance to crop improvement. *Theoretical and Applied Genetics*, 126, 867-887.

Dunbar-Co, S., Sporck, M.J. & Sack, L. (2009). Leaf trait diversification and design in seven rare taxa of the Hawaiian *Plantago* radiation. *Int. J. Plant Sci.*, 170, 61-75.

Edwards, E.J. (2006). Correlated evolution of stem and leaf hydraulic traits in *Pereskia* (Cactaceae). *New Phytologist*, 172, 479-489.

Hacke, U.G. & Sperry, J.S. (2001). Functional and ecological xylem anatomy. *Perspect. Plant Ecol. Evol. Syst.*, 4, 97-115.

Jordan, G.J., Brodribb, T.J., Blackman, C.J. & Weston, P.H. (2013). Climate drives vein anatomy in Proteaceae. *Am. J. Bot.*, 100, 1483-1493.

Larter, M., Pfautsch, S., Domec, J.C., Trueba, S., Nagalingum, N. & Delzon, S. (2017). Aridity drove the evolution of extreme embolism resistance and the radiation of conifer genus *Callitris*. *New Phytologist*, 215, 97-112.

Liu, C.M. (2010). *Arabidopsis as Model for Developmental Regulation and Crop Improvement*. Springer-Verlag Berlin, Berlin.

Medeiros, C.D., Scoffoni, C., John, G.P., Bartlett, M.K., Inman-Narahari, F., Ostertag, R. *et al.* (2019). An extensive suite of functional traits distinguishes Hawaiian wet and dry forests and enables prediction of species vital rates. *Funct. Ecol.*, 33, 712-734.

Pivovaroff, A., Sharifi, R., Scoffoni, C., Sack, L. & Rundel, P. (2014). Making the best of the worst of times: traits underlying combined shade and drought tolerance of *Ruscus aculeatus* and *Ruscus microglossum* (Asparagaceae). *Functional Plant Biology*, 41, 11-24.

Sack, L. & Holbrook, N.M. (2006). Leaf hydraulics. In: *Annual Review of Plant Biology*, pp. 361-381.

Sack, L. & Scoffoni, C. (2013). Leaf venation: structure, function, development, evolution, ecology and applications in the past, present and future. *New Phytologist*, 198, 983-1000.

Sack, L., Scoffoni, C., John, G.P., Poorter, H., Mason, C.M., Mendez-Alonzo, R. *et al.* (2013). How do leaf veins influence the worldwide leaf economic spectrum? Review and synthesis. *Journal of Experimental Botany*, 64, 4053-4080.

Sheffield, J. & Wood, E.F. (2008). Global trends and variability in soil moisture and drought characteristics, 1950-2000, from observation-driven simulations of the terrestrial hydrologic cycle. *J. Clim.*, 21, 432-458.

CHAPTER 2

EVOLUTION OF LEAF STRUCTURE AND DROUGHT TOLERANCE IN SPECIES OF CALIFORNIAN *CEANOTHUS*

ABSTRACT

Premise of the study: Studies across diverse species have established theory for the contribution of leaf traits to plant drought tolerance. For example, species of more arid climates tend to have smaller leaves of higher vein density, higher leaf mass per area, and more negative osmotic potential at turgor loss point (π_{TLP}). However, few studies have tested these associations for species within a given lineage that have diversified across an aridity gradient.

Methods: We analyzed the anatomy and physiology of 10 *Ceanothus* (Rhamnaceae) species grown in a common garden for variation between and within "wet" and "dry" subgenera (*Ceanothus* and *Cerastes* respectively), and analyzed a database for 35 species for leaf size and leaf mass per area (LMA). We used a phylogenetic generalized least squares approach to test hypothesized relationships among traits, and of traits with climatic aridity in the native range. We also tested for allometric relationships among anatomical traits.

Key results: Leaf form, anatomy and drought tolerance varied strongly among species within and between subgenera. *Cerastes* species had specialized anatomy including hypodermis and encrypted stomata that may confer superior water storage and retention. The osmotic potentials at turgor loss point (π_{TLP}) and full turgor (π_o) showed evolutionary correlations with the aridity index (AI) and precipitation of the 10 species' native distributions, and LMA with potential evapo-transpiration for the 35 species in the larger database. We found an allometric correlation

between upper and lower epidermal cell wall thicknesses, but other anatomical traits diversified independently.

Conclusions: Leaf traits and drought tolerance evolved within and across lineages of *Ceanothus* consistently with climatic distributions. The π_{TLP} has signal to indicate the evolution of drought tolerance within small clades.

Key words: California lilac; chaparral; leaf anatomy; leaf traits; leaf venation; Mediterranean climate; phylogenetic analysis; Rhamnaceae; stomatal crypts; trait evolution

INTRODUCTION

Plants in dry environments have adapted a wide variety of leaf-level mechanisms to tolerate drought stress (Chaves et al., 2002; Sofo et al., 2008; Chaves et al., 2009; Brodribb et al., 2014). The study of these mechanisms and their evolution gains in urgency because in many ecosystems plant drought tolerance is of major and growing importance for survival (Sheffield and Wood, 2008). California is projected to become drier and to increase by several degrees in mean annual temperature by the end of the twenty-first century, affecting seasonal water availability, and contributing to summer drought (Cook et al., 2004; Cayan et al., 2008; AghaKouchak et al., 2014; Diffenbaugh et al., 2015). Understanding drought tolerance and its evolution is thus increasingly critical to predict the influence of ongoing climate change on species and ecosystems (Cook et al., 2004).

There are two comparative approaches to establishing the traits that help plants tolerate harsh conditions. One is to analyze traits across a large number of taxa (Reich et al., 1997; Reich et al., 1999; Niinemets, 2001). Thus, studies conducted across diverse species sets have shown that variation in drought tolerance relates to leaf form, including traits such as leaf size, leaf mass per area (LMA); xylem and mesophyll anatomy; chemical composition; leaf and stem hydraulic conductance; root traits; and osmotic potential at turgor loss point (π_{TLP}) (Cooper, 1922; Givnish, 1987; Niinemets, 1999; Hacke and Sperry, 2001; Jacobsen et al., 2007; Dunbar-Co et al., 2009; Poorter et al., 2009; Blackman et al., 2010; Bartlett et al., 2012b; Sack and Scoffoni, 2013; Scoffoni et al., 2014; Pivovaroff et al., 2014; Marechaux et al., 2015; Ivanova et al., 2018). Some of these linkages are clearly mechanistic: smaller leaves have a thinner boundary layer, which facilitates cooling under hot and dry climates (Ackerly et al., 2002; Scoffoni et al., 2011; Wright et al., 2017) and a higher LMA can extend leaf lifespan and improve leaf economic return under

low resource conditions (Poorter et al., 2009; Bartlett et al., 2012b; Marechaux et al., 2015). Smaller xylem conduits can be less prone to embolism during drought (Hacke and Sperry, 2001), and root embolism and refilling may protect against loss of hydraulic conductance in other organs during severe drought (Alder et al., 1996). A more negative π_{TLP} can enable maintenance of turgor and stomatal opening with lower soil water availability (Bartlett et al., 2012b; Bartlett et al., 2014). However, such trait correlations discovered across diverse species do not necessarily reflect small-scale evolutionary patterns (Edwards, 2006; Edwards et al., 2014; Mason and Donovan, 2015; Blonder et al., 2016; McKown et al., 2016; Scoffoni et al., 2016). An alternative approach to determining the associations of traits with drought tolerance is to sample within an appropriate clade that can be analyzed using a well-documented phylogeny. Comparing one or more traits within a particular plant clade can establish their ancestral basis and their relationship to past and current environmental factors including temperature, precipitation, humidity, elevation, and drought stress (Edwards, 2006; Dunbar-Co et al., 2009; Poorter et al., 2009; Mason and Donovan, 2015). Surprisingly few studies have focused on the evolution of drought tolerance traits across species within given lineages. In an example from the Rhamnaceae, species that resprout after fire were more drought sensitive than those that re-establish from seedlings (Davis et al., 1999; Pratt et al., 2007), although in short periods of high-intensity drought, deep-rooted sprouters had an advantage (Venturas et al., 2016). Within the genus *Callitris*, species adapted to greater aridity had narrower wood xylem conduits and greater embolism resistance (Larter et al., 2017). Within the genus *Eucalyptus*, species adapted to greater aridity had narrower vessels of higher frequency, and higher sapwood density, although phylogenetic analyses were not performed (Pfautsch et al., 2016).

Ceanothus (the "California lilac") is a lineage of woody shrubs in the family Rhamnaceae that is diverse in form and ecology, and includes several of the most drought tolerant species of the California chaparral (Jacobsen et al., 2008). Much of the *Ceanothus* diversification took place across steep environmental gradients within California (Stebbins and Major, 1965; Ackerly, 2009; Burge et al., 2011). The modern *Ceanothus* lineage consists of two major subclades: *Ceanothus* and *Cerastes*, with 29 and 24 species respectively which diverged ~12.9 mya, with each subclade further diversifying from ca. 5.3-6.3 mya (Ackerly et al., 2006; Burge et al., 2011). The origin of the California Mediterranean (MT) climate is assumed to have occurred around 5mya, indicating that the ancestors of modern genus *Ceanothus* species may have been native to moister forest, yet pre-adapted to drought with small leaf size and high LMA (Ackerly, 2004; Burge et al., 2011), potentially being adapted to xeric habitats such as shallow soil lenses, south facing slopes, and post-fire open and exposed sites (Keeley et al., 2012). However, some have estimated the origin of the MT climate to have arisen earlier, at 12-15 mya (Keeley et al., 2012; Baldwin, 2014), and in that case the small leaves found in the genus as a whole may have evolved in this novel seasonally dry environment.

The aim of this study was to investigate the evolution of traits related to drought tolerance in *Ceanothus*, which has excellent potential to be developed as a model lineage for the study of traits across a strong aridity gradient (Burge et al., 2011). We tested the overarching hypothesis that leaf anatomical, structural, and hydraulic traits associated with drought tolerance would align with habitat aridity within the genus, consistent with trends previously established across diverse species. Notably, a previous study taking an evolutionary approach in *Ceanothus* reported a weak negative correlation of LMA with precipitation that disappeared after a phylogenetic independent contrast analysis, and a correlation of LMA and temperature within the

Ceanothus subgenus (Ackerly et al., 2006). We tested specific hypotheses for the variation of *Ceanothus* leaf anatomical, structural and drought tolerance traits in relation to aridity across the species' distributions (Table 2.1) based on relationships shown in diverse species sets (summarized in Table 2.2). We focused on ten species representing both subgenera (six in *Ceanothus* and four in *Cerastes*) and analyzed the Jepson Herbarium Ecological Flora Pilot database (http://ucjeps.berkeley.edu/EFT.html) for LMA and leaf size data available for a wider set of 35 species. We further hypothesized that traits would differ between the two subgenera reflecting the well-recognized greater drought tolerance of *Cerastes* (Table 2.2). We expected species of more arid climates to have smaller leaves, both to provide drought tolerance via higher major vein density (Sack and Scoffoni, 2013) and also to contribute to leaf cooling (Givnish, 1987; Wright et al., 2017). We also hypothesized shorter interveinal distances (IVDs) to provide more pathways for water transport despite potential embolism, damage or collapse of tissues (Sack and Scoffoni, 2013). We expected that LMA and leaf thickness and density would be positively associated with aridity to reduce the surface area to volume ratio of the leaf to better retain water, to provide greater mechanical strength, and increase leaf lifespan (Niinemets, 2001; Wright et al., 2004). Similarly, we expected the shrinkage of leaf thickness and area to be greater for species native to moister climates (Scoffoni et al., 2014). We hypothesized that saturated water content (SWC) would be lower and leaf dry matter content (LDMC) would be higher for species of more arid climates to increase leaf mechanical protection and lifespan (Diaz et al., 2016). We expected species native to drier climates to have higher values for both petiole to leaf area ratio, a metric of hydraulic supply to the leaf (Sack et al., 2003), and the petiole area to leaf dry mass ratio, reflecting stronger investment in mechanical support (Royer et al., 2007). We expected osmotic potential at full and zero turgor to be negatively related to native climate

aridity (Bartlett et al., 2012b). We also expected to find relationships between greater tissue thicknesses, smaller cells and thicker cell walls with greater aridity (Niinemets, 2001).

Recent work has shown that leaf anatomical traits may be constrained by allometries within and across tissues that link the sizes of cells, the thickness of cell walls and the thickness overall of leaves. Thicker leaves tend to have larger cells (Brodribb et al., 2013; John et al., 2013), yet, in apparent contradiction, drought tolerant species have been expected to have thicker leaves (Niinemets, 2001) but with smaller cells (Cutler et al., 1977). Thus we tested for allometries and departures from allometries among cell dimensions, cell wall thicknesses, tissue thicknesses and leaf thickness across *Ceanothus* species.

METHODS

***Study species, site, and sampling*—**All members of the *Ceanothus* genus are woody shrubs and the majority of species are evergreen (Kubitzki, 2004), including six of the species in this study (Table 2.1). We focused on 10 *Ceanothus* species that are diverse in form and representative of both *Ceanothus* subgenera (Table 2.1), grown in a common garden at the Rancho Santa Ana Botanical Garden in Claremont, California (34.110738, -117.713913; 507 mm precipitation per year; BioClim). The common garden approach was employed to ensure that the observed trait differences are due to heritable interspecies variation, and not to confounding environmental variables that may have elicited phenotypically plastic trait variation (Cordell et al., 1998; Dunbar-Co et al., 2009; Givnish and Montgomery, 2014; Mason and Donovan, 2015).

Sun exposed shoots with fully expanded leaves were collected from each of three individual mature plants for each of the study species, and brought to the laboratory in plastic bags with wet paper to maintain hydration, and rehydrated overnight covered with plastic.

***Measurements of leaf size and structure*—**Measurements of leaf size and structure were made for three leaves per individual for the three individuals per species (i.e., a total of nine leaves per species). Measurements were taken for leaf mass, area (using ImageJ version 1.42q; National Institutes of Health, Bethesda, Maryland, USA), leaf thickness (average of thicknesses at top, middle, and bottom of leaf; digital calipers, Fowler, Chicago, IL, USA), petiole diameter (average of top, middle, and bottom measurements from two different diameters per leaf), and petiole length for fully hydrated leaves, and after oven drying at least three days at >70^{o}C (XS205; Mettler, Toledo, OH, USA) at which time the dry mass of lamina, midrib, and petiole were also determined (Dunbar-Co et al., 2009). Leaf mass per area was calculated as leaf dry mass divided by fully hydrated leaf area (Ackerly et al., 2006). Leaf area shrinkage (LAS) was calculated as:

$$\text{LAS} = 1 - (\textit{dry leaf area} / \textit{fully hydrated leaf area}) \quad \text{eqn 1}$$

Similarly, leaf thickness shrinkage (LTS) was calculated as:

$$\text{LTS} = 1 - (\textit{dry leaf thickness} / \textit{fully hydrated leaf thickness}) \quad \text{eqn 2}$$

One species, *C. impressus*, had negligible shrinkage (a tiny negative mean value for thickness shrinkage, non-significant in a paired t-test), which was therefore converted to zero.

Saturated water content (SWC) was calculated as:

$$\text{SWC} = (\textit{Fully hydrated leaf mass} - \textit{dry leaf mass})/\textit{dry leaf mass} \quad \text{eqn 3}$$

Leaf dry matter content (LDMC) was calculated as:

$$LDMC = \textit{Dry leaf mass}\ /\textit{fully hydrated leaf mass} \quad \text{eqn 4}$$

The small leaf size of the majority of *Ceanothus* species renders the determination of pressure-volume curves difficult. Instead, we determined the osmotic potential at turgor loss point (π_{TLP}), a predictor of species' abilities to tolerate drought, using an osmometer (VAPRO

5520 vapor pressure osmometer, Wescor, Logan, UT; Bartlett et al., 2012a). Osmolality was determined for fresh fully hydrated leaves and used to calculate turgor loss point with a calibration curve previously established for 30 diverse species (Bartlett et al., 2012a).

***Preservation of anatomical samples*—**One leaf was sampled from each of three individuals per species for cross sectioning and preserved in Formalin Acetic Acid-Alcohol solution (FAA; 37% formaldehyde, glacial acidic acid, 95% ethanol in deionized water). A 1 × 0.5 cm subsample including the midrib was cut from the center of each leaf, and for very small leaves, the entire leaf was used. The samples were placed in capsules gradually filled with mixtures of ethanol and increasing concentrations of L.R. White acrylic resin (London Resin Co., UK) under vacuum over the period of one week (John et al., 2013). The capsules were then heated overnight in a drying oven at 55°C. One-micrometer thick transverse cross sections were obtained using a microtome (Leica Ultracut E, Reichert-Jung, California, USA) with glass knives (cut using an LKB 7800 KnifeMaker; LKB Produkter, Bromma, Sweden), and were stained with 0.01% toluidine blue in 1% sodium borate (John et al., 2013).

***Measurements of anatomical samples*—**Images were taken under a light microscope (Leica Lietz DMRB; Leica Microsystems) using 5× to 40× objectives and captured with SPOT advanced imaging software (SPOT Imaging Solutions; Diagnostic Instruments, Inc.; Sterling Heights, Michigan, USA). Measurements were taken using ImageJ (software version 1.49k; National Institutes of Health, Bethesda, Maryland, USA) including interveinal distances (IVD), tissue thickness (palisade, mesophyll, upper and lower epidermises, upper and lower cuticles,

and hypodermis for *Cerastes* species), and cell cross-sectional areas for the same tissues (Pasquet-Kok et al., 2010).

For leaves of species in the *Ceanothus* subgenus, measurements of leaf and tissue thicknesses were averaged for the left, middle, and right thirds of each image. For leaves of species in the *Cerastes* subgenus, due to the variable thickness caused by presence of stomatal crypts, the area of each tissue in the cross-section was measured, divided by the cross-sectional area of the whole leaf, and then multiplied by whole leaf thickness to obtain individual tissue thicknesses. For the cuticles, epidermises, hypodermises, and palisade and spongy mesophyll cells, three cells per tissue for each leaf cross-section were averaged (for a large, small, and medium cell in each image).

Collection of species range and climate information—Species range data were downloaded from the Global Biodiversity Information Facility (GBIF, 2012, https://ww.gbif.org, Table S2.1). Individual points were mapped for each species using ArcMap (ArcGIS version 10.2.2 for Desktop, Esri Inc.) and erroneous points were removed (including points found in the ocean or at botanical garden locations). Mean annual temperature (MAT) and annual precipitation (MAP) were obtained from WorldClim Global Climate Data (BioClim). These data have a resolution of 1 km^2 and represent values averaged from 1960 to 1990. Climate data for Global Aridity Index (AI, inversely related to climatic aridity) and Global Potential Evapo-transpiration (PET) were obtained from the Consultative Group for International Agriculture Research (CGIAR) Consortium for Spatial Information (CSI) database. Data from the CGIAR are also at 1 km^2 resolution and represent values averaged from 1950-2000. MAT, MAP, AI, and PET data were

extracted at each coordinate for each species using ArcMap, and averaged for each species (Table 2.1).

To visualize species' range distributions, average latitudes and longitudes for all occurrences of *Ceanothus* species (including the ten focal species) were mapped in ArcMap. When an averaged point appeared in the ocean due to individual points being clustered around a bay or curved coastline, the average was moved to the nearest location on land (Fig. 2.1).

***Compilation of available published trait data for Ceanothus*—**Data for leaf blade area and specific leaf area (the inverse of LMA, calculated as leaf area per mass) for an additional 35 *Ceanothus* species were collected from The Jepson Herbarium Ecological Flora Pilot database (http://ucjeps.berkeley.edu/EFT.html; data originally from Ackerly, 2004). Nineteen of these species were in the *Ceanothus* subgenus, and 16 were in the *Cerastes* subgenus. Specific leaf area values were converted to LMA values for comparison with our data.

***Divergence Time Estimation*—**MUSCLE alignments for *Ceanothus* nuclear ribosomal transcribed spacer (ITS), and the third intron from the nuclear gene nitrate reductase (NIA) were obtained from Burge et al. (2011). Alignments were pruned to a single individual from each species, covering 73 of the 78 taxa (including subspecies) of *Ceanothus.*

The rate-calibration method was used to estimate the divergence time of the two *Ceanothus* subgenera based on the known mutation rate of ITS to estimate divergence time, as was done in a previous study (Burge et al., 2011). The model of a relaxed clock with uncorrelated lognormal rate variation was run in BEAUti/BEAST version 1.8.3 (Drummond et al., 2012). The two subgenera were defined as monophyletic based on previous work (Ackerly, 2004; Burge et al.,

2011). Following Burge et al. (2011), the meanRate prior was set from estimates of ITS substitution rate (0.38×10^{-3} to 7.83×10^{-3} substitutions/site/yr) with a mean of 2.15×10^{-3} and Log(Stdev) of 0.84. BEAST uses substitutions per site per year, while Burge et al. (2011) reported the rates in millions of years, so the numbers from their paper were multiplied by one million. 3×10^{7} Markov chain Monte Carlo (MCMC) generations were performed, sampling every 1000 generations. The resulting tree was viewed in FigTree version 1.4.2 (Drummond et al., 2012; Fig. 2.2).

***Statistical and phylogenetic analyses*—**Nested ANOVAs were used to test for differences between the two subgenera and among species within subgenera in the R programming environment (R version 3.4.4). To apply a phylogenetic generalized least-squares (PGLS) approach, the tree was pruned to the ten species for which detailed trait data had been obtained (Fig. 2.2). The *caper* package in R (version 3.4.4) was used to conduct PGLS. PGLS used the constructed tree and pairings of environmental and leaf traits, and enabled calculations of correlations between variables independent of the phylogeny and comparisons between models of Brownian motion, Pagel's lambda, and Ornstein-Uhlenbeck (OU; Felsenstein, 1985; Freckleton et al., 2002; Garland et al., 2005). For π_{TLP}, which is a negative number, the values were multiplied by -1. For leaf thickness shrinkage, because one value was zero, +1 was added to all species values.

Correlations related to each of the following overarching hypotheses were tested, i.e., between each category of traits (structural, drought-tolerance, anatomical) and each climate variable (mean annual temperature, MAT; annual precipitation; aridity index, AI; and potential evapo-transpiration, PET), and among anatomical dimensions, i.e., cell cross-sectional areas, cell

wall thicknesses and leaf thickness. A Benjamini-Hochberg false discovery rate correction was applied to *p*-value of the model of evolution with the lowest AICc score for each hypothesis (Benjamini and Hochberg, 1995). For consistency, this was done even if the AICc scores for two models differed by less than 2. Due to the rigor of this *p*-value correction for multiple testing, the reported *p*-values might appear high, even given strong correlations with high *r*-values.

We also tested whether the significant cell and tissue allometric relationships shown for a more phylogenetically diverse species set (John et al., 2013) were upheld for *Ceanothus* in our study. To analyze allometric relationships, we used standard major axes (SMA; using SMATR; Warton et al., 2006). Standard major axes were used rather than ordinary least squares regression (OLS) to consider both *x* and *y* traits as independent variables with similar measurement error and to best estimate the functional relationship between the variables; OLS regression assumes that the error in one variable (*y*) is much greater than that in the other variable (*x*) and is most useful when the *y* variable is to be predicted from the *x* (Sokal and Rohlf, 1995; Sack et al., 2003; Poorter and Sack, 2012). For each relationship, we fitted a standard major axis to log-transformed data, determining *a* and *b* for $y = ax + b$, or, equivalently, using log-transformed data, $\log y = \log a + b \log x$. We tested whether allometric slopes differed from those reported for diverse species (John et al., 2013)

We performed a phylogenetic principal component analysis (pPCA) in R using the *phytools* package to test for multivariate associations between traits for the ten focal species (Revell, 2002). We applied the pPCA to five key traits from our study: leaf area, LMA, π_{TLP}, upper epidermal cell area, and palisade cell wall thickness. Variables were *z*-transformed ($xi - \bar{x} / sd$) for comparison using the "prcomp" function in the *stats* package. Correlations between traits, PC

axes, and PCA scores were calculated with the *BiodiversityR* package. Correlations between PC scores and climate variables were also calculated.

Notably, our study was not comprehensive as it focused on 10 of the 53 extant *Ceanothus* species. This design, following many previous ecophysiological studies (Garnier et al., 1999; Brodribb and Holbrook, 2003; Sperry et al., 2005; Edwards, 2006; Sack and Frole, 2006; Nardini et al., 2012; John et al., 2013), is rigorous for testing hypothesized trends that would be expected even in a subset of species. While a small sample may be at greater risk of missing significant trends, the species here were specifically sampled to represent both subgenera and thus are expected to encompass a wide range of traits (see John et al., 2013 for detailed discussion of the concerns with studies of small species sets and when the concerns would be misplaced). This group of species enabled testing hypotheses that can be further extended to broader datasets in the future. To further confirm that the species group studied here was representative of the genus as a whole, we tested correlations of leaf size and LMA values from our study with those for the same species in the Jepson Herbarium Ecological Flora Pilot database, described above, and we tested whether the phylogenetic relationships of leaf size and LMA to climate in our study were similar to those found for the 35 species represented in that database. A Benjamini-Hochberg false discovery rate correction was applied to *p*-values of these correlations.

RESULTS

***Variation across Ceanothus species and subgenera in leaf traits and genetics*—**We found pronounced variation in leaf traits across the ten *Ceanothus* species (Table 2.2; Table S2.2, see supplemental data with this article). Almost all traits varied significantly across species, from subtle (< 2-fold difference) to dramatic (i.e., many-fold variation). At the high end of the range

of variation, leaf size was 12-fold different from *C. cuneatus var. fascicularis* at 0.56 cm^2 to *C. incanus* at 6.71 cm^2. LMA varied by more than four-fold across all ten species, from 68.5 g/m^2 for *Ceanothus lemmonii* to 364 g/m^2 for *Ceanothus verrucosus* (Fig. 2.3A). This variation in LMA would have arisen from the 1.5-fold variation across all species in leaf density, and the two-fold difference between subgenera in leaf thickness (Fig. 2.3B). The hydraulic and biomechanical ratios of petiole area to leaf area and petiole area to leaf mass varied over 11-fold and 7.5-fold across species respectively (Fig. 2.3C). Species differed from -1.35 MPa to -2.62 in osmotic potential at full turgor (π_o), and from -1.60 to -2.81 MPa in turgor loss point (π_{TLP}; Fig. 2.3D). Leaf area shrinkage varied across species from 15-83%, and leaf thickness shrinkage varied from no significant shrinkage to 60%. Saturated water content (SWC) and leaf dry matter content (LDMC) varied 2.3- and 1.7-fold, respectively.

Anatomical traits also varied across species subtly or dramatically. Interveinal distance (IVD) varied 2.4-fold (from 151 μm for *C. oliganthus* to 359 μm for *C. megacarpus var. megacarpus;* Fig. 2.3E) as did the thickness of the upper epidermis (2.5-fold) and mesophyll (2.4-fold). Cell cross sectional areas varied across species for every cell type: 9.7-fold for upper epidermal cells, 2.5-fold for palisade mesophyll cells, 2-fold for spongy mesophyll cells, and 1.8-fold for lower epidermal cells. Upper epidermal and spongy mesophyll cell wall thicknesses also varied across species by 3.4- and 5.8-fold, respectively.

The two subgenera varied strongly in their leaf traits and in tissue organization, as did species within the subgenera. Indeed, across structural traits, 43-77% and 50-94% of the variation was between and within subgenera, respectively (nested ANOVA; Table 2.2); in drought tolerance traits, 47-54% and 26-32%; in tissue thicknesses, 52-75% and 61-70%; and for cell dimensions (area and cell wall thicknesses) 35-50% and 32-76%. Strikingly, leaves of

species of the *Cerastes* subgenus had hypodermal tissue and deep invaginations on the abaxial sides containing stomata, neither of which occurred in species of the *Ceanothus* subgenus (Fig. 2.4). The mean LMA and leaf thickness across the four subgenus *Cerastes* species was 2.4-fold and 2.5-fold greater than that for the six subgenus *Ceanothus* species (Fig. 2.3A, B). The ratio of petiole to leaf area was 4-fold higher for the subgenus *Cerastes* species (Fig. 2.3C). The subgenera differed on average in osmotic potential at full turgor and at turgor loss point (π_{TLP}) with *Cerastes* having more negative values than *Ceanothus* subgenus species by 0.40 and 0.48 MPa respectively (Fig. 2.3D). The percent difference in interveinal distance (IVD) between the *Cerastes* and *Ceanothus* subgenus was 46% greater in *Cerastes* (Fig. 2.3E). The upper cuticle was 58% thicker in *Cerastes* than *Ceanothus*, and lower epidermal thickness and lower cuticle thickness were 2.8-fold and 3.5-fold greater than those of *Ceanothus* (Fig. 2.3F). Upper epidermal cell area in *Ceanothus* was 3.5-fold higher than in *Cerastes* (Fig. 2.3G). The percent difference in upper and lower epidermal cell wall thicknesses ranged between 54-58% between subgenera, with *Cerastes* species having thicker cell walls (Fig. 2.3H).

In the phylogenetic principal component analysis (pPCA) applied to five traits (leaf area, LMA, π_{TLP}, upper epidermal cell area, and palisade cell wall thickness), the first two axes of the pPCA explained 82.3% of the trait variation (Fig. 2.5, Table S2.3). Variation in the first PC axis was driven by π_{TLP} and palisade mesophyll cell wall thickness, while variation in PC2 was driven by the leaf area, LMA and upper epidermal cell area.

Association of traits with climate in evolutionary analyses—Of the traits hypothesized to relate to the aridity of species' native ranges, i.e., annual precipitation and aridity index (AI), only the osmotic potential at full turgor (π_o) and turgor loss point (π_{TLP}) showed significant relationships

(Fig. 2.6; Tables S2.4-S2.5). Thus, species with more negative π_o and π_{TLP} were native to sites of greater aridity (r = 0.79; P = 0.007 for both; Fig. 2.6A) and lower mean annual precipitation (r = 0.77; P = 0.009 for both; Fig. 2.6B). Trait correlations with other climate variables were not significant after a multiple test correction. Additionally, PC1 scores correlated with AI, MAT, and annual precipitation (r = 0.85, -0.66, and 0.88; P = 0.002, 0.04, and 0.0008; Table S2.3), and log-transformed values of PC2 scores also correlated with AI and annual precipitation (r = 0.72 and 0.77; P = 0.02 and 0.009; Table S2.3).

***Tests of allometries of tissue and cell dimensions*—**Across species, the thickness of upper and lower epidermal cell walls were tightly correlated (r = 0.88, P = 0.02, Fig. 2.7), with an allometric slope that did not differ from 1 (i.e., isometry). The allometric slope b and intercept a were 0.863 (95% confidence intervals 0.587 to 1.27) and -0.446 (-0.0984 to -0.00917) respectively, statistically similar to those for a relationship previously published for diverse species (John et al., 2013; P = 0.37-0.46). Beyond that one relationship, across species, cell areas and cell wall thicknesses were statistically independent (Fig. 2.8). There were significant relationships between tissue thicknesses, such that thicker leaves had thicker upper and lower cuticles, and lower epidermises (r = 0.92, P = 0.0002; r = 0.91, P = 0.0002, r = 0.90, P = 0.0004). Upper and lower cuticle thickness also were positively related to each other and to lower epidermal thickness (r = 0.94-0.98, $P < 0.0001$; Tables S2.4-S2.5).

***Analyses of database information for the Ceanothus genus*—**The data for the larger set of 35 species of *Ceanothus* for which Ecological Flora Pilot database information was available showed a correlation with our data for both LMA and leaf size (r = 0.79, P = 0.006; r = 0.71, P =

0.02, respectively; Tables S2.6-S2.7). Consistent with our findings for the 10 study species, across the 35 species in the database, the species of subgenus *Cerastes* had a 53% higher LMA than species of subgenus *Ceanothus* (P <0.001; Fig. 2.9A; Tables S2.6-S2.7), but leaf size did not differ significantly between the subgenera (Fig. 2.9B). The larger dataset showed a significant relationship of LMA with the climate variable PET in a phylogenetic least squares regression, which was not observed across the ten focal species (r = 0.61, P = 0.0001; Fig. 2.10, Tables S2.8-S2.9).

DISCUSSION

Variation between and within Ceanothus subgenera in leaf traits—*Ceanothus* species showed a wide range of leaf trait variation, with stark contrasts between the two subgenera in several morphological traits. This was consistent with the finding of strong genetic divergence between subgenera. We found greater expression of multiple traits associated with aridity in the *Cerastes* subclade possibly contributing to the spread of this subgenus as the MT climate strengthened within the California Floristic Province over several million years (Ackerly, 2004; Burge et al., 2011). We note that leaf traits can contribute strongly to the overall plant life history (Givnish, 1987; Poorter et al., 2009) but the traits of other organs (e.g., stem hydraulic anatomy) and the whole-plant (e.g. sprouting versus non-sprouting life history, rooting depth, growth form, and biotic interactions) would also show adaptation to benefit growth and/or survival during drought and/or other environmental stresses (Keeley and Zedler, 1978; Davis et al., 1999; Pratt et al., 2007; Pfautsch et al., 2016; Venturas et al., 2016).

For the majority of measured leaf traits most of the overall variation arose among species within the subgenera. *Cerastes* species had thicker leaves of higher LMA and greater interveinal

distance, all features related to their unique anatomy, organized around stomatal crypts. *Cerastes* leaves also had a distinctive thick hypodermis under the upper epidermis, comprised of relatively large, closely packed cells with very little airspace, in between the veins. These cells stain darkly and may contain secondary compounds, whether for oil storage, to deter herbivores, and/or to increase osmotic concentration and thus turgor in dehydrating soil (Evert, 2006; Retamales and Scharaschkin, 2014). A study on mangroves suggested that the hypodermis may function in osmotic regulation by storing salts, although the applicability of this mechanism to other systems is unclear (Balsamo and Thomson, 1995). Previous work has also indicated that hypodermal tissue may provide greater water storage capacity and/or water transport pathways (Wylie, 1954). The presence of a hypodermis tends to be more common in species of xeric habitats, which supports the idea that hypodermal tissues may play a role in water retention (Carlquist, 1994).

Leaves of the four *Cerastes* species examined have mesophyll cells arranged around deep, conical crypts, with vascular tissue found only between crypts. Stomatal crypts are generally an adaptation for living in arid climates (Gibson, 1983), along with revolute margins and individually enclosed stomata (Hill, 1998; Jordan et al., 2008). In a study of *Banksia*, crypt depth was proposed as a useful trait diagnostic of past arid climates in fossils (Carpenter et al., 2014), but a more complete fossil record would be needed to draw similar conclusions for *Ceanothus*. One proposed function of crypts is to create humid pockets that allow stomata to remain open longer during soil and/or atmospheric drought, though the ability of stomatal crypts to importantly minimize transpirational water loss has also been questioned (Gibson, 1983; Evert, 2006; Roth-Nebelsick et al., 2009).

In addition, *Cerastes* species had thicker lower epidermal tissue, which would also act to prevent water loss. Given that epidermal cells were also smaller in *Cerastes* leaves, the greater

tissue thickness was mostly due to multiple epidermal layers, which is a rare trait in the Rhamnaceae family (Kubitzki, 2004). *Cerastes* species also have thicker upper and lower cuticles. All these properties are consistent with adaptation to reduce nonstomatal water loss, and potentially with inner epidermal water storage (Evert, 2006). Such characteristics contributing to drought tolerance and longer leaf lifetimes would be expected to repay the greater construction cost of *Cerastes* leaves, evident in their higher LMA. Greater investment in long-lasting organs was reported previously for *Cerastes* stems, which are sturdier than those of the *Ceanothus* subgenus species due to their unique anatomy (Keeley, 1975). In contrast with the epidermis and cuticle, there was limited variation between palisade and spongy mesophyll cell dimensions among species and between subgenera.

In addition to morphology, traits relating to physiological adaptation also differed between the subgenera. Petiole to leaf area ratio was significantly higher in *Cerastes* species, which may provide greater hydraulic supply to the leaf (Sack et al., 2003). *Cerastes* species also had more negative values of π_o and π_{TLP} than species of subgenus *Ceanothus* species. Across diverse species, a more negative π_{TLP} is typical of biomes and forests of greater aridity, and is correlated with other traits related to drought adaptation, specifically in their ability to tolerate increased water stress while maintaining photosynthetic function (Alder et al., 1996; Bartlett et al., 2012b; Bartlett et al., 2016). Indeed, the π_{TLP} is considered one of the traits most directly predictive of drought tolerance (Bartlett et al., 2012b). The values we found for π_{TLP} were consistent with those previously reported in the literature for well-watered plants of *C. cuneatus, C. megacarpus, C. oliganthus*, and *C. spinosus,* although more negative values can be observed under drought stress (Saruwatari and Davis, 1989; Pratt et al., 2007).

Several traits differed between subgenera in a way that contrasted with expectations. *Cerastes* species had greater IVD than species of the *Ceanothus*, despite expectations of the opposite given that *Cerastes* species are generally found in more arid locations. Higher vein density, related to lower IVD (Uhl and Mosbrugger, 1999), can provide redundant pathways for water transport, which would be beneficial if leaf vein xylem embolizes during drought, and, additionally, higher vein density can contribute to higher gas exchange rates in the shorter periods that water is available in more arid climates (Sack and Scoffoni, 2013). The greater IVD in *Cerastes* was apparently related to its distinctive tissue organization. The deep encryptions containing stomata, the large hypodermis cells and apparent water storage tissue accounted for the increased spacing between veins. These modifications also result in a short distance between veins and stomata, and future research is needed to resolve whether these adaptations, in addition to the potential advantages provided by stomatal crypts in enabling gas exchange under arid conditions, may reduce the need for greater vein density that is typical of most drought tolerant species. This unique tissue organization may additionally be related to the high photosynthetic rates previously observed in *Cerastes* species (Pratt et al., 2012). Future research is needed to quantify other leaf xylem traits, such as vein xylem conduit numbers and sizes to determine whether these too may contribute to higher hydraulic supply and photosynthetic rate in *Cerastes* species.

Among species within subgenera we found very strong diversification of many other leaf traits, including leaf area, LMA, leaf density, SWC, LDMC, leaf area and thickness shrinkage, petiole allocation, and tissue, cell and cell wall dimensions. These traits may contribute to other leaf functions such as adaptations to diverse microhabitats, as *Ceanothus* species thrive in a wide range of edaphic conditions (Burge et al., 2013; Burge, 2014).

***Evolutionary association of traits with climate*—**Our results generally supported the hypothesis that drought tolerance traits π_o and π_{TLP} are adaptive in more arid locations, shown by significant phylogenetic least squares regressions with aridity index. These correlations between π_{TLP} and climate establish an evolutionary basis for the trends previously described across diverse species. These trends support the hypothesis that plants evolve the capacity to maintain gas exchange for longer into drought without wilting given reduced water availability in the native range. The evolutionary correlations support the hypothesis that species evolved along these climate gradients even after the deep evolutionary split in the genus.

We also found support for a correlation of leaf mass per area (LMA) with potential evapotranspiration (PET) in phylogenetic least squares regression across a larger set of 35 *Ceanothus* species, which was most likely driven by relationships within each subgenus of LMA and PET. However, relationships of LMA with other climate variables were not observed, in contrast with patterns previously reported across diverse species. LMA tends to be inversely related to precipitation across disparate species (Lamont et al., 2002; Poorter et al., 2009), but this relationship was not supported either in our ten study species or across the larger group of species in this lineage. Indeed, a lack of correlation of LMA with precipitation was previously reported for 39 *Ceanothus* species (Ackerly et al., 2006), highlighting the need to quantify traits more directly related to drought tolerance. Notably, even though the *Ceanothus* species did not show a trend of LMA with aridity in a common garden, plasticity of LMA with aridity might still play a role in species performance under drought, as this trait shows a high degree of intraspecific variation (Messier et al., 2010; Fajardo and Piper, 2011). Other expected trends of traits with aridity were also unsupported. Across species, smaller and thicker leaves are generally found in high light and high temperature environments (Cooper, 1922; Poole and Miller, 1981;

Givnish, 1987; Niinemets, 2001; Scoffoni et al., 2011; Wright et al., 2017), as these minimize overheating and water loss (Ackerly et al., 2002; Scoffoni et al., 2011). However, we did not find significant differences in leaf size between *Ceanothus* subgenera, or a relationship between leaf size and climate in our ten study species or across the data compiled for 35 species in this lineage. This lack of support does not necessarily mean one can reject the possibility of trends that may be found in future studies of the entire *Ceanothus* genus when data become available.

Notably, the lack of support for some expected trends of LMA, leaf size and other traits with climate in the phylogenetic analysis of all species could also reflect the fact that the bulk of variation in leaf morphology and genetics was driven by the deep phylogenetic split between subgenera. The *Ceanothus* genus is particularly susceptible to a problem described by Felsenstein (1985): despite the consideration of multiple species from each subgenus, species are closely related within the subgenera and clustered in their trait values. This hinders the inference of correlation between traits within a subclade and weakens the overall phylogenetic correlation across all species. Thus, while trait differences between subgenera and/or relationships of traits with climate across all species do indicate evolutionary correlations, the lack of a relationship does not provide evidence against correlated evolution of traits with climate, but may simply be due to a lack of resolution within the analysis. Given the divergence between subgenera, the phylogenetic analysis would have made many correlations weaker (Carvalho et al., 2006) or non-significant. Considering evolutionary history highlights the lack of resolution of the historical factors underlying trait diversification, such as the timing of the advent of the Mediterranean (MT) climate. One possibility is that California flora evolved largely under the MT climate regime, beginning around 12-15 million years ago (Keeley et al., 2012; Baldwin, 2014); that scenario would suggest that *Ceanothus* leaf traits, including the relatively high LMA of all

species, evolved as adaptations to the MT climate. Another possibility, however, is that all *Ceanothus* species shared a common ancestor that already possessed drought tolerance, and the two subgenera diverged prior to the rise of the MT climate in California (Ackerly, 2004; Donoghue, 2008; Burge et al., 2011; Kauffman, 2015), and the *Cerastes* subgenus in particular evolved traits beneficial under high aridity.

Trait-trait correlations: structural traits and cell cross-sectional anatomy—We found mixed support for strict allometries among cell, cell wall and whole leaf dimensions within *Ceanothus*. The upper and lower epidermal cell wall thicknesses, and thicknesses of the upper and lower cuticles and of the lower epidermis and upper and lower cuticle showed correlated evolution. There were also linkages between upper and lower cuticle thicknesses, lower epidermal thickness, and whole leaf thickness. These relationships suggest allometries arising from developmental or functional linkages (Evert, 2006) even during fine-scale evolution of traits in different habitats, extending findings for such anatomical correlations in Proteaceae and in a study across diverse species (Brodribb et al., 2013; John et al., 2013). However, other trends reported in those studies were not found, i.e., the relationships among cell sizes, cell wall thickness and leaf thickness. In some cases, the lack of correlation between traits within *Ceanothus* may be due to certain traits spanning a relatively narrow range, such as spongy and mesophyll cell sizes, so an across-species trend would not be resolved. In other cases, expected linkages might have been broken by the diversification of a lineage across environments such as the California *Ceanothus*. This might occur when one trait shifts but not another that was expected to be correlated (e.g., the decoupling of spongy mesophyll and upper epidermal cell

sizes, among other relationships, Fig. 2.8), or, decoupling of cell and tissue allometries may arise due to the evolution of specialized tissues such as hypodermis and stomatal crypts.

Conclusions and future directions—This study demonstrated a substantial diversification of drought tolerance traits across species of *Ceanothus*, within and between subgenera. Further, these analyses supported the importance of π_{TLP} as a trait in signaling the adaptive radiation of drought tolerance across a lineage of closely related species. An urgent avenue for future research is the application of these findings to predict the climates and habitats of species to enable their conservation and protect sites of their future distributions, a current grand challenge in plant ecology. Recent studies have shown that leaf traits can provide a first step toward predicting site aridity for diverse species at continental scales (Stahl et al., 2014; Shipley et al., 2017), and our study supports this potential application of leaf traits within an evolutionary radiation, i.e., within a genus, and even within subgenera. The findings further attest to the excellent potential of *Ceanothus* to be used as model lineage to understand trait diversification, particularly in drought tolerance traits, and striking anatomical specialization, as is found in the *Cerastes* subgenus.

Table 2.1. Study species of the *Ceanothus* genus and their leaf habits (E, evergreen; D, deciduous) and environments, in order of ascending mean aridity index (± S.E.). An aridity index below 0.2 indicates an arid to hyper-arid climate, and above 0.5 indicates a sub-humid or humid climate (Global Biodiversity Information Facility 2012, Trabucco and Zomer, 2009). Nomenclature follows the Jepson Manual (Jepson Flora Project (eds.) 2017. Jepson eFlora, http://ucjeps.berkeley.edu/IJM.html).

Species	**Subgenus**	**Leaf habit**	**Average Aridity Index**	**Average Potential Evapo-Transpiration (mm/year)**	**Annual Precipitation (mm)**	**Mean Annual Temperature (°C)**	**Sample Size**
Ceanothus verrucosus	*Cerastes*	E	0.27 (0.006)	1230.02 (8.30)	324.61 (6.23)	16.77 (0.04)	310
Ceanothus megacarpus	*Cerastes*	E	0.37 (0.003)	1160.43 (5.82)	436.36 (4.31)	15.60 (0.05)	619
Ceanothus tomentosus	*Ceanothus*	D	0.39 (0.008)	1368.71 (3.17)	520.20 (9.56)	15.99 (0.05)	949
Ceanothus spinosus	*Ceanothus*	D	0.40 (0.005)	1277.12 (4.11)	505.27 (5.47)	15.56 (0.07)	457
Ceanothus cuneatus	*Cerastes*	E	0.42 (0.014)	1106.22 (8.52)	397.37 (7.13)	13.91 (0.05)	94
Ceanothus ferrisiae	*Cerastes*	E	0.43 (0.011)	1324.11 (9.22)	564.99 (8.71)	14.55 (0.14)	81
Ceanothus impressus	*Ceanothus*	D	0.48 (0.028)	1115.97 (10.69)	510.18 (22.60)	13.45 (0.16)	89
Ceanothus oliganthus	*Ceanothus*	E	0.53 (0.007)	1274.85 (3.45)	648.36 (6.50)	14.41 (0.05)	1642
Ceanothus lemmonii	*Ceanothus*	D	0.93 (0.012)	1270.00 (5.49)	1166.71 (12.58)	13.01 (0.13)	412
Ceanothus incanus	*Ceanothus*	E	1.04 (0.023)	1116.72 (6.71)	1150.53 (23.86)	12.33 (0.08)	367

Table 2.2. Leaf trait variation across ten *Ceanothus* species and the results of nested ANOVA tests of species and subgenus variation. The columns with subgenus headers show minimum, average (bold) and maximum values within each group for each trait. ANOVA results show mean square values, percent variation, and significance levels for each trait across all *Ceanothus* species and between subgenera. For two traits, thickness of the hypodermis and lower epidermis in crypts, which only existed in *Cerastes* species, degrees of freedom from an ANOVA are reported in parentheses. Boldface indicates a significant result. ns, $P>0.05$; *, $P<0.05$; **, $P<0.01$; ***, $P<0.001$. An H or L denotes if traits were expected to be higher or lower in *Cerastes* species, and the check mark indicates whether the trait followed our expectation. A (+/-) denotes the expected direction of a correlation with aridity (notably opposite of aridity index, where a low value indicates a more arid climate). A check denotes if a trait followed the expected correlation with aridity, and checks with asterisks indicate that this correlation was still significant following the Benjamini-Hochberg FDR test.

Trait	Unit	Higher or Lower for Cerastes	Expected correlation with aridity	*Ceanothus*	*Cerastes*	Between subgenera, df=1	Within subgenus (between species), df=8	Error, df=20
Structural Traits								
Leaf Area	cm^2	L	- ✔	0.89, **3.03,** 6.71	0.55, **1.16,** 1.49	22.8, 19.4	**8.97, 60.9*****	1.16, 20.3
Leaf Mass per Area	$g\ m^2$	H ✔	+	68.5, **119,** 169	243, **294,** 364	**210944, 76.4*****	**5109, 14.8****	1222, 37.4
Density	$g\ 0.001m^{-3}$	H	+	0.36, **0.45,** 0.55	0.42, **0.50,** 0.56	0.02, 8.38	**0.02, 61.2****	0.00, 0.76
Saturated Water Content	$g\ g^{-1}$	L	-	1.32, **1.81,** 3.05	1.30, **1.49,** 1.75	0.75, 7.51	**0.79, 62.7****	0.15, 17.8
Leaf Dry Matter Content	$g\ g^{-1}$	H	+	0.26, **0.37,** 0.43	0.39, **0.42,** 0.44	0.01, 14.8	**0.01, 61.6*****	0.00, 0.15
Leaf Area Shrinkage	%	NA	-	0.29, **0.31,** 0.35	0.15, **0.37,** 0.83	0.03, 2.71	**0.11, 94.0*****	0.00, 0.85
Leaf Thickness Shrinkage	%	NA	-	0.00, **0.17,** 0.40	0.09, **0.15,** 0.20	0.00, 0.56	**0.05, 73.8*****	0.01, 12.4
Leaf Thickness	mm	H	+	0.16, **0.26,** 0.31	0.46, **0.55,** 0.65	**0.72, 76.8*****	0.01, 9.34	0.01, 0.17
Petiole Area:Leaf Area		NA	+	0.04, **0.06,** 0.10	0.12, **0.25,** 0.50	**0.24, 42.8***	**0.04, 50.9*****	0.00, 0.08
Petiole Area:Dry Leaf Mass		NA	+	26.3, **52.3,** 72.4	37.3, **90.9,** 196	10723, 14.4	**6873, 73.9*****	434, 13.6
Drought Tolerance Traits								
Osmotic Potential at Turgor Loss Point	MPa	L ✔	- ✔*	-2.40, **-2.15,** -1.57	-2.81, **-2.64,** -2.52	**1.18, 53.7****	**0.07, 26.2***	0.02, 0.81
Osmotic Potential at Full Turgor	MPa	L ✔	- ✔*	-2.12, **-1.86,** -1.35	-2.62, **-2.42,** -2.27	**1.70, 53.7****	**0.10, 26.2***	0.03, 1.16
Interveinal Distance	µm	H	-	151, **170,** 188	195, **271,** 359	**67792, 47.2****	**5761, 32.1****	1493, 39.3
Anatomical Traits								
Tissue Cross-Sectional Thicknesses								
Upper Cuticle	µm	H ✔	+	2.31, **3.43,** 4.23	4.69, **5.89,** 6.66	**39.0, 52.2*****	1.40, 15.1	1.22, 27.8
Upper Epidermis	µm	H	+	32.5, **45.9,** 75.8	30.4, **34.3,** 39.0	1272, 21.2	**454, 60.7*****	54.1, 22.8
Mesophyll	µm	H	+	122, **195,** 291	173, **214,** 260	402, 0.31	**11257, 70.1*****	1897, 29.6
Lower Epidermis	µm	H ✔	+	10.3, **13.8,** 17.6	30.6, **40.0,** 43.6	**4840, 74.9*****	66.6, 8.24	54.5, 64.2
Lower Cuticle	µm	H ✔	+	1.09, **1.55,** 2.59	4.61, **5.68,** 6.49	**118, 74.3*****	1.29, 6.48	1.54, 26.7
Hypodermis	µm	NA	NA	NA	13.8, **15.8,** 20.3	NA	8277, 29.1 (3)	581, 70.9 (8)
Crypt Lower Epidermis	µm	NA	NA	NA	243, **311**, 370	NA	27.9, 29.9 (3)	24.6, 70.1 (8)
Cross-sectional Cell Areas								
Upper Epidermis	μm^2	NA	-	524, **1085,** 2140	221, **309,** 362	**5189996, 44.8***	**639323, 44.1*****	64704, 20.2
Palisade Mesophyll	μm^2	NA	-	231, **354,** 571	256, **306,** 389	51433, 8.60	**57098, 76.4*****	4487, 16.4
Spongy Mesophyll	μm^2	NA	-	141, **182,** 249	123, **169,** 244	3518, 3.82	**6894, 59.9****	1669, 37.7
Lower Epidermis	μm^2	NA	-	13,2, **18.1,** 23.5	12.7, **14.1,** 15.6	193331, 29.6	**42330, 51.8*****	6070, 26.5
Cell Wall Thicknesses								
Upper Epidermis	µm	NA	+	0.55, **0.71,** 0.84	0.98, **1.29,** 1.89	**2.03, 34.7***	**0.24, 32.4***	0.10, 5.00
Palisade Mesophyll	µm	NA	+ ✔	2.88, **3.53,** 4.21	3.11, **3.47,** 3.98	0.34, 1.47	1.32, 45.9	0.61, 50.1
Spongy Mesophyll	µm	NA	+	0.49, **0.60,** 0.67	0.65, **1.42,** 2.85	4.37, 20.5	**1.18, 44.2***	0.37, 20.0
Lower Epidermis	µm	NA	+	0.56, **0.65,** 0.74	0.89, **1.14,** 1.49	**1.48, 50.3****	0.08, 22.4	0.04, 1.55

FIGURE CAPTIONS

Figure 2.1 Map of the centers of distributions for each species overlaid on an annual precipitation grid, with values ranging from high precipitation in black, to low precipitation in white. Yellow circles represent the centers of distributions for all *Ceanothus* species included in this study. Orange stars represent centers of focal *Cerastes* subgenus species distributions, and blue stars represent centers of focal *Ceanothus* subgenus species distributions.

Figure 2.2 Phylogenetic tree of the genus *Ceanothus*, and pruned tree of the sampled species, reconstructed from alignments of nitrate reductase (NIA) and nuclear ribosomal transcribed spacer (ITS) DNA sequences. Tip labels are abbrevaited as the first three letters of the genus name, followed by the first three letters of the species name (and subspecies, if applicable), following Burge et al. (2011). Branch labels indicate branch lengths. Focal species are higlighted in the full tree. Branches are colored to distinugh subgenera, where blue branches indicate *Ceanothus* subgenus species, and orange branches indicated *Cerastes* subgenus species.

Figure 2.3 Trait means across ten *Ceanothus* species: (A) leaf mass per area (LMA), (B) leaf thickness, (C) petiole to leaf area ratio, (D) osmotic potential at turgor loss point (π_{TLP}), (E) interveinal distance (IVD), (F) upper cuticle thickness, (G) upper epidermal cell area, and (H) upper epidermal cell wall thickness (CWT). Mean ± S.E. values are shown. Species are arranged phylogenetically, with more closely related species closer together on the graph. Blue bars indicate species of the *Ceanothus* subgenus, and orange bars indicate species of the *Cerastes* subgenus. All traits showed significant variation between subgenera.

Figure 2.4 Leaf anatomy of ten *Ceanothus* species as seen from a scan of a typical leaf, and transverse cross-section of the lamina. Notably, *Cerastes* leaves contain hypodermal tissue not found in the *Ceanothus* subgenus (A). Transverse cross-sections showing stomatal crypts in *Cerastes* species on right (invaginations in leaf margin, indicated by arrow, scale = 1 mm), and *Ceanothus* subgenus species on left (B). Tissue types are labeled: Upper epidermis (UE), palisade mesophyll (PM), spongy mesophyll (SM), vascular tissue (V), lower epidermis (LE) and hypodermis (H).

Figure 2.5 Phylogenetic principal component analysis showing trait variation between species of *Ceanothus* (blue) and *Cerastes* (orange) subgenera, based on leaf area, leaf mass per area (LMA), osmotic potential at turgor loss point (TLP), upper epidermal cell area (UECA), and palisade mesophyll cell wall thickness (PCWT).

Figure 2.6 Relationships of osmotic potential at turgor loss point (π_{TLP}) to climate variables for ten *Ceanothus* species. Correlations are shown for π_{TLP} with aridity index (A) and annual precipitation (B). Blue points indicate species of the *Ceanothus* subgenus, and orange points the *Cerastes* subgenus. The *r*-values correspond to phylogenetic generalized least squared regressions, and asterisks denote significance after Benjamini-Hochberg correction. ns, $P>0.05$; *, $P<0.05$; **, $P<0.01$; ***, $P<0.001$.

Figure 2.7 Correlations of upper and lower epidermal cell wall thickness across ten *Ceanothus* species from this study (blue points) and a set of diverse species published previously (grey points; John et al., 2013), with statistically similar isometric relationship. Error bars represent

standard errors. A standard major axis line is shown. The *r*-values correspond to phylogenetic generalized least squared regressions, and asterisks denote significance after Benjamini-Hochberg correction.. ns, $P>0.05$; *, $P<0.05$; **, $P<0.01$; ***, $P<0.001$.

Figure 2.8 Examples of the lack of relationships between cell sizes, cell wall thickness and leaf thickness across 10 *Ceanothus* species (blue points) in contrast with trends found across a set of diverse species published previously (grey points; John et al., 2013): relationships between spongy mesophyll cell areas with upper epidermal cell areas (A), palisade cell areas (B), total leaf thickness (C), and spongy cell wall thickness (D; μm). Error bars represent standard errors.

Figure 2.9 Mean leaf mass per area (A; LMA) and leaf area (B) across 35 *Ceanothus* species. Blue bars indicate species of the *Ceanothus* subgenus (n = 19), and orange bars indicate species of the *Cerastes* subgenus (n = 16). In an ANOVA, subgenus means were significantly different for LMA ($P < 0.001$***), but not for leaf size ($P = 0.096$, ns).

Figure 2.10 Relationships of leaf mass per area (LMA) to potential evapo-transpiration (PET) variables for 35 *Ceanothus* species. Blue points indicate species of the *Ceanothus* subgenus, and orange points the *Cerastes* subgenus. The *r*-values correspond to phylogenetic generalized least squared regressions, and asterisks denote significance after Benjamini-Hochberg correction. ns, $P>0.05$; *, $P<0.05$; **, $P<0.01$; ***, $P<0.001$.

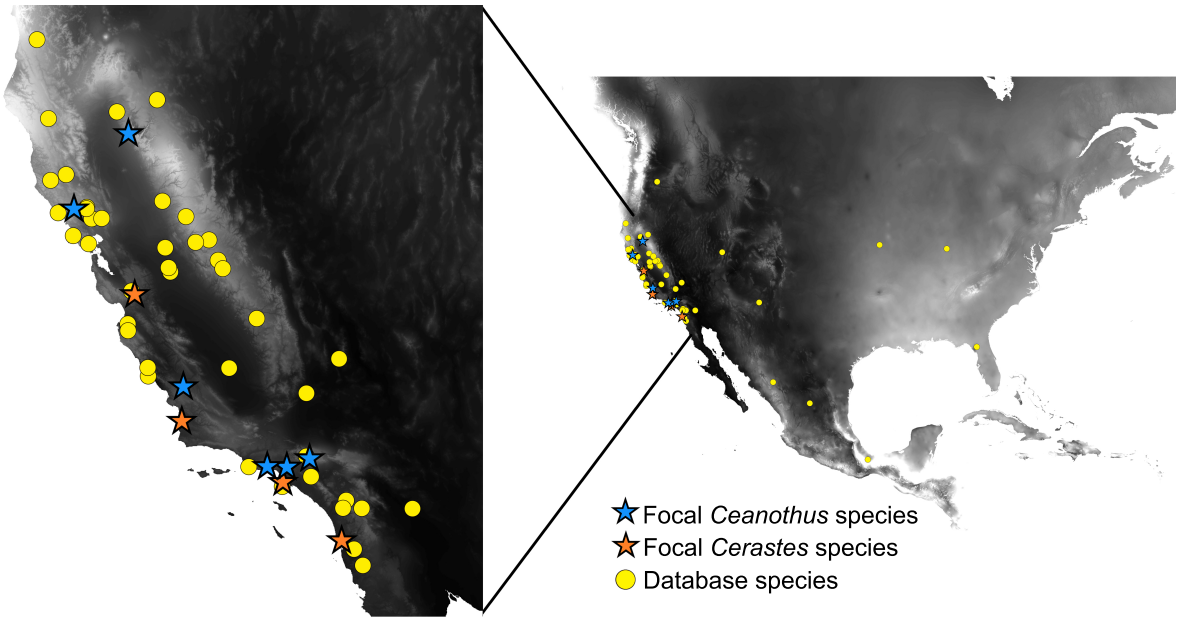
Focal *Ceanothus* species
Focal *Cerastes* species
Database species

FIGURE 2.1

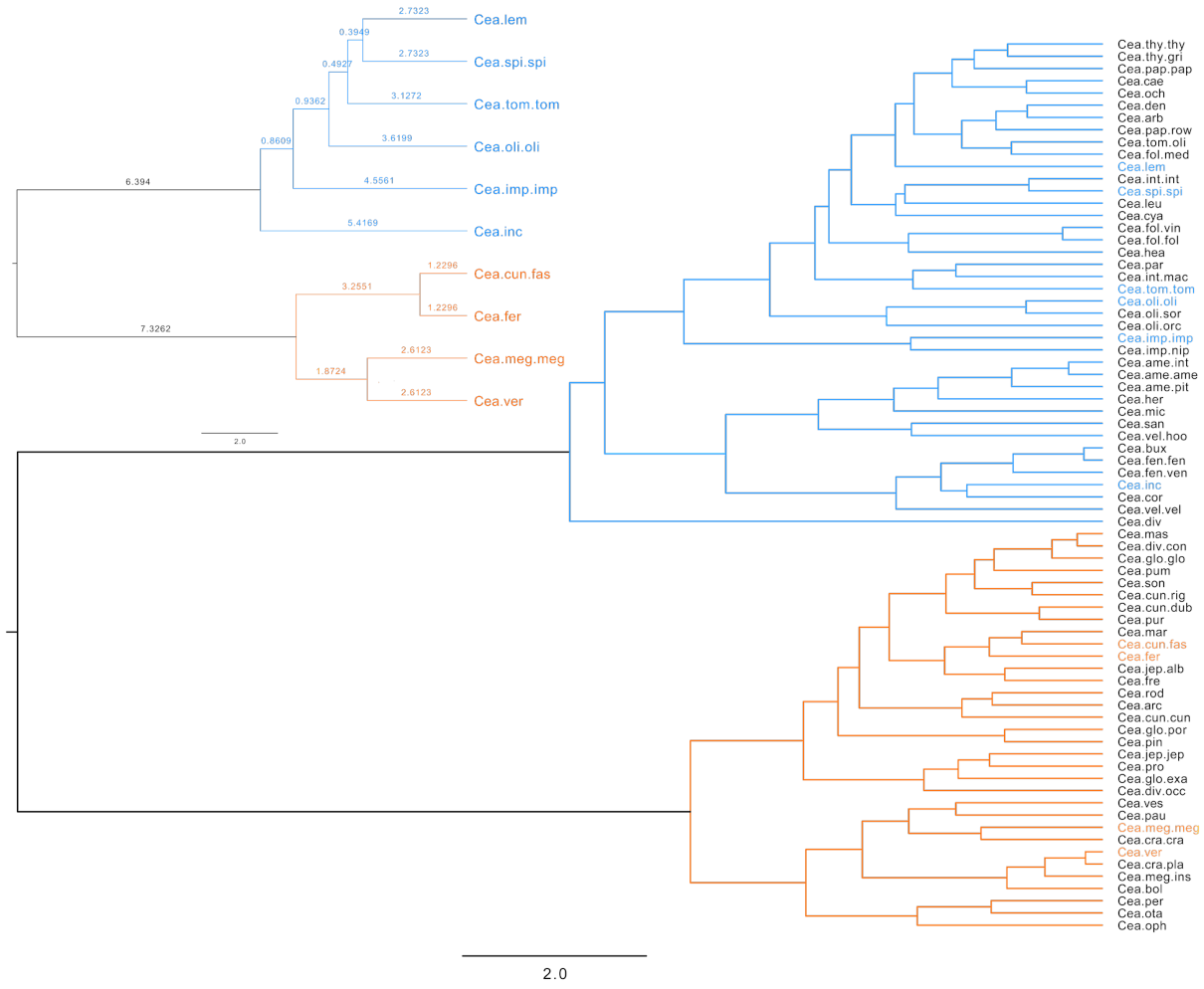
2.7323
Cea.lem
0.3949
2.7323
Cea.spi.spi
0.4927
3.1272
Cea.tom.tom
0.9362
3.6199
Cea.oli.oli
0.8609
4.5561
Cea.imp.imp
6.394
5.4169
Cea.inc
1.2296
Cea.cun.fas
3.2551
1.2296
Cea.fer
7.3262
2.6123
Cea.meg.meg
1.8724
2.6123
Cea.ver
2.0
Cea.thy.thy
Cea.thy.gri
Cea.pap.pap
Cea.cae
Cea.och
Cea.den
Cea.arb
Cea.pap.row
Cea.tom.oli
Cea.fol.med
Cea.lem
Cea.int.int
Cea.spi.spi
Cea.leu
Cea.cya
Cea.fol.vin
Cea.fol.fol
Cea.hea
Cea.par
Cea.int.mac
Cea.tom.tom
Cea.oli.oli
Cea.oli.sor
Cea.oli.orc
Cea.imp.imp
Cea.imp.nip
Cea.ame.int
Cea.ame.ame
Cea.ame.pit
Cea.her
Cea.mic
Cea.san
Cea.vel.hoo
Cea.bux
Cea.fen.fen
Cea.fen.ven
Cea.inc
Cea.cor
Cea.vel.vel
Cea.div
Cea.mas
Cea.div.con
Cea.glo.glo
Cea.pum
Cea.son
Cea.cun.rig
Cea.cun.dub
Cea.pur
Cea.mar
Cea.cun.fas
Cea.fer
Cea.jep.alb
Cea.fre
Cea.rod
Cea.arc
Cea.cun.cun
Cea.glo.por
Cea.pin
Cea.jep.jep
Cea.pro
Cea.glo.exa
Cea.div.occ
Cea.ves
Cea.pau
Cea.meg.meg
Cea.cra.cra
Cea.ver
Cea.cra.pla
Cea.meg.ins
Cea.bol
Cea.per
Cea.ota
Cea.oph
2.0

Figure 2.2

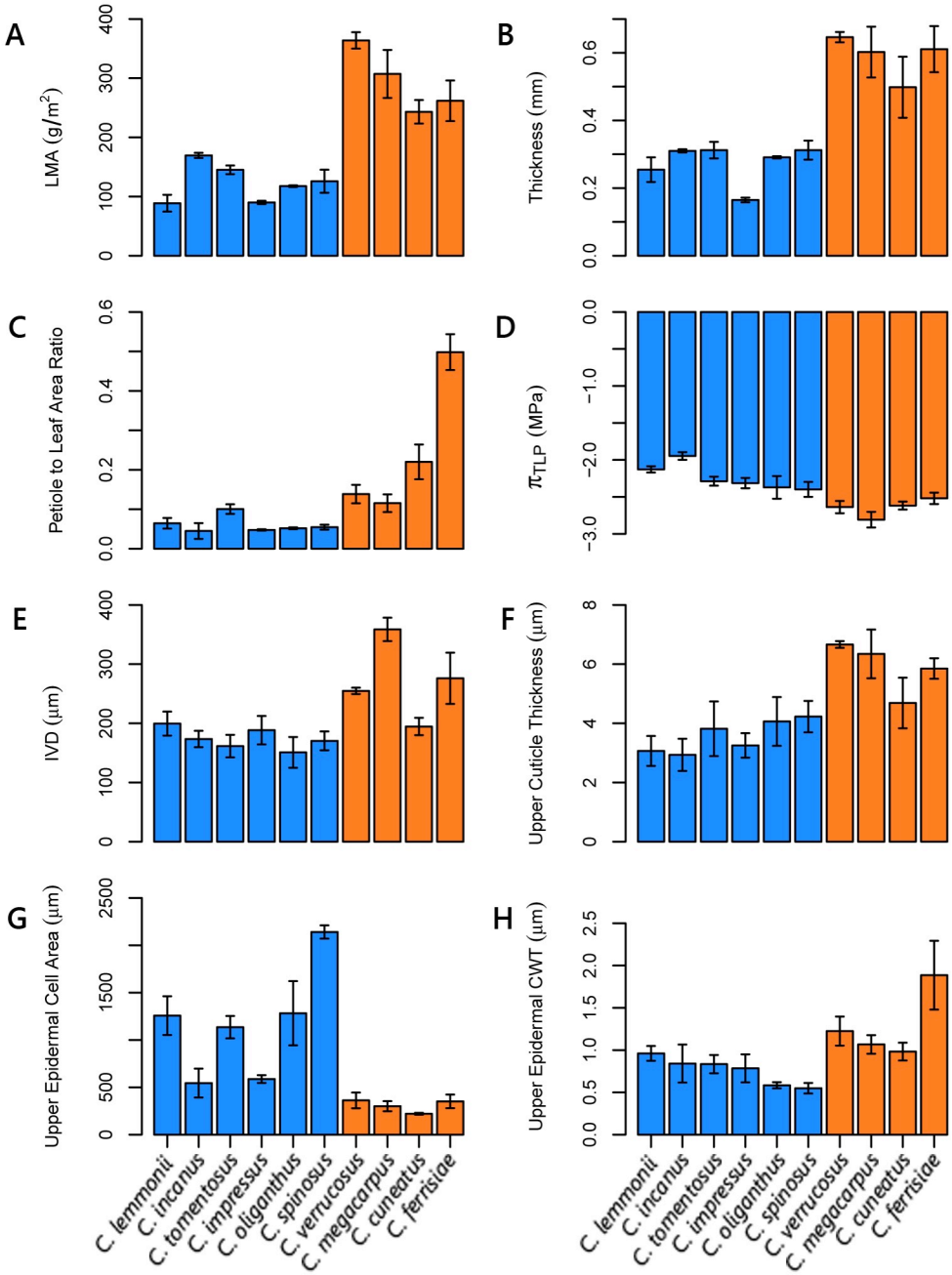
A
LMA (g/m²)
0
100
200
300
400
B
Thickness (mm)
0.0
0.2
0.4
0.6
C
Petiole to Leaf Area Ratio
0.0
0.2
0.4
0.6
D
π_{TLP} (MPa)
−3.0
−2.0
−1.0
0.0
E
IVD (µm)
0
100
200
300
400
F
Upper Cuticle Thickness (µm)
0
2
4
6
8
G
Upper Epidermal Cell Area (µm)
0
500
1500
2500
H
Upper Epidermal CWT (µm)
0.0
0.5
1.0
1.5
2.0
2.5
C. lemmonii
C. incanus
C. tomentosus
C. impressus
C. oliganthus
C. spinosus
C. verrucosus
C. megacarpus
C. cuneatus
C. ferrisiae

Figure 2.3

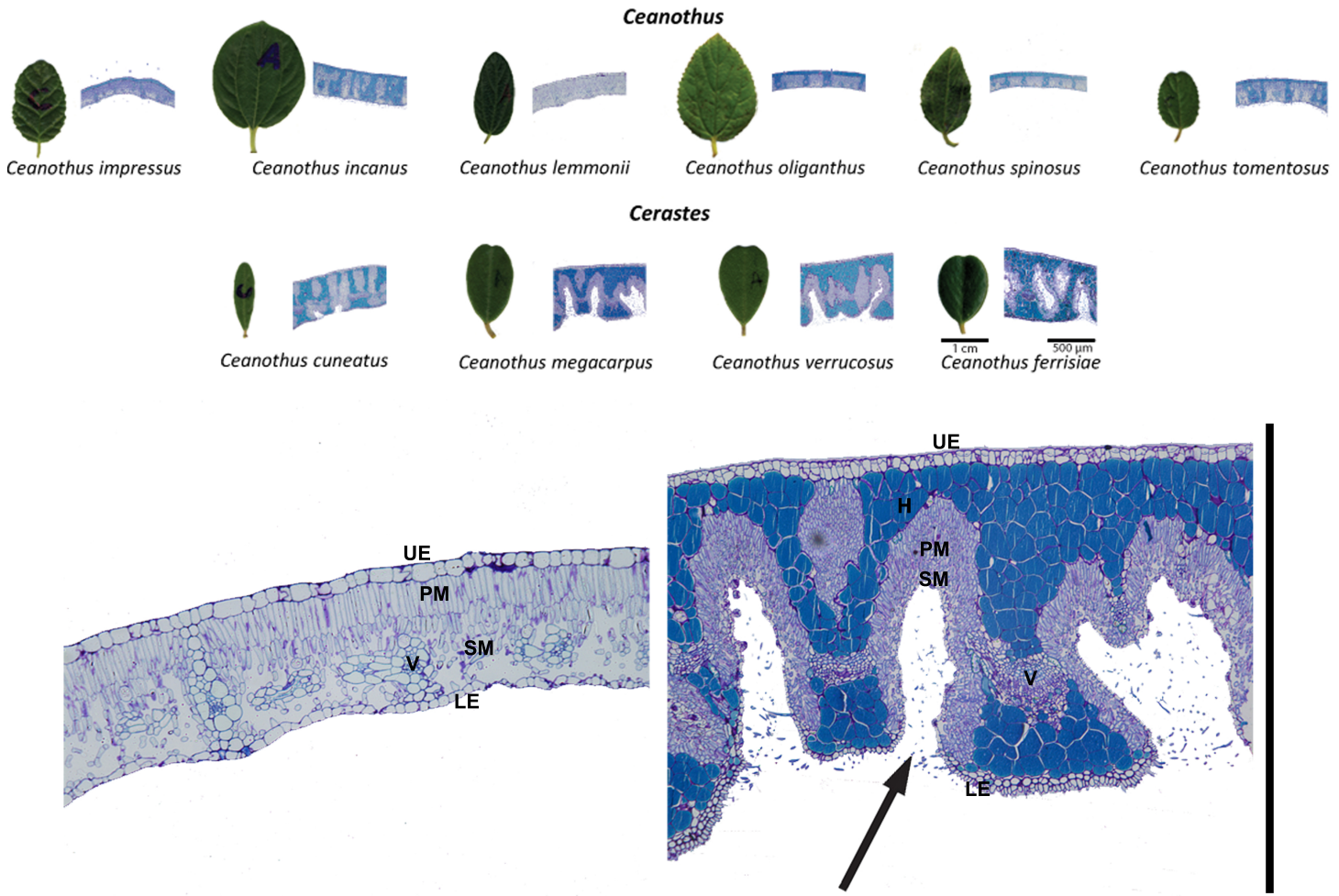
Ceanothus
Ceanothus impressus
Ceanothus incanus
Ceanothus lemmonii
Ceanothus oliganthus
Ceanothus spinosus
Ceanothus tomentosus
Cerastes
Ceanothus cuneatus
Ceanothus megacarpus
Ceanothus verrucosus
1 cm
500 µm
Ceanothus ferrisiae
UE
PM
SM
V
LE
UE
H
PM
SM
V
LE

Figure 2.4

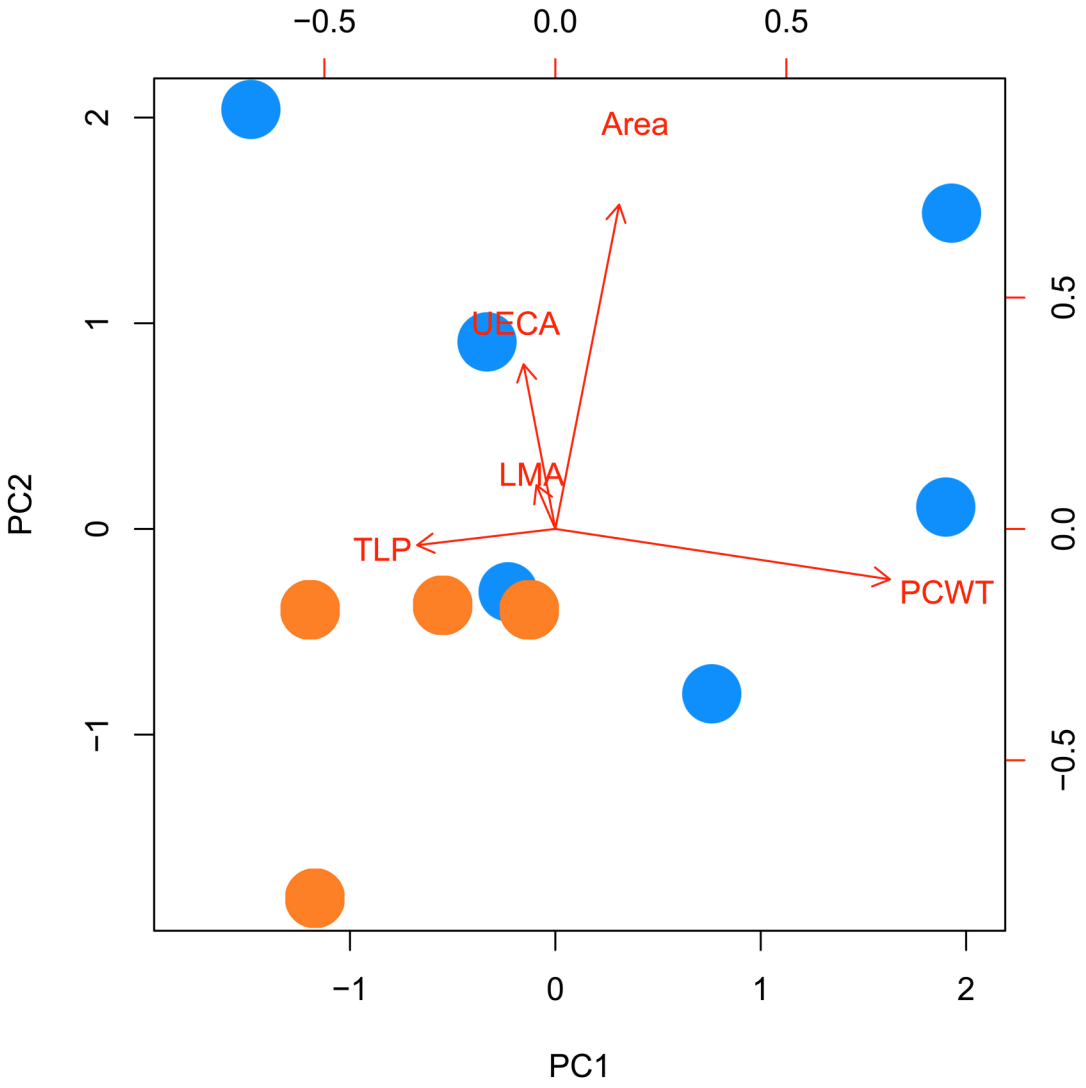

Figure 2.5

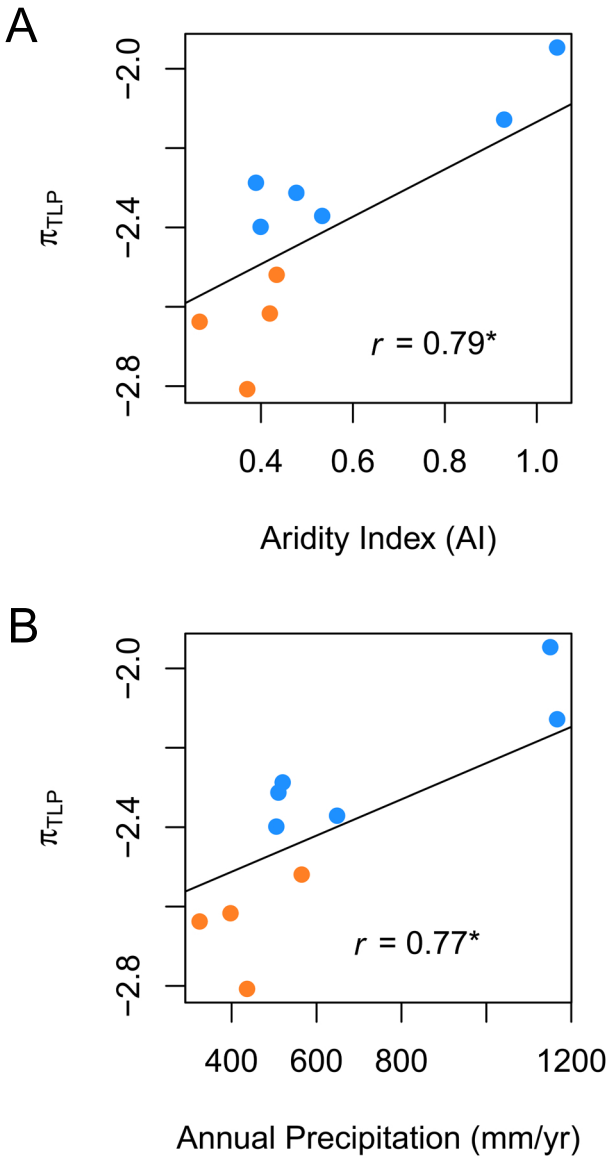
A
π_{TLP}
−2.0
−2.4
−2.8
r = 0.79*
0.4
0.6
0.8
1.0
Aridity Index (AI)
B
π_{TLP}
−2.0
−2.4
−2.8
r = 0.77*
400
600
800
1200
Annual Precipitation (mm/yr)

Figure 2.6

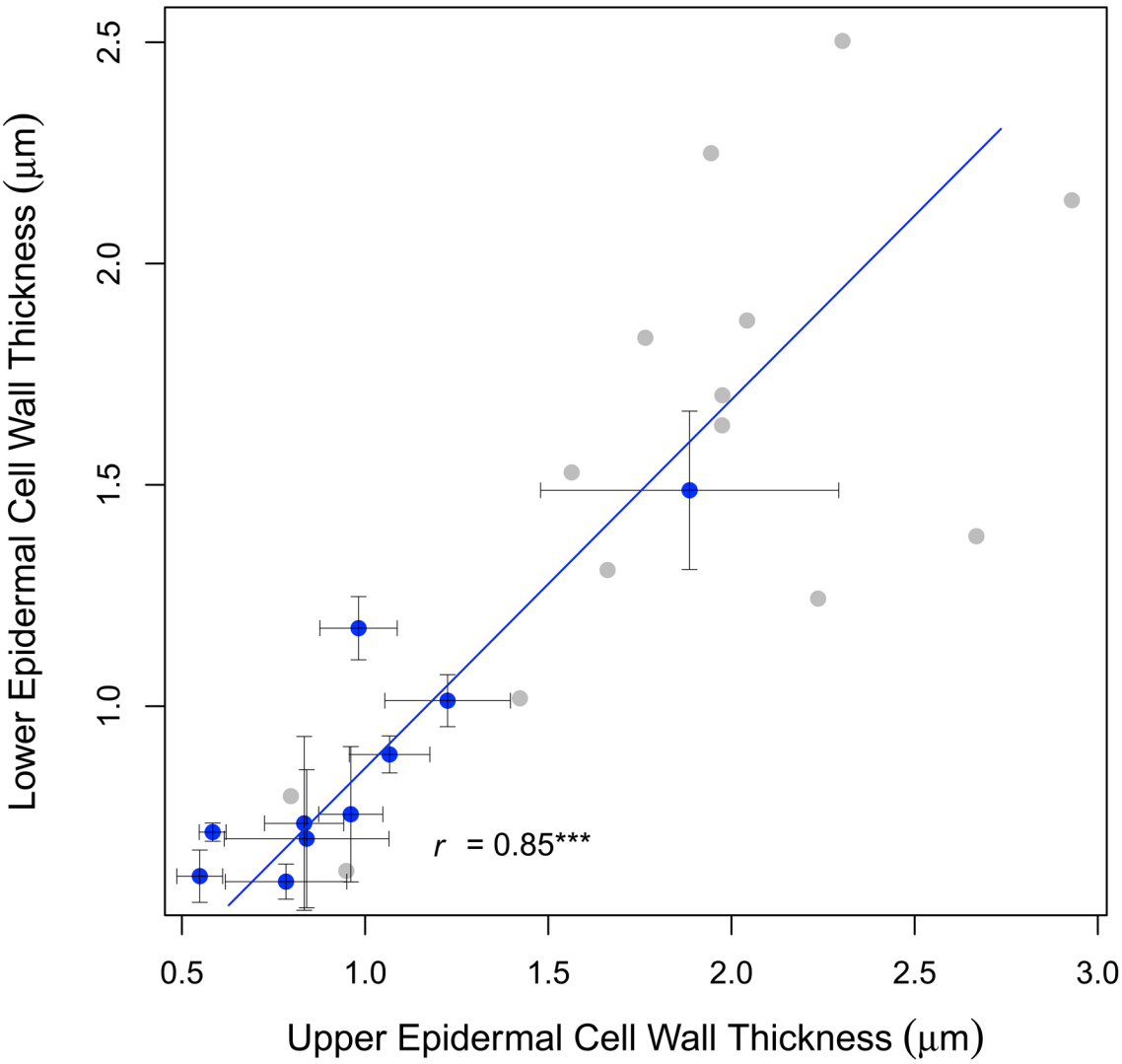
Lower Epidermal Cell Wall Thickness (µm)
Upper Epidermal Cell Wall Thickness (µm)
r = 0.85***
0.5
1.0
1.5
2.0
2.5
3.0
1.0
1.5
2.0
2.5

Figure 2.7

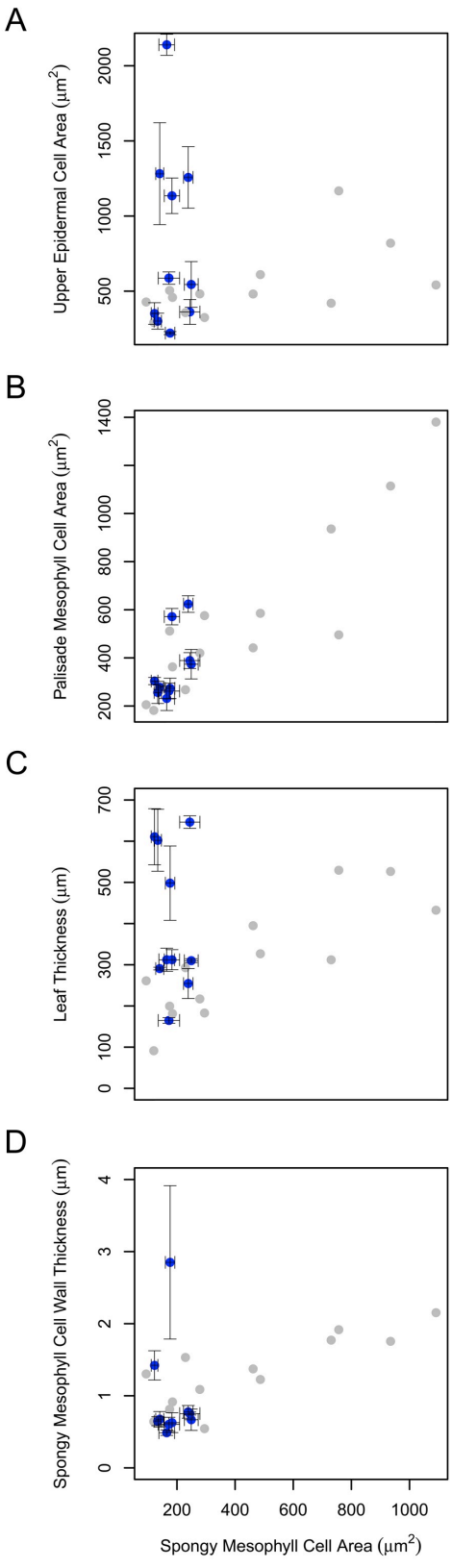
A
Upper Epidermal Cell Area (µm²)
500
1000
1500
2000
B
Palisade Mesophyll Cell Area (µm²)
200
400
600
800
1000
1400
C
Leaf Thickness (µm)
0
100
300
500
700
D
Spongy Mesophyll Cell Wall Thickness (µm)
0
1
2
3
4
200
400
600
800
1000
Spongy Mesophyll Cell Area (µm²)

Figure 2.8

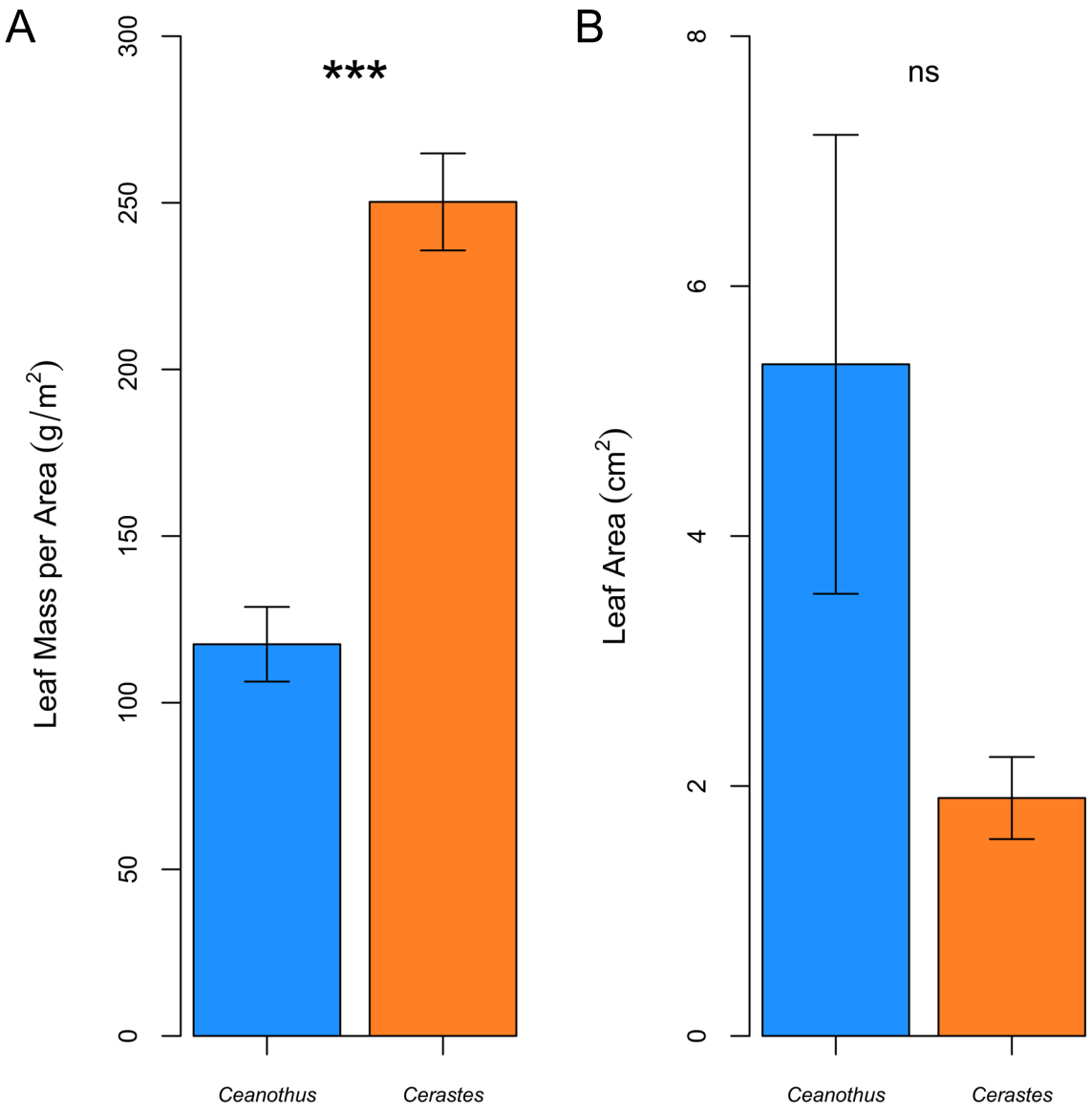
A
***
Leaf Mass per Area (g/m^2)
0
50
100
150
200
250
300
Ceanothus
Cerastes
B
ns
Leaf Area (cm^2)
0
2
4
6
8
Ceanothus
Cerastes

Figure 2.9

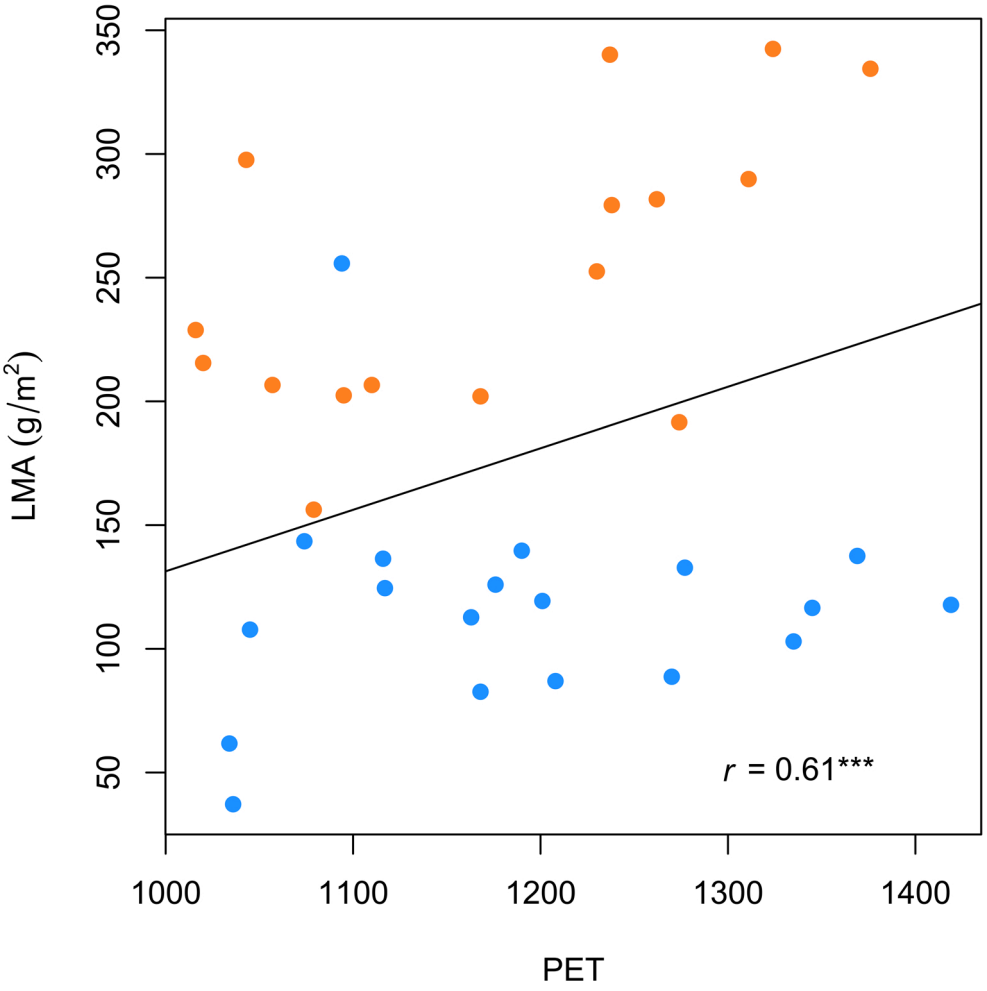
LMA (g/m^2)
350
300
250
200
150
100
50
1000
1100
1200
1300
1400
PET
r = 0.61***

Figure 2.10

SUPPLEMENTARY MATERIALS

Supplementary Data Captions (see attached Excel Workbook)

Table S2.1: DOIs for individual datasets downloaded from GBIF. These datasets were edited and/or combined to obtain occurrence data for the ten focal *Ceanothus* species used in this study.

Table S2.2: Individual and species mean values, standard deviations and standard errors for 10 *Ceanothus* species. Values are averages of three leaves per individual plant, and three plants per species for 26 traits.

Table S2.3: Correlation of traits with the first three axes from the phylogenetic principal components analysis (pPCA), and of climate with each of the five axes.

Table S2.4: Phylogenetic generalized least squares (PGLS) regression tests of each trait pair for ten focal *Ceanothus* species. Results are reported for three models of evolution: Brownian Motion, Pagel's Lambda, and Ornstein-Uhlenbeck (OU). The p-value from the best-fit model was extracted. Yellow highlights indicate significant p-values.

Table S2.5: Significance levels for trait-trait and trait-climate correlations after performing a Benjamini-Hochberg (BH) false discovery rate (FDR) analysis. These results include the 10 focal species. P-values prior to the FDR test are shown for the best-fit model from the phylogenetic generalized least squares regression. Yellow highlights indicate significant p-values.

Table S2.6: Data for species of *Ceanothus* obtained from the eFlora database for two traits on 35 species, and four climate variables obtained for each species' range (See Methods). Name codes follow Burge et al. 2011.

Table S2.7: Focal *Ceanothus* species data compared with data from the Jepson Herbarium eFlora database (http://ucjeps.berkeley.edu/EFT.html).

Table S2.8: Phylogenetic generalized least squares (PGLS) regression tests of each trait pair for 35 eFlora database species. Results are reported for three models of evolution: Brownian Motion, Pagel's Lambda, and Ornstein-Uhlenbeck (OU). The p-value from the best-fit model was extracted. Yellow highlights indicate significant p-values.

Table S2.9: Significance levels for trait-trait and trait-climate correlations after performing a Benjamini-Hochberg (BH) false discovery rate (FDR) analysis. These results include the 35 eFlora database species. P-values prior to the FDR test are shown for the best-fit model from the phylogenetic generalized least squares regression. Yellow highlights indicate significant p-values.

REFERENCES

Ackerly, D. D. 2004. Adaptation, niche conservatism, and convergence: Comparative studies of leaf evolution in the California chaparral. *American Naturalist* 163:654-671.

Ackerly, D. D. 2009. Evolution, origin and age of lineages in the Californian and Mediterranean floras. *Journal of Biogeography* 36:1221-1233.

Ackerly, D. D., C. A. Knight, S. B. Weiss, K. Barton, and K. P. Starmer. 2002. Leaf size, specific leaf area and microhabitat distribution of chaparral woody plants: Contrasting patterns in species level and community level analyses. *Oecologia* 130:449-457.

Ackerly, D. D., D. W. Schwilk, and C. O. Webb. 2006. Niche evolution and adaptive radiation: Testing the order of trait divergence. *Ecology* 87:S50-S61.

AghaKouchak, A., L. Cheng, O. Mazdiyasni, and A. Farahmand. 2014. Global warming and changes in risk of concurrent climate extremes: Insights from the 2014 California drought. *Geophysical Research Letters* 41:8847-8852.

Alder, N. N., J. S. Sperry, and W. T. Pockman. 1996. Root and stem xylem embolism, stomatal conductance, and leaf turgor in *Acer grandidentatum* populations along a soil moisture gradient. *Oecologia* 105:293-301.

Baldwin, B. G. 2014. Origins of plant diversity in the California Floristic Province. *Annual Review of Ecology, Evolution, and Systematics* 45:347-369.

Balsamo, R. A., and W. W. Thomson. 1995. Salt effects on membranes of the hypodermis and mesophyll-cells of *Avicennia germinans* (Avicenniaceae) – a freeze-fracture study. *American Journal of Botany* 82:435-440.

Bartlett, M. K., T. Klein, S. Jansen, B. Choat, and L. Sack. 2016. The correlations and sequence of plant stomatal, hydraulic, and wilting responses to drought. *Proceedings of the National Academy of Sciences of the United States of America* 113:13098-13103.

Bartlett, M. K., C. Scoffoni, R. Ardy, Y. Zhang, S. W. Sun, K. F. Cao, and L. Sack. 2012a. Rapid determination of comparative drought tolerance traits: Using an osmometer to predict turgor loss point. *Methods in Ecology and Evolution* 3:880-888.

Bartlett, M. K., C. Scoffoni, and L. Sack. 2012b. The determinants of leaf turgor loss point and prediction of drought tolerance of species and biomes: A global meta-analysis. *Ecology Letters* 15:393-405.

Bartlett, M. K., Y. Zhang, N. Kreidler, S. W. Sun, R. Ardy, K. F. Cao, and L. Sack. 2014. Global analysis of plasticity in turgor loss point, a key drought tolerance trait. *Ecology Letters* 17:1580-1590.

Benjamini, Y., and Y. Hochberg. 1995. Controlling the false discovery rate – a practical and powerful approach to multiple testing. *Journal of the Royal Statistical Society Series B-Methodological* 57:289-300.

Blackman, C. J., and T. J. Brodribb. 2011. Two measures of leaf capacitance: Insights into the water transport pathway and hydraulic conductance in leaves. *Functional Plant Biology* 38:118-126.

Blackman, C. J., T. J. Brodribb, and G. J. Jordan. 2010. Leaf hydraulic vulnerability is related to conduit dimensions and drought resistance across a diverse range of woody angiosperms. *New Phytologist* 188:1113-1123.

Blonder, B., B. G. Baldwin, B. J. Enquist, and R. H. Robichaux. 2016. Variation and macroevolution in leaf functional traits in the Hawaiian silversword alliance (Asteraceae). *Journal of Ecology* 104:219-228.

Bradbury, P. J., Z. Zhang, D. E. Kroon, T. M. Casstevens, Y. Ramdoss, and E. S. Buckler. 2007. TASSEL: Software for association mapping of complex traits in diverse samples. *Bioinformatics* 23: 2633–2635.

Brodribb, T. J., and N. M. Holbrook. 2003. Stomatal closure during leaf dehydration, correlation with other leaf physiological traits. *Plant Physiology* 132:2166-2173.

Brodribb, T. J., G. J. Jordan, and R. J. Carpenter. 2013. Unified changes in cell size permit coordinated leaf evolution. *New Phytologist* 199:559-570.

Brodribb, T. J., S. A. M. McAdam, G. J. Jordan, and S. C. V. Martins. 2014. Conifer species adapt to low-rainfall climates by following one of two divergent pathways. *Proceedings of the National Academy of Sciences of the United States of America* 111:14489-14493.

Burge, D. O. 2014. The role of soil chemistry in the geographic distribution of *Ceanothus otayensis* (Rhamnaceae). *Madroño* 61:276-289.

Burge, D. O., D. M. Erwin, M. B. Islam, J. Kellermann, S. W. Kembel, D. H. Wilken, and P. S. Manos. 2011. Diversification of *Ceanothus* (Rhamnaceae) in the California Floristic Province. *International Journal of Plant Sciences* 172:1137-1164.

Burge, D. O., R. Hopkins, Y. H. E. Tsai, and P. S. Manos. 2013. Limited hybridization across an edaphic disjunction between the gabbro-endemic shrub *Ceanothus roderickii* (Rhamnaceae) and the soil-generalist *Ceanothus cuneatus. American Journal of Botany* 100:1883-1895.

Carlquist, S. 1994. Anatomy of tropical alpine plants. *In* P. W. Rundel, A. P. Smith and F. C. Meinzer [eds.], Tropical alpine environments, 111-128. Cambridge University Press, Cambridge, Great Britain.

Carpenter, R. J., S. McLoughlin, R. S. Hill, K. J. McNamara, and G. J. Jordan. 2014. Early evidence of xeromorphy in angiosperms: Stomatal encryption in a new Eocene species of *Banksia* (Proteaceae) from Western Australia. *American Journal of Botany* 101:1486-1497.

Carvalho, P., J. A. Felizola Diniz-Filho, and L. M. Bini. 2006. Factors influencing changes in trait correlations across species after using phylogenetic independent contrasts. *Evolutionary Ecology* 20:591-602.

Cayan, D. R., E. P. Maurer, M. D. Dettinger, M. Tyree, and K. Hayhoe. 2008. Climate change scenarios for the California region. *Climatic Change* 87:S21-S42.

Chaves, M. M., J. Flexas, and C. Pinheiro. 2009. Photosynthesis under drought and salt stress: regulation mechanisms from whole plant to cell. *Annals of Botany* 103:551-560.

Chaves, M. M., J. S. Pereira, J. Maroco, M. L. Rodrigues, C. P. P. Ricardo, M. L. Osorio, I. Carvalho, T. Faria, and C. Pinheiro. 2002. How plants cope with water stress in the field, Photosynthesis and growth. *Annals of Botany* 89:907-916.

Cook, E. R., C. A. Woodhouse, C. M. Eakin, D. M. Meko, and D. W. Stahle. 2004. Long-term aridity changes in the western United States. *Science* 306:1015-1018.

Cooper, W. S. 1922. The broad-sclerophyll vegetation of California; An ecological study of the chaparral and its related communities. Cornegie Institution of Washington, Washington, USA.

Cordell, S., G. Goldstein, D. Mueller-Dombois, D. Webb, and P. M. Vitousek. 1998. Physiological and morphological variation in *Metrosideros polymorpha*, a dominant

Hawaiian tree species, along an altitudinal gradient: The role of phenotypic plasticity. *Oecologia* 113:188-196.

Cutler, J. M., D. W. Rains, and R. S. Loomis. 1977. Importance of cell-size in water relations of plants. *Physiologia Plantarum* 40:255-260.

Davis, S. D., F. W. Ewers, J. Wood, J. J. Reeves, and K. J. Kolb. 1999. Differential susceptibility to xylem cavitation among three pairs of *Ceanothus* species in the Transverse Mountain Ranges of southern California. *Ecoscience* 6:180-186.

Diaz, S., J. Kattge, J. H. C. Cornelissen, I. J. Wright, S. Lavorel, S. Dray, B. Reu, M. Kleyer, C. Wirth, I. C. Prentice, E. Garnier, G. Bonisch, M. Westoby, H. Poorter, P. B. Reich, A. T. Moles, J. Dickie, A. N. Gillison, A. E. Zanne, J. Chave, S. J. Wright, S. N. Sheremet'ev, H. Jactel, C. Baraloto, B. Cerabolini, S. Pierce, B. Shipley, D. Kirkup, F. Casanoves, J. S. Joswig, A. Gunther, V. Falczuk, N. Ruger, M. D. Mahecha, and L. D. Gorne. 2016. The global spectrum of plant form and function. *Nature* 529:167-U173.

Diffenbaugh, N. S., D. L. Swain, and D. Touma. 2015. Anthropogenic warming has increased drought risk in California. *Proceedings of the National Academy of Sciences of the United States of America* 112:3931-3936.

Donoghue, M. J. 2008. A phylogenetic perspective on the distribution of plant diversity. *Proceedings of the National Academy of Sciences of the United States of America* 105:11549-11555.

Drummond, A. J., M. A. Suchard, D. Xie, and A. Rambaut. 2012. Bayesian phylogenetics with BEAUti and the BEAST 1.7. *Molecular Biology and Evolution* 29:1969-1973.

Dunbar-Co, S., M. J. Sporck, and L. Sack. 2009. Leaf trait diversification and design in seven rare taxa of the Hawaiian *Plantago* radiation. *International Journal of Plant Sciences* 170:61-75.

Edwards, E. J. 2006. Correlated evolution of stem and leaf hydraulic traits in *Pereskia* (Cactaceae). *New Phytologist* 172:479-489.

Edwards, E. J., C. P. Osborne, C. A. E. Stromberg, S. A. Smith, W. J. Bond, P. A. Christin, A. B. Cousins, M. R. Duvall, D. L. Fox, R. P. Freckleton, O. Ghannoum, J. Hartwell, Y. S. Huang, C. M. Janis, J. E. Keeley, E. A. Kellogg, A. K. Knapp, A. D. B. Leakey, D. M. Nelson, J. M. Saarela, R. F. Sage, O. E. Sala, N. Salamin, C. J. Still, B. Tipple, and C. G. Consortium. 2010. The origins of C-4 grasslands: Integrating evolutionary and ecosystem science. *Science* 328:587-591.

Edwards, E. J., D. S. Chatelet, L. Sack, and M. J. Donoghue. 2014. Leaf life span and the leaf economic spectrum in the context of whole plant architecture. *Journal of Ecology* 102:328-336.

Evert, R. F. 2006. Esau's plant anatomy: Meristems, cells, and tissues of the plant body – their structure, function, and development, 3rd ed. John Wiley & Sons, Inc. Hoboken, New Jersey, USA.

Fajardo, A., and F. I. Piper. 2011. Intraspecific trait variation and covariation in a widespread tree species (*Nothofagus pumilio*) in southern Chile. *New Phytologist* 189:259-271.

Felsenstein, J. 1985. Phylogenies and the comparative method. *American Naturalist* 125:1-15.

Freckleton, R. P., P. H. Harvey, and M. Pagel. 2002. Phylogenetic analysis and comparative data: a test and review of evidence. *American Naturalist* 160:712-726.

Garland, T., A. F. Bennett, and E. L. Rezende. 2005. Phylogenetic approaches in comparative physiology. *Journal of Experimental Biology* 208:3015-3035.

Garnier, E., J. L. Salager, G. Laurent, and L. Sonie. 1999. Relationships between photosynthesis, nitrogen and leaf structure in 14 grass species and their dependence on the basis of expression. *New Phytologist* 143:119-129.

Global Biodiversity Information Facility, multiple contributors. 2012. GBIF Network Version 1.0. Website http://links.gbif.org/ [accessed 21 September 2016].

Gibson, A. C. 1983. Anatomy of photosynthetic old stems of nonsucculent dicotyledons from North American deserts. *Botanical Gazette* 144:347-362.

Givnish, T. J. 1987. Comparative studies of leaf form – assessing the relative roles of selective pressures and phylogenetic constraints. *New Phytologist* 106:131-160.

Givnish, T. J., and R. A. Montgomery. 2014. Common-garden studies on adaptive radiation of photosynthetic physiology among Hawaiian lobeliads. *Proceedings of the Royal Society B-Biological Sciences* 281.

Hacke, U. G., and J. S. Sperry. 2001. Functional and ecological xylem anatomy. *Perspectives in Plant Ecology Evolution and Systematics* 4:97-115.

Hill, R. S. 1998. Fossil evidence for the onset of xeromorphy and scleromorphy in Australian Proteaceae. *Australian Systematic Botany* 11:391-400.

Ivanova, L. A., P. K. Yudina, D. A. Ronzhina, L. A. Ivanov, and N. Holzel. 2018. Quantitative mesophyll parameters rather than whole-leaf traits predict response of C-3 steppe plants to aridity. *New Phytologist* 217:558-570.

Jacobsen, A. L., R. B. Pratt, S. D. Davis, and F. W. Ewers. 2007. Cavitation resistance and seasonal hydraulics differ among three arid Californian plant communities. *Plant Cell and Environment* 30:1599-1609.

Jacobsen, A. L., R. B. Pratt, S. D. Davis, and F. W. Ewers. 2008. Comparative community physiology: nonconvergence in water relations among three semi-arid shrub communities. *New Phytologist* 180:100-113.

Jepson Flora Project (eds.) 2017. Jepson eFlora, Website http://ucjeps.berkeley.edu/IJM.html [accessed 14 October 2017].

John, G. P., C. Scoffoni, and L. Sack. 2013. Allometry of cells and tissues within leaves. *American Journal of Botany* 100:1936-1948.

Jordan, G. J., P. H. Weston, R. J. Carpenter, R. A. Dillon, and T. J. Brodribb. 2008. The evolutionary relations of sunken covered, and encrypted stomata to dry habitats in Proteaceae. *American Journal of Botany* 95:521-530.

Kauffman, M., T. Parker, and M. Vasey. 2015. Field guide to manzanitas: California, North America, and Mexico, 1st ed. Backcountry Press, Oceanside, California, USA.

Keeley, J. E. 1975. Longevity of nonsprouting *Ceanothus. American Midland Naturalist* 93:504-507.

Keeley, J. E., W. J. Bond, R. A. Bradstock, J. G. Pausas, and P. W. Rundel. 2012. Fire in Mediterranean ecosystems: Ecology, evolution and management. Cambridge University Press, New York, New York, USA.

Keeley, J. E., and P. H. Zedler. 1978. Reproduction of chaparral shrubs after fire – comparison of sprouting and seeding strategies. *American Midland Naturalist* 99:142-161.

Kubitzki, K. 2004. Flowering Plants – Dicotyledons: Celstrales, Oxidales, Rosales, Cornales, Ericales. Springer, Hamburg, Germany.

Lamont, B. B., P. K. Groom, and R. M. Cowling. 2002. High leaf mass per area of related species assemblages may reflect low rainfall and carbon isotope discrimination rather than low phosphorus and nitrogen concentrations. *Functional Ecology* 16:403-412.

Larter, M., S. Pfautsch, J. C. Domec, S. Trueba, N. Nagalingum, and S. Delzon. 2017. Aridity drove the evolution of extreme embolism resistance and the radiation of conifer genus *Callitris*. *New Phytologist* 215:97-112.

Marechaux, I., M. K. Bartlett, L. Sack, C. Baraloto, J. Engel, E. Joetzjer, and J. Chave. 2015. Drought tolerance as predicted by leaf water potential at turgor loss point varies strongly across species within an Amazonian forest. *Functional Ecology* 29:1268-1277.

Mason, C. M., and L. A. Donovan. 2015. Evolution of the leaf economics spectrum in herbs: Evidence from environmental divergences in leaf physiology across *Helianthus* (Asteraceae). *Evolution* 69:2705-2720.

McKown, A. D., M. E. Akamine, and L. Sack. 2016. Trait convergence and diversification arising from a complex evolutionary history in Hawaiian species of *Scaevola*. *Oecologia* 181:1083-1100.

Messier, J., B. J. McGill, and M. J. Lechowicz. 2010. How do traits vary across ecological scales? A case for trait-based ecology. *Ecology Letters* 13:838-848.

Nardini, A., G. Peda, and N. La Rocca. 2012. Trade-offs between leaf hydraulic capacity and drought vulnerability: Morpho-anatomical bases, carbon costs and ecological consequences. *New Phytologist* 196:788-798.

Niinemets, U. 1999. Components of leaf dry mass per area – thickness and density – alter leaf photosynthetic capacity in reverse directions in woody plants. *New Phytologist* 144:35-47.

Niinemets, U. 2001. Global-scale climatic controls of leaf dry mass per area, density, and thickness in trees and shrubs. *Ecology* 82:453-469.

Oksanen, J., F. G. Blanchet, R. Kindt, P. Legendre, P. R. Minchin, R. B. O'Hara, G. L. Simpson, P. Solymos, M. H. Stevens, and H. Wagner. 2016. Vegan: community ecology package. R package version 2.3-4. http://CRAN.R-project.org/package=vegan

Pasquet-Kok, J., C. Creese, and L. Sack. 2010. Turning over a new 'leaf': Multiple functional significances of leaves versus phyllodes in Hawaiian *Acacia koa. Plant Cell and Environment* 33:2084-2100.

Pfautsch, S., M. Harbusch, A. Wesolowski, R. Smith, C. Macfarlane, M. G. Tjoelker, P. B. Reich, and M. A. Adams. 2016. Climate determines vascular traits in the ecologically diverse genus Eucalyptus. *Ecology Letters* 19:240-248.

Pivovaroff, A., R. Sharifi, C. Scoffoni, L. Sack, and P. Rundel. 2014. Making the best of the worst of times: Traits underlying combined shade and drought tolerance of *Ruscus aculeatus* and *Ruscus microglossum* (Asparagaceae). *Functional Plant Biology* 41:11-24.

Poole, D. K., and P. C. Miller. 1981. The distribution of plant water-stress and vegetation characteristics in Souhtern-California chaparral. *American Midland Naturalist* 105:32-43.

Poorter, H., U. Niinemets, L. Poorter, I. J. Wright, and R. Villar. 2009. Causes and consequences of variation in leaf mass per area (LMA): A meta-analysis. *New Phytologist* 182:565-588.

Poorter, H., and L. Sack. 2012. Pitfalls and possibilities in the analysis of biomass allocation patterns in plants. *Frontiers in Plant Science* 3: 259.

Pratt, R. B., A. L. Jacobsen, K. A. Golgotiu, J. S. Sperry, F. W. Ewers, and S. D. Davis. 2007. Life history type and water stress tolerance in nine California chaparral species (Rhamnaceae). *Ecological Monographs* 77:239-253.

Pratt, R. B., A. L. Jacobsen, J. Hernandez, F. W. Ewers, G. B. North, and S. D. Davis. 2012. Allocation tradeoffs among chaparral shrub seedlings with different life history types (Rhamnaceae). *American Journal of Botany* 99:464-1476.

Reich, P. B., D. S. Ellsworth, M. B. Walters, J. M. Vose, C. Gresham, J. C. Volin, and W. D. Bowman. 1999. Generality of leaf trait relationships: A test across six biomes. *Ecology* 80:1955-1969.

Reich, P. B., M. B. Walters, and D. S. Ellsworth. 1997. From tropics to tundra: Global convergence in plant functioning. *Proceedings of the National Academy of Sciences of the United States of America* 94:13730-13734.

Retamales, H. A., and T. Scharaschkin. 2014. A staining protocol for identifying secondary compounds in Myrtaceae. *Applications in Plant Sciences* 2: 1400063.

Revell, L. J. 2012. phytools: an R package for phylogenetic comparative biology (and other things). *Methods in Ecology and Evolution* 3:217-223.

Roth-Nebelsick, A., F. Hassiotou, and E. J. Veneklaas. 2009. Stomatal crypts have small effects on transpiration: A numerical model analysis. *Plant Physiology* 151:2018-2027.

Royer, D. L., L. Sack, P. Wilf, C. H. Lusk, G. J. Jordan, U. Niinemets, I. J. Wright, M. Westoby, B. Cariglino, P. D. Coley, A. D. Cutter, K. R. Johnson, C. C. Labandeira, A. T. Moles, M. B. Palmer, and F. Valladares. 2007. Fossil leaf economics quantified: Calibration, Eocene case study, and implications. *Paleobiology* 33:574-589.

Sack, L., P. D. Cowan, N. Jaikumar, and N. M. Holbrook. 2003. The 'hydrology' of leaves: Co-ordination of structure and function in temperate woody species. *Plant Cell and Environment* 26:1343-1356.

Sack, L., and K. Frole. 2006. Leaf structural diversity is related to hydraulic capacity in tropical rain forest trees. *Ecology* 87:483-491.

Sack, L., and C. Scoffoni. 2013. Leaf venation: Structure, function, development, evolution, ecology and applications in the past, present and future. *New Phytologist* 198:983-1000.

Saruwatari, M.W. and S. D. Davis. 1989. Tissue water relations of three chaparral shrub species after wildfire. *Oecologia* 80:303-308.

Scoffoni, C., D. S. Chatelet, J. Pasquet-kok, M. Rawls, M. J. Donoghue, E. J. Edwards, and L. Sack. 2016. Hydraulic basis for the evolution of photosynthetic productivity. *Nature Plants* 2:8.

Scoffoni, C., J. Kunkle, J. Pasquet-Kok, C. Vuong, A. J. Patel, R. A. Montgomery, T. J. Givnish, and L. Sack. 2015. Light-induced plasticity in leaf hydraulics, venation, anatomy, and gas exchange in ecologically diverse Hawaiian lobeliads. *New Phytologist* 207:43-58.

Scoffoni, C., M. Rawls, A. McKown, H. Cochard, and L. Sack. 2011. Decline of leaf hydraulic conductance with dehydration: Relationship to leaf size and venation architecture. *Plant Physiology* 156:832-843.

Scoffoni, C., C. Vuong, S. Diep, H. Cochard, and L. Sack. 2014. Leaf shrinkage with dehydration: Coordination with hydraulic vulnerability and drought tolerance. *Plant* Physiology 164:1772-1788.

Sheffield, J., and E. F. Wood. 2008. Global trends and variability in soil moisture and drought characteristics, 1950-2000, from observation-driven simulations of the terrestrial hydrologic cycle. *Journal of Climate* 21:432-458.

Shipley, B., M. Belluau, I. Kuhn, N. A. Soudzilovskaia, M. Bahn, J. Penuelas, J. Kattge, L. Sack, J. Cavender-Bares, W. A. Ozinga, B. Blonder, P. M. van Bodegom, P. Manning, T. Hickler, E. Sosinski, V. D. Pillar, V. Onipchenko, and P. Poschlod. 2017. Predicting habitat affinities of plant species using commonly measured functional traits. *Journal of Vegetation Science* 28:1082-1095.

Sofo, A., S. Manfreda, M. Fiorentino, B. Dichio, and C. Xiloyannis. 2008. The olive tree: A paradigm for drought tolerance in Mediterranean climates. *Hydrology and Earth System Sciences* 12:293-301.

Sokal, R. R., and F. J. Rohlf. 1995. Biometry, 3rd ed. Freeman, New York, New York, USA.

Sperry, J. S., U. G. Hacke, and J. K. Wheeler. 2005. Comparative analysis of end wall resistivity in xylem conduits. *Plant Cell and Environment* 28:456-465.

Stahl, U., B. Reu, and C. Wirth. 2014. Predicting species' range limits from functional traits for the tree flora of North America. *Proceedings of the National Academy of Sciences of the United States of America* 111:13739-13744.

Stebbins, G. L., and J. Major. 1965. Endemism and speciation in California flora. *Ecological Monographs* 35:1-35.

Tosens, T., U. Niinemets, M. Westoby, and I. J. Wright. 2012. Anatomical basis of variation in mesophyll resistance in eastern Australian sclerophylls: News of a long and winding path. *Journal of Experimental Botany* 63:5105-5119.

Trabucco, A., and Zomer, R.J. 2009. Global Potential Evapo-Transpiration (Global-PET) and Global Aridity Index (Global-Aridity) Geo-Database. CGIAR Consortium for Spatial Information. Website http://www.csi.cgiar.org [accessed 12 October 2015].

Uhl, D., and V. Mosbrugger. 1999. Leaf venation density as a climate and environmental proxy: A critical review and new data. *Palaeogeography Palaeoclimatology Palaeoecology* 149:15-26.

Venturas, M. D., E. D. MacKinnon, H. L. Dario, A. L. Jacobsen, R. B. Pratt, and S. D. Davis. 2016. Chaparral shrub hydraulic traits, size, and life history types relate to species mortality during California's historic drought of 2014. *Plos One* 11:22.

Warton, D. I., I. J. Wright, D. S. Falster, and M. Westoby. 2006. Bivariate line-fitting methods for allometry. *Biological Reviews of the Cambridge Philosophical Society* 81: 259–291.

Wright, I. J., N. Dong, V. Maire, I. C. Prentice, M. Westoby, S. Diaz, R. V. Gallagher, B. F. Jacobs, R. Kooyman, E. A. Law, M. R. Leishman, U. Niinemets, P. B. Reich, L. Sack, R. Villar, H. Wang, and P. Wilf. 2017. Global climatic drivers of leaf size. *Science* 357:917.

Wright, I. J., P. B. Reich, M. Westoby, D. D. Ackerly, Z. Baruch, F. Bongers, J. Cavender-Bares, T. Chapin, J. H. C. Cornelissen, M. Diemer, J. Flexas, E. Garnier, P. K. Groom, J. Gulias, K. Hikosaka, B. B. Lamont, T. Lee, W. Lee, C. Lusk, J. J. Midgley, M. L. Navas, U. Niinemets, J. Oleksyn, N. Osada, H. Poorter, P. Poot, L. Prior, V. I. Pyankov, C. Roumet, S. C. Thomas, M. G. Tjoelker, E. J. Veneklaas, and R. Villar. 2004. The worldwide leaf economics spectrum. *Nature* 428:821-827.

Wylie, R. B. 1954. Leaf organization of some woody dicotyledons from New-Zealand. *American Journal of Botany 41*:186-191.

CHAPTER 3

VARIATION IN RELATIVE GROWTH AND ADAPTATION TO ARIDITY ACROSS *ARABIDOPSIS* ECOTYPES: DOES LACK OF A TRADE-OFF CONTRIBUTE TO A WIDE SPECIES RANGE?

ABSTRACT

Fundamental ecophysiological theories have hypothesized intrinsic trade-offs between plant relative growth rate in high resource conditions (RGR) versus the ability to tolerate stresses, across and within species, arising from morphological and physiological traits. Yet, tests for a trade-off between RGR and cold or drought tolerance across species have yielded contrary results, and few studies have considered ecotypes within a species. For 15 ecotypes of *Arabidopsis thaliana* grown in a common garden we tested for the existence of a strict trade-off between RGR and adaptation to cold or dry native climates and its mediation by traits. Ecotypes native to warmer or drier climates had higher leaf density, leaf mass per area (LMA), root mass fraction (RMF), nitrogen per leaf area (N_{area}), carbon isotope ratio ($\delta^{13}C$) and lower osmotic potential at full turgor (π_o). However, RGR was unrelated to measured functional traits and was statistically independent of rainfall and cold climates of the native range. The lack of an intrinsic trade-off between RGR and cold or drought adaptation for *Arabidopsis* would contribute to both its large geographic range and its climate sensitivity.

Keywords: Climate, plant, trade-off, stress, *Arabidopsis*, relative growth rate

INTRODUCTION

Climate change is increasingly impacting plant populations and species across a diversity of ecological contexts worldwide, necessitating general principles for prediction (Cook *et al.* 2004; Cayan *et al.* 2008; AghaKouchak *et al.* 2014; Diffenbaugh *et al.* 2015; Fournier-Level *et al.* 2016). Many have hypothesized that one strong constraint on the physiology and distribution of species with respect to climate is an intrinsic trade-off within or among species between growth and adaptation to stress, including cold or arid climates (Grime, 1974; Grime, 1977; Smith & Huston 1990; Sartori *et al.* 2019). However, these trade-offs have remained controversial, and many tests within and across species have reported diverse "growth-stress tolerance relationships" (GSTRs; reviewed in Table S3.1). Some studies supported a trade-off within or across species (Polley *et al.* 2002; Griffith *et al.* 2007; Darychuk *et al.* 2012; Koehler & Cavender-Bares 2012; Molina-Montenegro *et al.* 2012; Lopez-Iglesias *et al.* 2014; Kaproth & Cavender-Bares 2016; Leites *et al.* 2019; Lubbe & Henry 2019; Sartori *et al.* 2019; Ramirez-Valiente *et al.* 2020), but others found that growth rate and adaptation to cold or dry climates were positively coordinated (Kenney *et al.* 2014; Ramirez-Valiente *et al.* 2017; Vasseur *et al.* 2018; Ramirez-Valiente *et al.* 2020), or concluded that growth rates were decoupled from cold or drought tolerance (Fernández & Reynolds 2000; Polley *et al.* 2002; McKay *et al.* 2003; Sack 2004; Sanchez-Gomez *et al.* 2006; Sanchez-Gomez *et al.* 2008; Atwell *et al.* 2010; Mukherjee *et al.* 2011; Bristiel *et al.* 2018; Leites *et al.* 2019; Jung *et al.* 2020). Notably, assessing the generality of GSTRs is complicated by the measurement of different variables for growth under controlled conditions in different studies (i.e., absolute or relative growth rates) and of different measures of adaptation to cold or drought (i.e., climatic aridity of the native range, or cold or drought tolerance with respect to experimental growth or survival under stress). Overall, of the

23 studies we reviewed, 8 showed support for a trade-off, 2 for positive coordination, 7 for decoupling, and 6 had mixed results (Table S3.1). The aim of this study was to test for an intrinsic trade-off between RGR and adaptation to cold and drought and their putative basis in functional traits. We focused on ecotypes of a particularly significant genetic and ecological model, an annual herb with a very wide climatic distribution, *Arabidopsis thaliana* (referred to as Arabidopsis henceforth). Our study is particularly novel in focusing on phenotypic traits related cold and drought tolerance and testing for a role in constraining RGR across ecotypes, which would have important implications for understanding the ecological ranges of ecotypes and species.

Indeed, the hypothesized general relationships across species between growth rates and adaptation to cold or aridity have been based on trait-based physiological mechanisms, relating to biomass allocation, morphology, and composition. Thus, some have hypothesized that trade-offs would arise if plants achieve tolerance of cold or drought by allocating to higher root mass fraction (RMF) and higher leaf mass per area (leaf dry mass divided by leaf area; LMA), which, by entailing allocation away from photosynthetic leaf surface, would reduce relative growth rate (RGR; Smith & Huston 1989; Sterck *et al.* 2011; Poorter *et al.* 2012). The general relationships among leaf traits often described across plant species as the "leaf economics spectrum" (LES; Wright *et al.* 2004) have been hypothesized to contribute to a trade-off. The LES hypothesizes relationships between several traits associated with carbon and nutrient acquisition that lead to either slow or rapid use of resources. Previous work in Arabidopsis has suggested that high leaf mass per area (LMA; the inverse of SLA) and low leaf nitrogen per area and per mass (N_{area} and N_{mass}) are aligned with rapid or slow completion of the lifecycle and thus with colder or drier habitats, at the expense of high RGR (Sartori *et al.* 2019). Further, many plants may achieve cold

or drought tolerance through additional adaptations that involve biochemical costs, which might reduce RGR, such as a high osmotic concentration, which results in a lower wilting point, and also may contribute to chilling or freezing tolerance (Parker 1963; Gonzalez-Zurdo *et la.* 2016). Further, a high osmotic concentration may increase epidermal pressure around the stomata in well hydrated leaves, potentially reducing maximum rates of gas exchange and RGR (Henry *et al.* 2019). By contrast, a positive coordination between RGR and success in cold or dry climates may arise in "stress-avoiding" or "pulse-driven" species, i.e., deciduous species, or annual species, if growth-promoting traits enable a high RGR when resources are available and thereby mitigate a shorter growing season (Maximov 1931; Grubb 1998; McKay *et al.* 2003; Kikuzawa *et al.* 2013; Kenney *et al.* 2014; Vitasse *et al.* 2014; Gonzalez-Zurdo *et al.* 2016; Table S3.1). Finally, RGR and stress tolerance may be decoupled if species can adapt to stress via traits without an overall direct detrimental effect on RGR, such as, for example, a smaller leaf size, or increased cell wall flexibility or cell membrane stability (Wanner & Junttila 1999; Fernández & Reynolds 2000; Sack 2004; Sanchez-Gomez *et al.* 2006; Sanchez-Gomez *et al.* 2008; Yadav 2010; Mukherjee *et al.* 2011; Wright *et al.* 2017; Bristiel *et al.* 2018; Ding *et al.* 2019; Jung *et al.* 2020; Table S3.1).

Notably, while GSTRs have been proposed based on individual plant-based ecophysiological theory, they can have profound effects on community ecology and biogeography and predictions of species responses to climate change (Grime 1974; Grime 1977; Orians & Solbrig 1977; Coley *et al.* 1985; Smith & Huston 1989; Latham 1992; Fine *et al.* 2006; Sterck *et al.* 2011). GSTRs, if general, could affect specialization in high versus low stress niches, their diversity within and across and their range widths (synthesis in 3. 1), and how these properties may shift with ongoing climate change (Midgley *et al.* 2002; Medina-Villar *et al.*

2020; Pareek *et al.* 2020). In particular, a trade-off in maximum RGR with cold or drought tolerance across ecotypes would in principle result in a smaller species climatic range relative to a positive coordination or decoupling (Appendix 3.1).

Ecotypes of model species *Arabidopsis thaliana* provide an ideal test bed for the putative trade-off between RGR and adaptation to cold or dry climates across ecotypes, and its basis in functional traits. Two previous studies have reported the growth of ecotypes of known native climates (Atwell *et al.* 2010; Vasseur *et al.* 2018; Fig. S3.1). One study tested linear correlations of growth with climate variables across 451 ecotypes and suggested a trade-off between RGR and cold adaptation, and a positive coordination of RGR with dry climate adaptation (Vasseur *et al.* 2018; Table S3.1). However, our re-analysis of these data showed a wide range of RGR across climates, including high RGR ecotypes both in cold and very warm climates, such that a U-shaped relationship was statistically selected over a linear model for RGR versus MAT (Fig. S3.1A-B; Tables S3.1 and S3.2). Data from a second study of 107 Arabidopsis ecotypes indicated positive coordination of RGR with cold climates and decoupling of RGR from dry climate adaptation (our analysis of data of Atwell *et al.* 2010; Fig. 3.1SC-D; Tables S3.1 and S3.2). Notably, these previous studies estimated RGR from rosette area expansion, which can differ from mass-based RGR, which better represents whole-plant function (Inman-Narahari *et al.* 2014; Falster *et al.* 2018), and did not quantify functional trait-based mechanisms for these patterns.

We tested for a strict intrinsic trade-off across ecotypes between growth in the common garden and adaptation to cold and/or dry climates. We further hypothesized that adaptation to climate may be related to the underlying components of RGR, i.e., specific leaf area (SLA), leaf mass fraction (LMF), leaf area ratio (LAR) and unit leaf rate (ULR), as RGR = ULR × LAR,

where LAR = SLA × LMF (Evans 1972; Hunt 1990; Lambers *et al.* 2017). Additionally, we hypothesized that traits, such as LMA, N_{area}, N_{mass} and chlorophyll per area would be correlated through the leaf economics spectrum (Wright *et al.* 2004), and would influence RGR. Finally, we hypothesized that RGR would be related to additional morphological and physiological traits, including root mass fraction (RMF), leaf thickness, density and size, and the leaf osmotic potential at full turgor (π_o), the main biophysical determinant of wilting point (i.e., turgor loss point; Bartlett *et al.* 2012a; Bartlett *et al.* 2012b; Fletcher *et al.* 2018; Griffin-Nolan *et al.* 2019), as described in the published literature comparing diverse species. We also hypothesized that ecotypes adapted to tolerance of cold or dry climates, or to avoiding climatic extremes, would differ in those traits in specific ways (reviewed in Table 3.1). We focused on 15 Arabidopsis ecotypes representing populations native to a range of climates across Europe and Asia, diverse in climate of origin and life history, from the 1001 Genomes Project (Weigel & Mott 2009), and grown in a greenhouse common garden (Table 3.2). We also considered the implications of the relationships of the maximum RGR in ideal conditions with adaptation to cold and/or dry climates for the native range of the species, and its responses to climate warming and aridification.

METHODS

Growth conditions

We grew 15 *Arabidopsis thaliana* ecotypes in a climate-controlled greenhouse common garden at the University of California, Los Angeles. Seeds were acquired from the collection of the 1001 Genotypes Project (Weigel & Mott 2009; Alonso-Blanco *et al.* 2016) and were maintained at The Arabidopsis Information Resource (TAIR; Huala *et al.* 2001), and bulked up in the

experimental greenhouse. Ecotypes therefore represent individual populations from which multiple individuals were sampled, to demonstrate phenotypic and genetic diversity within the populations. Our design focused on cultivated plants in a common garden under well-watered conditions and warm temperatures (19-33ºC) to provide detailed information of ecotypic variation in phenotypic traits and growth under favorable conditions, and to relate this to the native climates of the ecotypes in order to test for adaptations to different climates. Notably, the RGR in the experiment is that achieved under high resource conditions, to test for a trade-off between RGR and adaptation to stressful climates as hypothesized in the literature (see Introduction). We thus did not implement drought or cold treatments to directly assess drought or cold tolerance. Fifteen ecotypes were selected for variation in aridity index and temperature across seven of the Arabidopsis "origin" groups (Table 3.2; Trabucco & Zomer 2009). Seed for each ecotype was sown in lawns in trays of soil mix (18.75% washed plaster sand, 18.75% sandy loam, 37.5% peat moss, 12.5% perlite, 12.5% coarse vermiculite) in shallow pots (8 cm wide, 8 cm long, 9 cm deep) and placed in a cold room (4°C) on 13 April 2016, and moved to greenhouse benches on 18 April 2016. Seedlings of each ecotype were then transplanted two to a pot (n=17 pots per ecotype; 8 cm long, 12.3 cm wide, 6 cm deep) at the five true-leaf stage on 3-9 May 2016, randomized across two benches, and thinned to one seedling per pot two weeks later. Plants were staked after 3 weeks of growth. Ten plants of each ecotype were selected randomly for harvesting 21-23 June 2016. In the greenhouse, mean temperature was 22.9 °C (minimum and maximum were 20.6°C and 26.3°C, respectively), mean humidity was 48% (21-64%) and mean irradiance from 9:00 to 16:00 was 193 μmol photons m^{-2} s^{-1} (26-533 μmol photons m^{-2} s^{-1}; HOBO Micro Station with Smart Sensors, Onset, Bourne, MA, USA). Plants were watered 2-3 times per week with fertilized water (250 ppm of Peters Professional water

soluble fertilizer; N 20%; P 20%; K 20%; B 0.0125%; Cu 0.0125%; Fe 0.05%; Mn 0.025%; Mo 0.005%; Zn 0.025%).

Plant harvesting and biomass and trait measurements

The mass of fifty seeds of each ecotype divided by fifty was used to determine mean seed mass. On 3 May 2016, at the time of transplanting the five-leaf seedlings from lawns to pots, for the 12 ecotypes with seedlings abundantly available, an initial harvest was conducted of twenty-five seedlings per ecotype, enabling determination of mean initial seedling dry mass for this subset of the ecotypes. At maturity, i.e., between 69-71 days, after siliques had formed and just began to brown, ten individuals per ecotype were randomly selected for measurements, i.e., five plants for biomass harvesting and five for measurement of leaf osmotic potential at full turgor.

For biomass harvesting, plants were separated into photosynthetic and senescent leaves, inflorescence, basal stem and roots, which were washed free of soil, and all parts were dried at 70°C for at least 72 hours before dry mass was determined (XS205; Mettler, Toledo, OH, USA). Prior to drying, three randomly selected rosette leaves were traced for measurement of leaf area using ImageJ (version 1.46r), measured for leaf thickness (Fowler Digital Calipers, Chicago, IL, USA) and for chlorophyll concentration per leaf area, using a SPAD meter (SPAD-502; Konica Minolta Sensing Inc., Osaka, Japan), which provides measurements in SPAD units that correlate with total (a+b) chlorophyll per leaf area (Chl/area; Uddling *et al.* 2007). Root, leaf (rosette and inflorescence leaves), and other (basal stem, flower and fruit) mass fractions were calculated by dividing mass values by the plant total dry mass.

We note that the RGR in this study represents high resource growth in a greenhouse common garden. Relative growth rate (RGR; g g^{-1} day^{-1}) was calculated as

$$RGR = \frac{\ln\left(\frac{M_f}{M_0}\right)}{\Delta t} \qquad \text{(Eqn 1).}$$

where M_f is the dry mass at final harvest (g), M_0 is the initial mass (g), Δt is time (days between initial and final harvest). Absolute growth rate (AGR; g day^{-1}) was calculated as

$$AGR = \frac{M_f - M_0}{\Delta t} \qquad \text{(Eqn 2).}$$

RGR and AGR were determined in two ways; first, using M_0 for the seed mass for all 15 ecotypes (Kitajima 1994), and second, using the initial harvest seedling mass (five-leaf stage) for the 12 of 15 ecotypes for which sufficient seedlings were available for initial seedling harvest. As the AGR and RGR values resulting from these two calculations were highly correlated across ecotypes (r = 0.99 and 0.89 respectively; $P < 0.001$; n = 12), the more complete dataset for RGR using seed mass is presented, with the other dataset in the Table S3.3. M_f was also highly correlated with AGR (r = 0.99; $P < 0.001$), so AGR is presented in the text, with M_f data available in Table S3.3. Leaf mass fraction (LMF; g g^{-1}) was calculated as leaf mass (g) divided by M_f, leaf mass per area (LMA; g cm^{-2}) as leaf mass (g) divided by leaf area (cm^2), and leaf area ratio (m^2 g^{-1}) as leaf area divided by M_f. The unit leaf rate (ULR; g m^{-2} day^{-1}) was calculated as RGR divided by LAR. Leaf density (mg mm^{-3}) was calculated as LMA divided by leaf thickness (mm; Evans 1972). Root mass fraction (RMF; g g^{-1}) was also calculated as root mass (g) divided by M_f, and base and reproductive (including inflorescence stems, fruits and flowers) mass fractions were calculated as the mass of those parts (g) divided by M_f.

Nutrient data were obtained from 3 leaves each from 3-5 individual plants per genotype. Leaves were oven dried at 70°C for at least 72 hours. Liquid nitrogen was then poured over the leaves as they were ground with a mortar and pestle into a fine powder. 3-4mg of material were weighed into tin 4 × 6 capsules and were sent to the Center for Stable Isotope Biogeochemistry at the University of California, Berkeley. Carbon isotope ratio ($\delta^{13}C$) was measured by dual isotope analysis with an Elemental Analyzer interfaced to a mass spectrometer, along with the percent of nitrogen in the sample. Nitrogen per leaf mass (N_{mass}; mg g^{-1}) was determined as the mass nitrogen in the sample (mg) per the mass of the sample (g). Nitrogen per leaf area (N_{area}; g m^{-2}) was determined as N_{mass} multiplied by LMA.

The osmotic potential at full turgor (π_o) was estimated using the osmometer method (Bartlett *et al.* 2012a) on a randomly selected subset of eight ecotypes during the harvest period (Table 3.2). Whole plants were rehydrated overnight in plastic bags, and two leaf disks per each of five plants per ecotype were punched, immediately submerged in liquid Nitrogen, and placed into the osmometer to be measured for osmolality (VAPRO 5520 and 5600 vapor pressure osmometer, Wescor, Logan, UT, USA), which was then converted to π_o (Bartlett *et al.* 2012a). Individual and ecotype average data are available in Table S3.3. Notably, the turgor loss point (π_{TLP}) can be estimated from the osmometer measurement of π_o across species, but this was not done given that approach has not yet been validated within Arabidopsis (Bartlett *et al.* 2012a). Yet, previous studies have validated the use of π_o from the osmometer method as a test of drought tolerance across herb species (Griffin-Nolan *et al.* 2016) and across populations or cultivars of given species (Mart *et al.* 2015; Rosas *et al.* 2019).

Climate and flowering time data

We followed typical practice in the field by focusing on mean climate variables for our correlation tests using modeled climate variables at 1 km^2 based on the WorldClim database, assuming that the variation in modeled climate for the 15 ecotypes would correlate with true climate variation, given their large ranges in temperature and moisture in their sites of origin despite variation in microclimate experienced by Arabidopsis in the field. (Hancock *et al.* 2011; Lasky *et al.* 2012; Alonso-Blanco *et al.* 2016; Mojica *et al.* 2016; Vasseur *et al.* 2018; Sartori *et al.* 2019; Lorts & Lasky 2020). In addition, we estimated the maximum potential growing season based on climate variables (i.e., excluding the warmest, coldest, or driest months of the year; Lasky *et al.*, 2012). Coordinates for each ecotype were obtained from information provided by the 1001 Genomes Consortium 2016 (https://1001genomes.org/accessions.html). Mean annual temperature and annual precipitation climate variables were downloaded from WorldClim version 2.1 Global Climate Data (BioClim; http://www.worldclim.org/bioclim), and monthly temperature and precipitation variables were downloaded from WorldClim's historical climate database (Fick & Hijmans 2017). Additionally, aridity index was obtained from the Consultative Group for International Agriculture Research (CGIAR) Consortium for Spatial Information (CSI) database version 2 (Trabucco & Zomer 2019; Table S3.3). Climate information was extracted at each coordinate for each species using ArcMap (version 10.0). Growing season variables, including potential maximum length of the growing season, were calculated with historical climate data using data for the months with ≥ 4°C mean temperature and precipitation ≥ 2 × mean temperature (Lasky *et al.* 2012). Notably, Arabidopsis genotypes are very diverse in life history; some overwinter as rosettes and flower in early spring, while others germinate and complete their lifecycles in spring and/or early summer. However, this life history information is

not available for the genotypes in this study, and thus growing season variables are subject to a level of uncertainty. Consequently, we included these variables as previous studies have (Lasky *et al.* 2012), and describe these in the Results, though we feature mean annual variables in our plots, given they are subject to fewer assumptions, and they were correlated with growing season means (see Results). Flowering time information (days until first open flower) for each of the 15 ecotypes was obtained from the 1001 Genomes Consortium (Alonso-Blanco *et al.* 2016; Table S3.3), where plants were grown at a constant temperature of 10°C or 16°C after an initial cold treatment (FT10 and FT16, respectively).

Statistical analyses

Trait variation across ecotypes was tested using analyses of variance (*aov* function in the stats package) in the R Statistics environment (R version 3.5.1), which permitted testing for significant differences among ecotypes, and also quantification of the relative variation in traits within and among ecotypes.

To test relationships across ecotypes for growth variables, traits and climate variables, a linear mixed effects model with kinship was implemented using the *lmekin* function in the coxme package in R. Kinship matrices were pulled from the 1001 Genomes Project data release v3.1 (Weigel & Mott 2009). To test for both linear and nonlinear (power law) trends we used both untransformed and log-transformed data. Untransformed data with negative units (i.e. π_o and $\delta^{13}C$) were multiplied by -1 prior to analysis. Before log-transformation, for the mean annual temperature variable, which included a negative number, a constant equal to the lowest mean value for an ecotype +1 was added before log-transformation such that the lowest value for that variable was 1; for π_o and $\delta^{13}C$, all values were multiplied by -1. We present in the main text the

most significant of the findings (using untransformed or log-transformed data), with all results reported in Tables S3.4-S3.7.

Our analysis of the correlations of growth, traits and climate variables involved multiple significance tests. While published papers on trait-climate relationships often consider trait relationships with multiple climate variables without correction for multiple significance tests, to ensure the overall rigor of hypothesis testing, we added "omnibus" tests of each of the three overall hypotheses stated at the end of the Introduction, using proportion testing to consider the support for the overall hypotheses across multiple tests (Creese *et al* .2011; Pasquet-Kok *et al.* 2010; Waite & Sack 2010). We considered each overall hypothesis to be supported not if one of many relationships with multiple climate variables tested was significant in the expected direction, but only if the overall proportion of correlations tested for the hypothesis that were significant in the right direction was greater than 0.05 (with the difference in proportions tested using proportion tests, Minitab Release 15). Thus, for example, the overall hypothesis that LES traits would be inter-correlated was supported when 4/6 of the LES variables were related in the expected direction, i.e., a significantly higher proportion than 0.05 ($P < 0.001$).

Testing the correlations of RGR with its components can be influenced by the covariation among components. Therefore, to resolve the direct causal influences of components on RGR (i.e., ULR, LMF and SLA) responsible for differences in RGR among ecotypes, we used the causal partitioning approach of Buckley and Diaz-Espejo (2015). The idea behind this partitioning approach is that an infinitesimal change, dy, in some quantity y that depends on a number (N) of variables x_j (i.e., $y = f(x_1, x_2, ..., x_N)$), can be expressed as the sum of infinitesimal changes caused by each variable: $dy = \frac{\partial y}{\partial x_1} dx_1 + \frac{\partial y}{\partial x_2} dx_2 + \cdots + \frac{\partial y}{\partial x_N} dx_N = \sum_{j=1}^{N} \frac{\partial y}{\partial x_j} dx_j$. Integrating this expression between two conditions – a "reference state" ($y_r = f(x_{1r}, x_{2r}, ...)$) and a

"comparison" state ($y_c = f(x_{1c}, x_{2c}, ...)$) – produces a sum of finite terms representing the contributions of each variable x_j to the difference between y_c and y_r: $\int_r^c dy = y_c - y_r = \int_r^c \frac{\partial y}{\partial x_1} dx_1 + \int_r^c \frac{\partial y}{\partial x_2} dx_2 + \cdots + \int_r^c \frac{\partial y}{\partial x_N} dx_N = \sum_{j=1}^{N} \left[\int_r^c \frac{\partial y}{\partial x_j} dx_j \right]$. Expressing each term in this sum as a percentage of the total change in y then gives the % contribution of each x variable ($C(x_k)$) to the change in y:

$$\%\ contribution\ of\ x_k \equiv\ C(x_k) = 100 \cdot \frac{\int_r^c \frac{\partial y}{\partial x_k} dx_k}{\sum_{j=1}^{N} \left[\int_r^c \frac{\partial y}{\partial x_j} dx_j \right]} =\ 100 \cdot \frac{\int_r^c \frac{\partial y}{\partial x_k} dx_k}{y_c - y_r} \quad \text{(Eqn 3).}$$

The % contribution of any given variable can be positive or negative, but by definition they add up to 100%. A higher positive contribution for a factor indicates that on average, a species with higher RGR will tend to have it due that factor playing a more strong direct causative role; a negative contribution indicates that a species with higher RGR in fact tends to have that causative factor varying in the direction that would cause a lower RGR, and this effect is generally overcome by the other causative factors. We applied this method hierarchically: first we partitioned differences in ln(RGR) (= y) into contributions from ln(ULR) (= x_1) and ln(LAR) (= x_2); we then partitioned differences in ln(LAR) into contributions from ln(LMF) and ln(SLA). In each case, we repeated these calculations for every possible pairwise comparison between ecotypes (for 15 ecotypes, this gives 15!/[13!×2!] = 105 pairwise comparisons), with values for the ecotype with greater RGR representing the comparison state, and those for the ecotype with lesser RGR representing the reference state. The partial derivatives in each case were unity (e.g., $\partial \ln(RGR)/\partial \ln(ULR) = 1$), so the % contribution of each variable x_k was calculated simply as

$100 \cdot (x_{kr} - x_{kc})/(y_r - y_c)$. We then calculated the median value, over all 105 comparisons, for each variable's contribution (i.e., C(ln[ULR]) and C(ln[LAR]), and C(ln[LMF]) and C(ln[SLA])). Finally, we combined those results into a single set of three values (C(ln[ULR]), C'(ln[LMF]) and C'(ln[SLA[)) representing the contributions of ULR, LMF and SLA, respectively, to differences in RGR, by defining C'(ln[LMF]) = $0.01 \times C$(ln[LAR])$\times C$(ln[LMF]) and C'(ln[SLA]) = $0.01 \times C$(ln[LAR])$\times C$(ln[SLA])) so that C(ln[ULR]) + C'(ln[LMF]) + C'(ln[SLA]) = 100%.

RESULTS

Variation in growth and growth components across ecotypes

The 15 Arabidopsis ecotypes native to diverse climates varied substantially in growth rates (Table 3.1). Thus, absolute growth rate (AGR) varied 7.6-fold from 0.002-0.012 g g^{-1} day^{-1}, and relative growth rate (RGR) varied 1.3-fold from 0.12 to 0.16 g g^{-1} day^{-1} (Fig. 3.2A-B). The ecotypes varied over three-fold in specific leaf area (SLA) and seven-fold in leaf mass fraction (LMF) and unit leaf rate (ULR) (Fig. 3.2). Across ecotypes, the AGR, RGR correlated positively with flowering times published for the study ecotypes at 10°C (FT10) or 16°C (FT16), which themselves were correlated; $r = 0.57$, $P < 0.01$ Tables S3.4 and S3.5),

Variation in RGR was not correlated across ecotypes with any single one of its components, ULR, LAR, SLA or LMF. Comparing any pair of ecotypes showed that any component could be an important determinant of RGR differences. When one ecotype had greater RGR than another, this was primarily due to greater LMF (which contributed, on average across ecotypes, 100.9% of the difference in RGR), with much lesser contributions from greater ULR (10.5 on average) and smaller SLA (-11.4% on average). Thus, across ecotypes, LMF was the most important causal driver of RGR, with ULR and SLA having a comparatively small

impact on average, though important for explaining differences among a minority of the ecotypes (Table 3.3). Indeed, species with higher RGR values tended to have lower SLA values, and that influence is on average overcome by their higher ULR and especially higher LMF.

Variation in drought tolerance traits

Ecotypes varied strongly in all functional traits. Ecotypes varied by nearly tenfold in leaf area from 0.62 cm^2 to 5.88 cm^2 and in RMF from 0.018 g g^{-1} to 0.175 g g^{-1}, 2.6-fold in leaf thickness from 0.062 mm to 0.158 mm, and by -0.23 MPa in π_o from -0.79 MPa to -1.02 MPa (Fig. 3.2F). For most traits, two-thirds or more of the variation arose between rather than within ecotypes, except for root mass fraction (RMF) and osmotic potential at full turgor (π_o), for which half to a third of the variation arose between ecotypes, respectively (Table 3.1).

Correlations of traits with temperature variables

Across the 15 ecotypes, RGR and AGR were statistically independent of the mean precipitation, aridity and temperature of the native range (Fig. 3.1A-C; Fig. S3.2; Table S3.4). Notably, there was a nonsignificant empirical trend for higher RGR in ecotypes native to colder climate (P = 0.08; Fig. 3.1A). The π_o was related to two of the three temperature variables such that ecotypes with a more negative π_o were found in native climates with higher mean annual temperature and shorter growing seasons ($|r|$ = 0.62-0.76; P = 0.001-0.03). LMA and leaf thickness (LT) were also negatively related to length of the growing season (r = |0.50-0.56|, P = 0.01-0.02; Fig. 3.3C-D). However, across all traits expected to correlate with cold tolerance (Table 3.1), no relationships were significant in the expected direction (omnibus test P = 1.0).

Correlations of cold and drought-tolerance traits with climate

Across the 15 Arabidopsis ecotypes, 8/24 hypotheses of the relationships of morphological and physiological traits with native climate aridity were supported in the expected direction based on drought tolerance adaptation ($P < 0.001$; Table 3.1), while 2/42 were supported in the expected direction based on drought avoidance ($P = 0.63$; Table 3.1). LMA was higher and π_o was lower for ecotypes native to lower mean annual precipitation, precipitation of the growing season and aridity index ($|r| = 0.49\text{-}0.80$, $P < 0.05$; Fig. 3.3A-B; Tables S3.4, S3.5, S3.6 and S3.7). Leaf density, leaf nitrogen per area (N_{area}) and root mass fraction (RMF) were higher in species of more arid climates, i.e., negatively related to aridity index ($r = 0.48\text{-}0.51$, $P < 0.03$; Fig. 3.3C-E, Tables S3.4 and S3.5). A more negative value of $\delta^{13}C$ was associated with higher precipitation of the growing season ($r = 0.49$, $P = 0.03$; Fig. 3.4, Tables S3.4 and S3.5).

Correlations of leaf mass per area and economics traits

LMA was related to its components, leaf thickness and leaf density and with nitrogen per leaf mass (N_{mass}; $|r| = 0.47\text{-}82$, $P \leq 0.04$; Fig. 3.5A-C; Tables S3.4 and S3.5). Overall, LES traits were inter-correlated, with 4/6 trait-trait hypotheses supported in the expected direction. A higher LMA was associated with higher chlorophyll per area and N_{area} and a lower N_{mass} ($|r| = 0.068\text{-}0.89$, $P < 0.001$; Fig. 3.6A, Tables S3.4 and S3.5). Higher chlorophyll per area was correlated with higher N_{area} ($r = 0.89$, $P < 0.001$; Fig. 3.6B, Tables S3.4 and S3.5).

Correlations of leaf traits with relative growth rate and flowering times

The RGR was coordinated with several leaf traits, with 3/14 hypothesized relationships of RGR with other traits supported in the expected direction ($P < 0.005$; Table 3.1). Ecotypes with higher

RGR also had larger and thicker leaves with more chlorophyll per area (r = 0.46-0.59, P = 0.005-0.5; Fig. 3.7A-B, Tables S3.4 and S3.5). Leaf area was positively associated with LMF and LAR (r = 0.64-0.81, $P \leq 0.001$; Tables S3.4 and S3.5). RGR was negatively related to carbon isotope ratio ($\delta^{13}C$; r = -0.58, P = 0.006; Tables S3.4 and S3.5). Further, N_{mass} correlated with FT10, and leaf individual area and chlorophyll concentration (Chl/area), leaf mass fraction (LMF), $\delta^{13}C$ and nitrogen per area (N_{area}) with FT16 ($|r|$ = 0.45-0.63, P = 0.002-0.05; Tables S3.4 and S3.5).

DISCUSSION

Across the 15 *Arabidopsis* ecotypes, RGR under high resource conditions was not statistically associated with cold or arid native climates, or on average related to leaf economics traits or drought tolerance traits. While our study of 15 ecotypes could not preclude weak general trends that might emerge across a larger sampling of ecotypes, the lack of support for an RGR-stress tolerance trade-off across a diverse set of ecotypes measured in detail indicates no absolute or intrinsic physiologically-determined pattern as would have arisen according to hypotheses based on assumptions of trait-mediated trade-offs (Smith & Huston 1989; Fine *et al.* 2006; Sterck *et al.* 2011). We found that any potentially strict trait-based trade-off between growth and stress tolerance was overcome by independent variation in different traits. While some of the measured traits hypothesized to contribute to cold or drought tolerance were correlated across ecotypes with adaptation to cold or aridity, none of those traits were associated with RGR or AGR. The potential for traits to adapt independently to various climate stresses without cost to growth would contribute to the occupation of a very large climate range in this species. Indeed, the lack of an overall trade-off between RGR and climate variables is consistent with Arabidopsis ecotypes adapting to cold or dry climates through either tolerance mechanisms and/or avoidance,

i.e., mitigating the shorter growing period through rapid growth during a warm, moist growing period.

Coordination of RGR with adaptation to cold climates within Arabidopsis and trait-based mechanisms

Across the 15 ecotypes RGR was statistically independent of climate, with an empirical nonsignificant trend for more rapid growth of ecotypes native to colder climate ($P = 0.08$; Fig. 3.1A). This result is further evidence against a trade-off, and was consistent with our re-analysis of data for 107 ecotypes from Atwell *et al.* (2010; Fig. S3.1C-D), yet contrasted with a reported positive correlation of growth with climatic warmth by Vasseur *et al.* (2018) for 451 ecotypes (Fig. S3.1A-B). However, our re-analysis of the data of that study found a U-shaped relationship of RGR to MAT, indicating that the dominant trend over most of the climate range was for a higher RGR at lower MAT, with a high RGR also observed for ecotypes at the extreme hottest end of the range (Fig. S3.1A). Thus, the data are all consistent showing that while slow-growing ecotypes occur in cold climates, other ecotypes with high RGR may also be associated with regions experiencing cold winters, or very hot summers, i.e., stress-avoiding ecotypes that mitigate extreme temperatures through rapid growth in the shorter favorable season. Overall, weak or contrasting trends may be attributed to the fact that different ecotypes of Arabidopsis exhibit different life history strategies and can either tolerate stress or grow rapidly when resources are available and avoid growing through periods of stress (DeLeo *et al.* 2020).

Notably, flowering time is often considered a central trait in Arabidopsis ecology and evolution, linked with differences in growth and climate adaptation across ecotypes. Typically, species adapted to cold climates and faster RGR tend to have longer times to flowering, with a

great deal of variation around the trend (Debieu *et al.* 2013; Sartori *et al.* 2019). We found a non-significant trend across the ecotypes in our study, but a significant positive relationship of flowering time with RGR.

Decoupling of RGR from adaptation to aridity within Arabidopsis and trait-based mechanisms

We also found a lack of a trade-off between RGR and MAP across the 15 diverse ecotypes tested. This finding was consistent with our re-analysis of the data of Atwell *et al.* (2010) for 107 ecotypes, and that of Vasseur *et al.* (2018) for 451 ecotypes. Notably, Vasseur *et al.* (2018) did report that ecotypes native to drier climates had faster growth, as inferred from a scaling exponent of growth relative to size; our analysis of the RGR data from that study did not support that relationship, but instead supported statistical independence of RGR from native-climate aridity (Fig. S3.1). The decoupling of growth from adaptation to aridity in *Arabidopsis* indicates this adaptation is achieved via physiological and functional traits without a consistent directional influence on RGR. Thus, for example, a more negative π_o was associated with drier climates, and would provide drought tolerance by reducing leaf wilting point (Bartlett *et al.* 2012b). Though this trait would also constrain maximum stomatal conductance (Henry *et al.* 2019), the potential influence on reducing growth at plant scale could be offset by adjusting LMF or nitrogen allocation to photosynthesis. Other traits in our study likewise related to dry climates, i.e., leaf mass per area, seed mass and root mass fraction did not overall scale up to an influence on RGR.

Implications of decoupling of RGR from adaptation to cold and aridity

The lack of a strong intrinsic trade-off between RGR and adaptation to cold or arid climates across ecotypes has strong implications for the coexistence of genotypes and responses to

climate change. Overall, these findings suggest that ecotypes are likely to coexist. If trade-offs had existed, one would expect strong niche separation among fast-growing versus stress-tolerant ecotypes. The decoupling of RGR and climate adaptation is consistent with the existence of both stress tolerant and avoidant strategies under extreme climates. The decoupling of RGR from climatic aridity across ecotypes would also result in less niche separation than if a trade-off had existed, and thus contribute to the widespread distribution of Arabidopsis ecotypes and RGR with respect to water supply (Appendix 3.1). Indeed, slow or rapid RGR would not disadvantage given ecotypes across the range of aridity as ecotypes may adapt to climates with low annual rainfall by growing rapidly when water is available, and/or by extending their growth longer into the period of soil drying, consistent with the observed relationship of π_o to native climatic aridity in this set of ecotypes.

Based on our predictions from ecological theory and further considering the high degree of gene flow between most Arabidopsis populations in Europe (excluding populations of the Iberian Peninsula; Alonso-Blanco *et al.* 2016), the decoupling of growth from cold and drought adaptation would support a large species range given high gene flow (Appendix 3.1). This is consistent with the fact that Arabidopsis is spread across much of Europe and Asia, and now even occupies parts of North America (Alonso-Blanco *et al.* 2016). However, influence of climate change on this species' distribution is an avenue for future research. Indeed, a recent study of Arabidopsis leaves preserved in herbaria found that leaf traits such as carbon isotope ratio and C:N ratio shifted with climate change (DeLeo *et al.* 2020), and future work could investigate how physiological changes within a population may lead to exclusion or coexistence of genotypes with variable traits.

Drought tolerance and leaf economics trait correlations with RGR

Overall, drought tolerance traits such as π_o did not entail any constraint on RGR, indicating no support for a trade-off of growth and drought tolerance traits. However, several leaf traits were related to higher RGR and its most driving component, LMF, including larger, thicker leaves with greater water-use efficiency and higher chlorophyll concentration. Producing larger leaves can increase LMF and overall increase RGR in some cases (Conesa & Galmes 2019). Thicker leaves had a higher N_{area}, consistent with their having more cell layers, and would contribute to higher photosynthetic rates per leaf area (Ripullone *et al.* 2003; Wright *et al.* 2004). Yet, RGR was not strongly correlated with leaf economic spectrum traits, such as SLA, Narea or Nmass. Indeed, across the ecotypes, high RGR was driven strongly by multiple components, with high LMF being on average, and by far, the most important causal influence. These findings indicate that ecotypes may adapt to rapid RGR with a range of alternative trait combinations, i.e., via many-to-one mapping or trait multifunctionality (Marks & Lechowicz 2006; Sack & Buckley 2020).

Drawing inferences despite limitations of the experimental design

While our study was designed to test for strong intrinsic trade-offs between RGR and adaptation to cold and aridity using a set of 15 diverse ecotypes measured in detail, inference depends on several assumptions, which also highlight important aspects of the physiology of this widespread model species.

We considered the adaptation to cold and aridity by using the native range of the species, and tested the relationships with growth and traits as measured in a common garden. The strength of our common garden design is that it reduces the plastic changes with respect to the

environment, such that any observed differences are due to genetic variation between ecotypes (Cordell *et al.* 1998; Dunbar-Co *et al.* 2009; Givnish & Montgomery 2014; Mason & Donovan 2015). However, the growth measured in the common garden represents a maximum rate under high resource conditions, and plants in the field may achieve different RGRs according to abiotic and biotic field conditions, including nutrient and water availability (Fernández & Reynolds 2000). Further, the traits measured in the greenhouse do not reflect the potential acclimation of plants to cold or drought; in drying soil, plants may root more deeply, allocate more strongly to roots, and develop a higher LMA and a more negative osmotic potential (Huck *et al.* 1986; Poorter *et al.* 2009; Comas *et al.* 2013; Bartlett *et al.* 2014; Eziz *et al.* 2017). However, traits expressed in the common garden indicated adaptation to aridity without being associated with variation in RGR or AGR, indicating that these stress tolerance traits do not intrinsically constrain RGR or AGR across ecotypes.

The climate data we used represents the climate present at the sites from which seeds were originally collected for each ecotype (Weigel & Mott 2009). This method of climate data analysis is currently the standard in the field, though we acknowledge that climate data thus based on a single point may not fully represent of the mean climate of the ecotype's range, nor indeed the range of microclimates occupied in the field. Our ecotypes did not include ecotypes native to the hottest regions such as Spain, nor the full range of MAP represented in studies of more ecotypes, such as Vasseur *et al.* (2018) or Atwell *et al.* (2010), which may have contributed to the lack of a finding of association of RGR with climatic aridity. Nonetheless, the relationships of RGR with native climate in our study were consistent with those reported in the previous studies, and, indeed, if the trade-off between RGR and adaptation to dry climates were strict, we would have expected to find a relationship even in a small diverse ecotype set

representing semi-arid to humid climates. Similarly, our trait measurements for this set of 15 diverse ecotypes would likely not represent the full range of phenotypic variation across the species, which may decrease our ability to find relationships that have been shown across diverse species, though with this limited but diverse set of ecotypes, we could demonstrate the lack of an intrinsic, absolute growth versus stress tolerance trade-off (see John *et al.* 2013 for further discussion of inference from small sampling sets).

In our test of the putative growth versus stress tolerance trade-off we have assumed that cold- and drought-tolerances are represented by the temperature and aridity of ecotypes' native ranges. This assumption was supported by a recent study that has directly linked adaptation to dry climate in the native range with drought tolerance as assessed by survival in drying soil, showing for a set of 211 *Arabidopsis* ecotypes found that survival in a field experiment at a dry Mediterranean site correlated with survival in a drought experiment, and also with climatic aridity in the native range (our analysis of data of Exposito-Alonso *et al.* 2018; Fig. S3.3).

We note that our findings of the relationship of RGR with flowering time are dependent on the method of measurement. Studies that consider growth based on leaf area increment between germination and flowering, typically show in a negative correlation of AGR or RGR with flowering time, as ecotypes expand leaves more rapidly tend to do so over a shorter interval (Debieu *et al.* 2013; Sartori *et al.* 2019). However, in our study, we considered mass-based growth, focusing on a common growth interval, after which all the ecotypes had flowered, i.e., integrated across the full vegetative growth period, including the production of fruits, which is a typical approach when comparing species for their growth (Kitajima 1994; Sack 2004). In this design, we found a positive relationship between growth and flowering time, as expected, given that species that flowered later would grow over a longer interval. Thus, overall, the balance of

data suggest that flowering time is strongly linked with growth, but positively or negatively depending on the comparative growth measurements, but weakly with climate, and does not mediate a general trade-off.

Implications for seeking genes for variation in drought tolerance

Several studies have used Arabidopsis as a platform to discover genes and gene regions involved in climate adaptation. Previous studies have tested which climate variables explained genetic variation across Arabidopsis populations (Li *et al.* 2010; Hancock *et al.* 2011; Lasky *et al.* 2012; Bac-Molenaar *et al.* 2016; Frachon *et al.* 2018; Vasseur *et al.* 2018; Ferrero-Serrano & Assmann 2019), and sought to identify genes for water-use traits or drought survival across Arabidopsis populations (Ingram & Bartels 1996; Mojica *et al.* 2016; Exposito-Alonso *et al.* 2018). These studies have not tested many physiological traits most directly related to drought tolerance, such as π_o, which is an especially promising trait in conferring drought tolerance. Our results extend the theory of π_o diversification and the relationship of this trait to climate adaptation. Previous work had found the turgor loss point (π_{TLP}), of which π_o is the main determinant, to correlate with drought tolerance at multiple scales: across habitats (Bartlett *et al.* 2012b), diverse species (Bartlett *et al.* 2012b; Rosas *et al.* 2019), closely related species (Fletcher *et al.* 2018), and within species (Mart *et al.* 2016). Our results across Arabidopsis ecotypes confirm that traits such as π_o can predict plant drought tolerance. Bartlett *et al.* (2012b) found overall that despite the capacity of plants to osmotically adjust to different growth environments, this adjustment does not overwhelm the signal of the π_{TLP} and its relationship with drought tolerance except in certain crops. Future work should consider the importance of osmotic adjustment in Arabidopsis specifically. Such discoveries will have huge potential to be applied to crop breeding (Flavell

2005; Liu 2010; Chew & Halliday 2011) and in determining species' vulnerability to climate change (Exposito-Alonso *et al.* 2018). The lack of intrinsic trade-off between growth capacity and adaptation to aridity implies substantial flexibility that can enable crop breeding for combinations of rapid growth and climate tolerance.

Conclusions

Across ecotypes of Arabidopsis we found no evidence of a trade-off between relative growth rate (RGR) and cold or drought tolerance. We additionally found that RGR was not limited by any single one of its components, or constrained by functional traits related to cold or drought tolerance or avoidance. Based on ecological theory, these findings indicate that a lack of constraint on possible RGR values across ecotypes would contribute to the species' occupation of a large climatic range, and a decline in the diversity of ecotypes in response to climate change. Our results demonstrate a crucial need for understanding and establishing the physiological basis of trait-climate relationships and their implications for ecology.

ACKNOWLEDGMENTS

We thank Camila Medeiros, Jessica Smith and Weimin Deng for assistance with plant cultivation and data collection, Nathan Kraft for discussion of ecological principles and the National Science Foundation (Grants -#1457279, 1557906 and 1951244**)** and the National Institute of Food and Agriculture (Hatch project 1016439 and Award 2020-67013-30913) for support.

Table 3.1. Traits measured for 15 ecotypes of *Arabidopsis thaliana* grown experimentally, with hypotheses and rationales for expected correlation (positive, +, or negative, -) with cold or arid native climate due to adaptation for tolerance, or contribution to stress avoidance (i.e., contributing to rapid growth in the period with favorable climate), or contribution to a high relative growth rate (RGR). Hypotheses were compiled based on the published literature on Arabidopsis or other species, in general for comparisons of populations within species, or for comparisons across species. Measured trait variation is also presented (minimum, average (bold) and maximum mean ecotype values) with the results of an analysis of variance (ANOVA) testing for variation among ecotypes (mean squares, percentage of variance explained by differences among ecotypes (with the remainder being explained within ecotypes) significance levels for each trait; df, degrees of freedom; ns, $P>0.05$; *, $P<0.05$; **, $P<0.01$; ***, $P<0.001$). † Trait was measured using means; seed mass was measured as mean of 50 seeds per ecotype, and N_{area} was calculated using mean LMA and N_{mass}. ‡ Flowering times were reported as single mean values in Alonso-Blanco *et al.*, 2016. § df=7 for osmotic potential values.

Trait	Units	Hypothesized correlations with climatic temperature or moisture given adaptation to cold or aridity or to stress avoidance			Hypothe-sized relationship to RGR	Rationales for hypothesized linkages of traits with climate adaptation and RGR	Min Avg Max	ANOVA for differences among ecotypes; df=14
		Adaptation to cold	Adaptation to aridity	Stress avoidant				
Reproductive								
Seed Mass	g	+	+	+	+	Seedlings from large seeds tend to have greater cold or drought tolerance due to greater germination rates and greater ability to allocate to rapid root growth before stress, and, within a given species, seedlings from larger seeds tend to have higher RGR during establishment.[1, 2]	$1.56x10^{-5}$, **$2.14x10^{-5}$**, $3.86x10^{-5}$	na†
Flowering Time (FT10/FT16)	days	na	na	+/-	-	Early flowering genotypes can complete their life cycle earlier during favorable periods and better avoid stress[3] and tend to	60.5, **73.1**, 94.3/ 38.0, **57.0**, 89.3	na ‡

						have higher RGR.[3, 4, 5, 6, 7] Alternatively, early flowering can also increase the chance to experience late frost.[8]		
Components of Relative Growth Rate								
Unit Leaf Rate (ULR)	g m^{-2} day^{-1}	na	na	+	+	As a component of RGR, a higher ULR would confer faster growth during favorable periods and avoidance of stress periods.[9, 10]	4.93, **14.87**, 35.88	324.45, 0.65***
Leaf Mass Fraction (LMF)	g g^{-1}	-	-	+	+	A lower leaf mass fraction would confer greater tolerance of cold or drought due to a its representing a greater mass allocation to resource capture and storage below ground.[11] As a component of RGR, a higher LMF would confer faster growth during favorable periods and avoidance of stress periods.[9, 10]	0.11, **0.42**, 0.76	0.301, 0.79***
Leaf Mass per Area (LMA)	g m^{-2}	+	+	**-***	-	A higher LMA would confer greater tolerance of cold or drought, corresponding to lower evaporative surface and greater water mass per leaf area, and greater leaf mechanical protection.[11, 12] Specific leaf area, the inverse of LMA, is a component of RGR, and thus would confer faster growth during favorable periods and avoidance of stress periods.[9, 10, 13]	18.73, **30.51**, 59.18	760.87, 0.76***
Other biomass allocation								
Reproductive Mass Fraction (ReproMF)	g g^{-1}	na	na	+	-	Allocating more strongly to reproduction can potentially reflect earlier diversion of resources to complete the life cycle earlier during favorable periods and better avoid stress[2]. However, allocating more strongly to reproductive tissues may entail a cost to photosynthetic tissues contributing to RGR.[14]	0.07, **0.51**, 0.85	0.38, 0.81***
Root Mass Fraction (RMF)	g g^{-1}	+	+	-	-	A higher root mass fraction would confer greater tolerance of cold or drought due to a its representing a greater mass allocation to resource capture and storage below ground.[11] However, allocating more strongly to root tissues may entail a cost to photosynthetic tissues contributing to RGR.[15]	0.02, **0.08**, 0.17	0.012, 0.50***
Other leaf morphological traits								
Leaf Area (LA)	cm^2	-	-	+/-	+/-	Smaller leaf area results in a thinner boundary layer, and leaves more closely coupled with air temperature, thus avoiding overheating and chilling damage, and achieving higher photosynthetic rates and water use efficiency under dry conditions, as well as higher photosynthetic rates under	0.62, **2.57**, 5.88	11.35, 0.69***

						moist warm conditions, promoting more rapid growth in favorable climates.[16] Alternatively, larger leaves can increase LAR and thus increase RGR.[17]		
Leaf Thickness (LT)	mm	+	+	-	-	A thicker leaf would have higher LMA and the same influences as LMA, listed above.[12, 18]	0.06, **0.16**, 0.10	0.0049,0.77***
Leaf composition and biochemistry								
Chlorophyll per Area (Chl/area)	chlorophyll area^{-1}	na	na	+	+	A higher chlorophyll concentration may contribute to greater light harvesting and to faster RGR under favorable climates.[19]	19.49, **30.10**, 45.87	307.12, 0.80***
Osmotic potential at full turgor (π_o)	MPa	-	-*	+	+	A more negative osmotic potential may confer chilling tolerance and results in a more negative turgor loss point, directly conferring drought tolerance.[20, 21] However, the higher turgor pressure in hydrated leaves may restrict stomatal opening[22], with a negative consequence for RGR under favorable conditions.	-1.02, **-0.89**, -0.79	0.063, 0.33***§
Carbon isotope ratio ($\delta^{13}C$)	‰	na	-	+	-	A more negative carbon isotope ratio indicates greater discrimination against ^{13}C, suggesting more of their stomata are open, which would lead to increased photosynthesis and faster growth.[23, 24] Increases in $\delta^{13}C$ are related to increases in water use efficiency, aiding survival in arid climates.[25]	-33.53, **-31.65**, -29.01	7.28, 0.82***
Leaf nitrogen per mass (N_{mass})	mg g^{-1}	na	na	+	+	Higher leaf nitrogen content would enable faster photosynthetic rates per leaf mass or area[26], potentially allowing for rapid growth during periods of water availability.	34.11, **47.18**, 62.16	347.20, 0.58***
Leaf nitrogen per area (N_{area})	g m^{-2}	na	na	+	+	See above logic for N_{mass}	0.89, **1.36**, 2.31	na†

References: 1. Gomez 2004; 2. Turnbull *et al.* 2012; 3. Griffith & Watson 2005; 4. Kazan & Lyons 2016; 5. Kenney *et al.* 2014; 6. Meyre *et al.* 2001; 7. Vasseur *et al.* 2018; 8. Bigler & Bugmann 2018; 9. Hunt 1990; 10. Hunt & Cornelissen 1997; 11. Sack *et al.* 2003; 12. Gonzalez-Zurdo *et al.* 2016; 13. Poorter *et al.* 2009; 14. Sartori *et al.* 2019; 15. Poorter *et al.* 2012; 16. Wright *et al.* 2017; 17. Conesa & Galmes 2019; 18. Niinemets 2001; 19. Chaturvedi *et al.* 2011; 20. Bartlett *et al.* 2012b; 21. Parker 1963; 22. Henry *et al.* 2019; 23. Farquhar *et al.* 1989; 24. McKay *et al.* 2003; 25. Wang *et al.* 2003; 26. Wright *et al.* 2004

Table 3.2. Ecotypes of *Arabidopsis thaliana* grown experimentally, in order of ascending aridity index (with a larger value indicating greater humidity of the native climate), indicating substantial variation in leaf traits. Values of leaf mass per area are means with standard error in parentheses. Values of flowering time at 10°C (FT10) and 16°C (FT16) represent mean values for each ecotype (Alonso-Blanco *et al.* 2016). An asterisk indicates the ecotypes that were measured for osmotic potential at full turgor (π_o).

Ecotype	Origin Group	LMA (g m^2)	FT10 (days)	FT16 (days)	Aridity Index	MAP (mm $year^{-1}$)	MAT (°C)
CS76789*	Relict	46.4 (6.3)	62.75	47.25	0.1381	281	22.7
CS76649	Relict	24.7 (1.9)	63	41	0.2594	497	14.07
CS76532*	Asia	56.1 (5.4)	78.5	61.75	0.3047	493	14.21
CS77002*	Italy/Balkan/Caucasus	27.8 (1.1)	77.25	78.75	0.6707	773	12.16
CS76778 (Col-0)	Germany	22.6 (1.9)	70.5	38	0.7209	1023	13.12
CS76748	Central Europe	19.2 (1.5)	64	71.75	0.8632	806	10.93
CS76897*	Germany	20.9 (1.7)	68	48.75	0.789	640	7.32
CS76379*	Asia	59.2 (5.1)	79.25	73	0.5978	705	2.7
CS78855	Central Europe	26.1 (3.5)	94.25	58.75	0.8285	648	6.52
CS78888*	Admixed	30.0 (3.9)	71.75	51	0.923	838	9.54
CS76498	Germany	21.5 (3.2)	71	44.5	0.9858	801	8.35
CS78916*	Admixed	28.6 (1.8)	81.25	89.25	1.026	810	9.54
CS77170*	Central Europe	35.7 (3.6)	84.25	62.5	0.9717	705	4.72
CS76382	Asia	20.1 (2.5)	69.75	51.25	0.6389	557	-2.87
CS76623	Western Europe	18.7 (2.2)	60.5	38	1.7032	1572	10.03

Table 3.3. Causal partitioning of log-transformed values of relative growth rate (RGR) into its components, unit leaf rate (ULR), leaf mass fraction (LMF) and specific leaf area (SLA), to show how much of the observed differences in RGR across *Arabidopsis thaliana* ecotypes is due to differences in each component. Median values are displayed with the interquartile ranges.

Partitioning	Causal trait	Median % contribution	Interquartile range
RGR into ULR and LAR	ULR	10.5%	-734, 800
	LAR	89.5%	-700, 834
LAR into LMF and SLA	LMF	112.7%	59, 185
	SLA	-12.7%	-85, 41
RGR into ULR, LMF, and SLA	ULR	10.5%	-734, 800
	LMF	100.9%	-573, 1068
	SLA	-11.4%	-592, 225

FIGURE CAPTIONS

Figure 3.1. Relationships of relative growth rate (RGR) with native climate for 15 Arabidopsis ecotypes grown in a greenhouse common garden, i.e., with (A) mean annual temperature, (B) annual precipitation and (C) aridity index. The *r*-values with significance are based on linear regression analysis with kinship. ns, $P>0.05$; *, $P<0.05$; **, $P<0.01$; ***, $P<0.001$.

Figure 3.2. Variation across 15 Arabidopsis ecotypes grown in a greenhouse common garden in (A) relative growth rate, (B) leaf mass fraction, (C) absolute growth rate, (D) specific leaf area, (E) unit leaf rate and (F) root mass fraction. Ecotypes are ordered from lowest to highest value of relative growth rate. Error bars indicate standard error.

Figure 3.3. Relationships of aridity index (AI) with traits for Arabidopsis ecotypes grown in a greenhouse common garden, i.e., with (A) osmotic potential at full turgor (π_o); eight genotypes (B) leaf mass per area (LMA); 15 genotypes (C) leaf density; 15 genotypes (D) leaf nitrogen per area (N_{area}); 15 genotypes and (E) root mass fraction (RMF); 15 genotypes. The *r*-values with significance are based on linear or power law regressions with kinship. ns, $P>0.05$; *, $P<0.05$; **, $P<0.01$; ***, $P<0.001$.

Figure 3.4. Relationship of growing season precipitation with carbon isotope ratio ($\delta^{13}C$) for 15 Arabidopsis ecotypes grown in a greenhouse common garden. The *r*-value with significance is based on a linear regression with kinship. ns, $P>0.05$; *, $P<0.05$; **, $P<0.01$; ***, $P<0.001$.

Figure 3.5. Relationships of leaf mass per area (LMA) with (A) leaf nitrogen per mass (N_{mass}) and with its components (B) leaf thickness and (C) leaf density for 15 Arabidopsis ecotypes grown in a greenhouse common garden. The *r*-values with significance are based on linear or power law regressions with kinship. ns, $P>0.05$; *, $P<0.05$; **, $P<0.01$; ***, $P<0.001$.

Figure 3.6. Relationships between leaf economics traits for 15 Arabidopsis ecotypes grown in a greenhouse common garden, i.e. for (A) leaf mass per area with leaf nitrogen per area (N_{area}) and chlorophyll per area (inset panel) and for (B) chlorophyll per area with N_{area}. The *r*-values with significance are based on linear regressions with kinship. ns, $P>0.05$; *, $P<0.05$; **, $P<0.01$; ***, $P<0.001$.

Figure 3.7. Relationships leaf traits with relative growth rate (RGR) for 15 Arabidopsis ecotypes grown in a greenhouse common garden, i.e. for (A) leaf area and (B) leaf thickness with RGR. The *r*-values with significance are based on power law regressions with kinship. ns, $P>0.05$; *, $P<0.05$; **, $P<0.01$; ***, $P<0.001$.

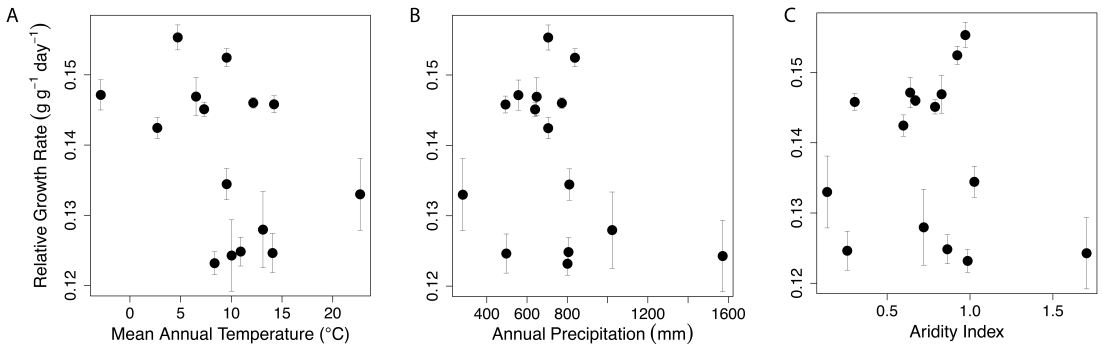
A
B
C
Relative Growth Rate (g g^{-1} day^{-1})
0.12
0.13
0.14
0.15
0
5
10
15
20
Mean Annual Temperature (°C)
400
600
800
1200
1600
Annual Precipitation (mm)
0.5
1.0
1.5
Aridity Index

Figure 3.1

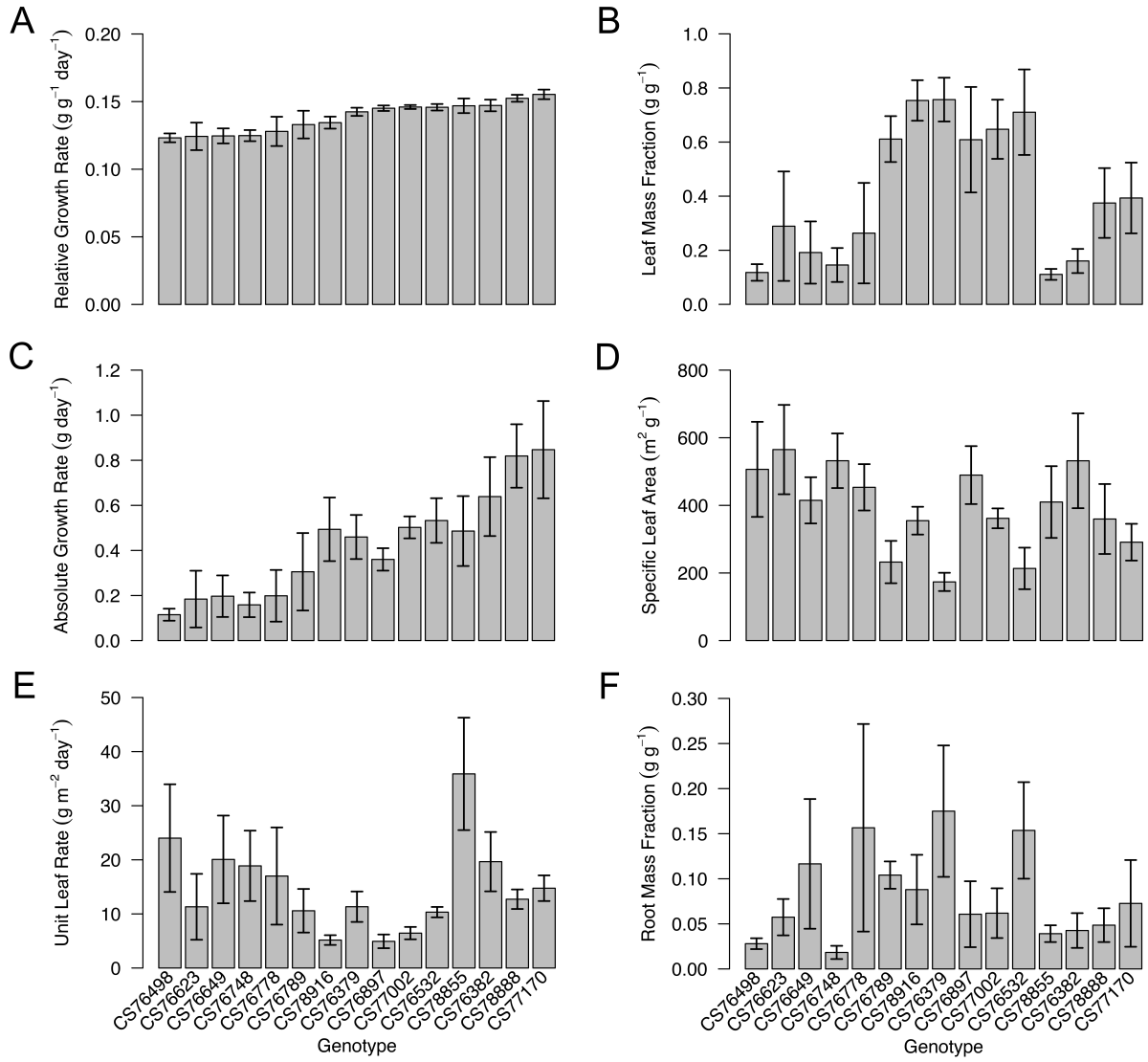
A
Relative Growth Rate (g g^{-1} day^{-1})
0.00
0.05
0.10
0.15
0.20
B
Leaf Mass Fraction (g g^{-1})
0.0
0.2
0.4
0.6
0.8
1.0
C
Absolute Growth Rate (g day^{-1})
0.0
0.2
0.4
0.6
0.8
1.0
1.2
D
Specific Leaf Area (m^2 g^{-1})
0
200
400
600
800
E
Unit Leaf Rate (g m^{-2} day^{-1})
0
10
20
30
40
50
F
Root Mass Fraction (g g^{-1})
0.00
0.05
0.10
0.15
0.20
0.25
0.30
CS76498
CS76623
CS76649
CS76748
CS76778
CS76789
CS78916
CS76379
CS76897
CS77002
CS76532
CS78855
CS76382
CS78888
CS77170
Genotype

Figure 3.2

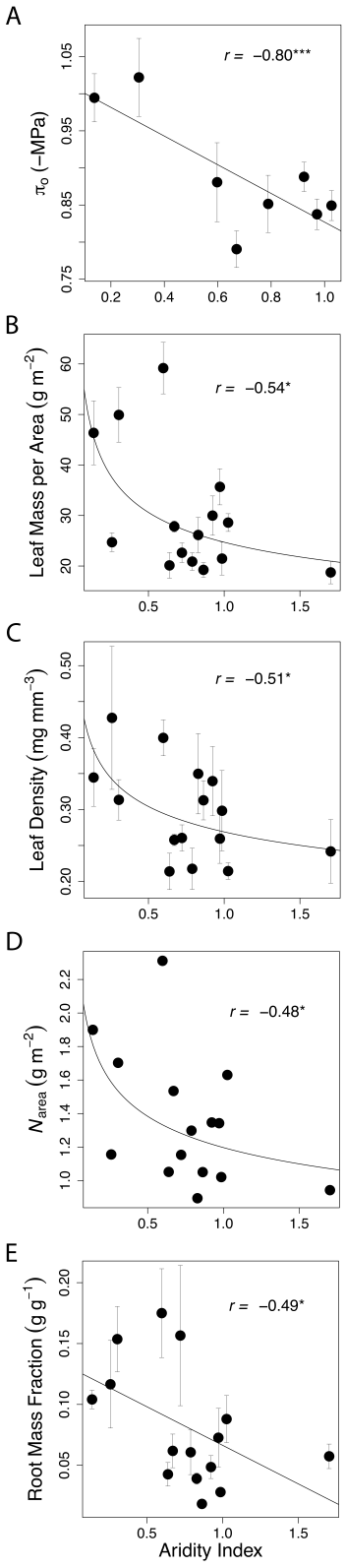
A
r = −0.80***
π_o (−MPa)
B
r = −0.54*
Leaf Mass per Area (g m^{-2})
C
r = −0.51*
Leaf Density (mg mm^{-3})
D
r = −0.48*
N_{area} (g m^{-2})
E
r = −0.49*
Root Mass Fraction (g g^{-1})
Aridity Index

Figure 3.3

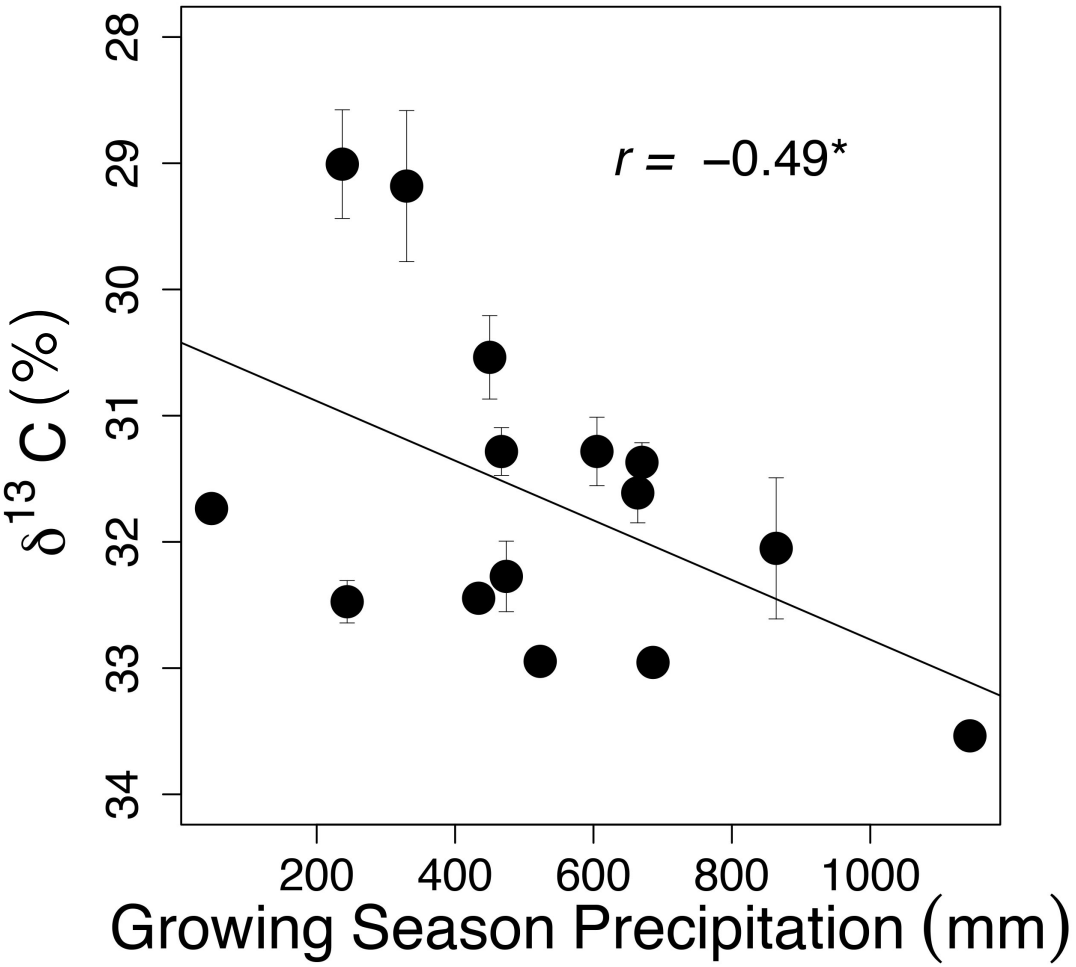
r = −0.49*
δ13 C (‰)
28
29
30
31
32
33
34
200
400
600
800
1000
Growing Season Precipitation (mm)

Figure 3.4

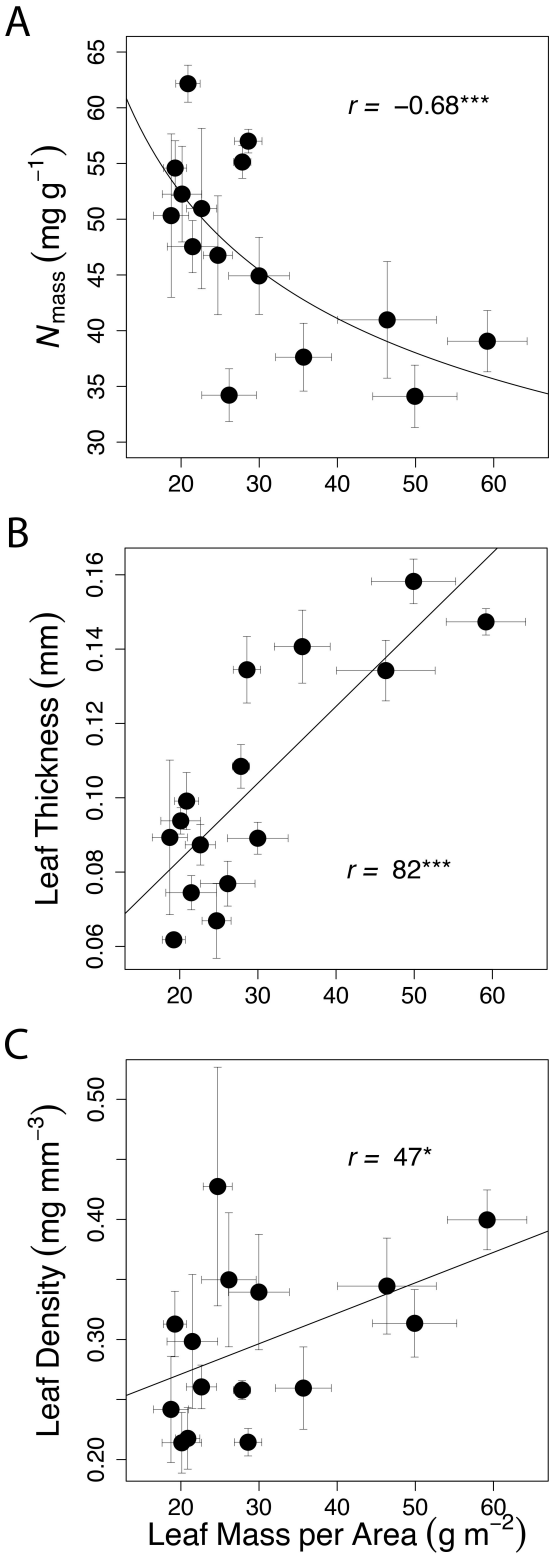
A
N_{mass} (mg g^{-1})
r = −0.68***
B
Leaf Thickness (mm)
r = 82***
C
Leaf Density (mg mm^{-3})
r = 47*
Leaf Mass per Area (g m^{-2})

Figure 3.5

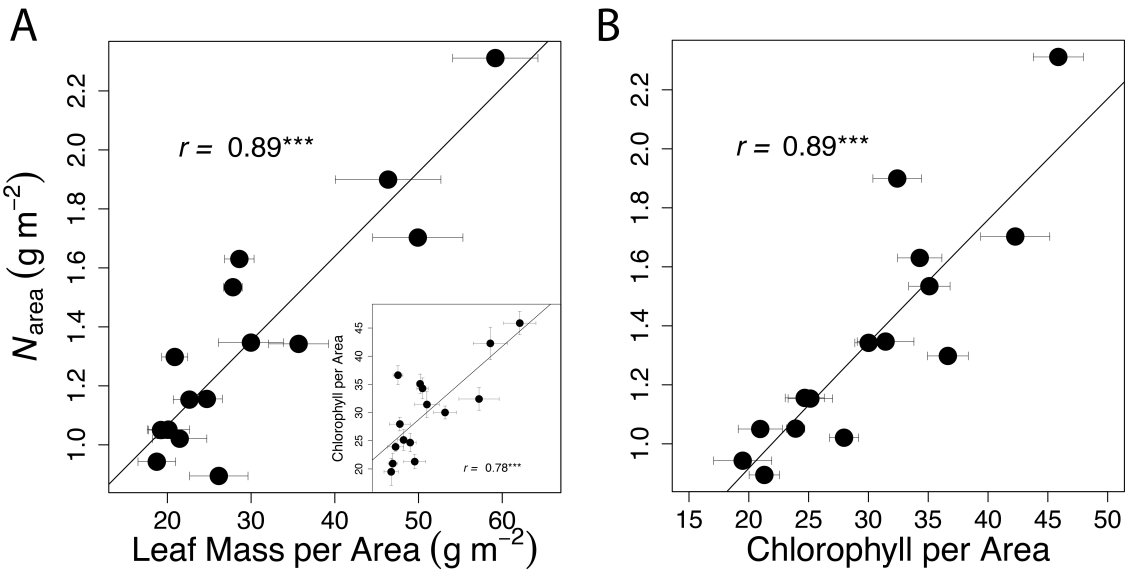
A
B
r = 0.89***
r = 0.89***
r = 0.78***
Chlorophyll per Area
Leaf Mass per Area (g m−2)
Chlorophyll per Area
Narea (g m−2)

Figure 3.6

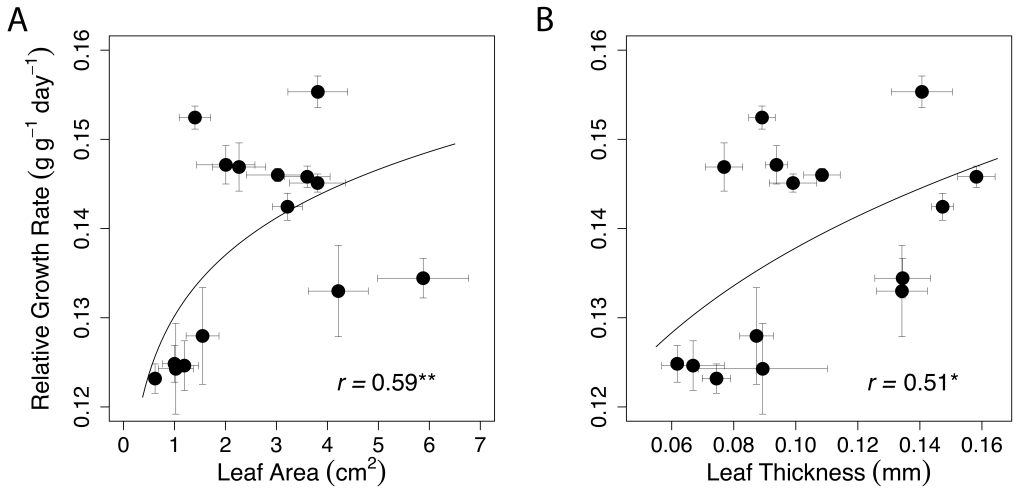
A
B
Relative Growth Rate (g g^{-1} day^{-1})
0.12
0.13
0.14
0.15
0.16
0
1
2
3
4
5
6
7
Leaf Area (cm^2)
r = 0.59**
0.06
0.08
0.10
0.12
0.14
0.16
Leaf Thickness (mm)
r = 0.51*

Figure 3.7

Appendix 3.1. The ecological consequences of within-species growth-stress tolerance relationships

To consider the potential ecological consequences of growth-stress tolerance relationships (GSTRs) across ecotypes of a given species, we synthesized theory based on the published literature using a simple framework (Appendix Figure 3.1). We considered a simple gradient of habitats from low to high climatic stress, where low climatic stress was assumed to be competitive habitat, given favorable conditions for most plants (Walter, 1979). Under a trade-off between maximum relative growth rate (RGR) and stress tolerance, ecotypes specializing in rapid RGR should dominate under favorable climates but would be replaced by stress-tolerant ecotypes under stressful climates (Appendix Fig. 3.1A). By contrast, under a positive coordination of RGR and stress tolerance, the same ecotypes should dominate across the climatic gradient (Appendix Fig. 3.1B). Finally, if RGR and stress tolerance are decoupled, ecotypes with any combination can exist, and thus ecotypes vary in their ranges across the gradient, with some confined to extremes and others with substantial ranges (Appendix Fig. 3.1C).

This framework provides a heuristic for prediction of how major ecological properties of the ecotypes and the species itself should vary under different GSTRs. We considered four properties: ecotype specialization in high versus low climatic stress niches, species differentiation into ecotypes across a climatic gradient, ecotype turnover across a climatic gradient, the width of the species range across continuous habitat, and the average range of an ecotype (Appendix Table 3.1).

Ecotype specialization in high vs. low climatic stress niches is represented by the total numbers of ecotypes existing within individual habitats (i.e., considering each of the single three squares vertically in Appendix Fig. 3.1, or averaging across them). Thus, under a trade-off, there is high ecotype specialization, relative to under positive coordination or decoupling (Kneitel & Chase, 2004; Ostman, Lin, & Adami, 2014; Appendix Fig. 3.1; Appendix Table 3.1). Ecotype differentiation across a climatic gradient is represented by the total numbers of ecotypes existing across the entire gradient (i.e., summing ecotypes across the three squares vertically in Appendix Fig. 3.1), and thus would thus be moderate, low and high respectively under a trade-off, positive coordination and decoupling (Farahpour, Saeedghalati, Brauer, & Hoffman, 2018; Kneitel & Chase, 2004; MacArthur & Levins, 1967; Mouquet & Loreau,

2002; Appendix Table 3.1). Ecotype turnover across a climatic gradient, assuming complete dispersal, is represented by the shift in species composition across the gradient (i.e., the change in species across the three squares vertically in Appendix Fig. 3.1) and would thus be high, moderate and low respectively under a trade-off, positive coordination and decoupling (Kneitel & Chase, 2004). An expectation for the width of the species range can be made, assuming continuous habitat and complete gene flow, given that gene flow would lead to a reduced range, because genetic adaptation to specific climates would be "diluted" by genes across the range. Finally, the width of the range of the species is represented by the degree that specialist ecotypes occur at the extremes (i.e., differentiated ecotypes in the highest and lowest squares of the vertical columns in Appendix Fig. 3.1) and would be relatively small, large and moderate respectively under a trade-off, positive coordination and decoupling (Antonovics, 1976; Kikpatrick & Barton, 1997; Mayr, 1963; Sexton, Strauss, & Rice, 2011; Appendix Fig. 3.1; Appendix Table 3.1).

Climate change would be expected to influence these effects of GSTRs on the ecological properties of a species and its ecotypes. Assuming that climate change tends overall to result in an increase in extreme habitat, one can hypothesize influences on each outcome (Appendix Table 3.1). In particular, greater representation of extreme climates would weaken some of the predicted trends associated with the influence of GSTRs across a climate gradient.

This theoretical synthesis is purely heuristic, and untested, but illustrates the potential for GSTRs to have strong impacts on fundamental ecological properties of ecotypes and species, and their responses to climate change. This importance of GSTRs explains why they have been a focus of enormous research effort (summarized in Table S3.1). These implications further highlight the urgency of further research in testing, establishing mechanisms for and determining the ecological consequences of GSTRs.

Appendix Table 3.1. Synthesis of literature indicating theoretical influences of growth-stress relationships (GSTRs) on major ecological properties of a species and its ecotypes of a given species, including ecotype specialization in high versus low climatic stress niches, ecotype differentiation into ecotypes across a climatic gradient, ecotype turnover across a climatic gradient, and the width of the species range across continuous habitat. Expectations are given for three GSTRs that have been hypothesized across ecotypes of given species, i.e., a trade-off between maximum relative growth rate (RGR) and stress tolerance, positive coordination of RGR with stress tolerance, and decoupling of RGR and stress tolerance. As climate change would tend to result in an increase in extreme habitat, expectations were also provided for the influence of climate change on each outcome; a minus sign indicates that climate change would decrease the hypothesized effect in a given category.

GSTR	**(1) Ecotype specialization in high versus low climatic stress niches**	**(2) Ecotype differentiation across a climatic gradient**	**(3) Ecotype turnover across large scale resource gradient with continuous habitat given complete dispersal**	**(4) Species range across continuous habitat (assuming complete gene flow)**
Trade-off	High-	Moderate-	High	Small-
Positive coordination	Low	Low	Low	Large-
Decoupling	Low-	High-	Moderate-	Moderate-
References	1, 2	1, 3, 4, 5	1	6, 7, 8, 9

References: 1. Kneitel & Chase 2004; 2. Ostman *et al.* 2014; 3. MacArthur & Levins 1967; 4. Mouquet & Loreau 2002; 5. Farahpour *et al.* 2018; 6. Mayr 1963; 7. Antonovics 1976; 8. Kirkpatrick & Barton 1997; 9. Sexton *et al.* 2011; 10. Holt & Barfield 2011.

APPENDIX FIGURE CAPTION

Appendix Figure 3.1. Schematic diagram showing ecological implications of contrasting growth-stress tolerance relationships for ecotypes of a species across a gradient from favorable climate (competitive habitat) to stressful climate. Green squares represent locations of varying climatic stress and shapes represent different ecotypes.

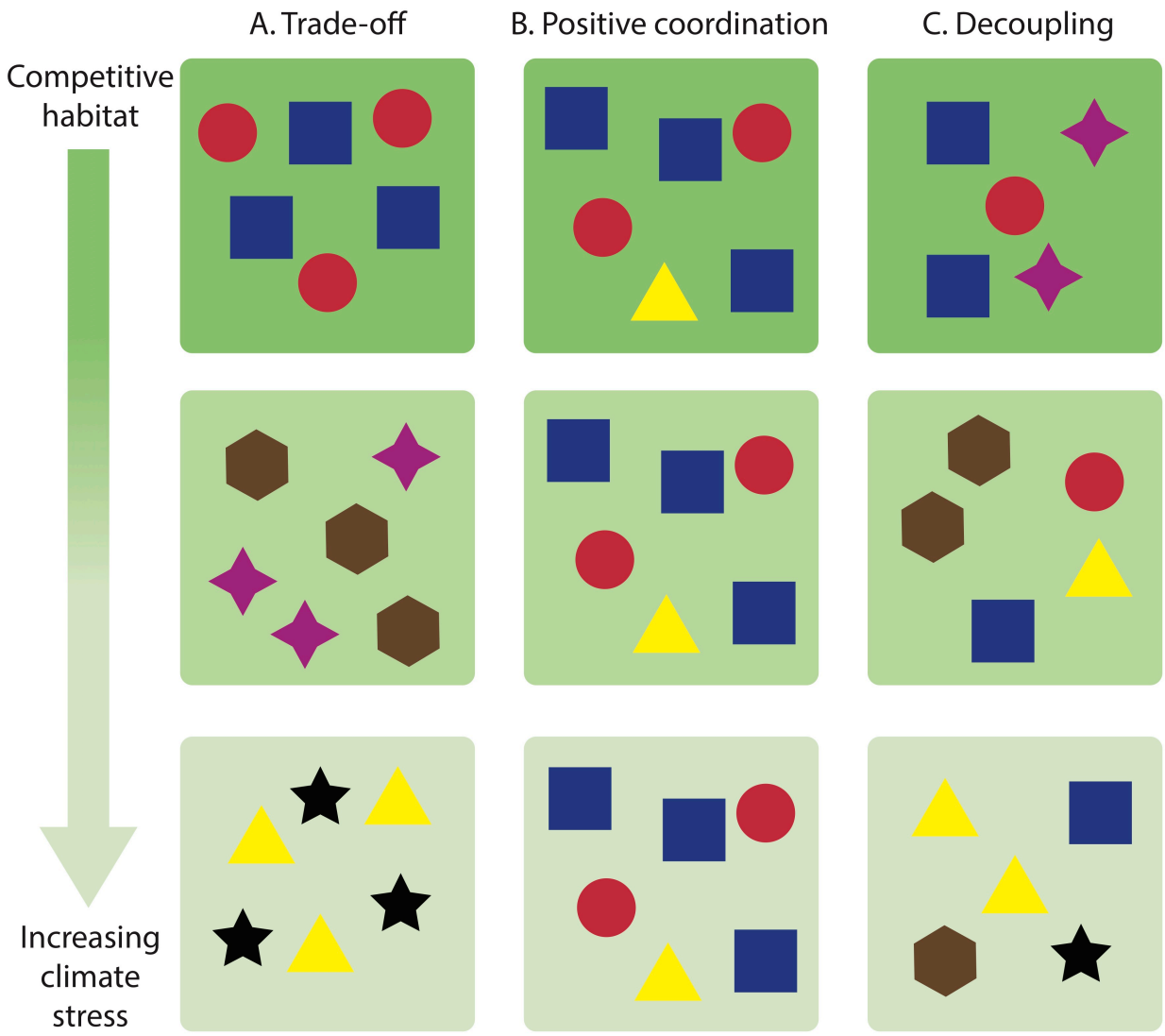

Appendix Figure 3.1

SUPPLEMENTARY MATERIALS

Supplementary Data Captions (see attached Excel Workbook)

Table S3.1. Previous studies investigating a trade-off between growth and stress tolerance across or within species. Columns include the study citation, growth variables investigated, drought or cold tolerance variables investigated, the relationship between the growth and tolerance variable (TO, tolerance; PC, positive coordination; NR, no relationship; NA, inconclusive), whether the study was performed in field or experimental conditions, whether the results were found in the original paper or were demonstrated through our analysis of the data (IP, in paper; OA, our analysis), the species used in the study, whether the relationship was demonstrated within or between species (WS, within species; BS, between species), whether the species investigated were annuals or perennials, and lists of the growth and tolerance traits measured (see legend below for variable names).

Table S3.2. Analyses of published data from studies considering relationships of relative growth rate with climate across *Arabidopsis thaliana* ecotypes (Atwell *et al.*, 2010; Vasseur et al,. 2018). Comparisons are made between linear (y = ax + b) and quadratic model (y = ax2 + bx + c) fits. Columns include names of the variables tested (RGR, relative growth rate), and the results of the analyses (df, degrees of freedom; AIC(c), Akaike Information Criterion; Delta_AICc, relative difference between the best model and each other model; AICcWt, Akaike weights indicating level of support for each model; Cum.Wt, cumulative Akaike weights; LL, log-likelihood of each model). AIC and AICc scores for fitted models of data show significant results from the AIC function in the stats package and the and AICc function in the MuMIn package in R verion 3.5.1.

The model selected by maximum likelihood is highlighted, and neither is highlighted if the difference in AIC scores is <2.

Table S3.3. Experimental data and native climate data for 15 genotypes of *Arabidopsis thaliana* grown in a greenhouse common garden including individual and ecotype mean values, standard deviations and standard errors. Average values are derived from 5 individual plants per genotype, with leaf traits being measured on three leaves per individual per genotype, and with two leaves per plant sampled for osmotic potential at full turgor (Pio). See "CHAPTER 3 Legend" tab for legend of symbols and units.

Table S3.4. Correlations accounting for kinship for all traits and climate variables on untransformed (raw) and log-transformed data for fifteen ecotypes of *Arabidopsis thaliana* grown in a common garden. Columns include the X and Y variables (See "CHAPTER 3 Legend" tab for legend of symbols and units), model estimates of the intercept, slope, and r-squared values, the p-value of the correlation. Significant p-values ($P < 0.05$) are highlighted. Note that Pio and d13C values were multiplied by -1 prior to running the analysis.

Table S3.5. Same as SI Table S3.4, just including the correlations significant at $P < 0.05$.

Table S3.6. Correlations accounting for kinship for osmotic potential at full turgor and climate variables on untransformed (raw) and log-transformed data for eight ecotypes of *Arabidopsis thaliana* grown in a common garden. Columns include the X and Y variables (See "CHAPTER 3 Legend" tab for legend of symbols and units), Model estimates of the intercept, slope, and r2

values, the p-value of the correlation. Significant p-values ($P < 0.05$) are highlighted. Note that Pio and d13C values were multiplied by -1 prior to running the analysis.

Table S3.7. Same as SI Table S3.6, just including the correlations significant at $P < 0.05$.

Supplementary figure captions

Figure S3.1. Analyses of the data of previously published studies of Arabidopsis ecotypes for relationships between relative growth rate and (A, C) mean annual temperature and (B, D) annual precipitation for 451 ecotypes (Vasseur *et al.*, 2018) and 107 ecotypes (Atwell *et al.*, 2010; our matching of ecotypes with origin climates based on the location data from the 1001 Genomes Project), respectively. Curves and *r*-values with significance are based on a fitted polynomial (panels A) or linear regression (panel C), according to the model selected by AICc score (Table S3.2). ns, $P>0.05$; *, $P<0.05$; **, $P<0.01$; ***, $P<0.001$. See Table S3.2 for the fits of the linear and polynomial models.

Figure S3.2. Plots of absolute growth rate (AGR) and flowering times with native climate for 15 Arabidopsis ecotypes grown in a greenhouse common garden, i.e. plots of AGR with (A) mean annual temperature (MAT) and (B) annual precipitation (MAP), (C) flowering time at 10°C with MAT and (D) MAP, and flowering time at 16°C with (E) MAT and (F) MAP. Flowering time data represent time until first flower opened (from Alonso-Blanco *et al.* 2016).

Figure S3.3. Data supporting the correspondence of experimental drought tolerance with native arid climate across 211 Arabidopsis ecotypes (Exposito-Alonso *et al.* 2018). Survival data are percentages of plants surviving in a drought-prone field site (Madrid). The r-value with significance was based on linear regression analysis. ns, $P>0.05$; *, $P<0.05$; **, $P<0.01$; ***, $P<0.001$.

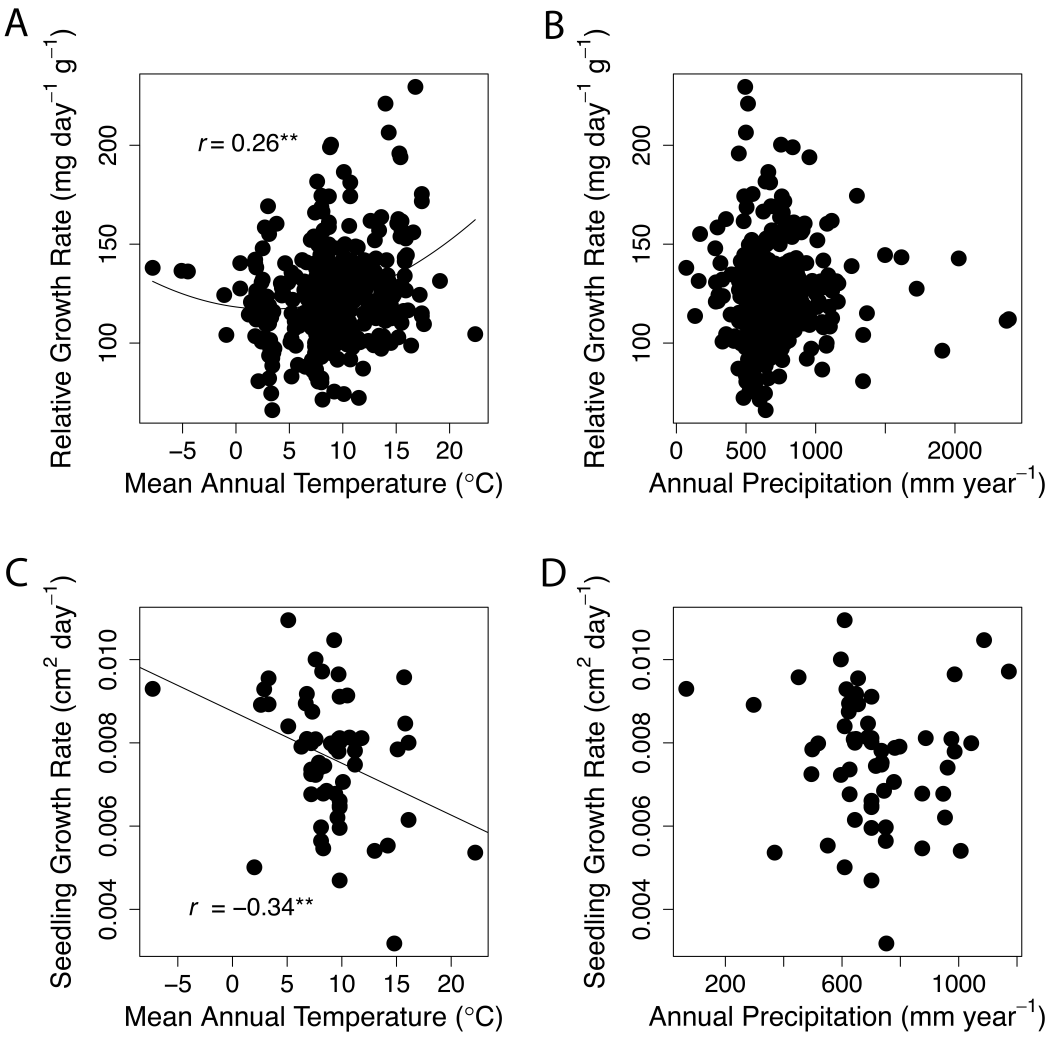
A
Relative Growth Rate (mg day^{-1} g^{-1})
r = 0.26**
Mean Annual Temperature (°C)
B
Relative Growth Rate (mg day^{-1} g^{-1})
Annual Precipitation (mm year^{-1})
C
Seedling Growth Rate (cm^2 day^{-1})
r = −0.34**
Mean Annual Temperature (°C)
D
Seedling Growth Rate (cm^2 day^{-1})
Annual Precipitation (mm year^{-1})

Figure S3.1

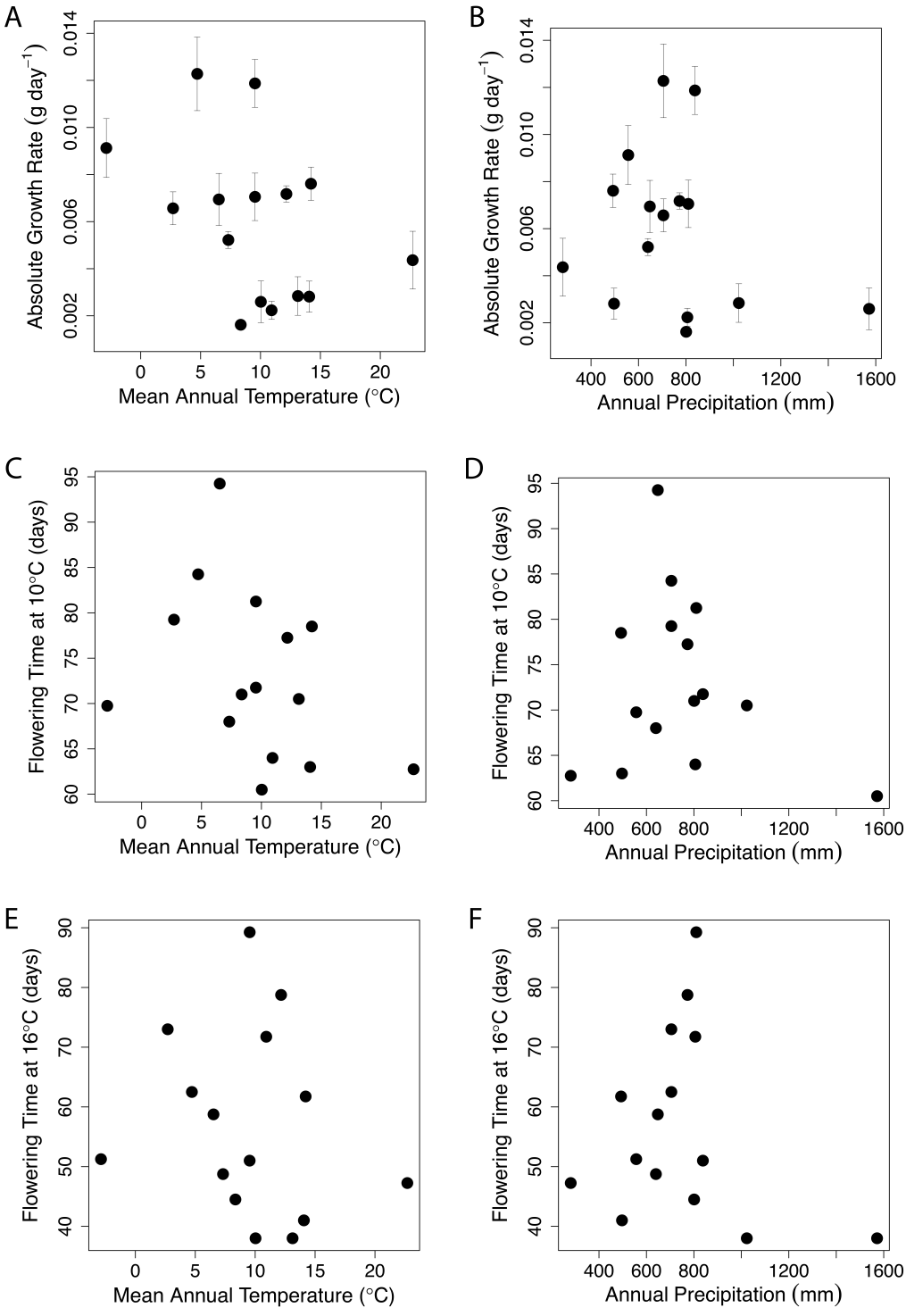
A
Absolute Growth Rate (g day^{-1})
0.002
0.006
0.010
0.014
0
5
10
15
20
Mean Annual Temperature (°C)
B
Absolute Growth Rate (g day^{-1})
0.002
0.006
0.010
0.014
400
600
800
1200
1600
Annual Precipitation (mm)
C
Flowering Time at 10°C (days)
60
65
70
75
80
85
90
95
0
5
10
15
20
Mean Annual Temperature (°C)
D
Flowering Time at 10°C (days)
60
65
70
75
80
85
90
95
400
600
800
1200
1600
Annual Precipitation (mm)
E
Flowering Time at 16°C (days)
40
50
60
70
80
90
0
5
10
15
20
Mean Annual Temperature (°C)
F
Flowering Time at 16°C (days)
40
50
60
70
80
90
400
600
800
1200
1600
Annual Precipitation (mm)

Figure S3.2

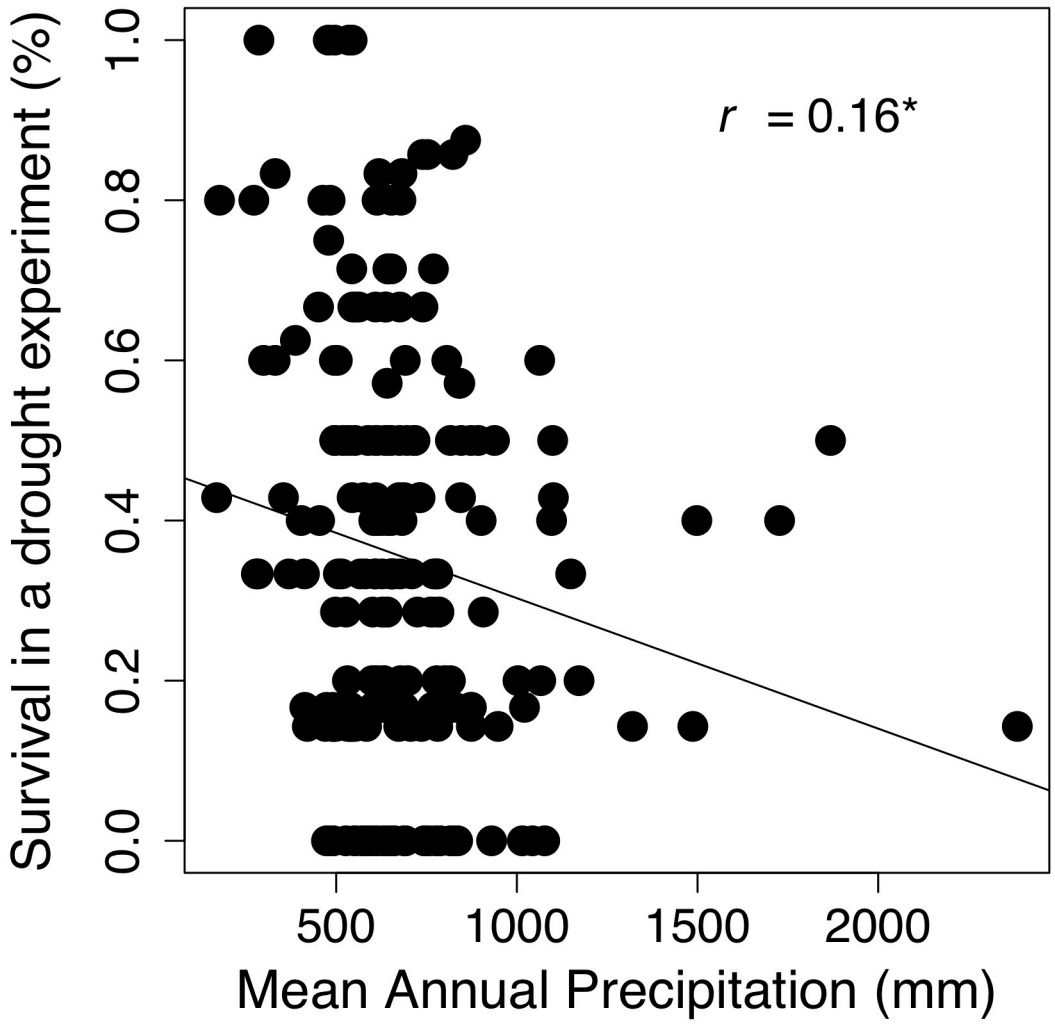
Survival in a drought experiment (%)
0.0
0.2
0.4
0.6
0.8
1.0
r = 0.16*
500
1000
1500
2000
Mean Annual Precipitation (mm)

Figure S3.3

REFERENCES

AghaKouchak, A., Cheng, L., Mazdiyasni, O., & Farahmand, A. (2014). Global warming and changes in risk of concurrent climate extremes: Insights from the 2014 California drought. *Geophysical Research Letters*, 41, 8847-8852.

Alonso-Blanco, C., Andrade, J., Becker, C., Bemm, F., Bergelson, J., Borgwardt, K. M. *et al.* (2016). 1,135 Genomes Reveal the Global Pattern of Polymorphism in *Arabidopsis thaliana*. *Cell*, 166, 481-491.

Ambroise, V., Legay, S., Guerriero, G., Hausman, J. F., Cuypers, A., & Sergeant, K. (2020). The roots of plant frost hardiness and tolerance. *Plant and Cell Physiology*, 61, 3-20.

Antonovics, J. (1976). Nature of limits to natural-selection. *Annals of the Missouri Botanical Garden*, 63, 224-247.

Atwell, S., Huang, Y. S., Vilhjalmsson, B. J., Willems, G., Horton, M., Li, Y. *et al.* (2010). Genome-wide association study of 107 phenotypes in *Arabidopsis thaliana* inbred lines. *Nature*, 465, 627-631.

Bac-Molenaar, J. A., Granier, C., Keurentjes, J. J. B., & Vreugdenhil, D. (2016). Genome-wide association mapping of time-dependent growth responses to moderate drought stress in *Arabidopsis*. *Plant Cell and Environment*, 39, 88-102.

Bartlett, M. K., Scoffoni, C., Ardy, R., Zhang, Y., Sun, S. W., Cao, K. F., & Sack, L. (2012). Rapid determination of comparative drought tolerance traits: using an osmometer to predict turgor loss point. *Methods in Ecology and Evol*ution, 3, 880-888.

Bartlett, M. K., Scoffoni, C., & Sack, L. (2012). The determinants of leaf turgor loss point and prediction of drought tolerance of species and biomes: a global meta-analysis. *Ecology Letters*, 15, 393-405.

Bartlett, M. K., Zhang, Y., Kreidler, N., Sun, S. W., Ardy, R., Cao, K. F., & Sack, L. (2014). Global analysis of plasticity in turgor loss point, a key drought tolerance trait. *Ecology Letters*, 17, 1580-1590.

Bigler, C., & Bugmann, H. (2018). Climate-induced shifts in leaf unfolding and frost risk of European trees and shrubs. *Scientific Reports*, 8, 9865-9865.

Bristiel, P., Gillespie, L., Ostrem, L., Balachowski, J., Violle, C., & Volaire, F. (2018). Experimental evaluation of the robustness of the growth-stress tolerance trade-off within the perennial grass *Dactylis glomerata*. *Functional Ecology*, 32, 1944-1958.

Buckley, T. N., & Diaz-Espejo, A. (2015). Partitioning changes in photosynthetic rate into contributions from different variables. *Plant Cell and Environm*ent, 38, 1200-1211.

Cayan, D. R., Maurer, E. P., Dettinger, M. D., Tyree, M., & Hayhoe, K. (2008). Climate change scenarios for the California region. *Climatic Change*, 87, S21-S42.

Chaturvedi, R. K., Raghubanshi, A. S., & Singh, J. S. (2011). Leaf attributes and tree growth in a tropical dry forest. *Journal of Vegetation Science*, 22, 917-931.

Chew, Y. H., & Halliday, K. J. (2011). A stress-free walk from Arabidopsis to crops. *Current Opinion in Biotechnology*, 22, 281-286.

Coley, P. D., Bryant, J. P., & Chapin, F. S. (1985). Resource availability and plant antiherbivore defense. *Science*, 230, 895-899.

Comas, L. H., Becker, S. R., Cruz, V. V., Byrne, P. F., & Dierig, D. A. (2013). Root traits contributing to plant productivity under drought. *Frontiers in Plant Science*, 4, 1-16.

Conesa, M. A., Mus, M., & Galmes, J. (2019). Leaf size as a key determinant of contrasting growth patterns in closely related *Limonium* (Plumbaginaceae) species. *Journal of Plant Physiology*, 240, 1-9.

Cook, E. R., Woodhouse, C. A., Eakin, C. M., Meko, D. M., & Stahle, D. W. (2004). Long-term aridity changes in the western United States. *Science*, 306, 1015-1018.

Cordell, S., Goldstein, G., Mueller-Dombois, D., Webb, D., & Vitousek, P. M. (1998). Physiological and morphological variation in *Metrosideros polymorpha*, a dominant Hawaiian tree species, along an altitudinal gradient: the role of phenotypic plasticity. *Oecologia*, 113, 188-196.

Creese, C., Lee, A., & Sack, L. (2011). Drivers of morphological diversity and distribution in the Hawaiian fern flora: trait associations with size, growth form, and environment. *American Journal of Botany*, 98, 956-966.

Darychuk, N., Hawkins, B. J., & Stoehr, M. (2012). Trade-offs between growth and cold and drought hardiness in submaritime Douglas-fir. *Canadian Journal of Forest Research*, 42, 1530-1541.

Debieu, M., Tang, C., Stich, B., Sikosek, T., Effgen, S., Josephs, E. *et al.* (2013). Co-variation between seed dormancy, growth rate and flowering time changes with latitude in *Arabidopsis thaliana*. *Plos One*, 8, 1-12.

DeLeo, V. L., Menge, D. N. L., Hanks, E. M., Juenger, T. E., & Lasky, J. R. (2020). Effects of two centuries of global environmental variation on phenology and physiology of *Arabidopsis thaliana*. *Global Change Biology*, 26, 523-538.

Diffenbaugh, N. S., Swain, D. L., & Touma, D. (2015). Anthropogenic warming has increased drought risk in California. *Proceedings of the National Academy of Sciences of the United States of America*, 112, 3931-3936.

Ding, Y. L., Shi, Y. T., & Yang, S. H. (2019). Advances and challenges in uncovering cold tolerance regulatory mechanisms in plants. *New Phytologist*, 222, 1690-1704.

Dunbar-Co, S., Sporck, M. J., & Sack, L. (2009). Leaf trait diversification and design in seven rare taxa of the Hawaiian *Plantago* radiation. *International Journal of Plant Sciences*, 170, 61-75.

Evans, G. C. (1972). The Quantitative Analysis of Plant Growth. Oxford: Blackwell Scientific Publications.

Exposito-Alonso, M., Vasseur, F., Ding, W., Wang, G., Burbano, H. A., & Weigel, D. (2018). Genomic basis and evolutionary potential for extreme drought adaptation in *Arabidopsis thaliana*. *Nature Ecology & Evolution*, 2, 352-358.

Eziz, A., Yan, Z. B., Tian, D., Han, W. X., Tang, Z. Y., & Fang, J. Y. (2017). Drought effect on plant biomass allocation: A meta-analysis. *Ecology and Evolution*, 7, 11002-11010.

Falster, D. S., Duursma, R. A., & FitzJohn, R. G. (2018). How functional traits influence plant growth and shade tolerance across the life cycle. *Proceedings of the National Academy of Sciences of the United States of America*, 115, E6789-E6798.

Farahpour, F., Saeedghalati, M., Brauer, V. S., & Hoffmann, D. (2018). Trade-off shapes diversity in eco-evolutionary dynamics. *Elife*, 7, 1-41.

Farquhar, G. D., Ehleringer, J. R., & Hubick, K. T. (1989). Carbon isotope discrimination and photosynthesis. *Annual Review of Plant Physiology and Plant Molecular Biology*, 40, 503-537.

Fernández, R. J., & Reynolds, J. F. (2000). Potential growth and drought tolerance of eight desert grasses: lack of a trade-off? *Oecologia*, 123, 90-98.

Ferrero-Serrano, A., & Assmann, S. M. (2019). Phenotypic and genome-wide association with the local environment of *Arabidopsis*. *Nature Ecology & Evolution*, 3, 274-285.

Fick, S.E., & Hijmans, R.J. (2017). WorldClim 2: new 1km spatial resolution climate surfaces for global land areas. *International Journal of Climatology*, 37, 4302-4315.

Fine, P. V. A., Miller, Z. J., Mesones, I., Irazuzta, S., Appel, H. M., Stevens, M. H. H. *et al.* (2006). The growth-defense trade-off and habitat specialization by plants in Amazonian forests. *Ecology*, 87, S150-S162.

Flavell, R. (2005). Model plants, with special emphasis on *Arabidopsis thaliana*, and crop improvement. In R Tuberosa, (eds R. L. Phillips, M. Gale), pp. 365-378. Proceedings of the International Congress "In the Wake of the Double Helix: From the Green Revolution to the Gene Revolution". Avenue Media, Bologna, Italy.

Fletcher, L. R., Cui, H., Callahan, H., Scoffoni, C., John, G. P., Bartlett, M. K. *et al.* (2018). Evolution of leaf structure and drought tolerance in species of Californian *Ceanothus*. *American Journal of Botany*, 105, 1672-1687.

Fournier-Level, A., Perry, E. O., Wang, J. A., Braun, P. T., Migneault, A., Cooper, M. D., *et al.* (2016). Predicting the evolutionary dynamics of seasonal adaptation to novel climates in *Arabidopsis thaliana*. *Proceedings of the National Academy of Sciences of the United States of America*, 113, E2812-E2821.

Frachon, L., Bartoli, C., Carrère, S., Bouchez, O., Chaubet, A., Gautier, M. *et al.* (2018). A genomic map of climate adaptation in *Arabidopsis thaliana* at a micro-geographic scale. *Frontiers in Plant Science*, 9, 1-15.

Gibert, A., Gray, E. F., Westoby, M., Wright, I. J., & Falster, D. S. (2016). On the link between functional traits and growth rate: meta-analysis shows effects change with plant size, as predicted. *Journal of Ecology*, 104, 1488-1503.

Givnish, T. J. (1987). Comparative studies of leaf form: assessing the relative roles of selective pressures and phylogenetic constraints. *New Phytologist*, 106, 131-160.

Givnish, T. J., & Montgomery, R. A. (2014). Common-garden studies on adaptive radiation of photosynthetic physiology among Hawaiian lobeliads. *Proceedings of the Royal Society B-Biological Sciences*, 281, 1-8.

Gomez, J. M. (2004). Bigger is not always better: Conflicting selective pressures on seed size in *Quercus ilex*. *Evolution*, 58, 71-80.

Gonzalez-Zurdo, P., Escudero, A., Babiano, J., Garcia-Ciudad, A., & Mediavilla, S. (2016). Costs of leaf reinforcement in response to winter cold in evergreen species. *Tree Physiology*, 36, 273-286.

Griffin-Nolan, R. J., Blumenthal, D. M., Collins, S. L., Farkas, T. E., Hoffman, A. M., Mueller, K. E. *et al.* (2019). Shifts in plant functional composition following long-term drought in grasslands. Journal of Ecology, 107, 2133-2148.

Griffin-Nolan, R. J., Ocheltree, T. W., Mueller, K. E., Blumenthal, D. M., Kray, J. A., & Knapp, A. K. (2019). Extending the osmometer method for assessing drought tolerance in herbaceous species. Oecologia, 189, 353-363.

Griffith, M., Timonin, M., Wong, A. C. E., Gray, G. R., Akhter, S. R., Saldanha, M. *et al.* (2007). Thellungiella: an Arabidopsis-related model plant adapted to cold temperatures. Plant *Cell and Environment*, 30, 529-538.

Griffith, T. M., & Watson, M. A. (2005). Stress avoidance in a common annual: reproductive timing is important for local adaptation and geographic distribution. *Journal of Evolutionary Biology*, 18, 1601-1612.

Grime, J. P. (1974). Vegetation classification by reference to strategies. *Nature*, 250, 26-31.

Grime, J. P. (1977). Evidence for existence of three primary strategies in plants and its relevance to ecological and evolutionary theory. *American Naturalist*, 111, 1169-1194.

Grubb, P. J. (1998). A reassessment of the strategies of plants which cope with shortages of resources. *Perspectives in Plant Ecology, Evolution and Systematics*, 1, 3-31.

Hancock, A. M., Brachi, B., Faure, N., Horton, M. W., Jarymowycz, L. B., Sperone, F. G. *et al.* (2011). Adaptation to climate across the *Arabidopsis thaliana* genome. *Science*, 334, 83-86.

Henry, C., John, G. P., Pan, R. H., Bartlett, M. K., Fletcher, L. R., Scoffoni, C., & Sack, L. (2019). A stomatal safety-efficiency trade-off constrains responses to leaf dehydration. *Nature Communications*, 10, 1-9.

Holt, R. D., & Barfield, M. (2011). Theoretical perspectives on the statics and dynamics of species' borders in patchy environments. *American Naturalist*, 178, S7-S25.

Huala, E., Dickerman, A. W., Garcia-Hernandez, M., Weems, D., Reiser, L., LaFond, F. *et al.* (2001). The Arabidopsis Information Resource (TAIR): a comprehensive database and web-based information retrieval, analysis, and visualization system for a model plant. *Nucleic Acids Research*, 29, 102-105.

Huck, M. G., Peterson, C. M., Hoogenboom, G., & Busch, C. D. (1986). Distribution of dry-matter between shoots and roots of irrigated and nonirrigated determinate soybeans. *Agronomy Journal*, 78, 807-813.

Hunt, R. 1990. Relative growth rates. In Basic Growth Analysis, pp. 25-34. Springer, Dordrecht.

Hunt, R., & Cornelissen, J. H. C. (1997). Components of relative growth rate and their interrelations in 59 temperate plant species. *New Phytologist*, 135, 395-417.

Ingram, J., & Bartels, D. (1996). The molecular basis of dehydration tolerance in plants. *Annual Review of Plant Physiology and Plant Molecular Biology*, 47, 377-403.

Inman-Narahari, F., Ostertag, R., Asner, G. P., Cordell, S., Hubbell, S. P., & Sack, L. (2014). Trade-offs in seedling growth and survival within and across tropical forest microhabitats. *Ecology and Evolution*, 4, 3755-3767.

John, G. P., Scoffoni, C., & Sack, L. (2013). Allometry of cells and tissues within leaves. *American Journal of Botany*, 100, 1936-1948.

Jung, E. Y., Gaviria, J., Sun, S. W., & Engelbrecht, B. M. J. (2020). Comparative drought resistance of temperate grassland species: testing performance trade-offs and the relation to distribution. *Oecologia*, 192, 1023-1036.

Kaproth, M., & Cavender-Bares, J. (2016). Drought tolerance and climatic distributions of the American oaks. *International Oaks*, 49-60.

Kazan, K., & Lyons, R. (2016). The link between flowering time and stress tolerance. *Journal of Experimental Botany*, 67, 47-60.

Kenney, A. M., McKay, J. K., Richards, J. H., & Juenger, T. E. (2014). Direct and indirect selection on flowering time, water-use efficiency (WUE, delta C-13), and WUE plasticity to drought in *Arabidopsis thaliana*. *Ecology and Evolution*, 4, 4505-4521.

Khurana, E., & Singh, J. S. (2004). Germination and seedling growth of five tree species from tropical dry forest in relation to water stress: impact of seed size. *Journal of Tropical Ecology*, 20, 385-396.

Kikuzawa, K., Onoda, Y., Wright, I. J., & Reich, P. B. (2013). Mechanisms underlying global temperature-related patterns in leaf longevity. *Global Ecology and Biogeography*, 22(8), 982-993.

Kirkpatrick, M., & Barton, N. H. (1997). Evolution of a species' range. *American Naturalist*, 150, 1-23.

Kitajima, K. (1994). Relative importance of photosynthetic traits and allocation patterns as correlates of seedling shade tolerance of 13 tropical trees. *Oecologia*, 98, 419-428.

Kneitel, J. M., & Chase, J. M. (2004). Trade-offs in community ecology: linking spatial scales and species coexistence. *Ecology Letters*, 7, 69-80.

Koehler, K., Center, A., & Cavender-Bares, J. (2012). Evidence for a freezing tolerance-growth rate trade-off in the live oaks (*Quercus* series *Virentes*) across the tropical-temperate divide. *New Phytologist*, 193, 730-744.

Lambers, H., Chapin, F. S. III, & Pons, T. L. (1998). Plant Physiological Ecology, 3rd edn. New York, USA: Springer.

Lasky, J. R., Des Marais, D. L., McKay, J. K., Richards, J. H., Juenger, T. E., & Keitt, T. H. (2012). Characterizing genomic variation of *Arabidopsis thaliana*: the roles of geography and climate. *Molecular Ecology*, 21, 5512-5529.

Latham, R. E. (1992). Cooccurring tree species change rank in seedling performance with resources varied experimentally. *Ecology*, 73, 2129-2144.

Leites, L. P., Rehfeldt, G. E., & Steiner, K. C. (2019). Adaptation to climate in five eastern North America broadleaf deciduous species: Growth clines and evidence of the growth-cold tolerance trade-off. *Perspectives in Plant Ecology Evolution and Systematics*, 37, 64-72.

Li, Y., Huang, Y., Bergelson, J., Nordborg, M., & Borevitz, J. O. (2010). Association mapping of local climate-sensitive quantitative trait loci in *Arabidopsis thaliana*. *Proceedings of the National Academy of Sciences of the United States of America*, 107, 21199-21204.

Liu, C. M. (2010). Arabidopsis as model for developmental regulation and crop improvement. In Plant Developmental Biology - Biotechnological Perspectives (eds E. C. Pua & M. R. Davey), pp. 21-33. Springer, Berlin.

Lopez-Iglesias, B., Villar, R., & Poorter, L. (2014). Functional traits predict drought performance and distribution of Mediterranean woody species. *Acta Oecologica-International Journal of Ecology*, 56, 10-18.

Lorts, C. M., & Lasky, J. R. (2020). Competition x drought interactions change phenotypic plasticity and the direction of selection on Arabidopsis traits. *New Phytologist*, 227, 1060-1072.

Macarthur, R., & Levins, R. (1967). Limiting similarity convergence and divergence of coexisting species. *American Naturalist*, 101, 377-385.

Marks, C. O., & Lechowicz, M. J. (2006). Alternative designs and the evolution of functional diversity. *American Naturalist*, 167, 55-66.

Mart, K. B., Veneklaas, E. J., & Bramley, H. (2016). Osmotic potential at full turgor: an easily measurable trait to help breeders select for drought tolerance in wheat. *Plant Breeding*, 135, 279-285.

Mason, C. M., & Donovan, L. A. (2015). Evolution of the leaf economics spectrum in herbs: Evidence from environmental divergences in leaf physiology across *Helianthus* (Asteraceae). *Evolution*, 69, 2705-2720.

Maximov, N. A. (1931). The physiological significance of the xeromorphic structure of plants. *Journal of Ecology*, 19, 273-282.

Mayr, E. (1963) Animal Species and Evolution. Cambridge, USA: Harvard University Press.

McKay, J. K., Richards, J. H., & Mitchell-Olds, T. (2003). Genetics of drought adaptation in *Arabidopsis thaliana*: I. Pleiotropy contributes to genetic correlations among ecological traits. *Molecular Ecology*, 12, 1137-1151.

Medina-Villar, S., Uscola, M., Perez-Corona, M. E., & Jacobs, D. F. (2020). Environmental stress under climate change reduces plant performance, yet increases allelopathic potential of an invasive shrub. *Biological Invasions*, 22, 2859-2881.

Meyre, D., Leonardi, A., Brisson, G., & Vartanian, N. (2001). Drought-adaptive mechanisms involved in the escape/tolerance strategies of *Arabidopsis* Landsberg *erecta* and Columbia ecotypes and their F1 reciprocal progeny. *Journal of Plant Physiology*, 158, 1145-1152.

Mickelbart, M. V., Hasegawa, P. M., & Bailey-Serres, J. (2015). Genetic mechanisms of abiotic stress tolerance that translate to crop yield stability. *Nature Reviews Genetics*, 16, 237-251.

Midgley, G. F., Hannah, L., Millar, D., Rutherford, M. C., & Powrie, L. W. (2002). Assessing the vulnerability of species richness to anthropogenic climate change in a biodiversity hotspot. *Global Ecology and Biogeography*, 11, 445-451.

Mojica, J. P., Mullen, J., Lovell, J. T., Monroe, J. G., Paul, J. R., Oakley, C. G., & McKay, J. K. (2016). Genetics of water use physiology in locally adapted *Arabidopsis thaliana*. *Plant Science*, 251, 12-22.

Molina-Montenegro, M. A., Gallardo-Cerda, J., Flores, T. S. M., & Atala, C. (2012). The trade-off between cold resistance and growth determines the *Nothofagus pumilio* treeline. *Plant Ecology*, 213, 133-142.

Mouquet, N., & Loreau, M. (2002). Coexistence in metacommunities: The regional similarity hypothesis. *American Naturalist*, 159, 420-426.

Mukherjee, J. R., Jones, T. A., Adler, P. B., & Monaco, T. A. (2011). Drought tolerance in two perennial bunchgrasses used for restoration in the Intermountain West, USA. *Plant Ecology*, 212, 461-470.

Niinemets, U. (2001). Global-scale climatic controls of leaf dry mass per area, density, and thickness in trees and shrubs. *Ecology*, 82, 453-469.

Orians, G. H., & Solbrig, O. T. (1977). Cost-income model of leaves and roots with special reference to arid and semiarid areas. *American Naturalist*, 111, 677-690.

Ostman, B., Lin, R., & Adami, C. (2014). Trade-offs drive resource specialization and the gradual establishment of ecotypes. *Bmc Evolutionary Biology*, 14, 1-10.

Pareek, A., Dhankher, O. P., & Foyer, C. H. (2020). Mitigating the impact of climate change on plant productivity and ecosystem sustainability. *Journal of Experimental Botany*, 71, 451-456.

Parker, J. (1963). Cold resistance in woody plants. *Botanical Review*, 29, 123-201.

Pasquet-Kok, J., Creese, C., & Sack, L. (2010). Turning over a new 'leaf': multiple functional significances of leaves versus phyllodes in Hawaiian *Acacia koa*. *Plant Cell and Environment*, 33, 2084-2100.

Polley, H. W., Tischler, C. R., Johnson, H. B., & Derner, J. D. (2002). Growth rate and survivorship of drought: CO2 effects on the presumed tradeoff in seedlings of five woody legumes. *Tree Physiology*, 22, 383-391.

Poorter, H., Niinemets, U., Poorter, L., Wright, I. J., & Villar, R. (2009). Causes and consequences of variation in leaf mass per area (LMA): a meta-analysis. *New Phytologist*, 182, 565-588.

Poorter, H., Niklas, K. J., Reich, P. B., Oleksyn, J., Poot, P., & Mommer, L. (2012). Biomass allocation to leaves, stems and roots: meta-analyses of interspecific variation and environmental control. *New Phytologist*, 193, 30-50.

Ramirez-Valiente, J. A., Center, A., Sparks, J. P., Sparks, K. L., Etterson, J. R., Longwell, T. *et al.* (2017). Population-level differentiation in growth rates and leaf traits in seedlings of the Neotropical live oak *Quercus oleoides* grown under natural and manipulated precipitation regimes. *Frontiers in Plant Science*, 8, 1-14.

Ramirez-Valiente, J. A., Lopez, R., Hipp, A. L., & Aranda, I. (2020). Correlated evolution of morphology, gas exchange, growth rates and hydraulics as a response to precipitation and temperature regimes in oaks (*Quercus*). *New Phytologist*, 227, 794-809.

Reich, P. B. (2014). The world-wide 'fast-slow' plant economics spectrum: a traits manifesto. Journal of Ecology, 102, 275-301.

Ripullone, F., Grassi, G., Lauteri, M., & Borghetti, M. (2003). Photosynthesis-nitrogen relationships: interpretation of different patterns between *Pseudotsuga menziesii* and *Populus x euroamericana* in a mini-stand experiment. *Tree Physiology*, 23, 137-144.

Rosas, T., Mencuccini, M., Barba, J., Cochard, H., Saura-Mas, S., & Martinez-Vilalta, J. (2019). Adjustments and coordination of hydraulic, leaf and stem traits along a water availability gradient. *New Phytologist*, 223, 632-646.

Sack, L. (2004). Responses of temperate woody seedlings to shade and drought: do trade-offs limit potential niche differentiation? *Oikos*, 107, 110-127.

Sack, L., & Buckley, T. N. (2020). Trait multi-functionality in plant stress response. *Integrative and Comparative Biology*, 60, 98-112.

Sack, L., Grubb, P. J., & Maranon, T. (2003). The functional morphology of juvenile plants tolerant of strong summer drought in shaded forest understories in southern Spain. *Plant Ecology*, 168, 139-163.

Sanchez-Gomez, D., Valladares, F., & Zavala, M. A. (2006). Performance of seedlings of Mediterranean woody species under experimental gradients of irradiance and water availability: trade-offs and evidence for niche differentiation. *New Phytologist*, 170, 795-805.

Sanchez-Gomez, D., Zavala, M. A., & Valladares, F. (2008). Functional traits and plasticity linked to seedlings' performance under shade and drought in Mediterranean woody species. *Annals of Forest Science*, 65, 1-10.

Sartori, K., Vasseur, F., Violle, C., Baron, E., Gerard, M., Rowe, N. *et al.* (2019). Leaf economics and slow-fast adaptation across the geographic range of *Arabidopsis thaliana*. *Scientific Reports*, 9, 1-12.

Sexton, J. P., Strauss, S. Y., & Rice, K. J. (2011). Gene flow increases fitness at the warm edge of a species' range. *Proceedings of the National Academy of Sciences of the United States of America*, 108, 11704-11709.

Smith, T., & Huston, M. (1989). A theory of the spatial and temporal dynamics of plant-communities. *Vegetatio*, 83, 49-69.

Sterck, F., Markesteijn, L., Schieving, F., & Poorter, L. (2011). Functional traits determine trade-offs and niches in a tropical forest community. *Proceedings of the National Academy of Sciences of the United States of America*, 108, 20627-20632.

Trabucco, A., & Zomer, R. J. (2019). Global Aridity Index and Potential Evapotranspiration (ET0) Climate Database v2 figshare. CGIAR Consortium for Spatial Information. Retrieved from https://doi.org/10.6084/m9.figshare.7504448.v3.

Turnbull, L. A., Philipson, C. D., Purves, D. W., Atkinson, R. L., Cunniff, J., Goodenough, A. *et al.* (2012). Plant growth rates and seed size: a re-evaluation. *Ecology*, 93, 1283-1289.

Uddling, J., Gelang-Alfredsson, J., Piikki, K., & Pleijel, H. (2007). Evaluating the relationship between leaf chlorophyll concentration and SPAD-502 chlorophyll meter readings. *Photosynthesis Research*, 91(1), 37-46.

Vasseur, F., Exposito-Alonso, M., Ayala-Garay, O. J., Wang, G., Enquist, B. J., Vile, D. *et al.* (2018). Adaptive diversification of growth allometry in the plant *Arabidopsis thaliana*. *Proceedings of the National Academy of Sciences of the United States of America*, 115, 3416-3421.

Vitasse, Y., Lenz, A., & Korner, C. (2014). The interaction between freezing tolerance and phenology in temperate deciduous trees. *Frontiers in Plant Science*, 5, 1-12.

Waite, M., & Sack, L. (2010). How does moss photosynthesis relate to leaf and canopy structure? Trait relationships for 10 Hawaiian species of contrasting light habitats. *New Phytologist*, 185, 156-172.

Walter, H. (1979). Vegetation of the Earth and Ecological Systems of the Geobiosphere. Germany: Heidelberg Science Library.

Wang, C., Liu, D. W., Luo, W. T., Fang, Y. T., Wang, X. B., Lu, X. T. *et al.* (2016). Variations in leaf carbon isotope composition along an arid and semi-arid grassland transect in northern China. *Journal of Plant Ecology*, 9, 576-585.

Wanner, L. A., & Junttila, O. (1999). Cold-induced freezing tolerance in Arabidopsis. *Plant Physiology*, 120, 391-399.

Weigel, D., & Mott, R. (2009). The 1001 Genomes Project for *Arabidopsis thaliana*. *Genome Biology*, 10, 1-5.

Wright, I. J., Dong, N., Maire, V., Prentice, I. C., Westoby, M., Diaz, S. *et al.* (2017). Global climatic drivers of leaf size. *Science*, 357, 917-921.

Wright, I. J., Reich, P. B., Westoby, M., Ackerly, D. D., Baruch, Z., Bongers, F. *et al.* (2004). The worldwide leaf economics spectrum. *Nature*, 428, 821-827.

Yadav, S. K. (2010). Cold stress tolerance mechanisms in plants. A review. *Agronomy for Sustainable Development,* 30, 515-527.

CHAPTER 4

BREAKING THE LAW: MIXED CLIMATE ADAPTATION STRATEGIES RESULTS IN CONTRARY TRAIT-CLIMATE RELATIONSHIPS ACROSS *ARABIDOPSIS* ECOTYPES

ABSTRACT

Leaf structural, hydraulic and gas exchange traits interact and scale up to affect whole plant growth. Little work has investigated the coordination among these traits and between these traits and climate across ecotypes of a single species. In common gardens, we tested for climate adaptation in drought resistance traits across a diverse set of 144 ecotypes of *Arabidopsis thaliana*, and focused on more detailed physiological traits for 12 ecotypes. We found strong variation across ecotypes in structure and function, with relationships contrasting with those that are well established as optimality principles across diverse species. These contrasting relationships arise due to the adaptation of *A. thaliana* ecotypes to climatic aridity through both stress tolerance and avoidance, a "rule breaking" ability that would contribute to its occupation of a wide climatic range and the expectation of strong evolution under climate change.

INTRODUCTION

Plant traits confer tolerance of climatic stresses such as drought in combination, achieving optimal suites (Wright *et al.* 2004). Studies on a range of diverse species have shown the centrality of the plant hydraulic system in this adaptation, given its major role in determining gas exchange, drought tolerance and plant growth (Meinzer 2002; Brodribb *et al.* 2005; Brodribb *et al.* 2007; Scoffoni & Sack 2017). On one hand, species can adapt to aridity through rapid growth when water is available, i.e., "stress avoidance". Such an ability would be enabled by traits related to high hydraulic conductance. According to theory, leaves need to maintain high levels of hydration (i.e., high leaf water potential, Ψ_{leaf}) to maintain open stomata and perform photosynthesis, and to avoid leaf damage. To maintain a high Ψ_{leaf} the leaves require sufficient hydraulic conductance to replenish the water lost to transpiration (see summary of literature in Table S4.1). Consequently, hydraulic supply must match evaporative demand, and leaf hydraulic conductance under high light (K_{max}) should be correlated with stomatal conductance (g_{op}) and with light-saturated photosynthetic rate per leaf area and mass (A_{area} and A_{mass}). These hypotheses have been supported across diverse species (Brodribb *et al.* 2007) and across evolution within closely related species of *Viburnum* (Scoffoni *et al.* 2016). Further, K_{max} varies based on conductivities both inside (K_x) and outside (K_{ox}) the xylem, with both of these components influenced by leaf anatomy and venation (Sack & Holbrook 2006; Scoffoni *et al.* 2011; Sack & Scoffoni 2013). The leaf vein system enables transport of water throughout the leaves and to the surrounding cells. A greater density of veins (vein length per area; VLA) should therefore lead to an increase in both K_x and K_{ox} (Sack & Frole 2006; Brodribb *et al.* 2007; Sommerville *et al.* 2012; Sack & Scoffoni 2013; McKown *et al.* 2016).

VLA has also been shown to be evolutionary correlated with stomatal traits across related (Zhang *et al.* 2012) and diverse species, with greater vein density leading to higher stomatal conductance and maintenance of photosynthetic function (Sack *et al.* 2008; Boyce *et al.* 2009; Scoffoni *et al.* 2011; Sack & Scoffoni 2012b, 2013). A greater VLA should therefore scale up to confer greater A_{area} and A_{mass}, as has been shown across diverse plant species (Brodribb *et al.* 2007; Sack *et al.* 2013). More xylem conduits with larger diameters will contribute to increases in K_x (Sommerville *et al.* 2012; Sack & Scoffoni 2013), and K_{ox} will be affected by many factors including cell membrane conductivities, ABA concentration, aquaporin function, and the length of pathways from veins to surrounding cells (Buckley *et al.* 2015; Scoffoni *et al.* 2017; Scoffoni *et al.* 2018). Previous studies across diverse species have found that higher vein length per area (VLA) is associated with warmer, drier climates to allow for a higher growth rate under water stress (Sack & Scoffoni 2013) by creating many pathways for water to move through the leaf. An increased K_{leaf} could confer the benefits of offsetting transpiration rates at higher vapor pressure deficit (VPD) in arid climates, and due to the coordination of K_{leaf} with A_{max}, a high K_{leaf} could also allow for fast growth of plants in times of water availability (Maximov 1931; Grubb 1998; Scoffoni *et al.* 2011; Sack *et al.* 2013). A plant's water use efficiency, or the ratio of water lost to carbon gained, depends on stomatal conductance, with more open stomata resulting in greater water loss. Water use efficiency can be measured as the ratio of ^{13}C to ^{12}C isotopes with a more negative value indicating greater discrimination against ^{13}C, usually indicating greater stomatal opening, as has been shown across 18 genotypes of *Arabidopsis thaliana* (Easlon *et al.* 2014).

Notably, achieving high hydraulic conductance may come at the cost of achieving the second major adaptive strategy for climatic extremes, the ability to function under extreme drought. Adaptation to drought could be achieved either through delaying desiccation (e.g., by

closing stomata) or by tolerating dehydration to maintain function under stress. For example, drought tolerant plants tend to have a more negative π_{TLP}, of which the osmotic potential at full turgor (π_o) is the major biophysical determinant (Bartlett *et al.* 2014). This trait is conferred by increased solute concentration in mesophyll cells. Across a number of species sets, the π_{TLP} can predict drought tolerance, and correlates with aridity across biomes, diverse species, closely related species, and genotypes of a single species (Bartlett *et al.* 2012b; Mart *et al.* 2016; Fletcher *et al.* 2018; Griffin-Nolan *et al.* 2019; Rosas *et al.* 2019). The π_o has been shown to correlate with other drought-related traits, such as leaf mas per area (LMA), across diverse species (Villagra *et al.* 2013; Scoffoni *et al.* 2014). The ability to maintain function during drought is also related to the water potential at 50 or 80 percent loss of hydraulic conductance (P_{50} and P_{80}) across species, and to other traits such as thick, dense leaves with high LMA (Nardini *et al.* 2012; Nardini *et al.* 2014) and more dense veins (Scoffoni *et al.* 2011; Nardini *et al.* 2012; Nardini *et al.* 2014). Across diverse species, a lower P_{50} and P_{80} have been associated with smaller leaves, which tend to have a greater major VLA due to major veins beginning to form prior to most of the leaf expansion (Scoffoni *et al.* 2011; Sack *et al.* 2012).

Thus, predictions for the direction of correlation of leaf traits with climate may vary across a set of plants if adaptation to an environmental stress occurs principally through avoidance or tolerance (see summary of predictions in Table S4.2; Maximov 1931; Evans 1972; Farquhar *et al.* 1989; Grubb 1998; Reich *et al.* 1999; Niinemets 2001; Wright *et al.* 2001; Hetherington & Woodward 2003; McKay *et al.* 2003; Wang *et al.* 2003; Wright *et al.* 2004; Westoby & Wright 2006; Brodribb *et al.* 2007; Franks & Farquhar 2007; Brodribb & Jordan 2008; Franks & Beerling 2009; Poorter *et al.* 2009; Scoffoni *et al.* 2011; Bartlett *et al.* 2012b; Klooster & Palmer-Young 2012; Sack *et al.* 2012; Zhu *et al.* 2012; Sack & Scoffoni 2013;

Blackman *et al.* 2014; Brodribb *et al.* 2014; Nardini & Luglio 2014; Wang *et al.* 2015; Wright *et al.* 2017; Fletcher *et al.* 2018; Jordan *et al.* 2020; Ramirez-Valiente *et al.* 2020; Oliveira *et al.* 2021; Fletcher *et al.* in prep.). Many traits can interplay to modulate overall plant growth in varying climates through coordination or trade-offs. For example, according to the leaf hydraulic safety-efficiency trade-off, plants with higher K_{max} may also be more vulnerable during drought due to disruption of K_{ox} and in some cases, embolism (Ocheltree *et al.* 2016; Scoffoni *et al.* 2017). Maximum stomatal conductance may also trade-off with another key drought tolerance trait, π_o. A more negative π_o causes water to be drawn into all cells, including those in the epidermis, creating a strong pressure against the stomata and preventing them from opening fully (Henry *et al.* 2019). Therefore, stomatal control also places a limit on A_{max} (Zhu *et al.* 2018), even if K_{leaf} is high in drought-adapted plants. In the case of annual plants, this trade-off with photosynthetic rate could lead to shorter lifecycles in plants with less negative π_o (Zhu *et al.* 2018).

Another major type of trade-off may act to distinguish stress avoiders from stress tolerant plants. An overarching theory for trait relationships in ecology is the leaf economics spectrum (LES), which describes how suites of structural and physiological traits contribute to slow and fast returns on investments (Wright *et al.* 2004). Leaf structural traits may be related to photosynthetic rates through the LES, e.g., greater leaf nitrogen concentration (N_{area} and N_{mass}) may contribute to higher A_{area} and A_{mass} (Wright *et al.* 2004). Greater LMA could lead to greater N_{area} due to the presence of multiple cell layers in the leaf (Ellsworth & Reich 1992). However, according to the LES, more investment into leaves with higher LMA that would have a longer lifespan could lead to a decreased A_{mass} (Wright *et al.* 2004).

While some trait-trait and trait-climate relationships have been tested across diverse species and across species within a lineage, the same relationships may differ at the intraspecific scale. Indeed, there was no support for a relationship between K_{leaf} and vein density (Caringella *et al.* 2015) or between VLA and stomatal density in other studies of Arabidopsis mutants (Carins Murphy *et al.* 2017). It is unclear whether these such relationships would be upheld across ecotypes within a given species. In addition, studying trait-trait and trait-climate relationships within a model species will potentially lead to gene discovery, creating genetic resources for future researchers.

The aim of this study was to test hydraulic design relationships among traits and between traits and climate (summarized in Tables S4.1 and S4.2) at multiple scales by combining a greenhouse common garden study of a few, diverse ecotypes of the model species *Arabidopsis thaliana* (referred to as Arabidopsis henceforth) with one encompassing Arabidopsis ecotypes found across a multi-continental native range. We tested a broad range of 144 ecotypes to examine the intraspecific relationship between π_o, LMA and climate (Fig. 4.1). For 12 diverse ecotypes (Table 4.1; Fig. 4.1A) grown in a common garden we also tested the association of the π_o with gas exchange and hydraulic traits, and of these traits with origin climate. We expected that traits would correlate with each other according to coordination between hydraulic and photosynthetic traits, trade-offs between traits, and leaf economics theory (summarized in Table S4.1). We additionally hypothesized that these traits would be correlated with climate by conferring drought tolerance and/or drought avoidance mechanisms according to a framework summarized in Table S4.2. Overall, this work scales from leaf form and anatomy up to gas exchange and growth in a model system, investigating the relationships of venation, drought tolerance, hydraulics, gas exchange, photosynthesis, growth, and climate.

METHODS

Growth conditions and trait data collection of 144 genotypes

144 naturally-occurring genotypes (ecotypes) of Arabidopsis that had been included in the 1001 Genomes Project (Alonso-Blanco *et al.* 2016) were selected to maximize the range of measured traits from the literature and past experiments (such as flowering time and growth rate) and the geographic distribution of the species. Ecotypes were grown across three experimental runs in a greenhouse at the Centre d'Ecologie Fonctionnelle et Evolutive (CEFE, Montpellier, France) from 8 December 2016 to 6 April 2017. Eight individuals of each ecotype were present in the first run, with half the individuals being harvested at bolting and half harvested at maturity. Two additional experimental runs were planted with four individuals each per genotype to ensure π_o could be measured for as many ecotypes as possible (n=133 of the 144 ecotypes). Leaf nitrogen content (LNC; 5) was also measured in each run (n=142 of the 144 ecotypes). Pots were filled with a 1:1 mixture of sand and soil that had been collected from a field at the CEFE and was supplemented with 2-3 mm of organic compost (Neuhaus N2). Three to five seeds were sown in each pot left in the dark at 8°C for one month for vernalization prior to being moved to the greenhouse. Pots were then thinned to one individual each after germination. The experiments were blocked, with two plants per genotype in each block, and with pots being distributed randomly in a checkerboard, leaving space around each pot to avoid shading. Blocks were rotated and moved within the greenhouse each day to reduce variation between them. During the experiment, consistent greenhouse temperature and light levels were maintained (18°C during the day and 15°C at night; 12.5 h photoperiod) Plants were watered twice per week.

Prior to measurement of the π_o, whole plants were removed from the soil and placed into tubes filled with deionized water. Plants were covered with opaque plastic bags and rehydrated

overnight. Leaf discs were punched and submerged immediately in liquid Nitrogen to release cell contents. The π_o was then measured using an osmometer (VAPRO 5520 or VAPRO 5600 vapor pressure osmometer; Wescor, Logan, UT, USA) on at least two samples per leaf for each of 3-12 individual plants (Bartlett *et al.* 2012a). Notably, tertiary veins could not be excluded from the measurements due to the small leaf size, which could potentially dilute the contents of the cell sap, but the midrib and secondary veins were avoided.

Repeated measures ANOVAs were performed on π_o for genotypes that were grown in more than one experimental round (either rounds 1 and 2 or rounds 1 and 3) using the *anova_test* function in the rstatix package. The π_o was not statistically significantly different between experimental rounds 1 and 3 ($F(1, 53) = 1.258$, $p = 0.267$, generalized eta squared = 0.012.) or between rounds 1 and 2, ($F(1, 13) = 4.477$, $p = 0.054$, generalized eta squared = 0.135). A correlation analysis using the *lm* function in the stats package was performed to test for correlations between traits and climate variables. Pearson's correlations were tested using untransformed and log-transformed data (data available in Tables S4.3 and S4.4), and Spearman's rank correlations were also tested. Results were considered significant if one of the Pearson's correlations was significant along with the rank correlation. The most significant of the correlations was reported in Table S4.5).

Growth conditions and trait measurements of 12 genotypes

Arabidopsis genotypes were selected from the 1001 Genomes Project (Alonso-Blanco *et al.* 2016) based on native climate, including genotypes originating in the most extreme ends of the climate ranges experienced by this species (based on aridity, precipitation and temperature, while still encompassing multiple origin groups; Table 4.1, Fig. 4.1A). Twelve focal genotypes were

grown in the UCLA greenhouse from July 2016 to May 2017 under standard growth conditions (22.3-32.6°C, 34.8-67.6% humidity, 116.8-206.5 μmol photons m^{-2} s^{-1}). Seeds were sown in pots (8 cm long, 12.3 cm wide, 6 cm deep) with 1:1:2:1:1 mixture of plaster sand, loam, peat moss, perlite and vermiculite. Pots were placed in a cold chamber for three days to cold acclimate at 4°C. After one week the pots were thinned to include one individual per pot. Plants were watered 2-3 times per week with fertilized water (250ppm of Peters Professional water soluble fertilizer; N 20%; P 20%; K 20%; B 0.0125%; Cu 0.0125%; Fe 0.05%; Mn 0.025%; Mo 0.005%; Zn 0.025%). Leaves were collected for various measurements as described below after they had 10-20 true leaves (approximately 6 weeks later).

The π_o and gas exchange measurements were made on two leaves each from three individuals per genotype. The π_o was measured using the osmometer method (VAPRO 5520 and 5600 vapor pressure osmometers; Wescor, Logan, UT, USA; (Bartlett *et al.* 2012a)). Photosynthetic and gas exchange rates (A_{area}; μmol of CO_2 m^{-2} s^{-1} and g_{op}; moles of H_2O m^{-2} s^{-1} or moles of CO_2 m^{-2} s^{-1}, respectively) along with transpiration rates (E; mmol H_2O m^{-2} s^{-1}) were recorded using a Li-Cor 6400 with a fluorescence head. If leaves were smaller than the area of the chamber, measurements were adjusted based on surface area inside the Li-Cor chamber which had its area traced and subsequently measured in ImageJ (software version 1.52k; National Institutes of Health, Bethesda, MD, USA). The whole leaf areas for 2-8 leaves per genotype were also traced in ImageJ. Leaves were then placed into a drying oven for at least 72 hours at 70°C (XS205; Mettler, Toledo, OH, USA) after which they were weighed to determine dry leaf mass. Leaf mass per area (LMA; g cm^{-2}) was calculated as leaf dry mass divided by leaf fresh area, and specific leaf area (SLA, m^2 kg^{-1}) was calculated as the inverse. The maximum

photosynthetic rate per mass (A_{mass}; μmol of CO_2 g^{-1} s^{-1}) was calculated as A_{area} divided by LMA, and the A_{area}:g_{op} ratio was calculated as A_{area} divided by g_{op}.

Leaf hydraulic measurements were made for each genotype using the evaporative flux method (Sack & Scoffoni 2012). Pots were moved from the greenhouse to the laboratory and were covered in opaque plastic bags filled with wet paper towels so plants could rehydrate over night prior to measurement. Vulnerability curves spanning a range of Ψ_{leaf} values were obtained by making measurements on at least 20 leaves from at least four individuals per genotype. A mature leaf was cut at the petiole with a razor blade under ultra pure water (0.22-μm Thornton 200 CR; Millipore) in preparation for measurement. The petiole was then wrapped in Parafilm and connected to tubing leading to a water source on a balance (models XS205 and AB265; Mettler Toledo). The balance was connected to a computer that logged flow rate into the leaf every five seconds. The leaf was placed onto a system designed to maximize its photosynthetic and subsquent transpiration rates: over a box fan and under a light with >1,000 μmol m^{-2} s^{-1} (model 73828 1,000-W UV filter; Sears Roebuck). There was a water bath below the light to prevent the leaf from overheating, and the leaf was maintainted between 23 to 28°C (monitored by measurement with a thermocouple; Cole-Parmer). The flow rate was recorded after the leaf had light-acclimated for at least 30 minutes on the evaporative flux system and only after flow had stabilized (the coefficient of variation was <0.05 in the last five-minute period before the measurement was recorded; coefficient of variation is the standard deviation divided by the mean). Leaf temperature was also recorded at this time. The leaf was then taken off the system and placed into a plastic bag into which the experiementer had previously exhaled. This bag was placed into a second bag with wet paper towels, was left for 30 minutes to allow the leaf to equilibrate before measurement of the Ψ_{leaf}. The final Ψ_{leaf} was measured using a pressure

chamber (Plant Moisture Stress model 1000: PMS Instrument) with a grass fitting in the compression lid. The leaf was also traced onto paper and the tracing was scanned and measured using ImageJ. Outlier points were removed based on Dixon's test for statistical outliers. K_{leaf} was calculated as the flow rate divided by the driving force (Ψ_{leaf}) and was corrected for area and temperature-based changes in water viscosity with a reference value of 25°C (Weast 1978; Yang & Tyree 1993). Vulnerability curves were plotted as K_{leaf} against Ψ_{leaf}. The best fitting curves of K_{leaf} against Ψ_{leaf} were modeled and selected by AIC scores in a model fitting comparison (to find the best fit between linear, logistic, exponential and sigmoidal curves). K_{max} was estimated as the value of K_{leaf} of the best-fit curve at a water potential of -0.1 MPa. The leaf water potential at 50 and 80% loss of K_{leaf} (P_{50} and P_{80}) were also estimated based on K_{max} at -0.1 MPa. The pressure drop across the leaf was calculated as E divided by K_{max}.

For vein and stomatal measurements, leaves were preserved in 70% formalin-acetic acid-alcohol (FAA; 48% ethanol: 10% formalin: 5% glacial acetic acid: 37% water). Then, for vein measurements, leaves were cleared with 2.5-5% sodium hydroxide in water or ethanol, and then with sodium hypochlorite bleach, following standard protocols (Scoffoni *et al.* 2013). Leaves were then stained with safranin and fast green, mounted between clear sheets (AF4300, 3M, St. Paul, MN, USA) and scanned at 1200dpi (Epson Perfection 4490, Long Beach, CA, USA). Leaf and vein measurements were made on 3-5 leaves per ecotype using ImageJ. Measurements included widths and vein length per area (VLA) for each vein order in the leaf blade, along with leaf size and dimension measurements made on cleared and stained leaves. The projected vein area per area (PAPA) was calculated as the sum of the VLA of each vein order times the average width of each corresponding vein order. The volume of veins per area (VPA) was also calculated

as the sum of the VLA for each vein order times the number π times the squared radius of each vein order.

Epidermal and stomatal traits were measured on one leaf from each of 3-5 individuals per ecotype. Epidermal measurements were obtained from microscopy images taken from nail varnish impressions of both leaf surfaces. Several traits were measured from microscope images of the nail varnish peels, including stomatal density (*s*), stomatal differentiation rate (or index; the number of stomata per numbers of stomata plus epidermal pavement cells, *i*), stomatal area (*s*), guard cell length and width (GC_l, GC_w), inner and outer stomatal pore length (SP_{il}, SP_{ol}), and epidermal pavement cell area (*e*) in the abaxial and adaxial surfaces. All images were analyzed and traits were measured using the software ImageJ. From the measured stomatal traits, we calculated the maximum theoretical stomatal conductance g_{max} two ways using the following equation (Franks & Farquhar 2007; Sack & Buckley 2016):

$$g_{\max} = \frac{bmds}{s^{0.5}} \qquad \text{eqn. 1}$$

In which *b* is a biophysical constant given as $b = \frac{D}{v}$, where *D* represents the diffusivity of CO_2 and water in air $m^2\ s^{-1}$ and *v* is the molar volume of air $m^3\ mol^{-1}$, so *b* = 0.00126; *d* is stomatal density, *s* is stomatal size and *m* is a morphological constant based on scaling factors representing the proportionality of stomatal dimensions $m = \frac{\pi c^2}{j^{0.5} 4hj + \pi}$ (Franks & Farquhar 2007; Franks *et al.* 2009; McElwain *et al.* 2016). For the calculation of $g_{max\ c}$, we treated *c*, *h*, and *j* as constants; *c*, *h* and *j* = 0.5. For the calculation of $g_{max\ m}$, *c*, *h*, and *j* were calculated using the measured stomatal dimensions; $c = \frac{SP_{ol}}{GC_l}$, $h = \frac{GC_w/_2}{GC_w}$ and $j = \frac{GC_w}{GC_l}$.

Stable carbon isotope data were obtained for 2-3 individual plants per genotype. Prior to processing, leaves were oven dried for at least 72 hours at 70°C. 3-4mg of ground leaf material

were sent to the Center for Stable Isotope Biogeochemistry at the University of California, Berkeley. Percent of nitrogen was measured along with carbon isotope ratio ($\delta^{13}C$; ‰; measured by dual isotope analysis with an Elemental Analyzer interfaced to a mass spectrometer). The leaf nitrogen per mass (N_{mass}; mg g^{-1}) was calculated as the mass of nitrogen in the sample (mg) divided by the mass of the sample (g), and leaf nitrogen per area (N_{area}; g m^{-2}) was calculated as N_{mass} multiplied by LMA.

Origin climate information was obtained using geolocation data available from the 1001 Genomes Project (Alonso-Blanco *et al.* 2016). Mean annual temperature and annual precipitation climate variables were downloaded from WorldClim version 2.1 Global Climate Data (BioClim), along with 4 monthly climate variables (precipitation, and minimum, average and maximum temperatures; Fick & Hijmans 2017). Annual values of aridity index and potential evapo-transpiration were downloaded from the Consultative Group for International Agriculture Research (CGIAR) Consortium for Spatial Information (CSI) database version 2 (Antonio & Robert 2019). Climate information was extracted at each coordinate for each genotype using ArcMap (version 10). Growing season monthly values were averaged for each genotype if they met previously the established criteria of ≥ 4°C and precipitation ≥ 2 × mean temperature (Lasky *et al.* 2012). This method was also used to determine growing season length and total precipitation of the growing season. Three additional climate variables of vegetation health index in spring and summer, and plant extractable water capacity of soil were obtained (Ferrero-Serrano & Assmann 2019). Flowering times for plants grown at a constant temperature of 10°C or 16°C after an initial cold treatment (FT10 and FT16, respectively, recorded as days until the first open flower appeared) for each ecotype were obtained from the 1001 Genomes Consortium (Alonso-Blanco *et al.* 2016). Data for plant lifespan, fruit number, relative growth rate (RGR),

rosette diameter and scaling exponent (as a proxy for RGR) were obtained for 9 of our 12 focal ecotypes (Vasseur *et al.* 2018).

An Analysis of Variance (ANOVA) was performed on all traits using the *aov* function in the stats package in the R Statistics environment (R version 4.0.4) to test for variation between individuals and across genotypes. Correlations were tested between all traits quantified in this study, and between traits and climate factors using a linear mixed effects model with kinship using the *lmekin* function in the coxme package in R. Kinship matrices were pulled from the 1001 Genomes Project data release v3.1 (Weigel & Mott 2009). Both untransformed and log-transformed data were used to test for both linear and nonlinear (power law) trends. In order to perform the log-transformation, a constant equal to the lowest mean value for an ecotype +1 was added to all variables that included negative numbers before log-transformation so that the lowest value for that variable was 1. This included such variables as mean annual temperature, average of the minimum temperatures occurring in each month of the growing season, and plant extractable water capacity of soil. For π_o, P_{50}, P_{80}, $\delta^{13}C$ and Ψ_{op} all values were multiplied by -1 before log transformation. The most significant of the findings are reported in the main text (using either untransformed or log-transformed data, data presented in Tables S4.6 and S4.7), with all results reported in Supplemental Table S4.8.

RESULTS

Trait and climate correlations across 133-142 ecotypes

In accordance with an overall pattern of adaptation via stress avoidance, across the 133 ecotypes for which π_o was measured, it was related to aridity index, with more negative values of π_o found in more humid climates ($|r|$ =0.19, P = 0.02; Table S4.5; Fig. 4.1B), and π_o also was less negative

for ecotypes originating from sites with higher potential evapo-transpiration ($|r| = 0.24$, $P < 0.01$; Table S4.5). Further, a higher LMA was also associated with lower potential evapo-transpiration, precipitation of the growing season (Fig. 4.1C), and maximum temperature of the growing season across 142 ecotypes ($|r| = 0.17$-0.19, $P < 0.05$; Table S4.5). Indeed, variables adapted to climate in accordance with stress avoidance were inter-correlated across the larger dataset, including LMA, leaf nitrogen concentration (LNC) and π_o, with genotypes with less negative π_o having lower LMA and higher LNC, and with LMA and LNC being negatively correlated ($|r| = 0.42$-0.84, $P < 0.001$; Table S4.5). All three of these traits were also related to lifecycle duration, with shorter-lived plants having lower LMA, higher LNC, and less negative π_o ($|r|$ 0.42-0.82, $P < 0.001$; Fig. 4.1D, Table S4.5).

Trait correlations with climate across 12 ecotypes

Hydraulic and photosynthetic traits showed many associations with climatic temperature and aridity. Higher A_{area} but lower A_{mass} was found in ecotypes originating from more arid climates with lower annual and growing season precipitation ($|r| = 0.51$-0.67, $P = 0.01$-0.04; Fig. 4.2A, Table S4.8). Higher A_{area} was also found in ecotypes native to climates with warmer temperatures of the growing season ($r = 0.5$, $P = 0.05$; Table S4.8), and the A_{area}:g_{op} ratio was lower in warmer climates ($r = -0.51$, $P < 0.05$; Table S4.8). Assuming a drought avoidance strategy, we hypothesized that A_{area} would be higher in places with shorter growing seasons or in ecotypes with shorter lifecycles. While we did not find support for a relationship of A_{area} with the length of the growing season, shorter-lived ecotypes had higher A_{area}, A_{mass} and g_{op}.

Stomatal conductance showed may correlations with climate, with a higher g_{op} being associated with more arid climates with lower annual precipitation and higher potential

evapotranspiration ($|r|$ = 0.54-0.62, $P < 0.03$; Fig. 4.2B, Table S4.8) and with higher minimum, average and maximum temperatures of the growing season ($|r|$ = 0.65-0.71, $P < 0.01$; Table S4.8). A higher ratio of g_{op}:g_{max} was found in climates with higher potential evapo-transpiration and warmer annual temperatures, as well as warmer minimum, maximum and average temperatures of the growing season ($|r|$ = 0.49-0.75, $P < 0.05$; Table S4.8). Stomatal density increased with decreasing annual temperature and with increasing minimum, average and maximum temperatures of the growing season ($|r|$ = 0.51-0.64, $P < 0.05$; Table S4.8). Stomatal size showed the opposite trend and increased with increasing annual temperatures and minimum, average and maximum temperatures of the growing season ($|r|$ = 0.52-0.65, $P < 0.05$; Table S4.8). Anatomical $g_{max\ m}$ was decoupled from climatic temperature and moisture.

Several leaf traits were also associated with climate. Larger leaves were found in wetter climates (r = 0.61, $P < 0.01$; Table S4.8). A high LMA was associated with low mean annual temperature across the 12 focal ecotypes (r = -0.50, $P < 0.05$; Table S4.8). There was support for the hypothesis that N_{mass} would decrease with increasing climatic moisture, as N_{mass} was negatively correlated with annual precipitation across ecotypes (r = -0.55, P = 0.02; Fig. 4.2C, Table S4.8).

Some traits showed the expected relationship with climate assuming the genotypes are adapted via drought tolerance. Along with the negative association of LMA with moisture across the larger ecotype set, we found that genotypes with more negative values of P_{80} were found in more arid climates with lower growing season precipitation ($|r|$ = 0.53-56, P = 0.02-0.03; Fig. 4.3B, Table S4.8), and in climates with lower spring vegetation health indices ($|r|$ = 0.43, P = 0.05; Table S4.8), but P_{80} was independent of temperature (Table S4.8).

Several traits related to climate in unexpected ways, or were decoupled from climatic stress despite predictions of correlation. As in the larger ecotype set, we found that ecotypes from arid climates with lower annual and growing season precipitation had less negative values of π_o ($|r|$ = 0.61-0.87, $P < 0.01$; Fig. 4.4A, Table S4.8). $\delta^{13}C$ was related to many climate variables, with more negative values of $\delta^{13}C$ being found in warmer climates with higher potential evapo-transpiration, and higher minimum, average and maximum temperatures of the growing season ($|r|$ = 0.59-0.70, $P \leq 0.01$; Fig. 4.4B, Table S4.8). Major vein density was independent of climate (Fig. 4.4C), but a higher minor vein density was found in more humid climates (r = 0.51, P = 0.04; Table S4.8). There was no significant trend for K_{max} or K_{max}:g_{op} with climate (Fig. 4.4D).

Trait correlations across 12 ecotypes

Across 12 Arabidopsis ecotypes, some hypothesized trait-trait relationships were supported, while others were not detected or were found in the opposite direction from the expected. Leaf size was negatively related to midrib, secondary and total major VLA (r = -0.69 to -0.77, $P \leq$ 0.001; Fig. 4.5A, Table S4.8), but was statistically independent from minor and total VLA (Table S4.5). There was no relationship between K_{max} and A_{max} (Fig. 4.5B, Table S4.8). We also hypothesized that K_{leaf} will be affected by venation architecture, with plants with more dense veins having a higher K_{leaf} and thus higher A_{max}. We found mixed support for this hypothesis, with higher major vein length per area (first and second order and total major VLA) being associated with higher rates of hydraulic conductance (r = 0.52-0.69, P = 0.001-0.04; Fig. 4.5C), but with no association between K_{leaf} and total or minor vein densities (Table S4.8). Contrary to our expectations, there was a negative association of both total and minor vein density and with

both g_{op} and A_{max} ($|r|$ = 0.53-0.69, P = 0.001-0.03; Table S4.8). There was no association of major vein densities with g_{op} or A_{max} (Table S4.8).

We found support for the hypothesis that plants with a more negative π_o would show smaller stomatal openings and thus lower stomatal conductance (r = 0.79, P < 0.001; Fig. 4.5D, Table S4.8). Additionally, the ratio of operating stomatal conductance to maximum measured anatomical stomatal conductance (g_{op}:$g_{max\ m}$) was lower for genotypes with a more negative π_o (r = 0.79-0.81, P < 0.001; Table S4.8). As predicted, ecotypes with more negative π_o also had a lower maximum rate of photosynthesis (r = 0.74, P <0.001; Table S4.8).

We found support for the hypothesis of a trade-off between max K_{leaf} and vulnerability (P_{80}), with ecotypes with higher K_{leaf} showing a drop off in leaf hydraulic conductance at a less negative water potential ($|r|$ = 0.81, P < 0.001; Fig. 4.5E, Table S4.8). A more negative P_{80} was additionally associated with thicker, denser leaves with higher LMA ($|r|$ = 0.80, P < 0.001; Fig. 4.5F, Table S4.8) but with less dense major veins, contrary to our hypothesis ($|r|$ = 0.52, P = 0.04; Fig. 4.5G, Table S4.8). A more negative carbon isotope ratio was associated with greater g_{op} but lower g_{max} ($|r|$ = 0.60-0.63, P < 0.01; Table S4.8).

Many traits were associated with plant lifespan across 9 ecotypes for which lifespan data were available. As had been found across the larger genotype set, a less negative π_o was found in ecotypes that were shorter-lived ($|r|$ = 0.77, P < 0.001; Table S4.5). A higher A_{mass}, A_{area}, g_{op} and g_{op}:g_{max} were related to shorter lifespan ($|r|$ = 0.69-0.95, P < 0.001; Fig. 4.5H, Table S4.8). Longer-lived plants had more dense minor veins (r = 0.59, P < 0.05; Table S4.8). Some LES traits also related to plant lifespan, with higher values of N_{mass}, N_{area} and N_{area}:g_{op} ratio found in plants with shorter lifespans ($|r|$ = 0.56-0.79, P < 0.05, Table S4.8). A more negative $\delta^{13}C$ was also found in shorter-lived plants ($|r|$ = 0.58, P < 0.05, Table S4.8).

There was some support for LES relationships across the 12 ecotypes. A higher LMA was associated with higher N_{area} (r = 0.82, P < 0.001; Fig. 4.6, Table S4.8) but was independent from N_{mass} (Fig. 4.6, Table S4.8). A higher A_{area} was associated with higher N_{area} and N_{mass} (r = 0.59-0.81, P < 0.01; Fig. 4.6, Table S4.8) but A_{mass} was independent of leaf nitrogen content (Fig. 4.6, Table S4.8).

Variation in structural, hydraulic and photosynthetic traits

Traits related to gas exchange showed substantial variation across the 12 ecotypes in most traits (Table 4.2; Tables S4.6 and S4.7), with A_{area} varying 5.2-fold from 3.0-15.8 μmol of CO_2 m^{-2} s^{-1}, A_{mass} varying 6.2-fold from 0.11-0.73 μmol of CO_2 g^{-1} s^{-1} and g_{op} varying 5.5-fold from 0.12-0.65 moles of CO_2 m^{-2} s^{-1}. The K_{max} varied 5.2-fold from 9.3-48.8 mmol m^{-2} s^{-1} MPa^{-1}. There was also variation in vein widths, where midrib width varied 1.7-fold from 0.56-0.93mm, secondary vein width varied 1.8-fold from 0.036-0.066 mm, and minor vein width varied 2.6-fold from 0.021-0.054 mm. Variation in major veins was greater than in minor veins, with total major VLA varying 2.6-fold from 0.05-1.23 mm mm^{-2} whereas minor VLA varied 1.6-fold from 1.8-2.8 mm mm^{-2}. Some variation was found in leaf composition traits, with $\delta^{13}C$ values ranging from -34.4 to -28.7‰, N_{mass} varying 2.3-fold from 25.8-60.4 mg g^{-1} and N_{area} varying over 4-fold from 0.45-1.86 g m^{-2}. All stomatal traits varied less than 2-fold except epidermal pavement cell area, which varied 2.4-fold from 520.1-1268.3 μm^2. All traits except guard cell width and stomatal initiation rate varied significantly across the 12 ecotypes (Table 4.2).

Variation in drought-related traits

In both experimental sets there was substantial variation in drought-related traits (Table 4.2; Tables S4.3, S4.4, S4.6 and S4.7). Leaf size varied 3.4-fold from 252.8-868.3 mm^2 across 12 ecotypes, and 11.9-fold (from 71.5-854.9 mm^2) when considering data across 136 ecotypes. Across 12 ecotypes, leaf mass per area varied 2.8-fold from 14.1-39.6 g m^{-2}, and across the larger set of 148 ecotypes, an 8.5-fold variation was shown from 9.5-80.7 g m^{-2}. Those 148 ecotypes also showed 1.9-fold variation in leaf nitrogen content from 4.0-7.5%. The π_o ranged from -1.08 to -0.71 across 12 ecotypes and from -1.13 to -0.79 across the set of 140 ecotypes.

Overall drought tolerance and drought avoidance trends

Of the 19 hypothesized trends for relationships of traits with climatic moisture, 8 reflected adaptation through drought avoidance (42%), and 4 reflected adaptation through drought tolerance (21%), while 7 showed a decoupling from climatic moisture (37%). Of the 19 hypotheses for trait relationships with climatic cold, 3 showed cold avoidance (16%), 7 showed cold tolerance (37%) and 9 showed a decoupling from cold (47%).

DISCUSSION

Overall our results indicate that there is some trait adaptation to aridity, but a drought avoidance strategy is dominant across Arabidopsis ecotypes, as evidenced by the correlations within several trait clusters and of traits with climate (e.g., π_o, $\delta^{13}C$, N_{area}, ratio, A_{area}, g_{op}). Leaf hydraulic traits are variable but indirectly related to other traits.

Coordination of hydraulics, photosynthesis, stomatal traits

We found support for some of the relationships between hydraulic, photosynthetic and stomatal traits that are well recognized across species when analyzing trends across genotypes within a species. Contrary to what has been shown across diverse and closely-related species (Brodribb *et al.* 2007; Scoffoni *et al.* 2016), we found no association between leaf photosynthetic and hydraulic capacity. Despite the lack of association between hydraulics and photosynthesis, we found that K_{max} was high and variable. This could potentially be due to the fact that Arabidopsis may avoid growing through stressful periods by instead when water is available and K_{max} is not limiting (Kenney *et al.* 2014; Ocheltree *et al.* 2016). One additional potential reason for the decoupling of A_{area} and K_{max} may be that there are multiple ways to increase photosynthetic rate, including by increasing leaf nitrogen concentration. Indeed, we found that greater concentrations of leaf nitrogen per area and mass (N_{area} and N_{mass}) were correlated with A_{area}, as predicted by the leaf economics spectrum (Wright *et al.* 2004), which could modulate the relationship of K_{max} and A_{area}.

While hydraulic and photosynthetic traits were not correlated, we did find support for the expected safety-efficiency trade-off between vulnerability (P_{80}) and K_{max} (Ocheltree *et al.* 2016; Scoffoni & Sack 2017), where ecotypes that transported water more effectively also lost that capacity during stress. Previous studies have found mixed support for this relationship across various scales (Blackman *et al.* 2010; Nardini *et al.* 2012; Nardini & Luglio 2014; Scoffoni & Sack 2017), but this work showed within-species support for the safety-efficiency trade-off. Several other traits such as outside xylem conductance, pit membrane thickness and bundle sheath and mesophyll cell characteristics may impact hydraulic efficiency and decline during dehydration (Scoffoni *et al.* 2014; Buckley *et al.* 2015; Ocheltree *et al.* 2016; Thonglim *et al.*

2020), and future studies should investigate the relationships between these traits and their role in climate adaptation.

Leaf venation and its effect on K_{max}, g_{op} and A_{max}

We found support for the hypothesis that ecotypes with more dense major veins also had higher values of K_{max} and less negative P_{80}, providing further evidence that hydraulic conductance is linked to leaf venation architecture (Scoffoni *et al.* 2011; Sommerville *et al.* 2012), but found that K_{max} was decoupled from minor vein density, as had been shown previously across Arabidopsis mutants (Caringella *et al.* 2015). We found that stomatal conductance and maximum photosynthetic rate were both decoupled from major vein densities and negatively associated with minor vein densities. In fact, building veins may actually take away from building photosynthetic mesophyll tissue, which will lead to a lower photosynthetic rate in ecotypes with dense veins. This was supported by a negative correlation of projected vein area per leaf area with A_{area} (r = -0.52, P = 0.04; Table S4.5). It should be noted, however, that the variation in vein density is relatively low as compared with the variation shown across diverse angiosperm species (Sack *et al.* 2013), indicating that venation is probably not the main driver for the patterns we observed in photosynthetic rate.

Vein scaling trends have previously been shown across diverse species, with smaller leaves having greater major vein length per area (VLA) while minor VLA has been shown to be decoupled from leaf size due to the fact that minor veins develop mostly after the leaf has fully expanded (Candela *et al.* 1999; Kang & Dengler 2004; Scoffoni *et al.* 2011; Sack & Scoffoni 2012; Sack *et al.* 2012; Sommerville *et al.* 2012). We found further support for this trend across

Arabidopsis genotypes, with major VLA decreasing with increasing leaf area, while minor VLA was independent of leaf size.

Associations of π_o with traits and climate

Previous work has shown π_o to be an excellent predictor of drought tolerance that correlates with climatic aridity at multiple scales (Bartlett *et al.* 2012b; Mart *et al.* 2016; Fletcher *et al.* 2018; Griffin-Nolan *et al.* 2019; Rosas *et al.* 2019) and even across ecotypes of Arabidopsis (Fletcher *et al.* in prep.), but our study found that ecotypes with more negative values of π_o were found in more humid climates. This is consistent with previous work which indicated that Arabidopsis ecotypes native to extremely warm or cool and dry climates tend to avoid drought by growing rapidly when water is available (Fletcher *et al.* in prep.) rather than investing in traits to keep stomata open during drought. This is further supported by the strong trade-off between π_o and both g_{op} and A_{area}, where having a less negative π_o through decreased solute concentration would lead to decreased pressure in leaf epidermal cells, allowing for leaves to open their stomata more widely in order to perform rapid photosynthesis in favorable conditions.

There are several possible reasons for the apparently contrasting trend of this work with a previously reported trend of more negative π_o being found in more arid climates across Arabidopsis ecotypes (Fletcher *et al.* in prep.). One explanation could simply be due to a sampling effect, but it would be unlikely to find a trend that opposes the broader results by random chance. Another explanation is that sampling across ecotypes of more extreme cold or dry native climates, as was done in this study which spanned a broader temperature range than in previous work, could reveal an overall drought avoidance trend, even though trait adaptations conveying drought tolerance may be found among ecotypes in more similar climates, i.e.,

ecotypes growing where the climate is more amenable may be benefitted by evolving some degree of stress tolerance in case they encounter stress during their lifecycles, but if all ecotypes found across a range of very cold and dry to warm and moist climates are included, the overall stress avoidance trend may become apparent. For example, the less negative π_o was associated with drier climates through a trade-off with g_{op} for drought avoidance, while a more negative π_o was associated with longer lifespan, which would confer survival of repeated droughts. Indeed, across the larger π_o dataset of 133 genotypes, thicker, denser leaves had lower leaf nitrogen content (LNC), more negative π_o and longer life cycle lengths, which further indicates that multiple traits may work in tandem to promote the strategy of growing slowly, but being able to tolerate environmental stresses that arise during the longer growth period in favorable climates.

Coordination of K_{max}, g_{op} and A_{max} with climate

We found that ecotypes native to more arid and colder climates had higher g_{op} and A_{area} which would contribute to rapid growth when water is available. Both of these traits, along with leaf nitrogen content, were higher in plants with shorter lifespans, consistent with previous work that indicated that genotypes native to colder climates may have faster growth (Fletcher *et al.* in prep.), but this study is unique in demonstrating increased photosynthetic activity in climates with lower rainfall and less available water. Hydraulic conductance was decoupled from climate, contrary to what has been found previously across diverse species (Nardini & Luglio 2014). This is consistent with the existence of stress-avoidance and stress tolerance adaptive trends existing simultaneously; in extreme climates, avoiders would benefit from high K_{max}, to enable high gas exchange rates when moisture is available, whereas tolerators would benefit from low K_{max}, given that high K_{max} corresponds with low P_{80}. Thus, the existence of two strategies of

adaptation would overall result in the absence of a trend. The same is true for relationships among traits. For example, high major VLA would be beneficial for avoiders in stressful climates through association with high K_{max}, even if major VLA does not contribute directly to A_{max}. A high major VLA would also be beneficial for tolerators by making redundant pathways in case of embolism, which may be expected to lead to a lower P_{80}. Overall, however, due to the strong trade-off between K_{max} and P_{80}, and major VLA being associated with K_{max} in Arabidopsis, we instead see the relationship of major VLA and P_{80} going the opposite direction from the expected, and we see decoupling of major VLA from climate.

Breaking the rules of trait-climate relationships

Despite an overall trend of traits showing adaptation to stress via stress avoidance, there are some traits that apparently adapt to stress via tolerance. For example, more negative values of P_{80}, which indicate reduced vulnerability to loss in hydraulic conductance, were found in ecotypes native to climates with lower annual and growing season precipitation (Oliveira *et al.* 2021). P_{80} was strongly correlated with LMA, which also showed climatic adaptation that would lead to stress tolerance; thicker, denser leaves were found in ecotypes native to colder climates (across the set of 12 ecotypes) with lower precipitation (across 142 ecotypes) consistent with previous work in a set of 378 ecotypes of Arabidopsis (Sartori *et al.* 2019). This relationship between P_{80} and LMA could relate to rehydration capacity, where a higher LMA leaf can dehydrate and rehydrate without becoming damaged (John *et al.* 2018).

Inferences of climate adaptation from leaf economics traits

Some stable isotope data supported the presence of a stress avoidance strategy, with greater leaf N_{mass} found in leaves with lower rainfall, which could allow for faster photosynthetic rates and growth (Craine *et al.* 2009). Combined with a greater LMA in arid climates, this would lead to an overall higher leaf N_{area} in these genotypes found at low rainfall (Wright *et al.* 2001). However, traits related to water use efficiency tended to confer stress tolerance, as seen in the higher ratio of A_{area} to stomatal conductance along with greater water-use efficiency as defined by $\delta^{13}C$ in colder places with higher LMA. A less negative $\delta^{13}C$ indicating greater water use efficiency was also found in longer-lived ecotypes, possibly as a stress adaptation, consistent with previous work in Arabidopsis (McKay *et al.* 2003). The N_{area}:g_{op} ratio was highly correlated with K_{max}, which showed a trade-off with P_{80}, which in turn showed drought adaptation, providing evidence that hydraulic traits may be indirectly linked to climate adaptation in Arabidopsis.

Considering inferences from and potential limitations of this study

Overall, this work shows the complexity of the relationships of plant traits with climate. One limitation of this study is that climate information is drawn from WorldClim, which even at the highest resolution only provides information within $1km^2$. Arabidopsis is a weedy plant that may utilize microclimatic variation to mitigate climatic effects that cannot be captured at this resolution (Lampei *et al.*). Additionally, annual variables may not be the most accurate to the growth periods of Arabidopsis given that Arabidopsis does not grow year-round, but due to the lack of information on the actual growing season months of various genotypes, these data were the best available, and are the standard used in the field (Hancock *et al.* 2011; Lasky *et al.* 2012;

Alonso-Blanco *et al.* 2016; Mojica *et al.* 2016; Vasseur *et al.* 2018; Sartori *et al.* 2019; Lorts & Lasky 2020). We also acknowledge that the native climate information is based on one point of collection for each genotype and may not represent the center of that genotype's range.

Our study showed the importance of considering drought tolerance traits such as the π_o at multiple scales. However, all traits measured in this study were from ideal conditions of high light and abundant water, which may not mimic conditions in the field. Future work should consider how the inferred trait-climate relationships may vary if Arabidopsis responds plastically under drought or cold stress. For example, plants may osmotically adjust in their π_o under different growing conditions, and future work should consider the role of osmotic adjustment in the correlation of π_o and climatic aridity. Previous work, however, has shown that alterations to the π_{TLP} through osmotic adjustment did not obscure the relationship of π_{TLP} with π_o in most species (Bartlett *et al.* 2012b).

Conclusions

Overall, leaf structural, hydraulic and gas exchange traits were shown to be variable across ecotypes. Arabidopsis can adapt to stress through drought avoidance and drought tolerance, but a drought avoidance strategy is dominant across ecotypes. The ability of Arabidopsis to adapt to stress in different ways allows it to break the rules of expected trait relationships with climate and of relationships between traits. In other words, mechanistic traits may show opposite trends of what is expected with climate if they are confounded with fast growth, and similarly trait-trait relationships can go in unexpected directions unless they are strictly mechanistically determined. This work illustrates the complex ways in which traits or suites of traits may adapt to climate and provides a deeper understanding of drought tolerance within a species.

ACKNOWLEDGEMENTS

The authors thank Jessica Smith and the staff of the plant growth center at the University of California, Los Angeles, including Weimin Deng for assistance with plant cultivation, Lauren Gillespie and undergraduate student Celine Ngo for assistance with data collection, Benjamin Blonder for discussion of ideas, and the National Science Foundation (Grants -#1457279, 1557906 and 1951244) and the European Research Council (ERC; 'CONSTRAINTS': grant ERC-StG-2014-639706-CONSTRAINTS) for support.

Table 4.1. Variation across 12 ecotypes of Arabidopsis grown in a greenhouse common garden, in order of ascending aridity index (where a smaller value indicates a more arid climate). Values of leaf mass per area are means with standard error in parentheses.

Genotype	Origin Group	Leaf Mass per Area ($g\ m^{-2}$)	Aridity Index	Annual Precipitation (mm)	Mean Annual Temperature (°C)
CS76789	Relict	21.80	0.14	281	22.7
CS78905	Asia	32.98	0.19	118	-11.5
CS76532	Asia	16.22	0.30	493	14.2
CS76802	Italy/Balkan/Caucasus	26.46	0.52	591	9.2
CS76375	Asia	39.62	0.53	520	4.3
CS76944	Admixed	25.84	0.53	578	9.9
CS76379	Asia	35.35	0.60	705	2.7
CS76778 (Col-0)	Germany	14.15	0.72	1023	13.1
CS78855	Central Europe	20.86	0.83	648	6.5
CS76710	North Sweden	17.21	0.99	637	3.0
CS77389	Admixed	26.01	1.52	1884	14.2
CS77156	Admixed	21.70	2.67	1809	7.1

Table 4.2. Variation in measured traits for 12 ecotypes of Arabidopsis grown in a greenhouse common garden with minimum, average (bold) and maximum mean ecotype values presented. Also presented are the results of an analysis of variance (ANOVA) testing for variation among ecotypes (mean squares, proportion of variance explained by the ANOVA and significance levels for each trait; df, degrees of freedom; ns, P>0.05; *, P<0.05; **, P<0.01; ***, P<0.001).

Trait	Symbol	Unit	Min, Avg, Max	df	ANOVA result
Leaf mass per area	LMA	g m^{-2}	14.15, 24.85, 39.62	52	289.36, 0.75***
Specific leaf area	SLA	m^2 kg^{-1}	25.45, 44.92, 70.73	52	838.69, 0.79***
Osmotic potential at full turgor	π_o	MPa	-1.08, -0.83, -0.71	96	0.063, 0.37***
Maximum photosynthetic rate per area	A_{area}	µmol CO_2 m^{-2} s^{-1}	3.03, 8.29, 15.84	62	87.28, 0.66***
Stomatal conductance	g_{op}	moles H_2O m^{-2} s^{-1}	0.12, 0.29, 0.65	62	0.12, 0.61***
Ratio of A_{area} to g_{op}	A_{area}:g_{op}	unitless	17.53, 29.34, 40.04	62	378.71, 0.29*
Operating leaf water potential	Ψ_{op}	-MPa	0.23, 0.42, 0.86	61	0.20, 0.26*
Leaf Area	LA	mm^2	252.80, 505.55, 868.35	46	133469, 0.41**
Midrib Width	Midrib.Width	mm	0.091, 0.14, 0.18	46	0.0039, 0.48***
Secondary vein width	2o.Vein.Width	mm	0.036, 0.052, 0.066	46	0.00047, 0.56***
Minor vein width	Minor.vein.width	mm	0.021, 0.033, 0.054	46	0.00039, 0.70***
Midrib vein length per area	Midrib VLA	mm mm^{-2}	0.070, 0.11, 0.17	46	0.0042, 0.53***
Secondary vein length per area	Secondary VLA	mm mm^{-2}	0.41, 0.66, 1.06	46	0.14, 0.61***
Major vein length per area	Major VLA	mm mm^{-2}	0.48, 0.77, 1.24	46	0.65, 0.44**
Minor vein length per area	Minor VLA	mm mm^{-2}	1.79, 2.17, 2.84	46	0.19, 0.61***
Total vein length per area	Total VLA	mm mm^{-2}	2.45, 2.94, 3.77	46	0.88, 0.44**
Projected vein area per area	PAPA	mm^2 mm^{-2}	0.087, 0.12, 0.23	46	0.0071, 0.78***
Volume of veins per area	VAPA	mm^3 mm^{-2}	0.0026, 0.0051, 0.012	46	0.000030, 0.80***
Ratio of stable isotopes 13C:12C	$\delta^{13}C$	‰	-34.39, -31.14, -28.67	21	7.93, 0.93***
Amount of nitrogen in a given unit of leaf mass	N_{mass}	mg g^{-1}	25.84, 40.18, 60.36	21	394.37, 0.78***
Total stomatal density	d_sum	# stomata mm^{-4}	447.35, 661.28, 824.03	43	61495, 0.41**
Mean inner pore length	Plinner_avg	µm	4.79, 6.09, 7.39	47	2.45, 0.45**

Mean outer pore length	Plouter_avg	µm	9.53, 11.12, 12.42	47	3.06, 0.35*
Mean guard cell length	GCL_avg	µm	16.75, 18.32, 20.14	47	6.73, 0.42**
Mean guard cell width	GCW_avg	µm	11.71, 12.79, 13.59	47	1.61, 0.27, ns
Mean stomatal area	s_avg	μm^2	165.14, 197.29, 224.87	47	1848.4, 0.34*
Mean epidermal pavement cell area	e_avg	μm^2	520.13, 727.61, 1268.34	47	205957, 0.39**
Mean stomatal initiation rate	i_avg	unitless	0.17, 0.18, 0.21	47	0.00078, 0.15, ns
Total measured maximum theoretical anatomical stomatal conductance	gmax_measured	mol m^2 s^{-1}	2.91, 4.20, 5.34	43	2.27, 0.42**
Total maximum theoretical anatomical stomatal conductance calculated using constants	gmax_c	mol m^2 s^{-1}	3.19, 4.38, 5.24	43	1.76, 0.36*

FIGURE CAPTIONS

Figure 4.1. Relationships of traits and climatic variables across the native distribution of focal Arabidopsis ecotypes. A, Distribution of the origin locations of Arabidopsis ecotypes from one set of 12 ecotypes grown in a common garden (black triangles) and another set of 152 ecotypes grown in a common garden (white circles). Climatic gradients represent annual precipitation modeled in the global WorldClim database, with moisture increasing from red to blue. B, The association of the osmotic potential at full turgor (π_o) with aridity index across 133 of those ecotypes of Arabidopsis. C, The association of leaf mass per area with growing season precipitation across 142 ecotypes of Arabidopsis. D, The association of the π_o with lifecycle duration across 133 ecotypes of Arabidopsis. Colors represent density of points in plots B-D. The *r*-values with significance are based on linear regression analysis with kinship. ns, $P>0.05$; *, $P<0.05$; **, $P<0.01$; ***, $P<0.001$.

Figure 4.2. Relationships of traits with origin climate demonstrating adaptations for stress avoidance across 12 ecotypes of Arabidopsis grown in a common garden. Relationship of annual precipitation with A, photosynthetic rate per unit area (A_{area}), B, stomatal conductance (g_{op}) and C, leaf nitrogen content per unit mass (N_{mass}). Error bars represent standard error. The *r*-values with significance are based on linear regression analysis of raw or log-transformed data accounting for kinship between ecotypes. ns, $P>0.05$; *, $P<0.05$; **, $P<0.01$; ***, $P<0.001$.

Figure 4.3. Relationship of annual precipitation with leaf water potential at 80% loss of hydraulic conductance (P_{80}) demonstrating an adaptation for stress tolerance across 12 ecotypes of Arabidopsis grown in a common garden. Error bars represent standard error. The *r*-value with

significance is based on linear regression analysis of raw or log-transformed data accounting for kinship between ecotypes. ns, $P>0.05$; *, $P<0.05$; **, $P<0.01$; ***, $P<0.001$.

Figure 4.4. Rule-breaking relationships of traits with origin climate across 12 ecotypes of Arabidopsis grown in a common garden. Relationship of A) aridity index with osmotic potential at full turgor (π_o), B, carbon isotope ratio ($\delta^{13}C$) with potential evapo-transpiration, C, major vein length per leaf area (VLA) with annual precipitation, and D, maximum hydraulic conductance (K_{max}) with annual precipitation. Error bars represent standard error. The *r*-values with significance are based on linear regression analysis of raw or log-transformed data accounting for kinship between ecotypes. ns, $P>0.05$; *, $P<0.05$; **, $P<0.01$; ***, $P<0.001$.

Figure 4.5. Relationships between and decoupling of traits across ecotypes of Arabidopsis grown in a common garden. A, the association of leaf area with major vein length per area (VLA). B, the lack of association between K_{max} and maximum photosynthetic rate per leaf area (A_{area}). C, The association of major VLA with maximum hydraulic conductance (K_{max}). D, the trade-off between the osmotic potential at full turgor (π_o) and stomatal conductance (g_{op}) and E, between water potential at 80% loss of hydraulic conductance (P_{80}) and K_{max}. F, The relationships of leaf mass per area (LMA) and G, major VLA with P_{80}. H, The relationship between lifecycle duration and A_{area}. Error bars represent standard error. The *r*-values with significance are based on linear regression analysis of raw or log-transformed data accounting for kinship between ecotypes. ns, $P>0.05$; *, $P<0.05$; **, $P<0.01$; ***, $P<0.001$. n=12 ecotypes for all plots except H, for which n=9 ecotypes.

Figure 4.6. Correlations between leaf economics traits across 12 ecotypes of Arabidopsis grown in a common garden. LMA, leaf mass per area (g m^{-2}); Narea, nitrogren per area (g m^{-2}); Nmass, leaf nitrogen per mass (mg g^{-1}); Amax_mass, maximum photosynthetic rate per mass (μmol of CO_2 g^{-1} s^{-1}); Amax_area, maximum photosynthetic rate per area (μmol of CO_2 m^{-2} s^{-1}). The *r*-values are based on linear regression analysis of raw or log-transformed data accounting for kinship between ecotypes. ns, $P>0.05$; *, $P<0.05$; **, $P<0.01$; ***, $P<0.001$.

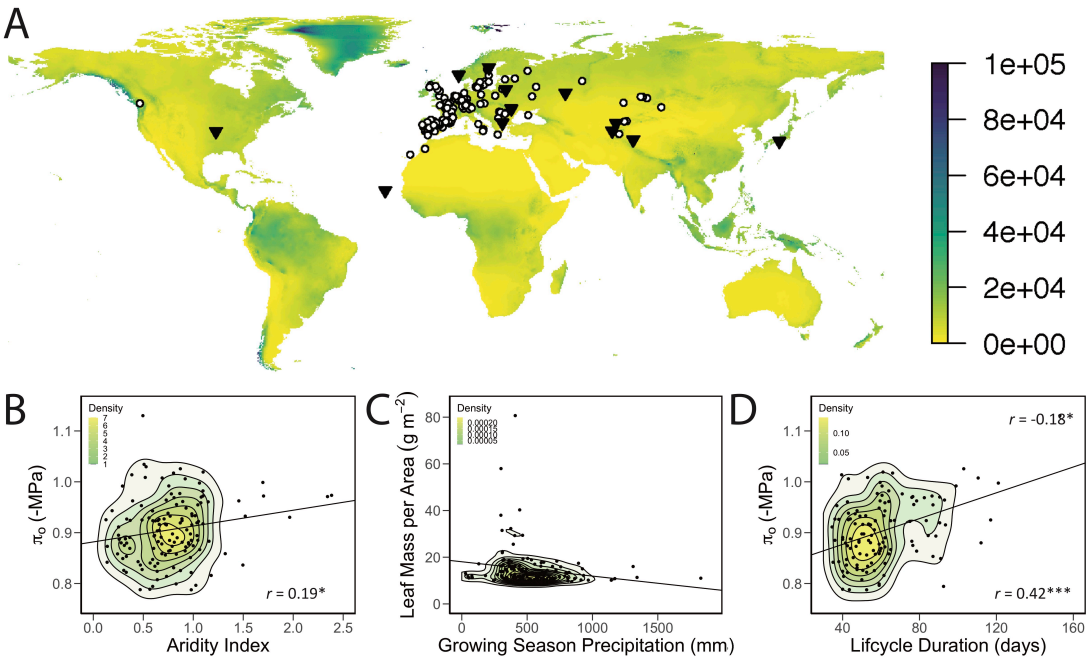
A
1e+05
8e+04
6e+04
4e+04
2e+04
0e+00
B
Density
π_0 (-MPa)
Aridity Index
r = 0.19*
C
Density
Leaf Mass per Area (g m^{-2})
Growing Season Precipitation (mm)
D
Density
r = -0.18*
π_0 (-MPa)
Lifcycle Duration (days)
r = 0.42***

Figure 4.1

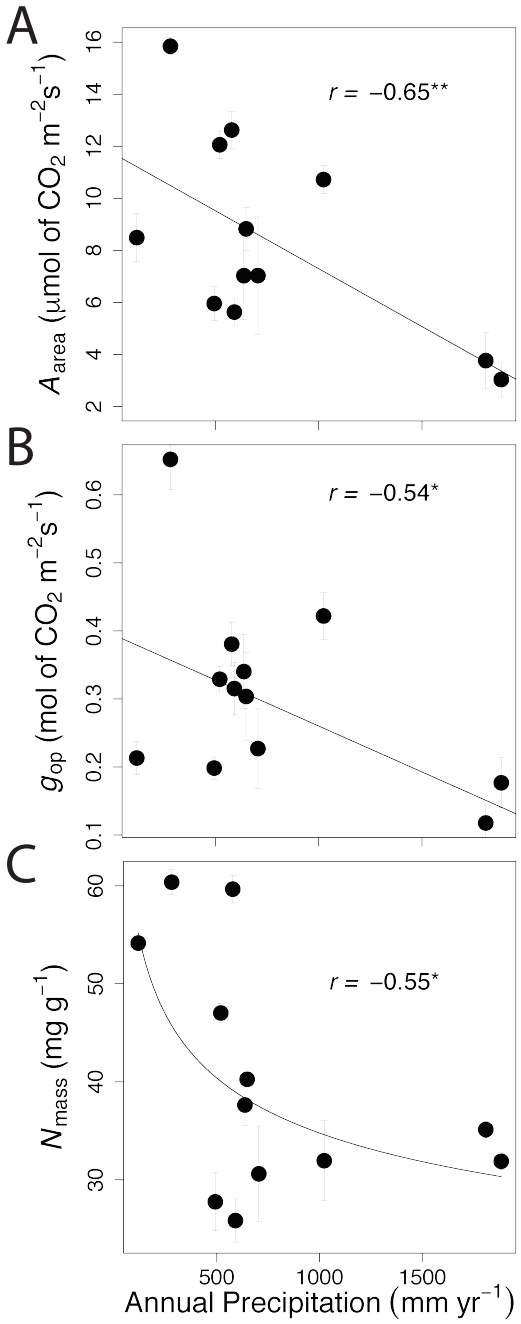
A
B
C
r = −0.65**
r = −0.54*
r = −0.55*
Aarea (μmol of CO2 m−2s−1)
gop (mol of CO2 m−2s−1)
Nmass (mg g−1)
Annual Precipitation (mm yr−1)
500
1000
1500

Figure 4.2

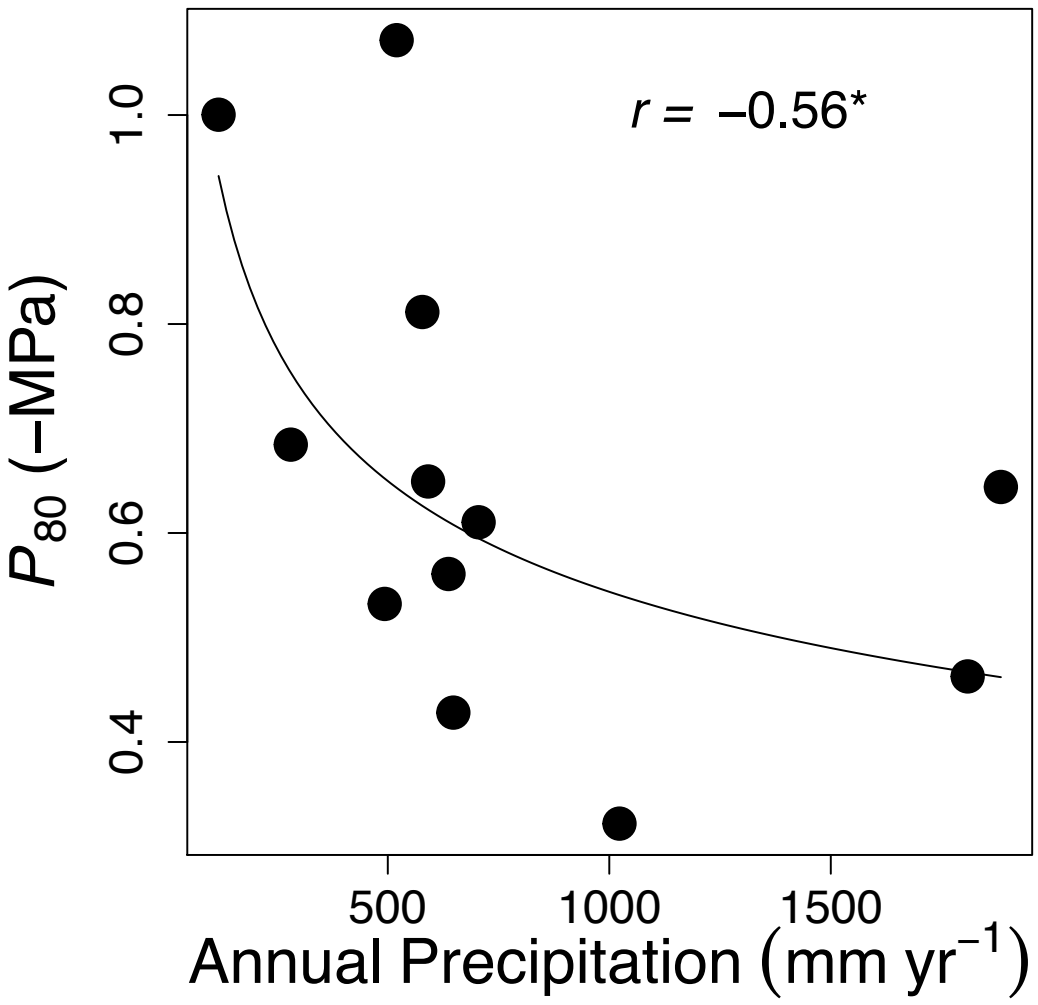
r = –0.56*
P80 (–MPa)
1.0
0.8
0.6
0.4
500
1000
1500
Annual Precipitation (mm yr−1)

Figure 4.3

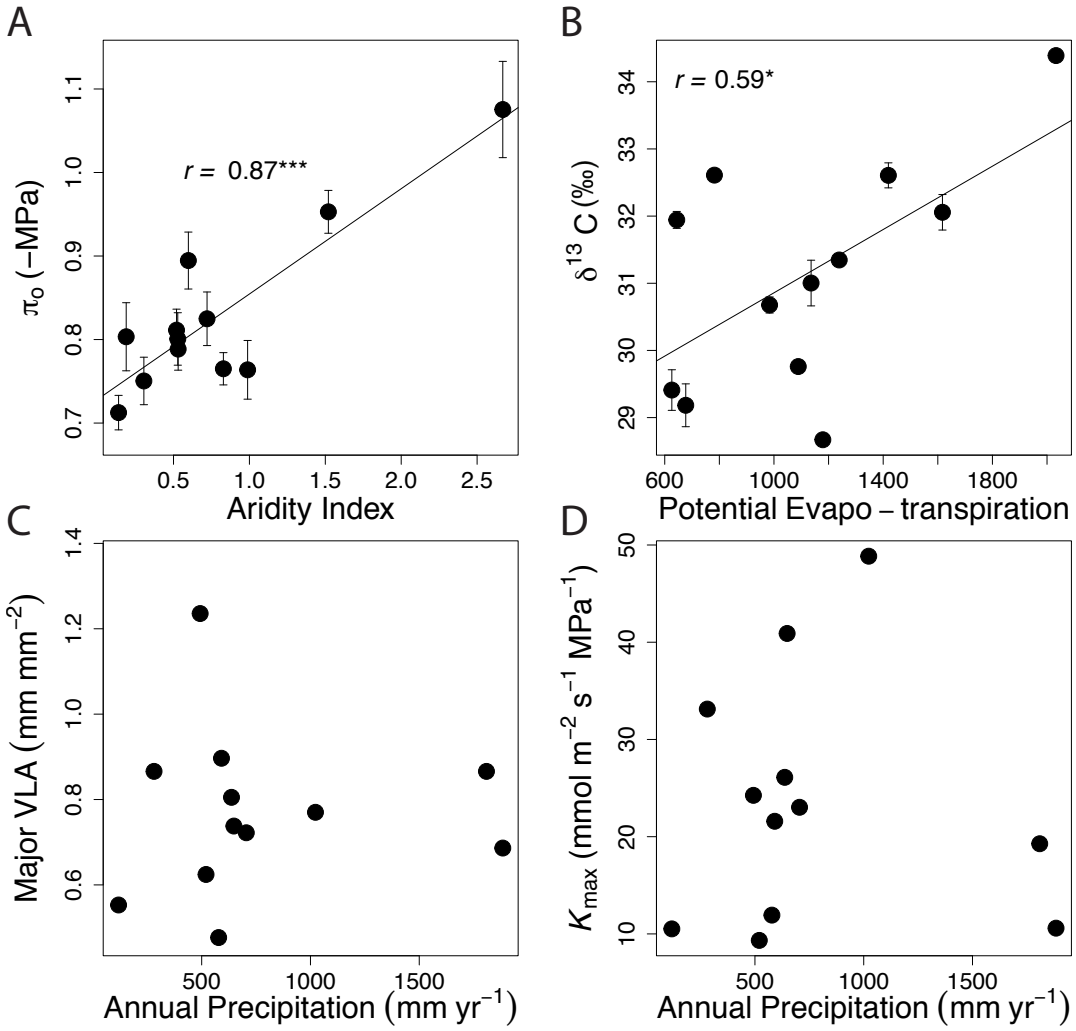
A
B
C
D
r = 0.87***
r = 0.59*
π₀ (−MPa)
Aridity Index
δ13 C (‰)
Potential Evapo − transpiration
Major VLA (mm mm−2)
Annual Precipitation (mm yr−1)
Kmax (mmol m−2 s−1 MPa−1)
Annual Precipitation (mm yr−1)

Figure 4.4

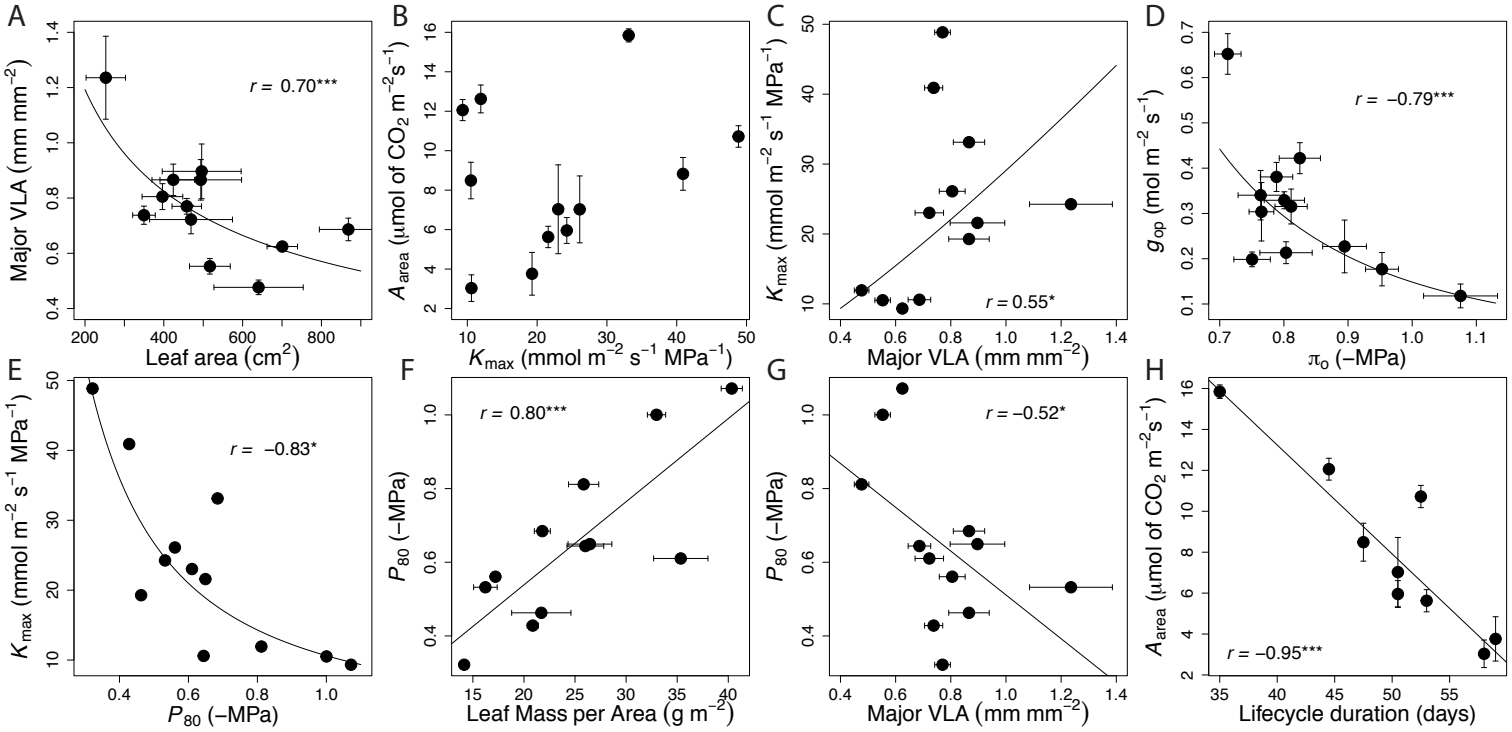
A
Major VLA (mm mm^{-2})
Leaf area (cm^2)
r = 0.70***
B
A_{area} (μmol of CO_2 m^{-2}s^{-1})
K_{max} (mmol m^{-2} s^{-1} MPa^{-1})
C
K_{max} (mmol m^{-2} s^{-1} MPa^{-1})
Major VLA (mm mm^{-2})
r = 0.55*
D
g_{op} (mol m^{-2} s^{-1})
π_o (–MPa)
r = –0.79***
E
K_{max} (mmol m^{-2} s^{-1} MPa^{-1})
P_{80} (–MPa)
r = –0.83*
F
P_{80} (–MPa)
Leaf Mass per Area (g m^{-2})
r = 0.80***
G
P_{80} (–MPa)
Major VLA (mm mm^{-2})
r = –0.52*
H
A_{area} (μmol of CO_2 m^{-2}s^{-1})
Lifecycle duration (days)
r = –0.95***

Figure 4.5

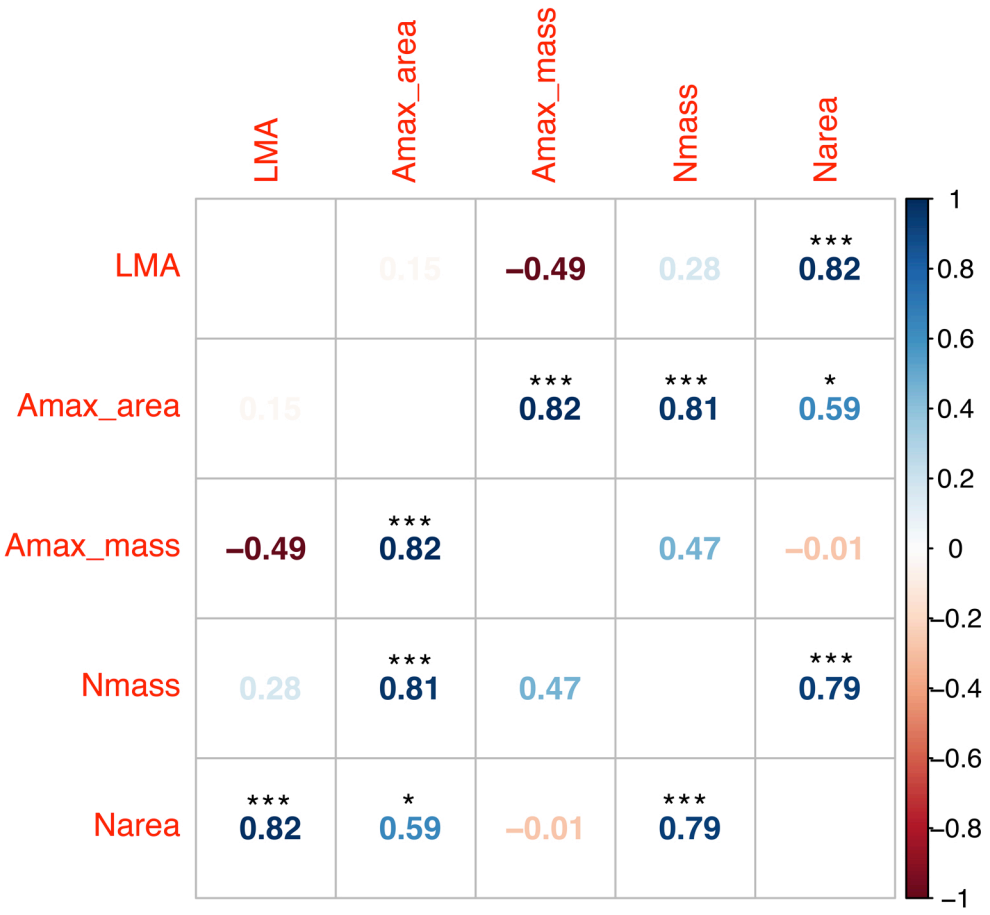
LMA
Amax_area
Amax_mass
Nmass
Narea
LMA
0.15
–0.49
0.28
*** 0.82
Amax_area
0.15
*** 0.82
*** 0.81
* 0.59
Amax_mass
–0.49
*** 0.82
0.47
–0.01
Nmass
0.28
*** 0.81
0.47
*** 0.79
Narea
*** 0.82
* 0.59
–0.01
*** 0.79
1
0.8
0.6
0.4
0.2
0
–0.2
–0.4
–0.6
–0.8
–1

Figure 4.6

SUPPLEMENTARY MATERIALS

Supplementary Data Captions (see attached Excel Workbook)

Table S4.1. Hypotheses for relationships between traits. Columns include hypotheses, citations of previous studies, variables involved, the expected direction of the correlation as found in the literature, and whether or not the hypothesis is supported in this study across 12 ecotypes of *Arabidopsis thaliana* grown in a common garden.

Table S4.2. Hypotheses for how traits could be associated with climate given various responses to drought or cold stress and/or association with growth. Responses to stress could include stress avoidance (fast growth), mechanistic drought resistance via tolerating drought or delaying desiccation. The leaf economics spectrum also provides predictions for how traits might confer drought tolerance. Columns include directions of correlation traits, predictions of their relationships with climate according to literature, actual directions of the relationships in this study across 12 ecotypes of *Arabidopsis thaliana* and a larger set of 133-142 ecotypes of *A. thaliana* grown in greenhouse experiments, and literature references.

Table S4.3. Experimental mean data and native climate data for 144 genotypes of *Arabidopsis thaliana* grown in a greenhouse common garden. See “CHAPTER 4 Legend” tab for legend of symbols and units.

Table S4.4. Experimental data for Pio for each individual of 144 genotypes of *Arabidopsis thaliana* grown in a greenhouse common garden. See " CHAPTER 4 Legend” tab for legend of symbols and units.

Table S4.5. Correlation matrix of all traits for 133-152 genotypes of *Arabidopsis thaliana* grown in a greenhouse common garden. Values show the r-values of correlations using raw, log-transformed, and ranked data. Highlighted cells represent tests for which either a raw and rank, or a log and rank correlation test were significant. Stars represent significance levels for each trait; df, degrees of freedom; ns, P>0.05; *, P<0.05; **, P<0.01; ***, P<0.001). See "CHAPTER 4 Legend" tab for legend of symbols and units.

Table S4.6. Experimental mean data and native climate data for 12 genotypes of *Arabidopsis thaliana* grown in a greenhouse common garden with standard errors. Average values are derived from 2-9 individual plants per genotype. See "CHAPTER 4 Legend" tab for legend of symbols and units.

Table S4.7. Experimental and native climate data for each individual of 12 genotypes of *Arabidopsis thaliana* grown in a greenhouse common garden. See " CHAPTER 4 Legend" tab for legend of symbols and units.

Table S4.8. Correlations accounting for kinship for all traits and climate variables on untransformed (raw) and log-transformed data for 12 ecotypes of *Arabidopsis thaliana* grown in a common garden. Columns include the X and Y variables (See "CHAPTER 4 Legend" tab for legend of symbols and units), model estimates of the intercept, slope, and r-squared values, the p-value of the correlation. Significant p-values (P < 0.05) are highlighted. Note that Pio, Psiop, P80 and d13C values were multiplied by -1 prior to running the analysis.

REFERENCES

Alonso-Blanco, C., Andrade, J., Becker, C., Bemm, F., Bergelson, J., Borgwardt, K.M. *et al.* (2016). 1,135 genomes reveal the global pattern of polymorphism in *Arabidopsis thaliana*. *Cell*, 166, 481-491.

Antonio, T. & Robert, Z. (2019). *Global Aridity Index and Potential Evapotranspiration (ET0) Climate Database v2*.

Bartlett, M.K., Scoffoni, C., Ardy, R., Zhang, Y., Sun, S.W., Cao, K.F. *et al.* (2012a). Rapid determination of comparative drought tolerance traits: using an osmometer to predict turgor loss point. *Methods in Ecology and Evolution*, 3, 880-888.

Bartlett, M.K., Scoffoni, C. & Sack, L. (2012b). The determinants of leaf turgor loss point and prediction of drought tolerance of species and biomes: a global meta-analysis. *Ecol. Lett.*, 15, 393-405.

Bartlett, M.K., Zhang, Y., Kreidler, N., Sun, S.W., Ardy, R., Cao, K.F. *et al.* (2014). Global analysis of plasticity in turgor loss point, a key drought tolerance trait. *Ecol. Lett.*, 17, 1580-1590.

Blackman, C.J., Brodribb, T.J. & Jordan, G.J. (2010). Leaf hydraulic vulnerability is related to conduit dimensions and drought resistance across a diverse range of woody angiosperms. *New Phytologist*, 188, 1113-1123.

Blackman, C.J., Gleason, S.M., Chang, Y., Cook, A.M., Laws, C. & Westoby, M. (2014). Leaf hydraulic vulnerability to drought is linked to site water availability across a broad range of species and climates. *Ann. Bot.*, 114, 435-440.

Boyce, C.K., Brodribb, T.J., Feild, T.S. & Zwieniecki, M.A. (2009). Angiosperm leaf vein evolution was physiologically and environmentally transformative. *Proc. R. Soc. B-Biol. Sci.*, 276, 1771-1776.

Brodribb, T.J., Feild, T.S. & Jordan, G.J. (2007). Leaf maximum photosynthetic rate and venation are linked by hydraulics. *Plant Physiology*, 144, 1890-1898.

Brodribb, T.J., Holbrook, N.M., Zwieniecki, M.A. & Palma, B. (2005). Leaf hydraulic capacity in ferns, conifers and angiosperms: impacts on photosynthetic maxima. *New Phytologist*, 165, 839-846.

Brodribb, T.J. & Jordan, G.J. (2008). Internal coordination between hydraulics and stomatal control in leaves. *Plant Cell and Environment*, 31, 1557-1564.

Brodribb, T.J., McAdam, S.A.M., Jordan, G.J. & Martins, S.C.V. (2014). Conifer species adapt to low-rainfall climates by following one of two divergent pathways. *Proc. Natl. Acad. Sci. U. S. A.*, 111, 14489-14493.

Buckley, T.N., John, G.P., Scoffoni, C. & Sack, L. (2015). How does leaf anatomy influence water transport outside the xylem? *Plant Physiology*, 168, 1616-1635.

Candela, H., Martinez-Laborda, A. & Micol, J.L. (1999). Venation pattern formation in *Arabidopsis thaliana* vegetative leaves. *Dev. Biol.*, 205, 205-216.

Caringella, M.A., Bongers, F.J. & Sack, L. (2015). Leaf hydraulic conductance varies with vein anatomy across *Arabidopsis thaliana* wild-type and leaf vein mutants. *Plant Cell and Environment*, 38, 2735-2746.

Carins Murphy, M.R., Dow, G.J., Jordan, G.J. & Brodribb, T.J. (2017). Vein density is independent of epidermal cell size in *Arabidopsis* mutants. *Functional Plant Biology*, 44, 410-418.

Craine, J.M., Elmore, A.J., Aidar, M.P.M., Bustamante, M., Dawson, T.E., Hobbie, E.A. *et al.* (2009). Global patterns of foliar nitrogen isotopes and their relationships with climate, mycorrhizal fungi, foliar nutrient concentrations, and nitrogen availability. *New Phytologist*, 183, 980-992.

Easlon, H.M., Nemali, K.S., Richards, J.H., Hanson, D.T., Juenger, T.E. & McKay, J.K. (2014). The physiological basis for genetic variation in water use efficiency and carbon isotope composition in *Arabidopsis thaliana*. *Photosynthesis Research*, 119, 119-129.

Ellsworth, D.S. & Reich, P.B. (1992). Leaf mass per area, nitrogen-content and photosynthetic carbon gain in acer-saccharum seedlings in contrasting forest light environments. *Funct. Ecol.*, 6, 423-435.

Evans, G.C. (1972). *The Quantitative Analysis of Plant Growth*. Blackwell Scientific Publications, Oxford.

Farquhar, G.D., Ehleringer, J.R. & Hubick, K.T. (1989). Carbon isotope discrimination and photosynthesis. *Annual Review of Plant Physiology and Plant Molecular Biology*, 40, 503-537.

Ferrero-Serrano, A. & Assmann, S.M. (2019). Phenotypic and genome-wide association with the local environment of *Arabidopsis*. *Nat. Ecol. Evol.*, 3, 274-+.

Fick, S.E. & Hijmans, R.J. (2017). WorldClim 2: new 1-km spatial resolution climate surfaces for global land areas. *Int. J. Climatol.*, 37, 4302-4315.

Fletcher, L.R., Cui, H., Callahan, H., Scoffoni, C., John, G.P., Bartlett, M.K. *et al.* (2018). Evolution of leaf structure and drought tolerance in species of Californian *Ceanothus*. *Am. J. Bot.*, 105, 1672-1687.

Fletcher, L.R., Scoffoni, C., Farrell, C., Buckley, T.N., Pellegrini, M. & Sack, L. (in prep.). Variation in relative growth and adaptation to aridity across *Arabidopsis* ecotypes: does lack of a trade-off contribute to a wide species range?

Franks, P.J. & Beerling, D.J. (2009). Maximum leaf conductance driven by CO2 effects on stomatal size and density over geologic time. *Proc. Natl. Acad. Sci. U. S. A.*, 106, 10343-10347.

Franks, P.J., Drake, P.L. & Beerling, D.J. (2009). Plasticity in maximum stomatal conductance constrained by negative correlation between stomatal size and density: an analysis using *Eucalyptus globulus*. *Plant, Cell & Environment*, 32, 1737-1748.

Franks, P.J. & Farquhar, G.D. (2007). The mechanical diversity of stomata and its significance in gas-exchange control. *Plant Physiology*, 143, 78-87.

Griffin-Nolan, R.J., Ocheltree, T.W., Mueller, K.E., Blumenthal, D.M., Kray, J.A. & Knapp, A.K. (2019). Extending the osmometer method for assessing drought tolerance in herbaceous species. *Oecologia*, 189, 353-363.

Grubb, P.J. (1998). A reassessment of the strategies of plants which cope with shortages of resources. *Perspectives in Plant Ecology, Evolution and Systematics*, 1, 3-31.

Hancock, A.M., Brachi, B., Faure, N., Horton, M.W., Jarymowycz, L.B., Sperone, F.G. *et al.* (2011). Adaptation to climate across the *Arabidopsis thaliana* genome. *Science*, 334, 83-86.

Henry, C., John, G.P., Pan, R.H., Bartlett, M.K., Fletcher, L.R., Scoffoni, C. *et al.* (2019). A stomatal safety-efficiency trade-off constrains responses to leaf dehydration. *Nat. Commun.*, 10, 9.

Hetherington, A.M. & Woodward, F.I. (2003). The role of stomata in sensing and driving environmental change. *Nature*, 424, 901-908.

John, G.P., Henry, C. & Sack, L. (2018). Leaf rehydration capacity: Associations with other indices of drought tolerance and environment. *Plant Cell and Environment*, 41, 2638-2653.

Jordan, G.J., Carpenter, R.J., Holland, B.R., Beeton, N.J., Woodhams, M.D. & Brodribb, T.J. (2020). Links between environment and stomatal size through evolutionary time in Proteaceae. *Proc. R. Soc. B-Biol. Sci.*, 287, 7.

Kang, J. & Dengler, N. (2004). Vein pattern development in adult leaves of *Arabidopsis thaliana*. *Int. J. Plant Sci.*, 165, 231-242.

Kenney, A.M., McKay, J.K., Richards, J.H. & Juenger, T.E. (2014). Direct and indirect selection on flowering time, water-use efficiency (WUE, delta C-13), and WUE plasticity to drought in *Arabidopsis thaliana*. *Ecology and Evolution*, 4, 4505-4521.

Klooster, B. & Palmer-Young, E. (2012). Water stress marginally increases stomatal density in *E. canadensis*, but not in *A. gerardii*. *Tillers*, 35-40%V 35.

Lampei, C., Wunder, J., Wilhalm, T. & Schmid, K.J. Microclimate predicts frost hardiness of alpine *Arabidopsis thaliana* populations better than elevation. *Ecology and Evolution*, 13.

Lasky, J.R., Des Marais, D.L., McKay, J.K., Richards, J.H., Juenger, T.E. & Keitt, T.H. (2012). Characterizing genomic variation of *Arabidopsis thaliana*: the roles of geography and climate. *Molecular Ecology*, 21, 5512-5529.

Lorts, C.M. & Lasky, J.R. (2020). Competition x drought interactions change phenotypic plasticity and the direction of selection on *Arabidopsis* traits. *New Phytologist*, 227, 1060-1072.

Mart, K.B., Veneklaas, E.J. & Bramley, H. (2016). Osmotic potential at full turgor: an easily measurable trait to help breeders select for drought tolerance in wheat. *Plant Breeding*, 135, 279-285.

Maximov, N.A. (1931). The physiological significance of the xeromorphic structure of plants. *J. Ecol.*, 19, 273-282.

McElwain, J.C., Yiotis, C. & Lawson, T. (2016). Using modern plant trait relationships between observed and theoretical maximum stomatal conductance and vein density to examine patterns of plant macroevolution. *New Phytologist*, 209, 94-103.

McKay, J.K., Richards, J.H. & Mitchell-Olds, T. (2003). Genetics of drought adaptation in *Arabidopsis thaliana*: I. Pleiotropy contributes to genetic correlations among ecological traits. *Molecular Ecology*, 12, 1137-1151.

McKown, A.D., Akamine, M.E. & Sack, L. (2016). Trait convergence and diversification arising from a complex evolutionary history in Hawaiian species of *Scaevola*. *Oecologia*, 181, 1083-1100.

Meinzer, F.C. (2002). Co-ordination of vapour and liquid phase water transport properties in plants. *Plant Cell and Environment*, 25, 265-274.

Mojica, J.P., Mullen, J., Lovell, J.T., Monroe, J.G., Paul, J.R., Oakley, C.G. *et al.* (2016). Genetics of water use physiology in locally adapted *Arabidopsis thaliana*. *Plant Sci.*, 251, 12-22.

Nardini, A. & Luglio, J. (2014). Leaf hydraulic capacity and drought vulnerability: possible trade-offs and correlations with climate across three major biomes. *Funct. Ecol.*, 28, 810-818.

Nardini, A., Ounapuu-Pikas, E. & Savi, T. (2014). When smaller is better: leaf hydraulic conductance and drought vulnerability correlate to leaf size and venation density across four *Coffea arabica* genotypes. *Functional Plant Biology*, 41, 972-982.

Nardini, A., Peda, G. & La Rocca, N. (2012). Trade-offs between leaf hydraulic capacity and drought vulnerability: morpho-anatomical bases, carbon costs and ecological consequences. *New Phytologist*, 196, 788-798.

Niinemets, U. (2001). Global-scale climatic controls of leaf dry mass per area, density, and thickness in trees and shrubs. *Ecology*, 82, 453-469.

Ocheltree, T.W., Nippert, J.B. & Prasad, P.V.V. (2016). A safety vs efficiency trade-off identified in the hydraulic pathway of grass leaves is decoupled from photosynthesis, stomatal conductance and precipitation. *New Phytologist*, 210, 97-107.

Oliveira, R.S., Eller, C.B., Barros, F.D., Hirota, M., Brum, M. & Bittencourt, P. (2021). Linking plant hydraulics and the fast-slow continuum to understand resilience to drought in tropical ecosystems. *New Phytologist*, 230, 904-923.

Poorter, H., Niinemets, U., Poorter, L., Wright, I.J. & Villar, R. (2009). Causes and consequences of variation in leaf mass per area (LMA): a meta-analysis. *New Phytologist*, 182, 565-588.

Ramirez-Valiente, J.A., Lopez, R., Hipp, A.L. & Aranda, I. (2020). Correlated evolution of morphology, gas exchange, growth rates and hydraulics as a response to precipitation and temperature regimes in oaks (*Quercus*). *New Phytologist*, 227, 794-809.

Reich, P.B., Ellsworth, D.S., Walters, M.B., Vose, J.M., Gresham, C., Volin, J.C. *et al.* (1999). Generality of leaf trait relationships: A test across six biomes. *Ecology*, 80, 1955-1969.

Rosas, T., Mencuccini, M., Barba, J., Cochard, H., Saura-Mas, S. & Martinez-Vilalta, J. (2019). Adjustments and coordination of hydraulic, leaf and stem traits along a water availability gradient. *New Phytologist*, 223, 632-646.

Sack, L. & Buckley, T.N. (2016). The developmental basis of stomatal density and flux. *Plant Physiology*, 171, 2358-2363.

Sack, L., Dietrich, E.M., Streeter, C.M., Sanchez-Gomez, D. & Holbrook, N.M. (2008). Leaf palmate venation and vascular redundancy confer tolerance of hydraulic disruption. *Proc. Natl. Acad. Sci. U. S. A.*, 105, 1567-1572.

Sack, L. & Frole, K. (2006). Leaf structural diversity is related to hydraulic capacity in tropical rain forest trees. *Ecology*, 87, 483-491.

Sack, L. & Holbrook, N.M. (2006). Leaf hydraulics. In: *Annual Review of Plant Biology*, pp. 361-381.

Sack, L. & Scoffoni, C. (2012). Measurement of leaf hydraulic conductance and stomatal conductance and their responses to irradiance and dehydration using the evaporative flux method (EFM). *Jove-Journal of Visualized Experiments*.

Sack, L. & Scoffoni, C. (2013). Leaf venation: structure, function, development, evolution, ecology and applications in the past, present and future. *New Phytologist*, 198, 983-1000.

Sack, L., Scoffoni, C., John, G.P., Poorter, H., Mason, C.M., Mendez-Alonzo, R. *et al.* (2013). How do leaf veins influence the worldwide leaf economic spectrum? Review and synthesis. *Journal of Experimental Botany*, 64, 4053-4080.

Sack, L., Scoffoni, C., McKown, A.D., Frole, K., Rawls, M., Havran, J.C. *et al.* (2012). Developmentally based scaling of leaf venation architecture explains global ecological patterns. *Nat. Commun.*, 3, 10.

Sartori, K., Vasseur, F., Violle, C., Baron, E., Gerard, M., Rowe, N. *et al.* (2019). Leaf economics and slow-fast adaptation across the geographic range of *Arabidopsis thaliana*. *Scientific Reports*, 9.

Scoffoni, C., Albuquerque, C., Brodersen, C.R., Townes, S.V., John, G.P., Bartlett, M.K. *et al.* (2017). Outside-xylem vulnerability, not xylem embolism, controls leaf hydraulic decline during dehydration. *Plant Physiology*, 173, 1197-1210.

Scoffoni, C., Albuquerque, C., Cochard, H., Buckley, T.N., Fletcher, L.R., Caringella, M.A. *et al.* (2018). The causes of leaf hydraulic vulnerability and its influence on gas exchange in *Arabidopsis thaliana*. *Plant physiology*.

Scoffoni, C., Chatelet, D.S., Pasquet-kok, J., Rawls, M., Donoghue, M.J., Edwards, E.J. *et al.* (2016). Hydraulic basis for the evolution of photosynthetic productivity. *Nat. Plants*, 2, 8.

Scoffoni, C., Rawls, M., McKown, A., Cochard, H. & Sack, L. (2011). Decline of leaf hydraulic conductance with dehydration: relationship to leaf size and venation architecture. *Plant Physiology*, 156, 832-843.

Scoffoni, C. & Sack, L. (2017). The causes and consequences of leaf hydraulic decline with dehydration. *Journal of Experimental Botany*, 68, 4479-4496.

Scoffoni, C., Sack, L. & contributors, P. (2013). Quantifying leaf vein traits. *PrometheusWiki*.

Scoffoni, C., Vuong, C., Diep, S., Cochard, H. & Sack, L. (2014). Leaf Shrinkage with Dehydration: Coordination with Hydraulic Vulnerability and Drought Tolerance. *Plant Physiology*, 164, 1772-1788.

Sommerville, K.E., Sack, L. & Ball, M.C. (2012). Hydraulic conductance of *Acacia* phyllodes (foliage) is driven by primary nerve (vein) conductance and density. *Plant Cell and Environment*, 35, 158-168.

Thonglim, A., Delzon, S., Larter, M., Karami, O., Rahimi, A., Offringa, R. *et al.* (2020). Intervessel pit membrane thickness best explains variation in embolism resistance amongst stems of *Arabidopsis thaliana* accessions. *Ann. Bot.*

Vasseur, F., Exposito-Alonso, M., Ayala-Garay, O.J., Wang, G., Enquist, B.J., Vile, D. *et al.* (2018). Adaptive diversification of growth allometry in the plant *Arabidopsis thaliana*. *Proc. Natl. Acad. Sci. U. S. A.*, 115, 3416-3421.

Villagra, M., Campanello, P.I., Bucci, S.J. & Goldstein, G. (2013). Functional relationships between leaf hydraulics and leaf economic traits in response to nutrient addition in subtropical tree species. *Tree Physiol.*, 33, 1308-1318.

Wang, G.A., Han, J.M. & Liu, D.S. (2003). The carbon isotope composition of C-3 herbaceous plants in loess area of northern China. *Sci. China Ser. D-Earth Sci.*, 46, 1069-1076.

Wang, M., Zhang, X.N. & Liu, J.H. (2015). Deep sequencing-based characterization of transcriptome of trifoliate orange (*Poncirus trifoliata* (L.) Raf.) in response to cold stress. *Bmc Genomics*, 16.

Weast, R.C. (1978). *CRC handbook of chemistry and physics : a ready-reference book of chemical and physical data*. CRC Press, West Palm Beach (Florida).

Weigel, D. & Mott, R. (2009). The 1001 Genomes Project for *Arabidopsis thaliana*. *Genome Biology*, 10, 5.

Westoby, M. & Wright, I.J. (2006). Land-plant ecology on the basis of functional traits. *Trends Ecol. Evol.*, 21, 261-268.

Wright, I.J., Dong, N., Maire, V., Prentice, I.C., Westoby, M., Diaz, S. *et al.* (2017). Global climatic drivers of leaf size. *Science*, 357, 917-921.

Wright, I.J., Reich, P.B. & Westoby, M. (2001). Strategy shifts in leaf physiology, structure and nutrient content between species of high- and low-rainfall and high- and low-nutrient habitats. *Funct. Ecol.*, 15, 423-434.

Wright, I.J., Reich, P.B., Westoby, M., Ackerly, D.D., Baruch, Z., Bongers, F. *et al.* (2004). The worldwide leaf economics spectrum. *Nature*, 428, 821-827.

Yang, S.D. & Tyree, M.T. (1993). Hydraulic resistance in acer-saccharum shoots and its influence on leaf water potential and transpiration. *Tree Physiol.*, 12, 231-242.

Zhang, S.B., Guan, Z.J., Sun, M., Zhang, J.J., Cao, K.F. & Hu, H. (2012). Evolutionary association of stomatal traits with leaf vein density in *Paphiopedilum*, Orchidaceae. *PLoS One*, 7, 10.

Zhu, S.D., Chen, Y.J., Ye, Q., He, P.C., Liu, H., Li, R.H. *et al.* (2018). Leaf turgor loss point is correlated with drought tolerance and leaf carbon economics traits. *Tree Physiol.*, 38, 658-663.

Zhu, Y.H., Kang, H.Z., Xie, Q., Wang, Z., Yin, S. & Liu, C.J. (2012). Pattern of leaf vein density and climate relationship of *Quercus variabilis* populations remains unchanged with environmental changes. *Trees-Struct. Funct.*, 26, 597-607.

CHAPTER 5

SCALING OF VENATION ARCHITECTURE WITHIN LEAVES OF DIVERSE ECOTYPES OF *ARABIDOPSIS THALIANA*

ABSTRACT

A reticulated vein system is essential for water transport in leaves, but also accounts for much of a plant's overall hydraulic resistance. Across species, vein tapering and ramification have been shown to increase with vein order to form an efficient vein system, but these vein scaling relationships vary with leaf size. We tested the scaling of vein length per area (VLA) with leaf size, and the effect of leaf size on vein tapering and branching in 169 ecotypes of *Arabidopsis thaliana*, including across different ontogenetic stages. We found that larger leaves showed increased vein tapering and branching across ecotypes within a single species. Major vein diameter and VLA scaled strongly with leaf size across ontogenetic stages, while minor VLA was influenced by ontogeny. These results demonstrate that scaling of leaf venation architecture with leaf size holds at multiple scales, and suggest that a cost-effective vein system is maintained across leaves of different sizes. This study also highlights the importance of ontogeny when considering vein scaling trends.

INTRODUCTION

Leaf veins include both xylem and phloem that are essential for water and sugar transport, and thus for sustaining the growth of the whole plant. When leaves open their stomata for the uptake of carbon dioxide required for photosynthesis, water is lost by transpiration and must be replaced by water that is transported through the leaf veins. Leaf vein architecture plays a major role in photosynthesis and transpiration, with 30% of the whole plant hydraulic resistance encountered in the leaf, and on average similar resistance within the vein system and in the pathways outside the veins to the stomata (Meinzer 2002; Sack *et al.* 2003; Brodribb *et al.* 2005; Sack & Holbrook 2006; Brodribb *et al.* 2007; McKown *et al.* 2010). Leaf venation varies strongly across species in architecture, diameter and density of veins (Uhl & Mosbrugger 1999; Roth-Nebelsick *et al.* 2001; Sack & Frole 2006), and there is substantial variation even within species (Uhl & Mosbrugger 1999; Roth-Nebelsick *et al.* 2001; Mediavilla *et al.* 2020). Leaf veins can be classified into branching orders, including first order (1°) veins, which run down the center of the leaf, second order (2°) veins, which branch off the first, and third order (3°) and/or minor veins that form a mesh between the secondaries (Ellis 2009). In most angiosperms, the vein system is hierarchical, such that the lower-order veins are wider and decrease in diameter with increasing vein order and branching, which maximizes hydraulic efficiency relative to construction cost (Coomes *et al.* 2007; Coomes *et al.* 2008; McKown *et al.* 2010).

In model organism *Arabidopsis thaliana* (referred to as Arabidopsis henceforth), much work has been dedicated to studying the development of the venation system (see summary in Kang & Dengler, 2004) and describing the sequential formation of veins branching from the primary vein into secondary loops and reticulating into third and higher order veins after. Early and late developed leaves of Arabidopsis differ strongly in their shape (heteroblasty) and vein

patterns (Candela *et al.* 1999; Perez-Perez *et al.* 2002). Leaf shape and vein architecture also show variation across natural populations (Candela *et al.* 1999; Perez-Perez *et al.* 2002).

The scaling of the vein system can reveal key principles for clarifying its functional design and how it emerges from developmental processes. For example, across diverse species, major vein diameters increase with leaf size and major vein length per area (VLA or vein density) declines with increasing leaf size, due to the formation of major veins when leaves are tiny primordia, and their ongoing diameter growth and spacing apart in ongoing expansion (Sack *et al.* 2008; Dunbar-Co *et al.* 2009; Scoffoni *et al.* 2011; Sack *et al.* 2012). This trend can provide a mechanism for the association of small leaves with dry and cold climates, given that small leaves have narrow veins containing narrow xylem conduits that resist cold and drought, and more redundancy in their major veins, in addition to properties of the boundary layer of small leaves (Sack *et al.* 2012; Baird *et al.* 2021). By contrast, across species, minor vein density is independent of leaf size, due to the continued patterning of minor veins during leaf expansion; the independence of minor VLA from leaf size can explain the ability of large leafed species to compete in high resource conditions, by adapting a high VLA to enable high photosynthetic rates. However, the scaling of vein density has not been tested across populations of given species that have diversified ecologically (i.e., ecotypes) to determine if intraspecific trends follow the same patterns as have been found using comparative and modeling approaches.

Beyond the scaling of vein diameters and density with leaf size, the changes in vein properties with increasing vein orders from the midrib to the minor veins can have important consequences. The tapering of vein diameter and increase in ramification and length with increasing vein order generates a cost-effective vein system (McKown *et al.* 2010). Yet, this tapering and ramification of veins across branching orders may depend on leaf area. In one study

of oak species, the tapering of xylem conduit diameters from the midrib to minor veins was stronger in smaller leaves (Coomes *et al.* 2008). If this size dependence of vein tapering and ramification is general, it would imply a mechanism to maintain the mass allocation to the vein system and the hydraulic distribution capacity of the vein systems across leaves of different sizes. Arabidopsis provides a key study system to test these such questions. We measured vein systems for 169 ecotypes of Arabidopsis from across their natural range and hypothesized that: (1) Major vein density will decrease with increasing leaf size due to the building of major veins early on in leaf development (prior to most of the leaf expansion), but (2) minor vein density will be decoupled from leaf size, as minor vein formation happens largely after leaf expansion is complete (Scoffoni *et al.* 2011; Sack *et al.* 2012; Baird *et al.* 2021). Further, we hypothesized that (3) the ratios of vein diameter and VLA across vein orders would indicate steeper vein tapering and ramification across higher vein orders in larger leaves and that (4) the scaling of vein diameter and VLA with vein orders will vary across leaves and with leaf size, with larger leaves showing steeper scaling slopes.

METHODS

Growing conditions

Seeds from 169 naturally occurring genotypes (ecotypes) of Arabidopsis were grown in a greenhouse in at the Centre D'Ecologie Fonctionnelle & Evolutive (CEFE, Montpellier, France) from 1 December 2015 to 19 April 2016. Genotypes were selected if they had been previously included as Regional Mapping (RegMap) lines (Horton *et al.* 2012) or in the 1001 Genomes Project (Alonso-Blanco *et al.* 2016), and were chosen specifically to both maximize the range of measured traits (such as flowering time and growth rate) based on previous literature

experiments, and to cover the natural geographic range of the species. Seeds were sown in pots and placed in a cold chamber at 4°C for four days. Four individuals of each genotype were grown in pots in four separate blocks, and were watered every other day. The blocks were rotated and moved in the greenhouse every day to reduce variation. The greenhouse was maintained at constant temperature and light levels of 18°C during the day and 16°C at night, with supplemental lighting to maintain a 12.5h photoperiod. At plant maturity (after bolting) the most recently developed, fully expanded and light-exposed leaf was harvested from each individual plant.

Vein data collection and trait calculations

Harvested leaves were placed in Formalin-Acid-Alcohol (FAA) two days prior to clearing and staining. Leaves were cleared with 95% ethanol and 5% glacial acetic acid for 24 hours. Leaves were then stained with 0.001% safranin, dipped in pure glycerol and mounted between glass sheets. Images were taken using a backlight and digital camera with a macro-lens (Nikon D300s; 100 pixels per millimeter resolution). Vein measurements were made on 169 ecotypes using ImageJ (version 1.52k) following standard protocols and as described below (Scoffoni *et al.* 2013). For 57 ecotypes, four leaves were measured, but when cleared leaves were broken during processing, measurements were not made; for 47 ecotypes, 3 leaves were measured, for 46 ecotypes 2 were measured, and for 19 ecotypes, 1 leaf was measured.

Leaf size and vein traits were measured at the University of California, Los Angeles (UCLA) using ImageJ (software version 1.52k; National Institutes of Health, Bethesda, MD, USA). Measurements included major and minor vein lengths and diameters, and leaf area, perimeter and length as described below. Vein diameters were measured on leaf scanned images

as follows: three measurements per leaf were made on the midrib at the tip, middle and base of the leaf, six measurements per leaf were made of the secondary veins, with two each for each of the three secondaries in the middle of the leaf, and three measurements per leaf were made on random higher order veins near the center of the leaf. The mean of these values for each leaf were used for each vein order. Vein length was measured for the midrib, all secondaries on one half of the leaf, and all minor veins within one focal secondary loop positioned near the center of each leaf. 1° VLA was calculated as the midrib length divided by the total leaf area. 2° VLA was calculated as the secondary vein length from half the leaf divided by half the leaf area. Minor VLA was calculated as the length of all minor veins, including 3° veins, in the focal secondary loop divided by the area of that focal secondary loop. Total major vein length per area (VLA) was calculated as the sum of 1° and 2° vein density, and minor vein density included third and higher order VLA. In Arabidopsis there are fewer vein orders than in most species, and it is common to consider first and second order veins as major veins, and third order and higher as minor (Kang & Dengler 2004). Vein order ratios of vein diameters and VLA were calculated, i.e., the ratio of values for 2° to 1°, 3° to 2° and 3° to 1°.

Leaves were categorized into groups having early type (E_t) or late type (L_t) leaves (Fig 1; Table S5.1) based on the assumed ontogenetic stage from which they were harvested. Leaves were considered E_t if they were round in shape without any teeth or lobes (similar to cotyledon leaves) and had relatively sparse venation. Leaves were considered L_t if they were lanceolate or spatulate and/or had teeth or lobes with greater vein reticulation. Leaves that showed some characteristics of both E_t and L_t were placed into an intermediate (*I*) category (see Fig. 5.1 for examples of each). Genotypes were categorized the same way with genotypes containing both E_t and L_t or only *I* leaves being placed into the *I* category (Table S5.2).

Statistical analyses

An ANOVA was performed in R (version 4.0.4) using the *aov* function in the stats package to determine whether leaf vein traits varied across genotypes, and coefficients of variation were calculated across all 480 leaves and across the 169 genotype means. To determine the scaling of vein diameter and vein density across the three vein orders, three-point power law allometries were fitted, as

$$\log y = \log a + \log x \qquad \text{eqn. 1}$$

The tightness of these relationships justifies the 3-point allometry approach (Scoffoni *et al.* 2011). Vein order scaling slopes were determined for each of the 480 individual leaves, for all 169 genotypes using the lm function in the *stats* package in R. These relationships were calculated between log-transformed vein order (1°, 2° and 3°) and both log-transformed values of leaf vein diameters and log-transformed values of VLA. The slopes of these regressions were then tested for correlations with the corresponding leaf areas both considering the all leaves and genotypes, and considering only those leaves and genotypes which had significant 3-point slopes. We also tested for an association of the vein order ratios of VLA and vein diameters with leaf size. The relationships between leaf area and major and minor vein densities were tested across all genotypes and across genotypes of each ontogenetic stage (E_t, L_t, and I). Correlations were tested between all traits using lm function in the *stats* package in R.

RESULTS

All vein traits varied significantly across ecotypes except minor vein diameter (Table 5.1 and Tables S5.1 and S5.2). Across all ecotypes, major vein density was negatively related to leaf area (r = -0.88, P < 0.001; Fig. 5.2A; Table S5.3), but minor VLA was positively related to leaf size (r = 0.54, P < 0.001; Fig. 5.2B; Table S5.3). The association of major VLA with leaf size held across genotypes in each leaf timing category (E_t, L_t and I leaves; $|r|$ = 0.81-0.85, P < 0.001; Fig. 5.2C, E, G; Tables S5.1-S5.3, slopes of log-transformed data = -0.38 to -0.60; Table S5.4), but when leaf timing was taken into account, minor VLA was independent of leaf size (Fig. 5.2D, F, H, Tables S5.1-S5.3; slopes of log-transformed data = -0.02 to 0.26; Table S5.4).

Leaf vein diameters decreased with increasing vein order, with the midrib being the widest and minor veins having the smallest diameters, as shown by two representative leaves (Fig. 5.3A). The VLA increased with increasing vein order with minor veins being more dense overall than major veins, as shown by two other representative leaves (Fig. 5.3B). Thus, overall the ratios of higher to lower order vein diameters were less than one, indicating tapering in vein diameter (Table 5.2), and the ratios of higher to lower order VLA were greater than one, indicating increased ramification in vein length (Table 5.1). The ratio of vein diameters between vein orders was higher between second and third orders than between first and third, but the opposite was true for the ratio of VLA between vein orders when looking across individual leaves (Table 5.2; Tables S5.1 and S5.2). Vein diameter ratios for all comparisons were negatively correlated with leaf size ($|r|$ = 0.26-0.43, P < 0.001; Table S5.3), and VLA ratios were positively correlated with leaf size across the 480 Arabidopsis leaves ($|r|$ = 0.49-0.88, P < 0.001; Table S5.3), indicating steeper conduit tapering and greater conduit branching in larger leaves. Consistent with that finding, there were significant 3-point slopes for the relationship of log-

transformed vein diameter with vein order for 132 of 480 leaves (27.5%; Table S5.5) and 75 of 169 genotypes (44.4%; Table S5.6). There were significant 3-point slopes for the relationship of log-transformed VLA with log-transformed vein order in 209 of 480 leaves (87.1%; Table S5.4) and in 93 of the 480 individual leaves (19.4%; Table S5.5), respectively. In general, genotypes with larger leaves showed a steeper negative slope for the relationship of vein diameter with vein order (Fig. 5.3A) and genotypes with larger leaves showed a steeper positive slope for the relationship of VLA with vein order (Fig. 5.3B). The slope of the relationship of vein diameter with vein order decreased with increasing leaf size across all leaves and genotypes ($|r|$ = 0.40-0.44, $P < 0.001$; Fig. 5.4A and B; Table S5.7), and the slope of the relationship of VLA with vein order increased (became steeper in the positive direction) with increasing leaf size across all leaves and genotypes ($|r|$ = 0.85-0.87, $P < 0.001$; Fig. 5.4C and D; Table S5.7). Across only leaves for which there was a significant 3-point slope for the relationship of log-transformed VLA or vein diameter with log-transformed vein order, the same leaf size trends were upheld ($|r|$ = 0.73-0.78, $P < 0.001$ for VLA; $|r|$ = 0.42-0.49, $P < 0.001$ for vein diameter; Table S5.7).

DISCUSSION

We found strong relationships for the scaling of major vein diameter and VLA with leaf size, and for the increased tapering and branching of veins in larger leaves across ecotypes of a single species. These findings establish the strong generality of the scaling of leaf venation architecture, both within and across species. Our results also demonstrate that relationships of vein traits with leaf size may vary with ontogenetic stages, highlighting the importance of considering leaf timing and development when analyzing trends of leaf vein traits.

The negative association of major VLA with leaf size upholds trends that had been found previously across diverse species (Scoffoni *et al.* 2011; Sack *et al.* 2012), but the positive association of minor VLA with leaf size has not been shown previously. However, when ontogenetic stage is considered, major and minor vein densities show the expected trends with leaf size. In Arabidopsis, leaves formed earlier in the plant lifecycle tend to have a smaller, rounder shape with less dense veins, while later-forming leaves become larger and lanceolate or spatulate with denser veins (Tsukaya *et al.* 2000; Perez-Perez *et al.* 2002). There are also differences between genotypes, with some retaining rounder shapes even at maturity (Perez-Perez *et al.* 2002), and some showing different and less developed venation as compared to a commonly studied Arabidopsis wild-type, *Ler* (Candela *et al.* 1999). Given that in this study, some genotypes displayed both the small, round leaves and large, spatulate leaves, different ontogeny is most likely causing the differences in leaf venation as opposed to natural ecotypic variation. However, care should be taken in future studies to ensure that all leaves are sampled at the same developmental stage to determine whether observed differences between leaves are genetically or developmentally based.

Our results show that the vein order scaling of vein diameter and vein density depend on leaf size, such that larger leaves in general have wider major veins that then taper more as they branch, and that these leaves have greater branching than smaller veins. This is consistent with the concept that larger leaves require more or wider veins to adequately supply water to all parts of the leaf surface (Coomes *et al.* 2008). Contrary to our expectations, we saw a larger ratio of branching from 2° to 1° veins as compared with the ratio from 3° to 2° veins, but this may have been observed due to the very lower midrib vein density. Overall, there was still a pattern of steep change in vein diameter and VLA from 3° to 1° order veins.

While our results show that smaller leaves may overall have denser veins, larger leaves tend to show greater increase in vein branching with increased vein order. The major veins are formed early in development and then become pushed apart as the leaf expands, while minor veins are formed throughout development but continue to form largely after the leaf has full expanded (Sack *et al.* 2012). This reduces major vein density and leads to an independence of minor vein length per area from leaf size. Therefore, minor VLA does not vary strongly with leaf size across genotypes of a single species. If minor VLA is relatively constant or even increases with leaf size, as our results across all leaves imply, but major VLA decreases with leaf size, then we would expect a steeper slope of VLA against vein order in larger leaves, as we found. These results imply that larger leaves have a greater increase in branching in order to ensure efficient water transport to all cells, as the average distance between major veins and the surrounding cells would be greater in large leaves. This is consistent with a positive correlation of vein density with branching points per leaf area, as had been shown previously in Arabidopsis (Candela *et al.* 1999). Similarly, the slope of the relationship of vein diameter with vein order also varies with leaf size, with larger leaves showing a steeper negative slope as compared with smaller leaves. This implies that larger leaves show a greater decrease in vein diameter as the veins branch. Minor vein diameter was relatively consistent across leaves of different sizes, while major vein diameter was wider in larger leaves. The greater ratio of third to second-order vein diameters as compared with the ratio of second to first-order vein diameters is consistent with previous developmental work in Arabidopsis which has shown that first and second-order veins are formed first in development and have larger vein diameters driven by a longer period of cell division and expansion in those veins as compared with third and higher order veins (Kang & Dengler 2002, 2004). The consistency of minor VLA across leaves of different sizes overall

reduces the variation in total VLA, a trait which indeed showed low variation relative to its mean (Table 5.2).

This work provides new clarity on the importance of optimizing leaf vein architecture with respect to transport capacity relative to construction cost. Further, our findings exemplify the importance of examining trends at fine scales across genotypes of a species, and even across individual leaves influenced by developmental changes during a plant's lifespan. A clearer understanding of the development and functional optimization of leaf venation is critical to fields outside of ecology, including agriculture, by clarifying intraspecific differences in leaf veins, to enable breeders to choose leaves with the most desirable traits (i.e., fewer large veins, larger leaf size, etc.). These results also have important implications for paleobotany, where vein scaling estimates could help predict leaf size, VLA and vein diameters from portions of fossil leaves (Hagen *et al.* 2019).

ACKNOWLEDGEMENTS

We thank undergraduate students Catherine Banh, Tiffany Dang, Danielle Hamadani, Brandon Ho, Sean Hormozian, Grace Hwang, Daniel Juarez, Jasper Kim, Ashley Lok, Matthew Myer, Celine Ngo, Andy Nguyen, Nathan Nguyen, Quang Pham, Amanda Phan, Brandon Phan, Ashley Tong and Erick Yeh for assistance with data collection, Benjamin Blonder for discussion of concepts, and the National Science Foundation (Grants -#1457279, 1557906 and 1951244) and the European Research Council (ERC; 'CONSTRAINTS': grant ERC-StG-2014-639706-CONSTRAINTS) for support.

Table 5.1. Variation in measured traits for 169 ecotypes of Arabidopsis grown in a greenhouse common garden with minimum, average (bold) and maximum mean ecotype values presented. Also presented are the results of an analysis of variance (ANOVA) testing for variation among ecotypes (mean squares, proportion of variance explained by the ANOVA and significance levels for each trait; df, degrees of freedom; ns, P>0.05; *, P<0.05; **, P<0.01; ***, P<0.001) Coefficients of variation (CV) are presented across all 480 measured leaves and across ecotype means, respectively, for each trait.

Trait	Symbol	Unit	Min, Avg, Max	ANOVA result df=168	CV
Leaf area	LA	mm^2	53.4, **333**, 721	65627, 0.810***	50.6, 41.8
Leaf width	LW	mm	7.01, **14.4**, 23.8	31.1, 0.812***	29.0, 21.8
Minor vein width	3° diameter	mm	9.83e-3, **3.52e-2**, 7.87e-2	1.39e-4, 0.393, ns	31.6, 21.4
Secondary vein width	2° diameter	mm	2.62e-2, **0.5.72e-2**, 0.116	5.75e-4, 0.601***	32.1, 26.0
Midrib width	1° diameter	mm	3.28e-2, **0.169**, 0.396	8.08e-3, 0.583***	41.2, 30.4
Minor vein length per area	Minor VLA	$mm\ mm^{-2}$	0.692, **1.78**, 3.23	0.546, 0.684***	29.8, 24.8
Secondary vein length per area	Secondary VLA	$mm\ mm^{-2}$	0.285, **0.621**, 1.53	5.53e-2, 0.583***	29.4, 23.3
Midrib vein length per area	Midrib VLA	$mm\ mm^{-2}$	3.74e-2, **0.114**, 0.276	3.95e-5, 0.739***	37.9, 32.7
Major vein length per area	Major VLA	$mm\ mm^{-2}$	0.352, **0.735**, 1.76	8.45e-2, 0.638***	29.3, 24.0
Total vein length per area	Total VLA	$mm\ mm^{-2}$	1.31, **2.51**, 4.28	0.446, 0.610***	20.2, 17.3
Projected vein area per area	PAPA	$mm^2\ mm^{-2}$	4.77e-2, **0.115**, 0.279	1.69e-3, 0.453***	31.4 22.0
Volume of veins per area	VAPA	$mm^3\ mm^{-2}$	1.49e-3, **0.6.22e-3**, 2.38e=2	1.51e-5, 0.414*	57.5, 37.3

Table 5.2. Ratios of vein diameter and vein length per area (VLA) between vein orders (second to first, third to second, and third to first) across 480 leaves of Arabidopsis from plants grown in a greenhouse. Reported are the minimum, average and maximum ratios for each category.

	2:1 Vein Diameter	3:2 Vein Diameter	3:1 Vein Diameter	2:1 VLA	3:2 VLA	3:1 VLA
Minimum	0.116	0.131	0.0392	2.49	0.879	4.73
Average	0.378	0.647	0.239	5.75	3.15	18.3
Maximum	0.997	1.00	0.795	14.1	10.2	62.0

FIGURE CAPTIONS

Figure 5.1. Early, intermediate and late timing Arabidopsis leaves (E_t, L_t and I, respectively). Genotypes represented are A) 6967, an E_t leaf, B) 8420, an I leaf and C) 7373, an L_t leaf.

Figure 5.2. Relationships between leaf size and vein length per area (VLA) across 480 leaves from 169 genotypes of Arabidopsis grown in a common garden. Plots show the association of A) major VLA and B) minor VLA with leaf area across all 169 genotypes where colors represent leaf ontogenetic stages (see below); the association of the mean values of C) major VLA and D) minor VLA with leaf size across genotypes categorized as having early-timing (E_t; white) leaves; the association of the mean values of E) major VLA and F) minor VLA with leaf size across genotypes categorized as having late-timing (L_t; black) leaves; the association of mean values of G) major VLA and H) minor VLA for genotypes categorized as intermediates (gray), meaning different individuals had leaves falling into both the E_t and L_t categories. The r-values with significance are based on linear regression analysis of raw or log-transformed data. ns, $P>0.05$; *, $P<0.05$; **, $P<0.01$; ***, $P<0.001$.

Figure 5.3. Relationships of vein order with logged values of A, vein diameter and B, vein length per area (VLA) across representative large (solid dots, solid lines) and small (open circles, dashed lines) leafed-genotypes. Genotypes in A: large leafed, 8235; small leafed, 6960. Genotypes in B: large leafed, 673; small leafed, 6911.

Figure 4. Relationship of leaf area with (A) the slope of the vein diameter between vein orders across 480 individual leaves and (B) across 169 ecotypes of Arabidopsis grown in a greenhouse

common garden. (C) The slope of the vein length per area across 480 individuals and (D) 169 ecotypes of Arabidopsis grown in a common garden. The *r*-values with significance stars are based on linear regression models. Colors represent leaf ontogenetic stages where early-timing (E_t) leaves or genotypes are white, late-timing (L_t) leaves or genotypes are black, and intermediate leaves or genotypes are gray. ns, $P>0.05$; *, $P<0.05$; **, $P<0.01$; ***, $P<0.0001$.

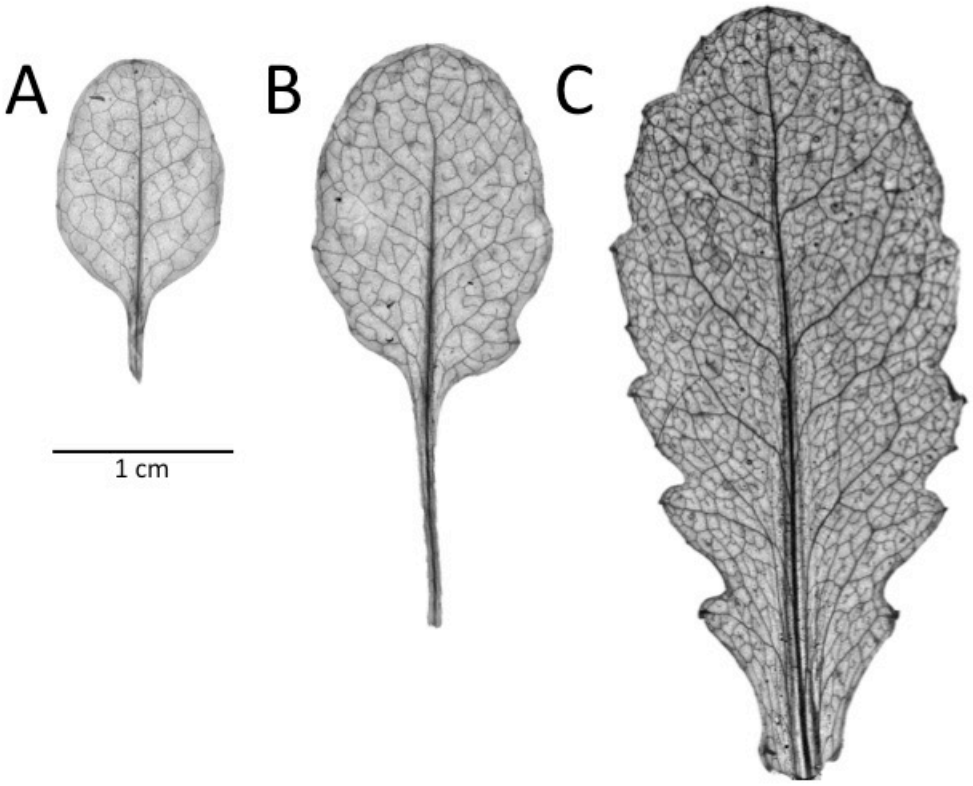

Figure 5.1

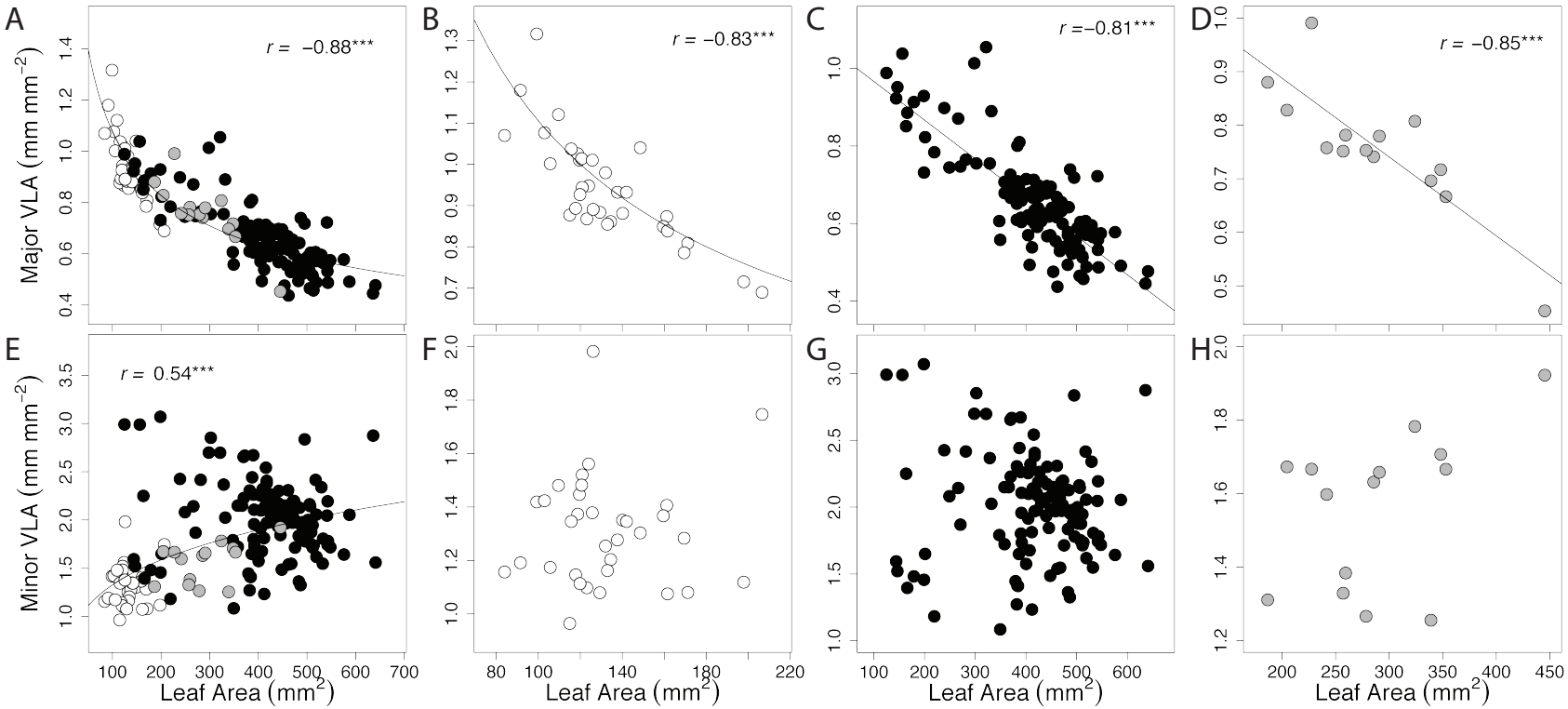
A
B
C
D
E
F
G
H
Major VLA (mm mm^{-2})
Minor VLA (mm mm^{-2})
Leaf Area (mm^2)
r = −0.88***
r = −0.83***
r = −0.81***
r = −0.85***
r = 0.54***

Figure 5.2

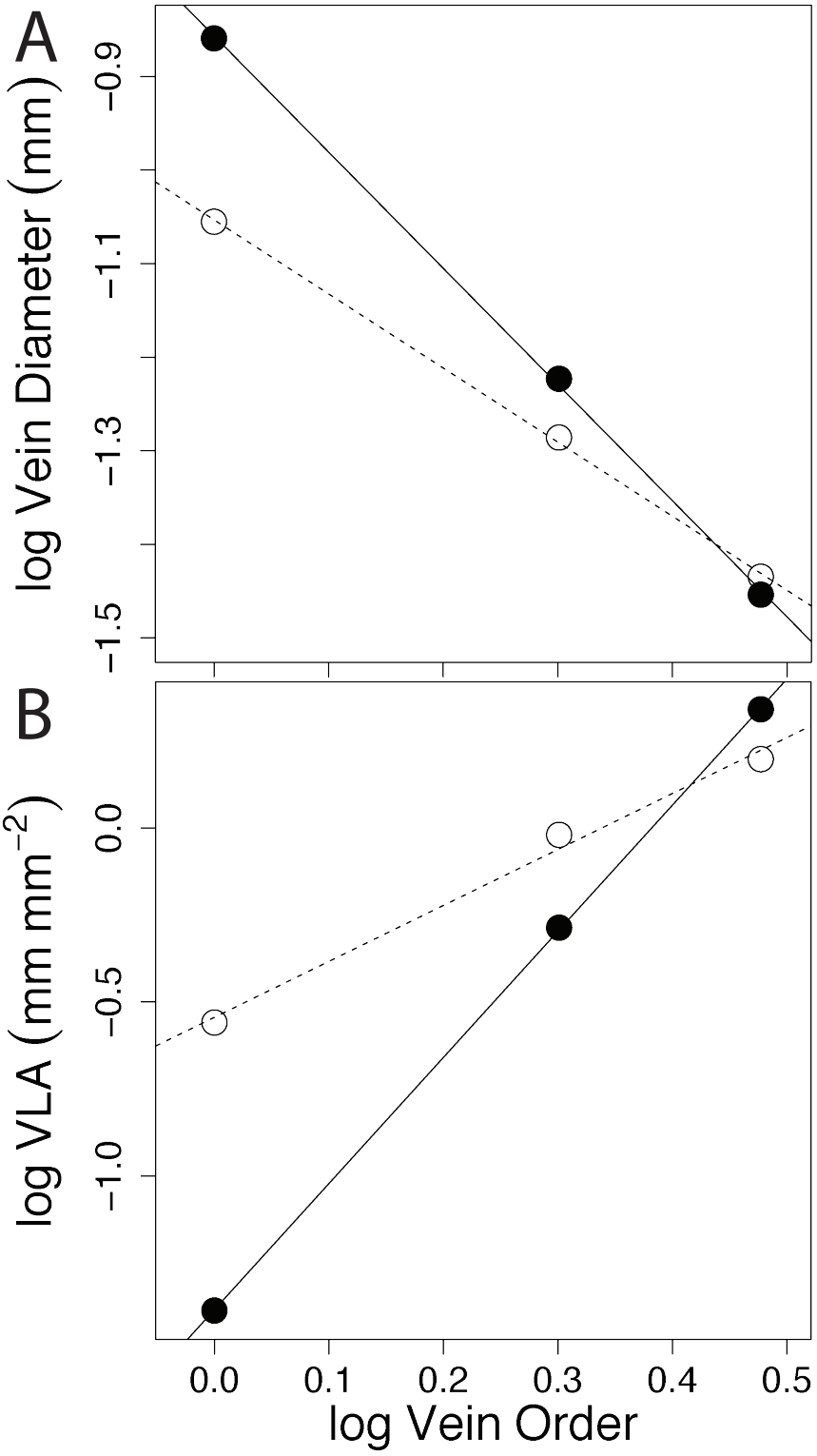
A
B
log Vein Diameter (mm)
log VLA (mm mm^{-2})
log Vein Order
−0.9
−1.1
−1.3
−1.5
0.0
−0.5
−1.0
0.0
0.1
0.2
0.3
0.4
0.5

Figure 5.3

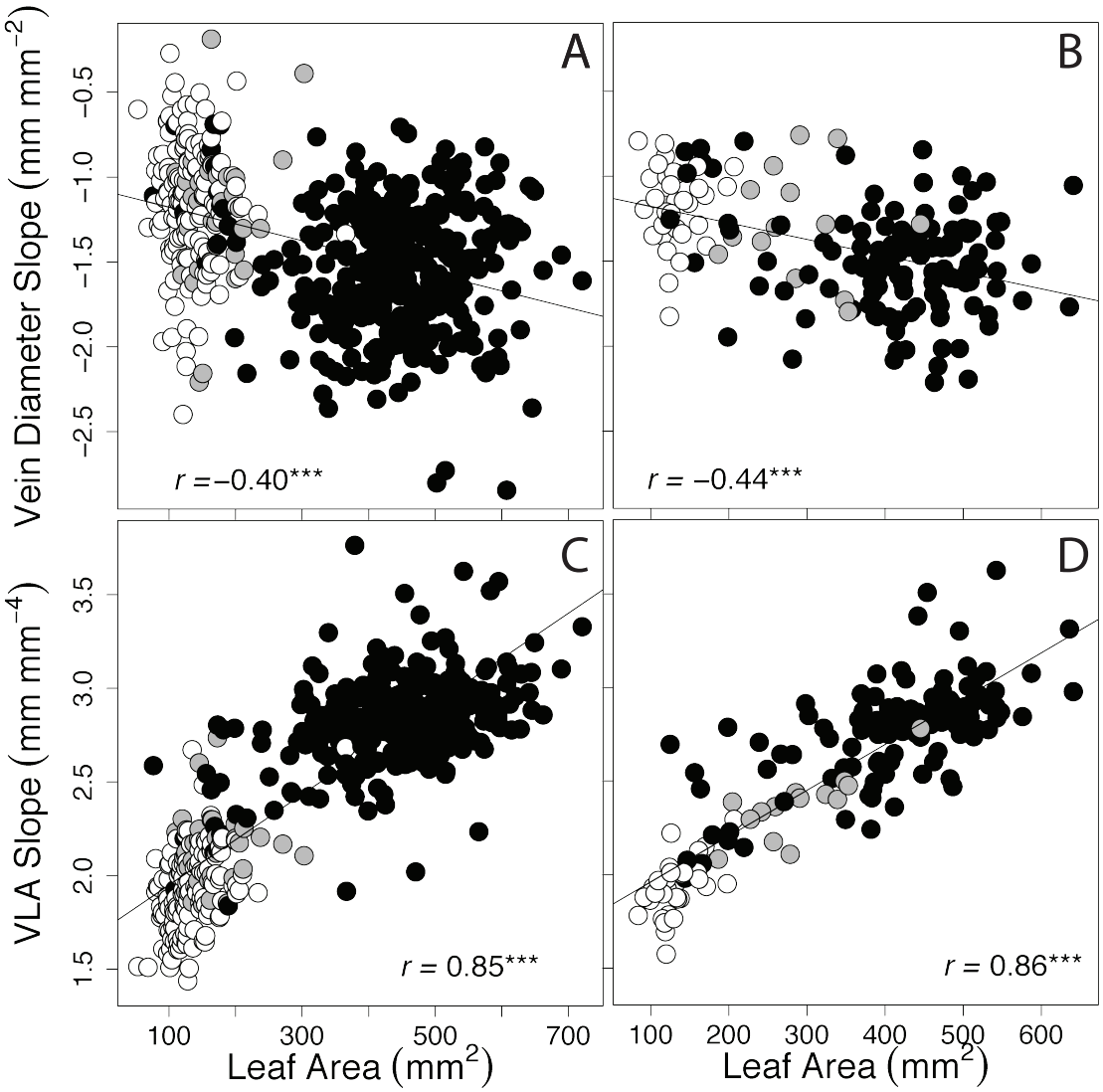
A
B
C
D
Vein Diameter Slope (mm mm^{-2})
VLA Slope (mm mm^{-4})
r =−0.40***
r = −0.44***
r = 0.85***
r = 0.86***
−2.5
−2.0
−1.5
−1.0
−0.5
1.5
2.0
2.5
3.0
3.5
100
300
500
700
100
200
300
400
500
600
Leaf Area (mm^2)
Leaf Area (mm^2)

Figure 5.4

SUPPLEMENTARY MATERIALS

Supplementary Data Captions (see attached Excel Workbook)

Table S5.1. Experimental data 480 leaves from 169 genotypes of *Arabidopsis thaliana* grown in a greenhouse common garden. See "CHAPTER 5 Legend" tab for legend of symbols and units.

Table S5.2. Experimental mean data 169 genotypes of *Arabidopsis thaliana* grown in a greenhouse common garden. See "CHAPTER 5 Legend" tab for legend of symbols and units.

Table S5.3. Correlation matrices of all traits for 480 individual leaves and 169 genotype means of *Arabidopsis thaliana* grown in a greenhouse common garden. Values show the r-values of correlations using raw, log-transformed, and ranked data. Highlighted cells represent tests for which either a raw and rank, or a log and rank correlation test were significant. Stars represent significance levels for each trait; df, degrees of freedom; ns, $P>0.05$; *, $P<0.05$; **, $P<0.01$; ***, $P<0.001$). See "CHAPTER 5 Legend" tab for legend of symbols and units.

Table S5.4. Slopes of the relationships of major and minor vein length per area (VLA) with leaf area across 169 genotypes of *Arabidopsis thaliana* grown in a greenhouse common garden. Columns include: Ontogenetic stage (E_t, early timing; L_t, late timing; *I*, intermediate, consisting of genotypes with leaves in both groups; All genotypes, a combination of all genotypes across all ontogenetic stages); Category of either major (first and second order) or minor (third and higher order) veins; Raw slope, which is the slope of the linear regression of untransformed data for VLA with leaf size; Log slope, which is the slope of the linear regression of log-transformed VLA and leaf size data.

Table S5.5. Linear regression coefficients for the relationship of log-transformed values of vein order versus vein diameter and log-transformed values of vein length per area for each of 480 leaves of *Arabidopsis thaliana* grown in a greenhouse common garden. Column names include the name of the individual leaf tested (IndivCode), the estimated slope and intercept values (estimate), the value of the statistic (statistic), the p-value for the regression (p.value), the associated leaf area for each leaf (see " CHAPTER 5 Legend" tab for units), and the logged value of that leaf area.

Table S5.6. Linear regression coefficients for the relationship of log-transformed values of vein order versus vein diameter and log-transformed values of vein length per area for genotypes means of each of 169 genotypes of *Arabidopsis thaliana* grown in a greenhouse common garden. Column names include the genotype accession number (Accession_ID), the estimated slope and intercept values (estimate), the value of the statistic (statistic), the p-value for the regression (p.value), the associated leaf area for each leaf (see " CHAPTER 5 Legend" tab for units), and the logged value of that leaf area.

Table S5.7. Linear regression results for the relationships of leaf area against the slope of VLA or vein diameter with vein order. Tests were performed across 480 individual leaves and 169 genotypes of *Arabidopsis thaliana* grown in a greenhouse common garden in Montpellier, France, and were tested using all data and only samples for which there were significant slopes for VLA or vein diameter with vein order. Column names include the intercept and slope of the regression (estimate), the standard error (Std. Error), the t-value of the regression (t values), the

p-value of the regression (Pr(>|t|)), significance level of the regression where ns, P>0.05; *, P<0.05; **, P<0.01; ***, P<0.0001(significance), the r-squared value (r.sqr) and the r-value (r).

REFERENCES

Alonso-Blanco, C., Andrade, J., Becker, C., Bemm, F., Bergelson, J., Borgwardt, K.M. *et al.* (2016). 1,135 genomes reveal the global pattern of polymorphism in *Arabidopsis thaliana*. *Cell*, 166, 481-491.

Baird, A.S., Taylor, S.H., Pasquet-Kok, J., Vuong, C., Zhang, Y., Watcharamongkol, T. *et al.* (2021). Developmental and biophysical determinants of grass leaf size worldwide. *Nature*, 592, 242-+.

Brodribb, T.J., Feild, T.S. & Jordan, G.J. (2007). Leaf maximum photosynthetic rate and venation are linked by hydraulics. *Plant Physiology*, 144, 1890-1898.

Brodribb, T.J., Holbrook, N.M., Zwieniecki, M.A. & Palma, B. (2005). Leaf hydraulic capacity in ferns, conifers and angiosperms: impacts on photosynthetic maxima. *New Phytologist*, 165, 839-846.

Candela, H., Martinez-Laborda, A. & Micol, J.L. (1999). Venation pattern formation in *Arabidopsis thaliana* vegetative leaves. *Dev. Biol.*, 205, 205-216.

Coomes, D.A., Heathcote, S., Godfrey, E.R., Shepherd, J.J. & Sack, L. (2008). Scaling of xylem vessels and veins within the leaves of oak species. *Biology Letters*, 4, 302-306.

Coomes, D.A., Jenkins, K.L. & Cole, L.E.S. (2007). Scaling of tree vascular transport systems along gradients of nutrient supply and altitude. *Biology Letters*, 3, 86-89.

Dunbar-Co, S., Sporck, M.J. & Sack, L. (2009). Leaf trait diversification and design in seven rare taxa of the Hawaiian *Plantago* radiation. *Int. J. Plant Sci.*, 170, 61-75.

Ellis, B. (2009). Manual of leaf architecture.

Hagen, E.R., Royer, D.L., Moye, R.A. & Johnson, K.R. (2019). No large bias within species between the reconstructed areas of complete and fragmented fossil leaves. *Palaios*, 34, 43-48.

Horton, M.W., Hancock, A.M., Huang, Y.S., Toomajian, C., Atwell, S., Auton, A. *et al.* (2012). Genome-wide patterns of genetic variation in worldwide *Arabidopsis thaliana* accessions from the RegMap panel. *Nature Genetics*, 44, 212-216.

Kang, J. & Dengler, N. (2002). Cell cycling frequency and expression of the homeobox gene ATHB-8 during leaf vein development in *Arabidopsis*. *Planta*, 216, 212-219.

Kang, J. & Dengler, N. (2004). Vein pattern development in adult leaves of *Arabidopsis thaliana*. *Int. J. Plant Sci.*, 165, 231-242.

McKown, A.D., Cochard, H. & Sack, L. (2010). Decoding Leaf Hydraulics with a Spatially Explicit Model: Principles of Venation Architecture and Implications for Its Evolution. *Am. Nat.*, 175, 447-460.

Mediavilla, S., Martin, I. & Escudero, A. (2020). Vein and stomatal traits in leaves of three co-occurring *Quercus* species differing in leaf life span. *Eur. J. For. Res.*, 139, 829-840.

Meinzer, F.C. (2002). Co-ordination of vapour and liquid phase water transport properties in plants. *Plant Cell and Environment*, 25, 265-274.

Perez-Perez, J.M., Serrano-Cartagena, J. & Micol, J.L. (2002). Genetic analysis of natural variations in the architecture of *Arabidopsis thaliana* vegetative leaves. *Genetics*, 162, 893-915.

Roth-Nebelsick, A., Uhl, D., Mosbrugger, V. & Kerp, H. (2001). Evolution and function of leaf venation architecture: A review. *Ann. Bot.*, 87, 553-566.

Sack, L., Cowan, P.D., Jaikumar, N. & Holbrook, N.M. (2003). The 'hydrology' of leaves: co-ordination of structure and function in temperate woody species. *Plant Cell and Environment*, 26, 1343-1356.

Sack, L., Dietrich, E.M., Streeter, C.M., Sanchez-Gomez, D. & Holbrook, N.M. (2008). Leaf palmate venation and vascular redundancy confer tolerance of hydraulic disruption. *Proc. Natl. Acad. Sci. U. S. A.*, 105, 1567-1572.

Sack, L. & Frole, K. (2006). Leaf structural diversity is related to hydraulic capacity in tropical rain forest trees. *Ecology*, 87, 483-491.

Sack, L. & Holbrook, N.M. (2006). Leaf hydraulics. In: *Annual Review of Plant Biology*, pp. 361-381.

Sack, L., Scoffoni, C., McKown, A.D., Frole, K., Rawls, M., Havran, J.C. *et al.* (2012). Developmentally based scaling of leaf venation architecture explains global ecological patterns. *Nat. Commun.*, 3, 10.

Scoffoni, C., Rawls, M., McKown, A., Cochard, H. & Sack, L. (2011). Decline of leaf hydraulic conductance with dehydration: relationship to leaf size and venation architecture. *Plant Physiology*, 156, 832-843.

Scoffoni, C., Sack, L. & contributors, P. (2013). Quantifying leaf vein traits. *PrometheusWiki*.

Tsukaya, H., Shoda, K., Kim, G.T. & Uchimiya, H. (2000). Heteroblasty in *Arabidopsis thaliana* (L.) Heynh. *Planta*, 210, 536-542.

Uhl, D. & Mosbrugger, V. (1999). Leaf venation density as a climate and environmental proxy: a critical review and new data. *Paleogeogr. Paleoclimatol. Paleoecol.*, 149, 15-26.

CHAPTER 6

VARIATION IN GROWTH AND VENATION ARCHITECTURE ACROSS *ARABIDOPSIS* LEAF VEIN MUTANTS

ABSTRACT

Leaf veins are fundamental determinants of plant growth. While the importance of leaf vein traits has been studied across diverse species, far less is known of its contribution to differences in function within species, such as within a model system such as *Arabidopsis thaliana*. Further, little work has been dedicated to determining the impact of vein mutations on whole plant performance. We applied an experimental approach to determine the consequences of variation in leaf vein architecture for whole plant growth across *A. thaliana* vein mutants. One wild-type (Col-0) and 89 *A. thaliana* mutant genotypes were measured for vein traits in early and late forming leaves, and whole plant relative growth rate (RGR) and its components were assessed. Across genotypes, we found that vein length per area (VLA) differed between early and late forming leaves, and that major VLA was negatively associated with leaf size at both stages, while minor VLA was independent of leaf area. Additionally, most vein mutants showed decreased RGR as compared with Col-0. However, RGR was independent of total VLA. This work provides insight into the influence of vein traits on higher-level plant function, and provides knowledge that may be transferrable to other species, including crops.

INTRODUCTION

Leaf veins are essential for mechanical stability and the transport of water, sugar, hormones and nutrients (Niklas 1999; Sack & Holbrook 2006; Kehr & Buhtz 2007). Many tests of the importance of leaf venation have been performed across diverse species (Uhl & Mosbrugger 1999; Roth-Nebelsick *et al.* 2001; Sack & Frole 2006; Sack *et al.* 2008; Dunbar-Co *et al.* 2009; Scoffoni *et al.* 2011; Sack *et al.* 2012) but few have focused within a single species or a model system such as *Arabidopsis thaliana* (referred to as Arabidopsis henceforth). Many Arabidopsis vein mutants have been identified (Petricka *et al.* 2008) making it an ideal system in which to study the effects of altered venation on whole plant performance. Some Arabidopsis leaves are known to exhibit altered vein traits in early-forming leaves but not in leaves formed later in their lifecycle (Perez-Perez *et al.* 2002). However, little is known of the consequences of these altered vein patterns for whole plant performance. Our goals were to quantify vein patterns at multiple developmental stages and to determine the effect of vein mutants on relative growth rate (RGR). We hypothesized that mutant genotypes would display altered venation at multiple developmental stages when compared to wild-types, and that the RGR of mutant genotypes may be negatively impacted as compared with a wild-type (Col-0) due to a reduced hydraulic supply, or due to extra construction costs of creating disrupted veins that would not provide any gains in growth.

METHODS

Plant growth conditions and DNA extraction

Seeds for 89 venation and stomatal mutants were identified and ordered using The *Arabidopsis* Information Resource (TAIR) database (Huala *et al.* 2001). Mutant genotypes and one naturally

occurring genotype (ecotype; Col-0) were grown in a UCLA greenhouse from 5 April 2017 to 10 May 2017. In the greenhouse, mean temperature was 23.9 °C (minimum and maximum were 21.3°C and 29.1°C, respectively), mean humidity was 44% (15-63%) and mean irradiance from 9:00 to 16:00 was 201µmol photons m-2 s-1 (61-861µmol photons m-2 s-1; HOBO Micro Station with Smart Sensors, Onset, Bourne, MA, USA). Seeds were sown as lawns in pots (8 cm long, 12.3 cm wide, 6 cm deep) with 1:1:2:1:1 mixture of plaster sand, loam, peat moss, perlite and vermiculite and plants were watered 2-3 times per week with fertilized water (250ppm of Peters Professional water soluble fertilizer; N 20%; P 20%; K 20%; B 0.0125%; Cu 0.0125%; Fe 0.05%; Mn 0.025%; Mo 0.005%; Zn 0.025%). Pots were placed in a cold chamber for three days to cold acclimate at 4°C. 100mg of leaf tissue for DNA extraction was harvested from the lawns of each genotype and DNA extractions were later performed with the Qiagen DNeasy Plant Mini Kit for all genotypes to allow for whole-genome sequencing. Twenty-five seedlings per genotype were also harvested between 22 April 2017 and 28 April 2017 to be used later for initial mass calculations for relative growth rate (RGR; g g^{-1} day^{-1}). Seedling roots were washed and groups of five seedlings were placed together into coin envelopes that were put into a drying oven at 70°C for at least 72 hours before dry mass was determined (XS205 and AB265-S; Mettler, Toledo, OH, USA). The mass of these seedlings together was divided by five and used as the initial mass (M_0) for RGR calculation described below. After one week of growth the pots were thinned to include one individual plant per pot, for a total of 11 individuals per mutant genotype. After three weeks of growth, plants were staked.

Growth and biomass harvesting, and collection of trait data

Three of the 11 individuals were harvested for phenotyping of leaf morphology and venation architecture. To investigate phenotypic changes caused by leaf heteroblasty, leaves were harvested from two growth stages: the first and third whorl rosette leaves (cohorts 1 and 3, representing early and late development). These leaves were preserved in 70% formalin-acetic acid-alcohol (FAA; 48% ethanol: 10% formalin: 5% glacial acetic acid: 37% water), and at least one leaf from each developmental stage was then measured for each vein mutant. Leaves were then cleared with 2.5-5% sodium hydroxide in water or ethanol, and then with sodium hypochlorite bleach, following standard protocols (Scoffoni *et al.* 2013). Leaves were finally stained with safranin and fast green, mounted between clear sheets (AF4300, 3M, St. Paul, MN, USA) and scanned at 1200dpi (Epson Perfection 4490, Long Beach, CA, USA). Vein traits were measured using ImageJ (software version 1.52k; National Institutes of Health, Bethesda, MD, USA). Measured vein traits included: widths (mm) and vein length per area (VLA; vein density; mm mm^{-2}) for each vein order in the leaf blade, along with leaf area (mm^2). The projected vein area per area (PAPA; mm^2 mm^{-2}) was calculated as the sum of the VLA of each vein order (first, second and third) times the average width of each corresponding vein order. The volume of veins per area (VPA; mm^3 mm^{-2}) was calculated as the sum of the VLA for each vein order multiplied by π and the squared radius of each vein order.

Five of the 11 individuals for 54 of the 90 genotypes that had not been affected by greenhouse pests were harvested to use for measurements of RGR (Evans 1972; Hunt & Cornelissen 1997). The plants were separated into rosette leaves (with three being weighed separately to later use for measurement of leaf mass per area; LMA; g m^2), inflorescence, and roots that were washed free of soil. All parts were oven-dried at 70°C for at least 72 hours before

dry mass was determined. Prior to drying, the three randomly selected rosette leaves were traced for measurement of leaf area using ImageJ, and were also measured for leaf thickness (LT; mm; Fowler Digital Calipers, Chicago, IL, USA) and chlorophyll concentration per leaf area using a SPAD meter (Chl area^{-1}; SPAD-502; Konica Minolta Sensing Inc., Osaka, Japan). The SPAD meter provides measurements in SPAD units that correlate with total (a+b) chlorophyll per leaf area (Uddling *et al.* 2007).

RGR and absolute growth rate (AGR; g day^{-1}) were determined using the initial seedling mass and the final mass. RGR was calculated as

$$RGR = \frac{\ln\left(\frac{M_f}{M_0}\right)}{\Delta t} \qquad \text{(Eqn 1)}$$

where Δt is time (days between initial and final harvest), M_f (g) is the plant total dry mass, and other variables are as described above. Absolute growth rate was calculated as

$$AGR = \frac{M_f - M_0}{\Delta t} \qquad \text{(Eqn 2).}$$

The components of RGR were also calculated following standard protocol (Hunt & Cornelissen 1997). Leaf mass fraction (LMF; g g^{-1}) was calculated as rosette leaf mass (g) divided by M_f, leaf mass per area (LMA; g cm^{-2}) as leaf mass (g) divided by leaf area (cm^2), leaf area ratio (m^2 g^{-1}) as leaf area divided by M_f and unit leaf rate (ULR; g m^{-2} day^{-1}) as RGR divided by LAR. Leaf density (mg mm^{-3}) was also calculated as LMA divided by LT (Evans 1972). Root mass fraction

(RMF; g g^{-1}) was determined as root mass (g) divided by M_f, and reproductive mass fraction was calculated as the mass of the inflorescence stem (g) divided by M_f.

Statistical analyses

All statistical analyses were performed in the R Statistics environment (R version 4.0.4). An Analysis of Variance (ANOVA) was performed on all traits using the *aov* function in the stats package. Paired t-tests were conducted to determine if leaf size and vein traits differed between the two cohorts (1 and 3) for each genotype using the *t.test* function in the stats package. Orthogonal contrasts were also performed to determine how each mutant genotype differed from the wild-type, Col-0, using the *aov* and *lm* functions in the stats package. Lastly, a matrix of all trait correlations on raw, log-transformed and ranked data was produced using the *lm* function in the stats package. For rigorousness, results were considered significant only if they were significant in both raw and Spearman's rank correlations, or both log-transformed and Spearman's rank correlations. The most significant correlation using raw or log-transformed data was reported given that the rank correlation was also significant.

RESULTS

Mutants varied from the wild-type in all traits except leaf thickness, and leaf area, midrib VLA and total VLA of cohort 1 leaves, but these traits too did vary significantly in leaves produced later (cohort 3; Table 6.1; Fig. 6.1; Tables S6.1 and S6.2). Leaf size and all vein traits varied in a paired t-test between first and third cohort leaves (Table S6.3), with leaf size and minor VLA overall increasing in late development leaves, while major VLA overall decreased (Fig. 6.2). 90.7% of the mutant genotypes (49 out of 54 compared to Col-0) showed altered RGR as

compared with Col-0 (Table S6.4). For all but three of these genotypes, RGR was reduced as compared with the wild-type (it was significantly higher for genotypes 1128, CS68723 and CS78905; Table S6.4).

In both cohort 1 and cohort 3 leaves, major VLA was negatively correlated with leaf size while minor VLA was independent of leaf size ($|r|$ = 0.56-0.71, $P < 0.05$; Table S6.5). RGR increased with increasing chlorophyll per area, leaf thickness ($|r|$ = 0.31-45, $P < 0.05$; Table S6.5), but was independent of total VLA (Table S6.5). RGR was also higher when either of its components, ULR or LMF, was higher (r = 0.39-0.83, $P < 0.05$; Table S6.5). A greater portion of the leaf surface being dedicated to veins (higher PAPA) and a higher VPA was associated with a reduced RGR ($|r|$ = 0.36-0.41, $P < 0.05$; Table S6.5).

DISCUSSION

Across Arabidopsis vein mutants, we found that most traits varied substantially, and that vein traits varied between early and late stage leaves. The finding of increased minor VLA in later-stage leaves is consistent with previous work on Arabidopsis genotypes showing that minor veins form later in development (Candela *et al.* 1999; Perez-Perez *et al.* 2002; Kang & Dengler 2004). Reduced major VLA is related to increased leaf size in later-stage leaves, where major veins are pushed apart more during leaf expansion (Scoffoni *et al.* 2011; Sack *et al.* 2012). The negative relationship of leaf area with major VLA but independence of minor VLA with leaf size has been well documented across diverse and closely related species (Sack *et al.* 2008; Dunbar-Co *et al.* 2009; Scoffoni *et al.* 2011; Sack *et al.* 2012), and across naturally occurring genotypes (ecotypes) of Arabidopsis (Fletcher *et al.* in prep.-a; Fletcher *et al.* in prep.-b), and has been shown here to hold across Arabidopsis vein mutants, indicating that this is a strong

developmental trend. The reduction in RGR in vein mutants is consistent with greater portions of the leaf surface being dedicated to veins, which may reduce photosynthetic mesophyll cell area, especially if mutants invest in veins that are improperly connected. However, this trend has also been shown previously across Arabidopsis ecotypes (Fletcher *et al.* in prep.-b), indicating that it may be upheld across natural and mutant Arabidopsis plants.

While most mutants showed a reduced RGR as compared with the wild-type, this is not necessarily indication of a causal relationship between vein traits and RGR. The lack of a correlation between VLA and RGR may indicate that the conductivity of veins, or other leaf traits may complicate this relationship. Indeed, the mutants included in this study also come from diverse genetic backgrounds and are not all single-knockout mutants, meaning other traits aside from venation pattern may have been impacted. Additionally, some mutated genes may be pleiotropic, affecting multiple aspects of the observed phenotypes. Future work should focus on determining which loci are affected in these mutants, and what potential impacts these may have on leaf traits (Atwell *et al.* 2010; Brachi *et al.* 2011; Filiault & Maloof 2012; Korte & Farlow 2013). Investigation into the genomes of these mutants may also help determine whether many or few loci control vein traits, and if these loci also show variation across natural Arabidopsis populations. The insight generated in this work can be applied to further research in agriculture by identifying target loci that influence the traits contributing to whole plant performance (Dhondt *et al.* 2010; Liu 2010; Chew & Halliday 2011; Cobb *et al.* 2013; Feldman *et al.* 2014).

ACKNOWLEDGEMENTS

We thank Jessica Smith, Weimin Deng and the staff of the plant growth center at the University of California, Los Angeles for assistance with plant cultivation, Ruihua Pan and undergraduate

students Andre Anvari, Chaiti Bhagawat, Rebecca Chen, Chu Chow, Brandon Ho, Grace Hwang, Jasper Kim, Ashley Lok, Andy Nguyen, Nathan Nguyen, Celine Ngo, Brandon Phan, Thomas Smith and Ashley Tong for assistance with data collection, Suhua Feng and Steve Jacobsen for assistance with DNA extraction, and the National Science Foundation (Grants -#1457279, 1557906 and 1951244) for support.

Table 6.1. Variation in measured traits for 89 mutants and one wild-type (Col-0) of Arabidopsis grown in a greenhouse common garden with minimum, average (bold) and maximum mean ecotype values presented. Also presented are the results of an analysis of variance (ANOVA) testing for variation among genotypes (mean squares, proportion of variance explained by the ANOVA and significance levels for each trait; df, degrees of freedom; ns, P>0.05; *, P<0.05; **, P<0.01; ***, P<0.001). C1: cohort 1, C3: cohort 3.

Trait	Symbol	Unit	Min, Avg, Max	ANOVA result	dfs
Whole plant growth and reproduction					
Seedling mass	Ms	g	3.38e-4, **1.84e-3**, 9.97e-3	7.76e-6, 0.500***	85, 363
Leaf thickness	LT	mm	7.72e-2, **0.197**, 0.972	5.81e-2, 0.220, ns	57, 140
Chlorophyll per area	SPAD	chl/area	6.63, **21.8**, 36.0	74.1, 0.856***	58, 145
Final mass	Mf	g	8.88e-3, **6.93e-2**, 0.605	4.13e-2, 0.549***	57, 152
Root mass fraction	RootMf	g g-1	1.98e-2, **0.111**, 0.402	1.61e-2, 0.596***	57, 152
Inflorescence mass fraction	IFMF	g g-1	0.230, **0.405**, 0.565	3.36e-2, 0.443***	57, 152
Absolute growth rate	AGR	g day-1	3.65e-4, **3.92e-3**, 4.51e-2	1.87e-4, 0.959***	54, 138
Relative growth rate	RGR	g g-1 day-1	4.54e-2, **0.200**, 0.449	2.09e-2, 0.898***	54, 138
Leaf mass fraction	LMF	g g-1	0.259, **0.487**, 0.664	3.89e-2, 0.450***	57, 151
Leaf mass per area	LMA	g m-2	6.41, **12.4**, 24.9	19.3, 0.531***	72, 168
Leaf density	LD	mg mm-3	4.42e-2, **7.42e-2**, 0.170	1.60e-3, 0.556***	56, 128
Specific leaf area	SLA	cm2 g-1	559, **872**, 2071	135763, 0.531***	72, 168
Unit leaf rate	ULR	g m-2 day-1	1.23, **5.77**, 14.0	25.2, 0.647***	54, 134
Leaf area ratio	LAR	m2 g-1	2.21e-2, **4.08e-2**, 7.07e-2	4.16e-4, 0.458***	58, 143
Leaf venation					
Leaf area C1	LA	mm2	220, **44.7**, 107	514.2, 0.447, ns	58, 59
Midrib diameter C1	Midrib Diam	mm	4.39e-2, **7.03e-2**, 0.109	4.67e-4, 0.705***	58, 58
Midrib vein length per area C1	Midrib VLA	mm mm-2	0.133, **0.209**, 0.277	2.10e-3, 0.470, ns	58, 59
Secondary width C1	Secondary Diam	mm	2.81e-2, **4.55e-2**, 7.35e-2	2.02e-4, 0.783***	58, 55
Secondary vein length per area C1	Secondary VLA	mm mm-2	0.655, **1.08**, 1.83	7.80e-2, 0.664**	58, 55
Minor vein width C1	Minor Diam	mm	2.26e-2, **3.45e-2**, 5.42e-2	9.61e-5, 0.630*	57, 55

Minor vein length per area C1	Minor VLA	mm mm-2	0.335, **1.24**, 2.52	0.328, 0.671**	57, 55
Major vein length per area C1	Major VLA	mm mm-2	0.830, **1.29**, 2.05	9.00e-2, 0.634*	58, 55
Total vein length per area C1	Total VLA	mm mm-2	1.60, **2.53**, 3.96	0.446, 0.616, ns	57, 55
Projected vein area per area C1	PAPA	mm2 mm-2	5.50e-2, **0.108**, 0.217	1.78e-3, 0.758***	57, 55
Volume of veins per area C1	VAPA	mm3 mm-2	1.32e-3, **3.95e-3**, 1.11e-2	6.85e-6, 0.768***	57, 55
Leaf area 3	LA	mm2	30.5, **121**, 342	9495, 0.673***	71, 122
Midrib diameter 3	Midrib Diam	mm	5.00e-2, **9.77e-2**, 0.195	1.47e-3, 0.608***	70, 117
Midrib vein length per area 3	Midrib VLA	mm mm-2	7.26e-2, **0.157**, 0.299	3.41e-3, 0.577***	70, 119
Secondary width 3	Secondary Diam	mm	3.23e-2, **5.31e-2**, 9.22e-2	2.76e-4, 0.611***	70, 116
Secondary vein length per area 3	Secondary VLA	mm mm-2	0.575, **0.970**, 2.38	0.169, 0.536**	70, 115
Minor vein width 3	Minor Diam	mm	2.12e-2, **4.21e-2**, 8.78e-2	2.23e-4, 0.628**	70, 116
Minor vein length per area 3	Minor VLA	mm mm-2	0.787, **1.64**, 2.76	0.246, 0.664***	70, 116
Major vein length per area 3	Major VLA	mm mm-2	0.696, **1.12**, 2.68	0.209, 0.546***	70, 115
Total vein length per area 3	Total VLA	mm mm-2	1.82, **2.77**, 4.65	0.660, 0.669***	70, 116
Projected vein area per area 3	PAPA	mm2 mm-2	5.96e-2, **0.135**, 0.225	2.77e-3, 0.658***	70, 115
Volume of veins per area 3	VAPA	mm3 mm-2	1.64e-3, **5.90e-3**, 1.57e-2	1.28e-5, 0.609***	70, 115

FIGURE CAPTIONS

Figure 6.1. Examples of Arabidopsis leaf mutants demonstrating the variety of leaf shapes and vein patterns observed.

Figure 6.2. Violin plots showing the variation in major (yellow) and minor (green) vein length per area (VLA) between leaf cohorts from early timing (cohort 1) to late timing (cohort 3) leaves.

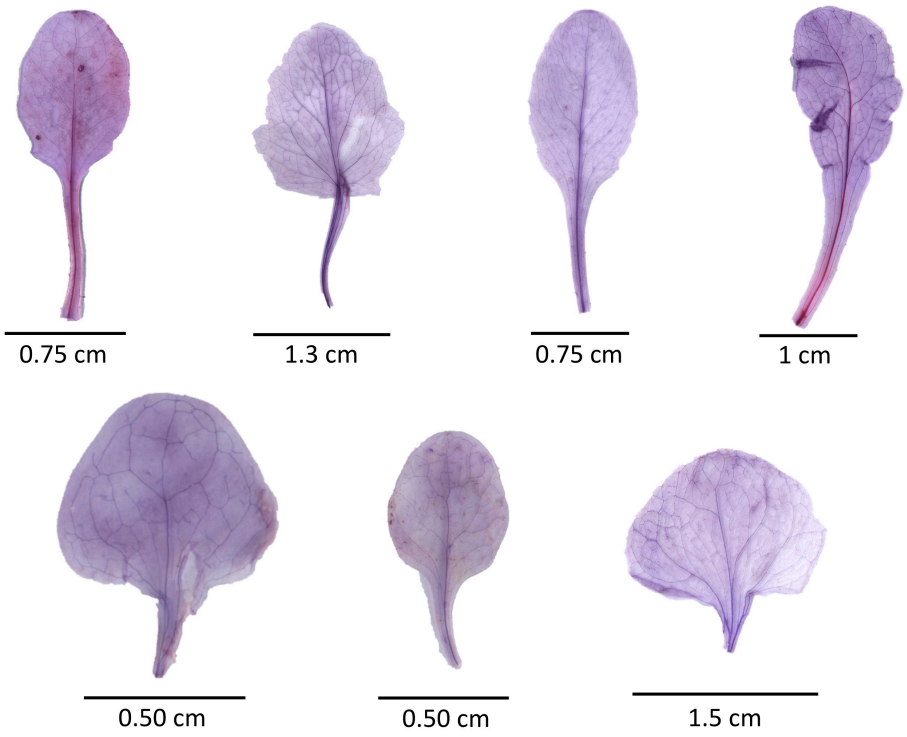

Figure 6.1

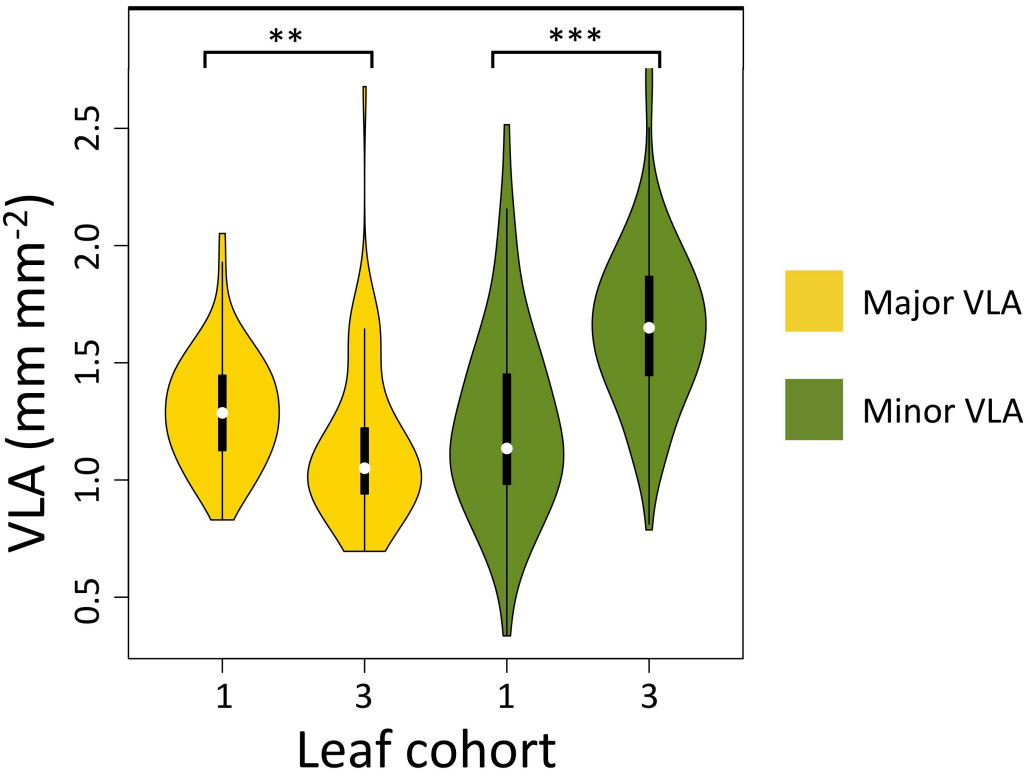

Figure 6.2

SUPPLEMENTARY MATERIALS

Supplementary Data Captions (see attached Excel Workbook)

Table S6.1. Experimental mean data for 90 genotypes (89 mutants and one wild-type; Col-0) of *Arabidopsis thaliana* grown in a greenhouse common garden. See "CHAPTER 6 Legend" tab for legend of symbols and units.

Table S6.2. Experimental data for all individuals of 90 genotypes (89 mutants and one wild-type; Col-0) of *Arabidopsis thaliana* grown in a greenhouse common garden. See "CHAPTER 6 Legend" tab for legend of symbols and units.

Table S6.3. Results of a paired t-test for leaf vein traits between early and late stage leaves (Cohorts 1 and 3) across all genotypes of for which vein trait data collection was possible at both developmental stages. Column names include the name of the trait variable tested, the estimated difference in means between the cohorts (estimate), the value of the t-statistic (statistic), the p-value for the test (p.value), the degrees of freedom for the t-statistic (parameter), the confidence intervals for the means (conf.low and conf.high), the type of test performed (method) and the alternative hypothesis (alternative).

Table S6.4. Results of an orthogonal contrast analysis for the relative growth rate (RGR) comparing all 54 mutant genotypes for which growth data were available with the wild-type, Col-0. Column names include the genotype name (term), the difference between the mean genotype values, or the mean genotype value in the case of Col-0 (estimate), the standard error (std.error), the value of the test statistic (statistic) and the p-value for the test (p.value). Yellow

highlights show genotypes for which RGR was greater than or equal to that of Col-0. Pink highlights show genotypes that were significantly different from Col-0 in their RGR.

Table S6.5. A correlation matrix of all traits for 90 genotypes of *Arabidopsis thaliana* (89 mutants and one wild-type, Col-0). Values show the r-values of correlations using raw, log-transformed, and ranked data. Highlighted cells represent tests for which either a raw and rank, or a log and rank correlation test were significant. Stars represent significance levels for each trait; df, degrees of freedom; ns, $P>0.05$; *, $P<0.05$; **, $P<0.01$; ***, $P<0.001$). C1: cohort 1, C3: cohort 3. See "CHAPTER 6 Legend" tab for units.

REFERENCES

Atwell, S., Huang, Y.S., Vilhjalmsson, B.J., Willems, G., Horton, M., Li, Y. *et al.* (2010). Genome-wide association study of 107 phenotypes in *Arabidopsis thaliana* inbred lines. *Nature*, 465, 627-631.

Brachi, B., Morris, G.P. & Borevitz, J.O. (2011). Genome-wide association studies in plants: the missing heritability is in the field. *Genome Biology*, 12.

Candela, H., Martinez-Laborda, A. & Micol, J.L. (1999). Venation pattern formation in *Arabidopsis thaliana* vegetative leaves. *Dev. Biol.*, 205, 205-216.

Chew, Y.H. & Halliday, K.J. (2011). A stress-free walk from *Arabidopsis* to crops. *Current Opinion in Biotechnology*, 22, 281-286.

Cobb, J.N., DeClerck, G., Greenberg, A., Clark, R. & McCouch, S. (2013). Next-generation phenotyping: requirements and strategies for enhancing our understanding of genotype-phenotype relationships and its relevance to crop improvement. *Theoretical and Applied Genetics*, 126, 867-887.

Dhondt, S., Coppens, F., De Winter, F., Swarup, K., Merks, R.M.H., Inze, D. *et al.* (2010). SHORT-ROOT and SCARECROW regulate leaf growth in *Arabidopsis* by stimulating S-Phase progression of the cell cycle. *Plant Physiology*, 154, 1183-1195.

Dunbar-Co, S., Sporck, M.J. & Sack, L. (2009). Leaf trait diversification and design in seven rare taxa of the Hawaiian *Plantago* radiation. *Int. J. Plant Sci.*, 170, 61-75.

Evans, G.C. (1972). *The Quantitative Analysis of Plant Growth*. Blackwell Scientific Publications, Oxford.

Feldman, A.B., Murchie, E.H., Leung, H., Baraoidan, M., Coe, R., Yu, S.M. *et al.* (2014). Increasing leaf vein density by mutagenesis: laying the foundations for C-4 rice. *PLoS One*, 9.

Filiault, D.L. & Maloof, J.N. (2012). A genome-wide association study identifies variants underlying the *Arabidopsis thaliana* shade avoidance response. *Plos Genetics*, 8.

Fletcher, L.R., Sartori, K., Vasseur, F., Medeiros, C.D., Farrell, C., Pellegrini, M. *et al.* (in prep.-a). Scaling of venation architecture within leaves of diverse ecotypes of *Arabidopsis thaliana*.

Fletcher, L.R., Scoffoni, C., Medeiros, C.D., Sartori, K., Vasseur, F., Violle, C. *et al.* (in prep.-b). Breaking the law: mixed climate adaptation strategies results in contrary trait-climate relationships across *Arabidopsis* ecotypes.

Huala, E., Dickerman, A.W., Garcia-Hernandez, M., Weems, D., Reiser, L., LaFond, F. *et al.* (2001). The *Arabidopsis* Information Resource (TAIR): a comprehensive database and web-based information retrieval, analysis, and visualization system for a model plant. *Nucleic Acids Res.*, 29, 102-105.

Hunt, R. & Cornelissen, J.H.C. (1997). Components of relative growth rate and their interrelations in 59 temperate plant species. *New Phytologist*, 135, 395-417.

Kang, J. & Dengler, N. (2004). Vein pattern development in adult leaves of *Arabidopsis thaliana*. *Int. J. Plant Sci.*, 165, 231-242.

Kehr, J. & Buhtz, A. (2007). Long distance transport and movement of RNA through the phloem. *Comp. Biochem. Physiol. A-Mol. Integr. Physiol.*, 146, S240-S240.

Korte, A. & Farlow, A. (2013). The advantages and limitations of trait analysis with GWAS: a review. *Plant Methods*, 9.

Liu, C.M. (2010). *Arabidopsis as Model for Developmental Regulation and Crop Improvement*. Springer-Verlag Berlin, Berlin.

Niklas, K.J. (1999). A mechanical perspective on foliage leaf form and function. *New Phytologist*, 143, 19-31.

Perez-Perez, J.M., Serrano-Cartagena, J. & Micol, J.L. (2002). Genetic analysis of natural variations in the architecture of *Arabidopsis thaliana* vegetative leaves. *Genetics*, 162, 893-915.

Petricka, J.J., Clay, N.K. & Nelson, T.M. (2008). Vein patterning screens and the defectively organized tributaries mutants in *Arabidopsis thaliana*. *Plant Journal*, 56, 251-263.

Roth-Nebelsick, A., Uhl, D., Mosbrugger, V. & Kerp, H. (2001). Evolution and function of leaf venation architecture: A review. *Ann. Bot.*, 87, 553-566.

Sack, L., Dietrich, E.M., Streeter, C.M., Sanchez-Gomez, D. & Holbrook, N.M. (2008). Leaf palmate venation and vascular redundancy confer tolerance of hydraulic disruption. *Proc. Natl. Acad. Sci. U. S. A.*, 105, 1567-1572.

Sack, L. & Frole, K. (2006). Leaf structural diversity is related to hydraulic capacity in tropical rain forest trees. *Ecology*, 87, 483-491.

Sack, L. & Holbrook, N.M. (2006). Leaf hydraulics. In: *Annual Review of Plant Biology*, pp. 361-381.

Sack, L., Scoffoni, C., McKown, A.D., Frole, K., Rawls, M., Havran, J.C. *et al.* (2012). Developmentally based scaling of leaf venation architecture explains global ecological patterns. *Nat. Commun.*, 3, 10.

Scoffoni, C., Rawls, M., McKown, A., Cochard, H. & Sack, L. (2011). Decline of leaf hydraulic conductance with dehydration: relationship to leaf size and venation architecture. *Plant Physiology*, 156, 832-843.

Scoffoni, C., Sack, L. & contributors, P. (2013). Quantifying leaf vein traits. *PrometheusWiki*.

Uddling, J., Gelang-Alfredsson, J., Piikki, K. & Pleijel, H. (2007). Evaluating the relationship between leaf chlorophyll concentration and SPAD-502 chlorophyll meter readings. *Photosynthesis Research*, 91, 37-46.

Uhl, D. & Mosbrugger, V. (1999). Leaf venation density as a climate and environmental proxy: a critical review and new data. *Paleogeogr. Paleoclimatol. Paleoecol.*, 149, 15-26.

CHAPTER 7

CONCLUSIONS AND FUTURE DIRECTIONS

As the climate changes, droughts are becoming more frequent and severe in many areas around the globe (Sheffield & Wood 2008). While many studies have investigated the influence of drought on biomes and across diverse species, little work has considered how trait-trait and trait-climate relationships may differ across closely-related species or genotypes of a given species. My dissertation addresses this knowledge gap by studying drought tolerance traits and their relationships with plant growth, development and adaptation to climatic stress at a fine scale. The traits conferring adaptation to drought that I quantify in *Arabidopsis thaliana* also open the door for future work to uncover the genetic bases of drought tolerance traits.

In my first chapter I demonstrated the importance of studying drought tolerance traits in a narrower sampling scheme by showing that trait-trait and trait-climate relationships may either be supported or show unexpected results depending on scale. I showed that a key drought tolerance trait, the osmotic potential at turgor loss point (π_{TLP}) can be used an indicator of drought tolerance across closely related species of *Ceanothus* (Rhamnaceae), upholding a trend that had been found across biomes and diverse species (Bartlett *et al.* 2012; Mart *et al.* 2016; Fletcher *et al.* 2018; Griffin-Nolan *et al.* 2019; Rosas *et al.* 2019). However, I also showed that expected cell allometries based on studies across diverse species (Brodribb *et al.* 2013; John *et al.* 2013) do not always hold when looking across closely-related species. In addition, I found that specialized anatomy may play a role in altering allometries due to strong anatomical differences even between species within a genus, but that specialized leaf anatomy (e.g. stomatal

crypts and hypodermal cells found in arid-adapted species) can potentially contribute to plant drought tolerance.

My next two chapters highlighted the complexity of plant drought adaptation within a species and demonstrated how suites of traits can scale up to confer adaptation to stress. I utilized the naturally occurring genotypes (ecotypes) of the model organism, *Arabidopsis thaliana* (Brassicaceae; referred to as Arabidopsis henceforth) to test a rich array of concepts. First, in Chapter 3 I tested for any intrinsic trade-offs between growth and drought tolerance traits, and between growth and climatic drought across 15 ecotypes of Arabidopsis. I found that the relative growth rate (RGR) was not constrained by drought tolerance traits such as the osmotic potential at full turgor ($\pi_{o,}$ the main determinant of π_{TLP}), nor was there any strong trade-off of growth with cold or drought of the genotypes' native ranges. However, certain traits were adapted to climatic drought and warmth, such as π_o, leaf mass per area (LMA), root mass fraction (RMF), among others. Thus, this study showed that traits can adapt independently to climate without a strong negative influence on growth. I then provided a novel theoretical framework for how this decoupling of growth from drought tolerance could allow a species to occupy a wide range of climates, as is found in Arabidopsis.

In Chapter 4 I again demonstrated how trait relationships could depend on scale, even varying within subsets of genotypes within a species. I used a large group of Arabidopsis ecotypes to show that the expected relationship of π_o being more negative in dry climates could be confounded by rapid growth in ecotypes that have adapted to climate by growing quickly when conditions were favorable. Other mechanistic traits expected to correlate with climate, such as the maximum leaf hydraulic conductance under well-watered conditions and in high light (K_{max}), were decoupled from climate, likely due to trade-offs with other traits that were climate-

adaptive. For example, K_{max} showed a strong trade-off with the water potential at 80% loss of hydraulic conductance (P_{80}), which was more negative in climates with lower rainfall, as expected, to maintain leaf function during drought. K_{max} was in turn decoupled from maximum photosynthetic rate (A_{max}), which was high in dry climates and thus would allow for fast growth when water is available (i.e., drought avoidance). Therefore, expected trait-trait and trait-climate trends could be unsupported or even occur in unexpected directions due to drought avoidance and drought tolerance adaptations operating in different ecotypes of a single species.

The leaf vein system is central to whole plant hydraulic function and growth. Traits such as greater major vein length per area (VLA) confer drought tolerance by creating redundant pathways for water movement in case of embolism (Scoffoni *et al.* 2011). In Chapter 5, I found strong scaling of greater major VLA in smaller leaves that was upheld across differing developmental stages, supporting a trend that had been shown at broader scales (Scoffoni *et al.* 2011; Sack *et al.* 2012). This work also emphasized the need to consider ontogeny in studies of vein traits, as minor VLA may seem to increase with leaf size if developmental stage is not considered, due to greater minor vein development occurring in later-forming leaves (Candela *et al.* 1999). I also explained how construction of large leaves can be beneficial by showing that veins in larger leaves had increased tapering and ramification as compared with smaller leaves, allowing for a reduction of hydraulic resistance (Mediavilla *et al.* 2021) and ample dedication of the leaf volume to photosynthetic mesophyll cells.

Chapter 6 provided novel data for vein development in Arabidopsis mutants and for understanding the influence of vein mutations on plant growth. I found that minor vein density was higher in later-development leaves, and that mutations in vein traits could potentially impact growth as evidenced by reduced RGR in mutants as compared with a wild-type, although further

investigation is required to disentangle the potential role of other traits that may have been affected by the mutations. I also generated genetic data that can be used in future research to determine which loci control vein traits.

My dissertation overall contributes to our knowledge of drought adaptation and opens the door to future studies in several key areas. First, my work adds to a body of literature that was previously lacking in studies of traits and climate using narrow sampling schemes, i.e. among closely-related species, genotypes within a species, and even comparing different genotype sets or ontogenetic stages within a given species. In the future, my findings can be used in tandem with field or drought experiments to gain a full understanding of plant drought response. Plants can respond plastically to their environments, and those types of responses should be quantified in key drought tolerance traits such as the π_{TLP}, which can osmotically adjust (Turner 2018). Future work should also integrate the knowledge we have gained from inter- and intra-specific studies to better predict how traits will scale up to impact plant growth, survival, reproduction and fitness, and therefore species ranges and interactions.

My work in Arabidopsis specifically will encourage an in-depth look into the many questions that still remain about the role of genetics in climate adaptation and the applicability of findings in mutant plants to natural populations. Some open questions include: Do genes vary across ecotypes at the same loci shown to be linked with leaf venation in mutants? Are leaf vein traits controlled by many or few loci, and which loci are these? Do mutants with more extreme phenotypes also have multiple mutations or mutations in genes with pleiotropic effects? The knowledge generated in this work can be applied to further research in agriculture by identifying target loci that influence the traits contributing to whole plant performance (Dhondt *et al.* 2010; Liu 2010; Chew & Halliday 2011; Cobb *et al.* 2013).

REFERENCES

Bartlett, M.K., Scoffoni, C. & Sack, L. (2012). The determinants of leaf turgor loss point and prediction of drought tolerance of species and biomes: a global meta-analysis. *Ecol. Lett.*, 15, 393-405.

Brodribb, T.J., Jordan, G.J. & Carpenter, R.J. (2013). Unified changes in cell size permit coordinated leaf evolution. *New Phytologist*, 199, 559-570.

Candela, H., Martinez-Laborda, A. & Micol, J.L. (1999). Venation pattern formation in *Arabidopsis thaliana* vegetative leaves. *Dev. Biol.*, 205, 205-216.

Chew, Y.H. & Halliday, K.J. (2011). A stress-free walk from *Arabidopsis* to crops. *Current Opinion in Biotechnology*, 22, 281-286.

Cobb, J.N., DeClerck, G., Greenberg, A., Clark, R. & McCouch, S. (2013). Next-generation phenotyping: requirements and strategies for enhancing our understanding of genotype-phenotype relationships and its relevance to crop improvement. *Theoretical and Applied Genetics*, 126, 867-887.

Dhondt, S., Coppens, F., De Winter, F., Swarup, K., Merks, R.M.H., Inze, D. *et al.* (2010). SHORT-ROOT and SCARECROW regulate leaf growth in *Arabidopsis* by stimulating S-Phase progression of the cell cycle. *Plant Physiology*, 154, 1183-1195.

Fletcher, L.R., Cui, H., Callahan, H., Scoffoni, C., John, G.P., Bartlett, M.K. *et al.* (2018). Evolution of leaf structure and drought tolerance in species of Californian *Ceanothus*. *Am. J. Bot.*, 105, 1672-1687.

Griffin-Nolan, R.J., Ocheltree, T.W., Mueller, K.E., Blumenthal, D.M., Kray, J.A. & Knapp, A.K. (2019). Extending the osmometer method for assessing drought tolerance in herbaceous species. *Oecologia*, 189, 353-363.

John, G.P., Scoffoni, C. & Sack, L. (2013). Allometry of cells and tissues within leaves. *Am. J. Bot.*, 100, 1936-1948.

Liu, C.M. (2010). *Arabidopsis as Model for Developmental Regulation and Crop Improvement*. Springer-Verlag Berlin, Berlin.

Mart, K.B., Veneklaas, E.J. & Bramley, H. (2016). Osmotic potential at full turgor: an easily measurable trait to help breeders select for drought tolerance in wheat. *Plant Breeding*, 135, 279-285.

Mediavilla, S., Martín, I. & Escudero, A. (2021). Plant ontogenetic changes in vein and stomatal traits and their relationship with economic traits in leaves of three Mediterranean oaks. *J. Plant Ecol.*

Rosas, T., Mencuccini, M., Barba, J., Cochard, H., Saura-Mas, S. & Martinez-Vilalta, J. (2019). Adjustments and coordination of hydraulic, leaf and stem traits along a water availability gradient. *New Phytologist*, 223, 632-646.

Sack, L., Scoffoni, C., McKown, A.D., Frole, K., Rawls, M., Havran, J.C. *et al.* (2012). Developmentally based scaling of leaf venation architecture explains global ecological patterns. *Nat. Commun.*, 3, 10.

Scoffoni, C., Rawls, M., McKown, A., Cochard, H. & Sack, L. (2011). Decline of leaf hydraulic conductance with dehydration: relationship to leaf size and venation architecture. *Plant Physiology*, 156, 832-843.

Sheffield, J. & Wood, E.F. (2008). Global trends and variability in soil moisture and drought characteristics, 1950-2000, from observation-driven simulations of the terrestrial hydrologic cycle. *J. Clim.*, 21, 432-458.

Turner, N.C. (2018). Turgor maintenance by osmotic adjustment: 40 years of progress. *Journal of Experimental Botany*, 69, 3223-3233.